

**Ice-nucleation by mineral dust applied to cell  
cryopreservation and atmospheric science**

**by**

**Martin Ian Daily**

Submitted in accordance with the requirements for the degree of Doctor of  
Philosophy

University of Leeds  
School of Earth and Environment

March 2022



The candidate confirms that the work submitted is his own, except where work which has formed part of jointly authored publications has been included. The contribution of the candidate and the other authors to this work has been explicitly indicated below. The candidate confirms that appropriate credit has been given within the thesis where reference has been made to the work of others. The work in Chapters Two to four of the thesis has appeared in the following publications:

**Daily, M.I., Whale, T.F., Partanen, R., Harrison, A.D., Kilbride, P., Lamb, S., Morris, G. J., Picton H.M., and Murray, B.J. ‘Cryopreservation of primary cultures of mammalian somatic cells in 96-well plates benefits from control of ice nucleation’**, published in *Cryobiology* (2020). This publication forms Chapter Two. Study was conceived by BJM, TFW, and HMP with PK, SL and GJM providing industrial motivation and expertise. I carried out all experiments, conceived the manual nucleation technique data analysis, produced all plots and diagrams and wrote the paper with edits from TFW, KP, SL, HMP and BJM. RP and TFW assisted and trained me with the granulosa cell isolation. ADH gave guidance on use of the IR-NIPI apparatus. HMP provided guidance with cell culture, statistical analysis and overall supervision along with BJM.

**Daily, M.I., Whale, T.F., Kilbride, P., Lamb, S., Morris, G. J., Picton H.M., and Murray, B.J. ‘A highly active mineral ice nucleating agent supports in-situ high throughput cell cryopreservation’**. This manuscript draft forms Chapter Three. Study was conceived by me, BJM, TFW, and HMP with PK, SL and GJM providing industrial motivation and expertise. I performed all experiments and data analysis, produced all plots and diagrams sourced the LDH1 sample, and I wrote the paper and edits from TFW, KP, HMP and BJM. HMP provided guidance with cell culture and overall supervision along with BJM.

**Daily, M. I., Tarn, M.D., Whale, T.F., and Murray, B.J. ‘An evaluation of the heat test for the ice-nucleating ability of minerals and biological material.’** This publication forms Chapter Four and has been accepted for publication with *Atmospheric Measurement Techniques* with minor revisions (February 2022). I conceived this study with discussions with BJM and designed and conducted all the experiments myself, performed all data analysis and produced all plots and diagrams. The paper was written by myself with input and edits by MDT, TFW and BJM.

This copy has been supplied on the understanding that it is copyright material and that no quotation from the thesis may be published without proper acknowledgement.

The right of Martin Ian Daily to be identified as Author of this work has been asserted by him in accordance with the Copyright, Designs and Patents Act 1988.

© 2022 The University of Leeds and Martin Ian Daily

## Acknowledgements

I would like to firstly thank my brilliant supervision team, without whom this project and thesis would not have been possible. My primary supervisor Ben Murray kept my head up during the tougher parts of the coronavirus lockdown and also was particularly helpful through the writing process. Tom Whale has been a great mentor providing plenty of ideas and fun science discussions throughout. I was also lucky to have Helen Picton to guide me through an area of science previously totally new to me.

I am very grateful to the Natural Environment Research Council for a PhD studentship and the additional funding and resources provided by Cytiva (formerly Asymptote Ltd), Cambridge, UK. The support from the people at Cytiva, particularly John Morris, Peter Kilbride, Stephen Lamb and Julie Meneghel, was crucial to this project and they made me feel welcome during my visits to Cambridge.

The support staff at Cohen (Andy Connelly, Andy Hobson) and the LIGHT Laboratories (Claire Hills, Phil Warburton) deserve my thanks for tolerating my chaos and keeping my labwork running to schedule.

I was lucky to share many happy times in the office, the Ice Lab, and the Old Bar with other members of the Ice-Nucleation group at the School of Earth and Environment including Mark Tarn, Sarah Barr, Elena Maters, Grace Porter, Mike Adams, Seb Sikora, Mark Holden, Alberto Sanchez-Marroquin, Sandy James, Beth Wyld, Leon King, Alex Harrison and many others.

Much of this project took place during the coronavirus lockdowns of 2020-2021 and my support bubble of Tom W, Anna, Tom F, Harriet and Ogs kept me going through this period. Finally, I thank my all other friends and my family (Mum, Dad and Peter) for their encouragement, love and welcome distractions throughout.

## Abstract

Heterogeneous ice-nucleation is a poorly understood physical process. This poses great challenges to understanding how ice formation in mixed-phase clouds affects Earth's current and future climate. Also, cryopreservation of biological material is hampered by the physical hazards of uncontrolled ice-nucleation. The aim of this thesis is to apply understanding about materials known to trigger heterogeneous ice-nucleation, and in particular, mineral particles to improving cryopreservation processes. The learnings from this are fed back into atmospheric sciences.

Cell monolayers frozen in multiwell plate format could be used for *in-vitro* high-throughput toxicology screening which could streamline the development of new lifesaving drugs and therapies. In this thesis it is shown how controlling ice-nucleation is essential for good recovery when cells are frozen in this way. First it is described how aqueous liquid aliquots will supercool to degree that is related to volume and in 96-well plates this can be by over 20 °C before freezing occurs. Using plated cultures of both primary and immortalized animal cells it was then shown unambiguously that when ice-nucleation is controlled post-thaw recovery is significantly improved. Moreover, a causal link was established by correlating ice-nucleation temperature with cell survival rates. Following on from this a strategy for controlling ice-nucleation in 96-well plates in a scaled up and biocompatible manner was tested. A highly effective mineral ice-nucleator previously discovered by the atmospheric science community, LDH1, was incorporated into IceStart arrays to control ice-nucleation in 96-well plates. The remarkable ice-nucleating properties of LDH1 were characterized and it was found that supercooling could almost be eliminated in 100 µL water and cryoprotectant solution droplets with as little as 0.05 mg. When trialed with plated immortalised hepatocyte cell cultures, post-thaw survival was significantly improved.

Finally, the stability of mineral ice-nucleators was investigated, particularly in response to heat. This has been overlooked to date and has a crucial role in the detection of biological ice-nucleating particles the atmosphere. While some minerals such as K-feldspar are largely stable, quartz particles lose ice-nucleating activity when heated in water. This is a surprising result which drives refinement of the established heat test for biological INP and gives some clues about nature of ice-nucleating sites on minerals.

## Table of Contents

<b>Acknowledgements</b> .....	<b>iii</b>
<b>Abstract</b> .....	<b>iv</b>
<b>Table of Contents</b> .....	<b>v</b>
<b>List of Tables</b> .....	<b>ix</b>
<b>List of Figures</b> .....	<b>ix</b>
<b>List of Abbreviations</b> .....	<b>xiii</b>
<b>1 Introduction</b> .....	<b>1</b>
1.1 Fundamentals of ice nucleation .....	1
1.1.1 Classical Nucleation Theory .....	3
1.1.2 Modes of Heterogeneous Ice-Nucleation.....	7
1.1.3 Relationship of freezing temperature of ‘pure’ water droplets with volume .....	8
References .....	11
1.2 Measurement of ice-nucleating materials in immersion mode .....	15
1.2.1 Experimental methods .....	15
1.2.2 Quantitative description of immersion mode heterogeneous ice- nucleation .....	19
References .....	22
1.3 Ice-nucleation in Cryobiology .....	27
1.3.1 Introduction to cryopreservation .....	27
1.3.2 Approaches to animal cell cryopreservation .....	27
1.3.3 Cryoprotectants.....	30
1.3.4 Role of controlled ice-nucleation in cryopreservation.....	31
References .....	36
1.4 Ice-nucleation in Earth’s atmosphere .....	41
1.4.1 Importance of ice-nucleation in clouds.....	41
1.4.2 Atmospheric aerosol and ice-nucleating particles.....	44
1.4.3 Climate change feedbacks controlled by ice-nucleation in clouds.....	47
References .....	49
1.5 Ice-nucleating materials .....	55
1.5.1 Fundamental prerequisites for ice-nucleating materials .....	55
1.5.2 Insoluble or particulate ice-nucleating materials.....	56
1.5.3 Soluble or non-particulate ice-nucleating materials .....	59
References .....	60
1.6 Project objectives.....	65

1.6.1	Demonstrate importance of controlling ice-nucleating in 96-well plates and the effectiveness of IceStart™ for cryopreserving cells.....	66
1.6.2	Optimise performance of mineral ice-nucleator.....	67
1.6.3	Investigate stability of mineral ice-nucleators and compare with biological ice-nucleators .....	67
	References .....	67
1.7	Thesis Overview .....	70
<b>2</b>	<b>Cryopreservation of primary cultures of mammalian somatic cells in 96-well plates benefits from control of ice nucleation.....</b>	<b>72</b>
2.1	Introduction .....	73
2.2	Materials and methods .....	76
2.2.1	Controlled and uncontrolled ice nucleation temperatures within 96-well plates .....	76
2.2.2	Bovine granulosa cell cultures.....	77
2.2.3	Cryopreservation of 96-well plates.....	78
2.2.4	Manual induction of Ice nucleation in 96-well plates.....	79
2.2.5	Thawing of cryopreserved 96-well plates .....	80
2.2.6	Neutral Red assessment of cell number and viability .....	80
2.2.7	Assessment of cell morphology.....	80
2.2.8	Cryoprotectant toxicity testing .....	81
2.2.9	Experimental design and statistical analysis of post-thaw cell viability.. .....	81
2.3	Results .....	82
2.3.1	Freezing temperatures with controlled and uncontrolled nucleation... ..	82
2.3.2	The effect of controlling nucleation on post thaw cell viability.....	85
2.3.3	Effect of cryopreservation on cell morphology.....	86
2.4	Discussion.....	88
2.5	Conclusions .....	91
	References .....	93
<b>3</b>	<b>A highly active mineral ice nucleating agent supports in-situ high throughput cell cryopreservation .....</b>	<b>96</b>
3.1	Introduction .....	96
3.2	Results .....	100
3.2.1	The ice-nucleating ability of LDH1 .....	100
3.2.2	Link between aliquot ice-nucleation temperature and post-thaw survival rates of cryopreserved cells.....	105

3.2.3	High-throughput cryopreservation of HepG2 cell monolayers in situ within 96-well plate with LDH1 delivered via IceStart™ arrays.....	108
3.3	Discussion .....	113
3.4	Materials and Methods.....	117
3.4.1	Sourcing and preparation of LDH1 and other ice-nucleating materials ..	117
3.4.2	Droplet freezing assays and derivation of INA.....	118
3.4.3	HepG2 cell culture and plate cryopreservation .....	120
3.5	Supplementary Information (SI).....	123
3.5.1	Source of LDH1 and ice-nucleating ability of its components .....	123
3.5.2	Long term stability of LDH1 in water and DMSO solution .....	125
3.5.3	Optimisation of cryoprotectant and toxicity trials.....	127
	References .....	135
<b>4</b>	<b>An evaluation of the heat test for the ice-nucleating ability of minerals and biological material.....</b>	<b>142</b>
4.1	Introduction .....	143
4.2	Materials and methods .....	151
4.2.1	Sample selection.....	151
4.2.2	Sample preparation .....	156
4.2.3	Heat treatments.....	157
4.2.4	Ice nucleation measurements by droplet freezing assay and determination of samples' heat deactivations .....	158
4.3	Results and discussion .....	160
4.3.1	Heat sensitivity of mineral-based INP samples.....	162
4.3.2	Biological INP surrogates .....	177
4.4	Summary and implications for using INP heat treatments.....	179
4.5	Conclusions .....	184
4.6	Appendix A: The effect of vessel type used for wet heating of silica INP suspensions. ....	186
4.7	Appendix B: Dependence of INA heat deactivations on temperature, duration and suspension concentration.....	188
4.8	Supplementary Information.....	193
4.8.1	Background information on classes of mineral INPs .....	193
4.8.2	Mass changes of samples after dry heating.....	196
4.8.3	Supplementary figures .....	197
	References .....	200

<b>5</b>	<b>Conclusions and future work.....</b>	<b>214</b>
5.1	Objective one: Demonstrate importance of controlling ice-nucleating in 96-well plates and the effectiveness of IceStart™ for cryopreserving cells.....	214
5.1.1	Conclusions .....	214
5.1.2	Future work .....	215
5.2	Objective two: Optimise performance of mineral ice nucleator.....	216
5.2.1	Conclusions .....	216
5.2.2	Future work .....	217
5.3	Objective three: Investigate stability of mineral ice-nucleators and compare with biological ice-nucleators .....	219
5.3.1	Conclusions .....	219
5.3.2	Future work .....	220
5.4	Final remarks .....	221
	References .....	221

### List of tables

Table 1.1. Comparison of methods for controlling ice-nucleation in cryopreservation applications.....	34
Table 3.1 HepG2 cell count data obtained by neutral red viability assay for plate cryopreservation trials shown in Fig 3.7.....	130
Table 4.1: List of past studies in which heat treatments were used to infer the presence of biological INPs in samples of various environmental media. ....	146
Table 4.2: Sample information for mineral-based INP samples. Sources of data for purity and specific surface area (SSA) are detailed in the annotations. ....	153
Table 4.3: Sample information for biological-based INP samples.....	155
Table 4.4: Summary of the characteristic responses of classes of INPs to wet and dry heat treatments.....	181
Table 4.5: Mass changes of samples after dry heat treatment (250 °C for 4 h) .....	196

### List of figures

Figure 1.1 Illustration of critical cluster size ( $r^*$ ) resulting from competing volume and interface terms according to Classical Nucleation Theory.....	5
Figure 1.2: Illustration of heterogeneous nucleation according to Classical Nucleation Theory. ....	6
Figure 1.3: Illustration of mode of ice-nucleation .....	8
Figure 1.4: Empirical relationship between volume and median freezing temperature for supercooled water aliquots.....	10
Figure 1.5: Droplet freezing assay demonstration.....	16
Figure 1.6: Idealised slow freezing cell cryopreservation, adapted from Hunt (2019). .....	29
Figure 1.7: Schematic of two-factor hypothesis of cell injury during slow-cooling cell cryopreservation (Mazur, 1972).....	30
Figure 1.8: Supercooling of liquid within 96-well plates and expected effect on post-thaw cell viability. ....	33
Figure 1.9: Three different concepts on the effects of solutes on heterogeneous ice-nucleation temperatures. ....	36
Figure 1.10: Wegener-Bergeron-Findeisen process, diagram from Koop and Mahowald (2013) .....	42
Figure 1.11: Fallstreak or ‘hole-punch’ cloud photographed within an altostratus cloud layer on 18 <sup>th</sup> January 2022, Leeds, UK. ....	43
Figure 1.12: Cloud model output showing effect of INP concentration on clouds in the cold-sector of mid-latitude cyclone over the Southern Ocean, a figure from	

Murray et al., (2021) which was adapted from Vergara-Temprado et al., (2018) .....	43
Figure 1.13: Summary of INP measurements taken globally from Kanji et. al., (2017). .....	46
Figure 1.14: Mixed phase clouds' possible responses to climate change, taken from Murray et al. (2021). .....	48
Figure 1.15: a) Feldspar group compositions plotted on ternary diagram (taken from Harrison et al (2016)). b) Thin section of perthitic orthoclase under crossed polarised light showing exsolution microtexture lamellae. c) Specimen of amazonite, a green variant of microcline, showing exsolution microtexture on a larger scale. ....	58
Figure 1.16: Compilation of literature data taken from Kanji et al. (2017) showing relative ice-nucleating active site densities of biological INP (a) and feldspar variants (b). .....	60
Figure 1.17: Schematic of IceStart array for 96-well plate, adapted from Morris and Lamb, 2018. ....	66
Figure 2.1: Description of 96-plate cryopreservation procedure and manual ice nucleation technique. ....	77
Figure 2.2: Droplet fraction frozen against well ice nucleation temperature for ensembles of 100 $\mu$ L droplets of water prepared in different conditions of sterility and of CPA with and without a cell monolayer in polypropylene 96- well plates. ....	83
Figure 2.3: (Left): IR NIPI temperature log of 96-well plate loaded with 50 $\mu$ L aliquots of CPA where half of the wells were nucleated manually with ice mist (green lines) and half left to nucleate without control (blue lines). The data gap at around 1300 s is due to the apparatus being disabled to allow the manual nucleation procedure. ....	85
Figure 2.4: (A) Boxplots of viable granulosa cell number pre- and post- cryopreservation as determined by Neutral Red assays. ....	87
Figure 2.5: Freezing temperatures of purified water droplet ensembles at a range of volumes with an empirical trend. ....	91
Figure 3.1: a) Cartoon of IR-NIPI instrument with example IR images of 96-well plate and well ice-nucleation events used to obtain all the data in this figure. b) Demonstration of thermal history of well and determination of $T_{nuc}$ .....	100
Figure 3.2: Boxplot showing IR-NIPI results of droplet freezing assays for 50 $\mu$ L droplets of suspensions of several ice-nucleating materials in water at different concentrations. ....	101
Figure 3.3: a-e) Thermal history traces of droplet freezing assays shown in c) at concentrations of 1% w/w. f-i) Detailed thermal history of LDH1 runs at all concentrations illustrating the apparent elimination of supercooling. For plots	

in d-k) numbers indicate droplet temperature ( $^{\circ}\text{C}$ ) on $x$ -axis and time into freezing run (s) on $y$ -axis.....	102
Figure 3.4: Number of active sites per unit mass of LDH1 and other strong ice-nucleators as a function of temperature ( $n_m(T)$ ). .....	104
Figure 3.5: Schematics for a) HepG2 plate cryopreservation protocol; b) and c) IceStart <sup>TM</sup> arrays. ....	106
Figure 3.6: Results for a 96-well plate with HepG2 culture cryopreserved with IR-NIPI instrument: a) Individual well $T_{\text{nuc}}$ ; b) Individual well post-thaw neutral red dye absorbance; c) Thermal history of wells with detail for wells spiked with LDH1 d). Correlation plot of data from a) and b) .....	107
Figure 3.7: Results for high-throughput trials of HepG2 cells cryopreserved in 96-well plate with and without controlled ice-nucleation with viability assays performed immediately post-thaw (a, c, d) and 5 days post-thaw (b, e, f). Example results for individual plates within the groups are shown in a) and b) with bar height and colour strength indicating post-thaw viability. Boxplots and ANOVA results for individual freezing runs are shown in c) and e). Overall post-thaw survival rates averaged over all 8 runs shown as d) and f). .....	111
Figure 3.8: Microscope images of cell monolayers after neutral red staining illustrating differences in cell morphology dependent on ice-nucleation control. ....	113
Figure 3.9 Source material for LDH1. ....	123
Figure 3.10: Close up of dark inclusion crystal shown in Fig. 3.9 under stereomicroscope at 4x magnification. ....	124
Figure 3.11: Fragment of sample shown in Fig. 3.9 broken along cleavage plane showing interior. ....	124
Figure 3.12: Plot of $f_{\text{ice}}$ for microlitre droplets of suspensions of ground constituents of sample shown in Fig. 3.9. ....	125
Figure 3.13 Stability of LDH1 (a) and BCS-376 Microcline (b) in water and 10% DMSO solution. ....	126
Figure 3.14: Effect of CPA formulations on unfrozen HepG2 cell viability. ....	128
Figure 3.15: Effect of CPA formulation on cryopreserved HepG2 viability. ....	128
Figure 3.16: Effect of IceStart arrays on unfrozen HepG2 cells. ....	129
Figure 4.1: Fraction of droplets frozen ( $f_{\text{ice}}(T)$ ) spectra illustrating characteristic heat treatment responses for: (a) A dry heat-sensitive mineral INP (BCS-376 Microcline). (b) A wet heat-sensitive mineral INP (Fluka Quartz). (c) A wet heat-sensitive proteinaceous biological INP (Snomax <sup>®</sup> ). (d) A wet heat-insensitive non-proteinaceous biological INP (birch pollen washing water). .....	161
Figure 4.2 (a) Boxplot showing freezing temperatures before (black) and after heat treatments (red for wet heat, blue for dry heat) for all K-feldspar samples... ..	164

Figure 4.3 Boxplot showing freezing temperatures before (black) and after heat treatments (red for wet heat, blue for dry heat) for all plagioclase feldspar samples .....	168
Figure 4.4 (a) Boxplot showing freezing temperatures before (black) and after heat treatments (red for wet heat, blue for dry heat) for all silica samples .....	169
Figure 4.5 Boxplot showing freezing temperatures before (black) and after heat treatments (red for wet heat, blue for dry heat) for clays based mineral samples .....	173
Figure 4.6. a). Boxplot showing freezing temperatures before (black) and after heat treatments (red for wet heat, blue for dry heat) for mineral dust analogues and calcite. ....	175
Figure 4.7: Boxplot showing freezing temperatures before (black) and after heat treatments (red for wet heat, blue for dry heat) for biological INP samples. .	178
Figure 4.8 Plot showing the fraction of droplets frozen ( $f_{ice}(T)$ ) for wet heated Fluka Quartz suspensions (all 1 % w/v) repeated using a range of different container types. ....	187
Figure 4.9: Thermocouple measurements of suspension temperature inside both glass and plastic vessels during the wet heat treatment procedure.....	187
Figure 4.10a-d: Plots of $n_s(T)$ or $n_m(T)$ illustrating heat test responses over an extended range of suspension concentrations for a) BCS-376 Microcline, b) Fluka Quartz, c) ATD, d) NX-Illite .....	189
Figure 4.11 a-b Boxplots of freezing temperatures for droplet freezing assays of suspensions of a) BCS-376 Microcline (1 % w/v) and b) Snomax <sup>®</sup> (0.05 % w/v) before and after wet heating and dry heating at varying temperatures and durations. ....	191
Figure 4.12: Fraction of droplets frozen ( $f_{ice}(T)$ ) curves for all mineral-based INP samples. ....	198
Figure 4.13 Fraction of droplets frozen ( $f_{ice}(T)$ ) curves for all biological analogue INP samples.....	199
Figure 4.14 Plot showing $f_{ice}(T)$ data for background water in borosilicate glass vials (Blanks #1 to #5) and handling blanks for various modes of wet and dry heat tests in borosilicate and polypropylene containers. ....	200

**List of abbreviations**

ANOVA	Analysis of variance
ATD	Arizona Test Dust
BET	Brunauer-Emmet-Teller (surface area measurement)
BPWW	Birch pollen washing water
CCN	Cloud condensation nuclei
cGMP	Current good manufacturing practice
CM	Culture media
CNT	Classical Nucleation Theory
CPA	Cryoprotectant
DFA	Droplet freezing assay
DMSO	Dimethyl Sulphoxide
IIF	Intracellular ice formation
INP	Ice-nucleating particle
IN	Ice-nucleation
INA	Ice-nucleating ability
IM	Incubation media
IPCC	Intergovernmental Panel on Climate Change
LDH1	Leeds hyperactive feldspar 1
LN <sub>2</sub>	Liquid nitrogen
MCC	Microcrystalline cellulose
MeSO <sub>2</sub>	Dimethyl sulphoxide
μl-NIPI	Microlitre Immersion by Immersed Particle Instrument
IR-NIPI	Infra-Red Immersion by Immersed Particle Instrument

PBAP	Primary biological aerosol particle
NR	Neutral Red
PTV	Post-thaw viability
PTS	Post-thaw survival
SD	Standard deviation
SEM	Scanning electron microscope / Standard error of the mean
SSA	Specific surface area
XRD	X-ray diffraction

# 1 Introduction

At the Earth's surface ice is the thermodynamically stable phase of pure water at temperatures below 0°C. However, water can cool below 0° C and remain liquid in a metastable, supercooled state without freezing (Bigg, 1953; Koop et al., 2000). This phenomenon plays a critical role in the behaviour of clouds in Earth's troposphere and in biological systems at low temperatures (Clarke et al., 2013; Murray et al., 2012). Freezing above around -33° C requires a surface or impurity to catalyse the initial appearance of the ice phase. This process is known as heterogeneous ice-nucleation (Pruppacher and Klett, 1997) and can be difficult to predict because it is a poorly understood process compared to homogeneous ice-nucleation. This limits our understanding of ice formation in clouds and the consequent effects on the hydrological cycle and radiative balance. Also, uncontrolled ice nucleation poses challenges to the successful cryopreservation of biological materials such as animal cells (Morris and Acton, 2013). This opening Chapter introduces the fundamental theories that underpin current understanding of ice-nucleation, outlines how ice-nucleation and the ability of materials to nucleate ice is quantified, the importance of ice-nucleation in cryopreservation and in clouds, and finally reviews the materials that are known to act as efficient ice-nucleators.

## 1.1 Fundamentals of ice nucleation

The phase transition from liquid water or supersaturated vapour to ice must be preceded by a nucleation event, where water molecules spontaneously assemble into a cluster with a crystalline structure. Without the nucleation event water can remain liquid in a metastable, supercooled (or supersaturated) state. Homogeneous ice-nucleation (IN) of water at temperatures ranging from -38°C to -33°C (Herbert et al., 2015) can readily be achieved using relatively unsophisticated laboratory techniques and very pure water droplets (Bigg, 1953; Polen et al., 2018). However, in common experience IN is triggered much closer to the freezing point via heterogeneous nucleation by the presence of an impurity or the surface that the water is in contact with. Nucleation in a supercooled liquid begins with the random and constant formation and disintegration of clusters of molecules in a solid, ice-like state. Initial

growth of these temporary clusters is thermodynamically unfavourable meaning they are likely to disintegrate. If, however, a cluster reaches a critical size threshold addition of water molecules to the cluster becomes thermodynamically favourable. The cluster is then said to have reached a critical size, meaning it will grow spontaneously, typically resulting in freezing of the whole body of supercooled liquid. Whether a critical cluster appears in supercooled water depend on various factors. Classical Nucleation Theory (CNT) can be used to predict ice nucleation rates (Ickes et al., 2015; Koop and Murray, 2016; Pruppacher and Klett, 1997).

Crystallisation of ice is associated with release of latent heat of crystallisation which has consequences for both atmospheric processes and cryopreservation protocols. For example, the release of latent heat by freezing cloud droplets can provide energy for up draughts in convective clouds (Fan et al., 2017). In cryopreservation protocols latent heat release after ice nucleation causes in-vessel temperature fluctuations which must be accounted for. The rate of homogeneous freezing as a function of temperature has been measured fairly precisely, meaning homogeneous freezing temperature of pure water droplets can be predicted to within a few degree if their sizes are known. In contrast, heterogeneous freezing is much harder to predict due to the poorly understood properties and occurrences of heterogeneous ice nucleating sites (Kanji et al., 2017; Maeda, 2021). Being able to predict or control of the rate of heterogeneous IN would therefore be advantageous in both these fields.

The nature of ice which nucleates from supercooled water is not well understood at present. At current, there are 19 known phases of ice, most of which form at high pressure (Hansen, 2021). Ice  $I_h$  is the thermodynamically stable phase at atmospheric pressure (Salzmann et al., 2011). However, metastable polymorphs of ice I may play an important role in ice nucleation (Murray et al., 2005). Cubic ice was previously only thought to exist naturally in cirrus clouds at low temperatures (below  $-80^\circ\text{C}$ ) in the upper troposphere due to evidence from cloud haloes (Murray et al., 2005; Riikonen et al., 2000). However, x-ray diffraction experiments have established that following nucleation (either homogeneous or heterogeneous) ice initially crystallises as randomly alternating layers of Ice  $I_h$  and Ice  $I_c$ , known as stacking disordered ice – Ice  $I_{sd}$  (Lupi et al., 2017; Malkin et al., 2012; Malkin et al., 2015). This has been observed at temperatures as warm as  $-15^\circ\text{C}$ , although it is likely a transient state which re-crystallises to Ice  $I_h$  (Huang and Bartell, 1995; Murray et al., 2010). This knowledge

allowed the calculations that lead to prediction of nucleation rates - which traditionally assume all ice formed is ice  $I_h$  under common environmental conditions (Murray et al., 2012) - to be refined (Koop and Murray, 2016).

### 1.1.1 Classical Nucleation Theory

Classical Nucleation Theory (CNT) is the theoretical framework most usually employed to predict the rate of nucleation of stable solid phase (ice) from a metastable supersaturated phase (supercooled water or supersaturated water vapour) (Ickes et al., 2015; Koop and Murray, 2016; Pruppacher and Klett, 1997). In the case of nucleation of ice from supercooled water it finds applications underpinning models that attempt predict the rate of ice formation in clouds and also quantifying how efficient specific substances can be at raising the IN temperature via heterogeneous nucleation. However, there are limitations to CNT due to the uncertainties of some physical parameters of supercooled water (Ickes et al., 2015) and in which phase of ice nucleates (Murray et al., 2012). Moreover, while a number of frameworks to describe heterogeneous IN have been developed, the prevailing method used is based on a singular or active-site model (Pruppacher and Klett, 1997; Vali, 1994) rather than CNT, where time dependence (stochasticity) is assumed to be insignificant. Instead, a characteristic active site temperature is typically used to due to the great variability and complexity of materials that initiate heterogeneous IN (Kanji et al., 2017).

#### 1.1.1.1 Homogeneous Nucleation

IN occurs via the homogeneous route where there is absence of any surface or impurity and this scenario becomes increasingly likely with decreasing droplet volume (Bigg, 1953). As we will show, CNT dictates that the probability of homogeneous IN increases with decreasing temperature and larger droplet volume and also increases over longer timescales due to the stochastic nature of the process. CNT has been used to describe the data produced by experiments aimed at measuring the rate of freezing of pure water droplets (Atkinson et al., 2016; Ickes et al., 2015; Tarn et al., 2021). The homogeneous nucleation rate,  $J_{hom}$  ( $\text{cm}^{-3}\text{s}^{-1}$ ), describes the rate of appearance of ice germs of critical size (i.e. nucleation events leading to droplet freezing) within a given volume of supercooled water per unit time:

$$J_{hom} = A \exp\left(-\frac{\Delta G^*_{cluster}}{k_b T}\right) \quad (1.1)$$

Where  $A$  is a pre-exponential factor mostly related to the self-diffusion of water,  $\Delta G^*_{cluster}$  is the Gibbs free energy barrier to reaching a critically sized ice cluster,  $k_b$  is the Boltzmann constant and  $T$  is the ambient temperature. Due to the exponential nature of this equation  $J_{hom}$  is very sensitive to changes in temperature and the value of  $\Delta G^*_{cluster}$ . The free energy change for forming a cluster ( $\Delta G_{cluster}$ ) is the product of two competing terms: the free energy gain of forming bulk solid from supercooled liquid ( $\Delta G_{bulk}$  is negative) versus the free energy cost of forming an interface between them ( $\Delta G_{int}$ : is positive):

$$\Delta G_{cluster} = \Delta G_{bulk} + \Delta G_{int} \quad (1.2)$$

For a spherical ice cluster forming in supercooled water it can be shown that:

$$G_{int} = 4\pi r^2 \gamma \quad (1.3)$$

Where  $r$  is the cluster radius and  $\gamma$  is the interfacial energy between supercooled water and ice. It can also be shown that for the same spherical cluster:

$$G_{bulk} = \frac{4\pi r^3}{3v} k_b T \ln S \quad (1.4)$$

Where  $v$  is the volume of a water molecule, and  $S$  is the supersaturation of supercooled water and ice. Clearly, the terms  $\Delta G_{bulk}$  and  $\Delta G_{int}$  scale with the square and cube of the cluster radius respectively which means that when increasing  $r$  from zero  $\Delta G^*_{cluster}$  is initially positive but reaches a maximum and decreases when the  $\Delta G_{bulk}$  term starts to win out. This value of  $r$  when  $\Delta G^*_{cluster}$  reaches a maximum (i.e.,  $d\Delta G_{cluster} / dr = 0$ ) corresponds to the critical cluster radius  $r^*$ . It can therefore be shown that:

$$r^* = \frac{2v\gamma}{k_b \ln S} \quad (1.5)$$

When this equation for  $r^*$  is combined with equations (1.3) and (1.4) this enables us to calculate a value for the free energy barrier for formation of a critical cluster which can be inserted into equation (1.1) to calculate  $J_{hom}$ :

$$\Delta G^*_{cluster} = \frac{16\pi\gamma^3 v^2}{3(k_b T \ln S)^2} \quad (1.6)$$

This relationship is illustrated in Fig 1.1.

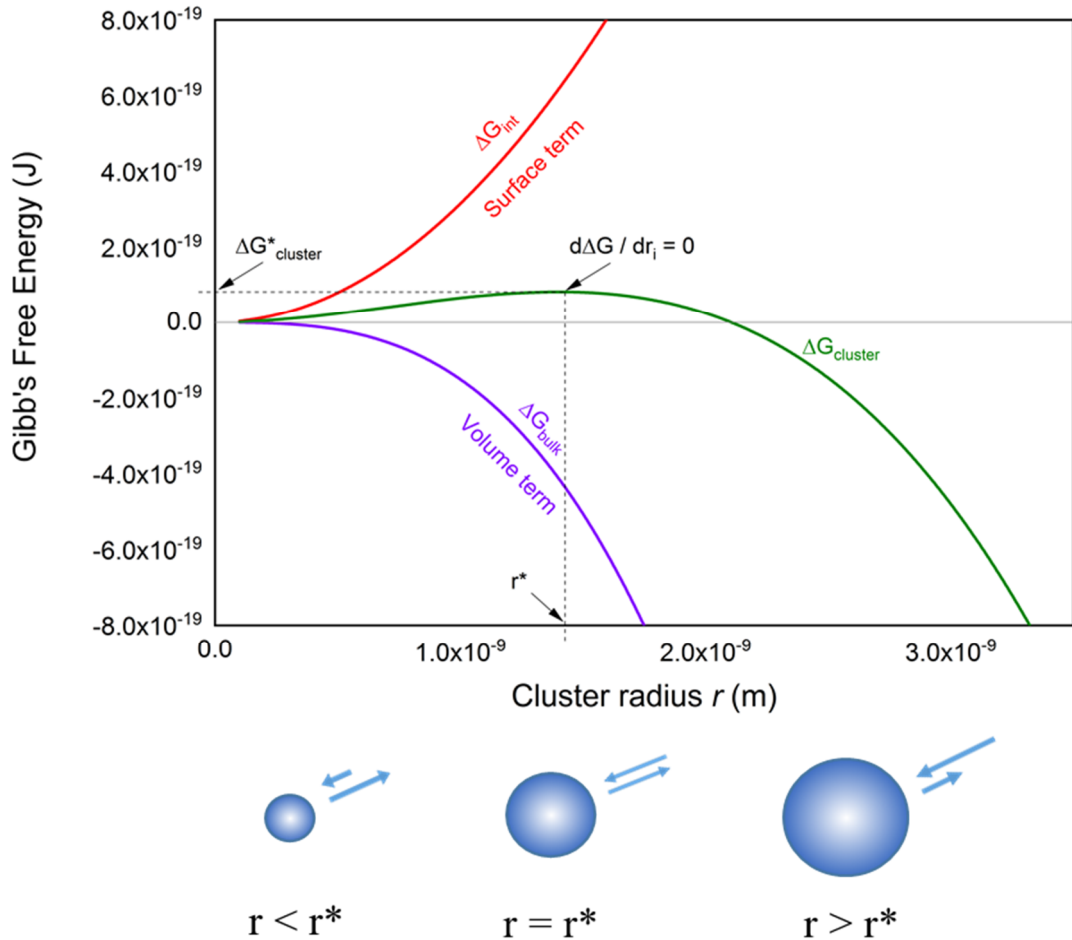


**Figure 1.1 Illustration of critical cluster size ( $r^*$ ) resulting from competing volume (purple) and interface (red) terms according to Classical Nucleation Theory. Droplets below represent thermodynamically driven likelihoods for droplets at and either side of critical radius to shrink or grow. Blue arrows represent addition or loss of water molecules.**

### 1.1.1.2 Heterogeneous Nucleation

Heterogeneous nucleation occurs if the free energy barrier for critical cluster formation  $\Delta G^*_{\text{cluster}}$  can be lowered by the presence of a surface (Pruppacher and Klett, 1997). Within the framework of CNT this process is often conceptualised as spherical cap-shaped cluster forming on the nucleating surface, akin to a water droplet sitting on a surface. As this ‘costs’ less interfacial energy ( $\Delta G_{\text{int}}$ ) compared with a spherical cluster of equal radius, this means  $\Delta G^*_{\text{cluster}}$  is lowered (Fig. 1.2). The heterogeneous nucleation rate  $J_{\text{het}}$  is therefore analogous to the homogeneous nucleation rate in equation (1.1):

$$J_{het} = A \exp\left(-\frac{\Delta G^*_{cluster} \varphi}{k_b T}\right) \quad (1.7)$$

But, with the addition of  $\varphi$  which is simply a factor of between 0 and 1 applied to  $\Delta G^*_{cluster}$ , this reduces the barrier, increases  $J_{het}$  and therefore the probability of freezing at a given temperature. The contact angle between the cluster and the nucleating surface,  $\theta$ , is used to calculate  $\varphi$  using the equation:

$$\varphi = \frac{1}{4}((2 + \cos\theta)(1 - \cos\theta)^2) \quad (1.8)$$

It follows that very efficient nucleating material would produce clusters with contact angles approaching  $180^\circ$  while materials with no ice-nucleating ability approaching  $0^\circ$  (effectively a spherical cluster undergoing homogeneous nucleation), akin to water droplets sitting on very hydrophilic and hydrophobic surfaces respectively (Fig. 1.2b-d). The spherical cap nucleus model is unlikely to be an exact physical representation of heterogeneous nucleation processes. However, using observations of  $J_{het}$  from freezing experiments, contact angles can be derived and used to describe the efficiency of an ice-nucleating surface or material (Marcolli et al., 2007; Welti et al., 2009). In reality, the actual substances that nucleate ice have complex surfaces with a diversity of sites, each having their own nucleation rates. Approaches to describing the heterogeneous ice-nucleating abilities of materials are outlined later in this Chapter in Section 1.2.

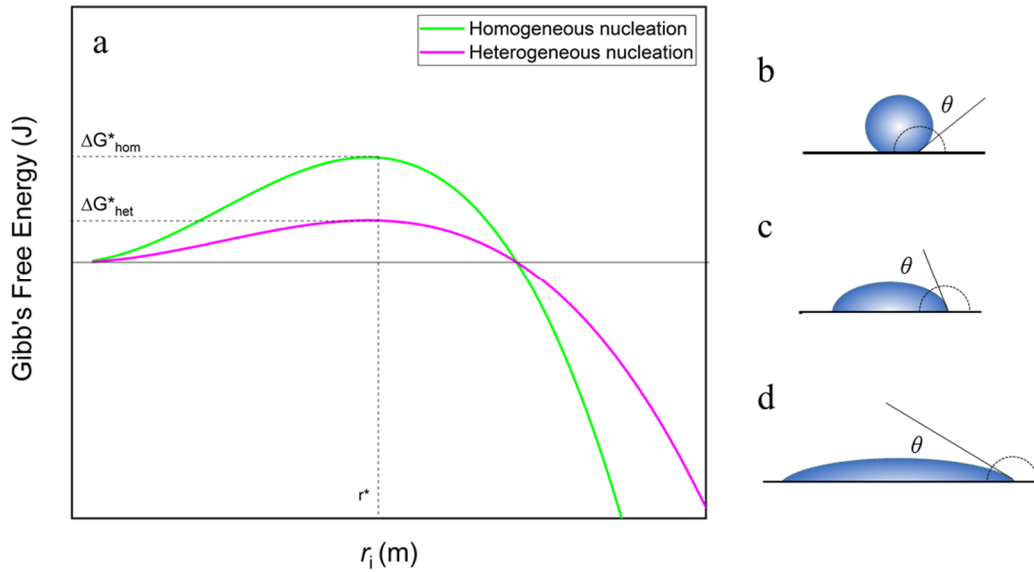


**Figure 1.2: Illustration of heterogeneous nucleation according to Classical Nucleation Theory. a) Gibb's Free Energy barriers for clusters forming via**

**homogeneous and heterogeneous nucleation. b)-d): Contact angle concept used to describe reduction of nucleation energy barrier. Poor ice nucleator b) has large contact angle  $\theta$  and nucleus is almost spherical; good ice nucleator d) has small contact angle  $\theta$  and is almost flat surface.**

### 1.1.2 Modes of Heterogeneous Ice-Nucleation

Heterogeneous ice-nucleation occurs via different pathways depending on how the nucleating surface interacts with water (Fig. 1.3). The two principal modes of heterogeneous ice-nucleation are immersion freezing and deposition freezing where ice nucleates from the supercooled liquid or supersaturated vapour phases respectively (Vali et al., 2015). As such, immersion nucleation events are measured only as a function of temperature, while both temperature and relative humidity (with respect to ice) must be taken into account to determine supersaturation with respect to ice for deposition mode nucleation. In cryobiological systems immersion freezing is the only IN mode of relevance. However, in clouds ice nucleation occurs via both type of pathways with immersion being most relevant to mixed-phase clouds at temperatures below homogeneous freezing temperatures (Ansmann et al., 2008) and deposition being important for cirrus cloud formation (Cziczo et al., 2013). Freezing of supercooled liquid clouds droplets in the heterogeneous mode is triggered by ice-nucleating particles (INP) and is proposed to occur via two pathways (Vali et al., 2015):

- 1 Immersion freezing: Droplet containing INP becomes supercooled and subsequently nucleates
- 2 Contact freezing: External INP encounters supercooled droplet and immediately triggers nucleation

Deposition nucleation has often been seen as occurring in the absence of any liquid phase, where nucleation occurs at a favourable site on the ice-nucleating substrate followed by crystal growth via diffusion of ice-supersaturated water vapour. An alternative mechanism has been proposed involving an initial stage where supercooled liquid water forms in pores or cracks in conditions subsaturated with respect to liquid water via capillary condensation, followed by homogeneous or heterogeneous nucleation of ice (Christenson, 2013; Marcolli, 2014).

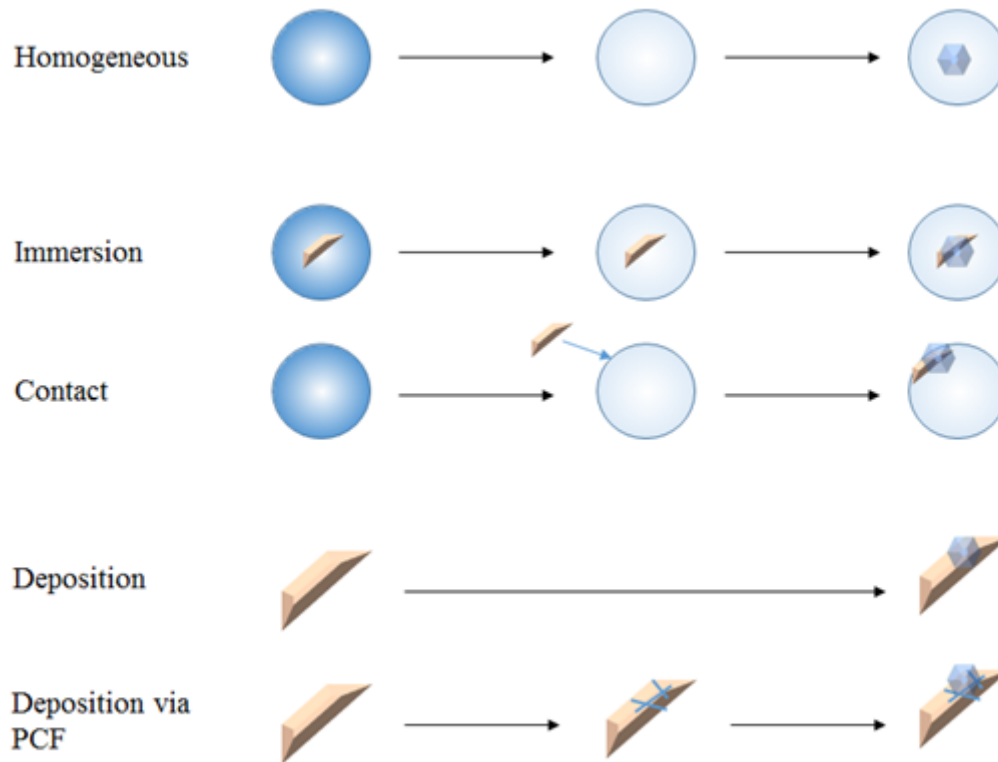


**Figure 1.3: Illustration of modes of ice-nucleation. Water droplets are cooled left to right, dark blue represents water above freezing, pale blue represents supercooled water. PCF = pore condensation and freezing.**

### 1.1.3 Relationship of freezing temperature of ‘pure’ water droplets with volume

Droplets or aliquots of water become more likely to supercool with reducing volume because the chance of heterogeneous ice-nucleating sites being present on impurities or its container wall reduces (Bigg, 1953; Morris and Acton, 2013). The amount of supercooling is, therefore, mostly controlled by both the presence and potency of heterogeneous ice-nucleating sites. If, however, the droplet and container were ‘clean’ enough to contain no heterogeneous ice-nucleating sites then in theory freezing would occur via homogeneous ice-nucleation at temperatures predicted by CNT which varies with droplet volume. This is illustrated with a CNT based parameterisation from Koop and Murray (2016) plotted in Fig 1.4. In practice, however, droplets of ‘pure’ water freeze at temperatures higher than predicted by CNT (Polen et al., 2018). This instead indicates freezing due to heterogeneous IN. Literature data for observed freezing

temperatures 'pure' water aliquots of various volumes are plotted in Fig. 1.4 and illustrate the characteristic behaviour of uncontrolled ice-nucleation of purified water droplets. Although this trend is purely empirical, it is notable that it encompasses data from a wide range of droplet formats (multiwell plates, sessile droplets, vials, water-oil emulsions) and container materials (glass, plastics). It shows that freezing temperatures start to deviate from homogeneous ice-nucleation into a heterogeneous ice-nucleation regime for droplet sizes above around a nanolitre and with a consistent range of around 10°C for any given volume. The spread in freezing temperatures at any given volume illustrates the 'randomness' of freezing temperatures seen that is often termed 'stochastic', akin to that associated with homogeneous IN. However, at temperatures warmer than the homogeneous IN regime this randomness is partly controlled by the distribution and potency of heterogeneous IN sites rather than it being truly stochastic.

Uncontrolled IN is major hurdle in cryopreservation due to small volumes of liquid and cleanliness and sterility requirements involved (Hunt, 2019; Morris and Acton, 2013). Firstly, large degrees of supercooling are likely to occur due to clean and sterile conditions employed in biological applications which minimise the impurities acting as heterogeneous ice-nucleating sites – this becoming more severe with smaller aliquot volumes. Secondly, even with standardised and cleaned containers some 'randomness' in freezing temperatures is seemingly unavoidable.

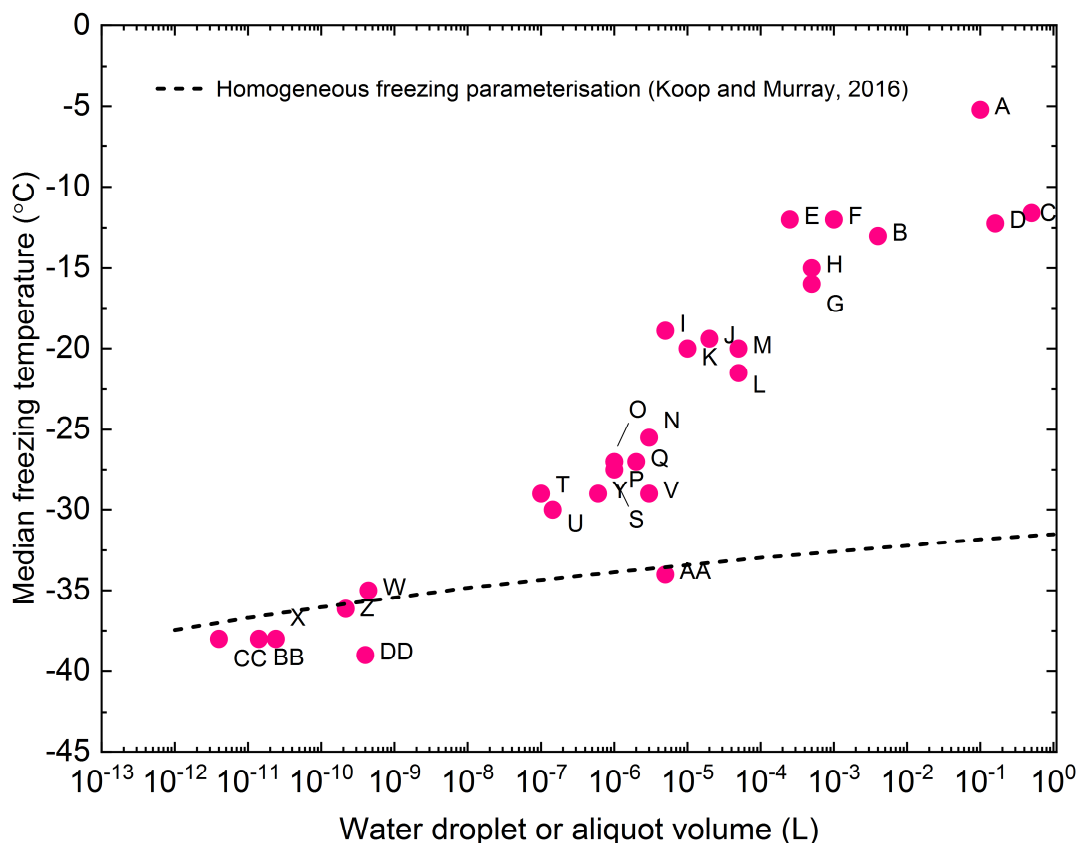


**Figure 1.4: Empirical relationship between droplet volume and median freezing temperature for supercooled water aliquots - values taken from literature. Homogeneous freezing parameterisation is shown for comparison illustrating modest volume dependence on freezing temperature. References: A: Widehem and Cochet (2003), B: Dorsey (1948), C: (Inada et al.), D: Kobayashi et al. (2018). E: Morris and Acton (2013). F: Wragg et al. (2020), G: Jiang et al. (2021), H: Jiang et al. (2021), I: Desnos et al. (2018), J: (2020), K: Du et al. (2017), L: Gong et al. (2020), M: Harrison et al. (2018), N: Kunert et al. (2018), O:Whale et al. (2015), P:Yadav et al. (2019), Q:Chong et al. (2019), S: Polen et al. (2018), T: Polen et al. (2018), U: Hader et al. (2014), V: Kunert et al. (2018), W: Tarn et al. (2018), X:Weng et al. (2016), Y: Irish et al. (2017), Z: Peckhaus et al. (2016), AA: Tobo (2016), BB: Zolles et al. (2015), CC: Kunert et al. (2018), DD: Hader et al. (2014)**

## References

- Ansmann, A., Tesche, M., Althausen, D., Müller, D., Seifert, P., Freudenthaler, V., Heese, B., Wiegner, M., Pisani, G., Knippertz, P., and Dubovik, O.: Influence of Saharan dust on cloud glaciation in southern Morocco during the Saharan Mineral Dust Experiment, *Journal of Geophysical Research: Atmospheres*, 113, 2008.
- Atkinson, J. D., Murray, B. J., and O'Sullivan, D.: Rate of Homogenous Nucleation of Ice in Supercooled Water, *The Journal of Physical Chemistry A*, 120, 6513-6520, 2016.
- Bigg, E. K.: The Supercooling of Water, *Proceedings of the Physical Society. Section B*, 66, 688-694, 1953.
- Bogler, S. and Borduas-Dedekind, N.: Lignin's ability to nucleate ice via immersion freezing and its stability towards physicochemical treatments and atmospheric processing, *Atmos. Chem. Phys.*, 20, 14509-14522, 2020.
- Chong, E., King, M., Marak, K. E., and Freedman, M. A.: The Effect of Crystallinity and Crystal Structure on the Immersion Freezing of Alumina, *J Phys Chem A*, 123, 2447-2456, 2019.
- Christenson, H. K.: Two-step crystal nucleation via capillary condensation, *CrystEngComm*, 15, 2030-2039, 2013.
- Clarke, A., Morris, G. J., Fonseca, F., Murray, B. J., Acton, E., and Price, H. C.: A Low Temperature Limit for Life on Earth, *PLOS ONE*, 8, e66207, 2013.
- Cziczo, D. J., Froyd, K. D., Hoose, C., Jensen, E. J., Diao, M., Zondlo, M. A., Smith, J. B., Twohy, C. H., and Murphy, D. M.: Clarifying the Dominant Sources and Mechanisms of Cirrus Cloud Formation, *Science*, 340, 1320-1324, 2013.
- Desnos, H., Baudot, A., Teixeira, M., Louis, G., Commin, L., Buff, S., and Bruyère, P.: Ice induction in DSC experiments with Snomax®, *Thermochimica Acta*, 667, 193-206, 2018.
- Dorsey, N. E.: The Freezing of Supercooled Water, *Transactions of the American Philosophical Society*, 38, 247-328, 1948.
- Du, R., Du, P., Lu, Z., Ren, W., Liang, Z., Qin, S., Li, Z., Wang, Y., and Fu, P.: Evidence for a missing source of efficient ice nuclei, *Sci Rep*, 7, 39673, 2017.
- Fan, J., Leung, L. R., Rosenfeld, D., and DeMott, P. J.: Effects of cloud condensation nuclei and ice nucleating particles on precipitation processes and supercooled liquid in mixed-phase orographic clouds, *Atmos. Chem. Phys.*, 17, 1017-1035, 2017.
- Gong, X., Wex, H., van Pinxteren, M., Triesch, N., Fomba, K. W., Lubitz, J., Stolle, C., Robinson, T. B., Müller, T., Herrmann, H., and Stratmann, F.: Characterization of aerosol particles at Cabo Verde close to sea level and at the cloud level – Part 2: Ice-nucleating particles in air, cloud and seawater, *Atmos. Chem. Phys.*, 20, 1451-1468, 2020.
- Hader, J. D., Wright, T. P., and Petters, M. D.: Contribution of pollen to atmospheric ice nuclei concentrations, *Atmos. Chem. Phys.*, 14, 5433-5449, 2014.

Hansen, T. C.: The everlasting hunt for new ice phases, *Nature Communications*, 12, 3161, 2021.

Harrison, A. D., Whale, T. F., Rutledge, R., Lamb, S., Tarn, M. D., Porter, G. C. E., Adams, M. P., McQuaid, J. B., Morris, G. J., and Murray, B. J.: An instrument for quantifying heterogeneous ice nucleation in multiwell plates using infrared emissions to detect freezing, *Atmos. Meas. Tech.*, 11, 5629-5641, 2018.

Herbert, R. J., Murray, B. J., Dobbie, S. J., and Koop, T.: Sensitivity of liquid clouds to homogenous freezing parameterizations, *Geophysical Research Letters*, 42, 1599-1605, 2015.

Huang, J. and Bartell, L. S.: Kinetics of Homogeneous Nucleation in the Freezing of Large Water Clusters, *The Journal of Physical Chemistry*, 99, 3924-3931, 1995.

Hunt, C. J.: Technical Considerations in the Freezing, Low-Temperature Storage and Thawing of Stem Cells for Cellular Therapies, *Transfusion Medicine and Hemotherapy*, 46, 134-150, 2019.

Ickes, L., Welti, A., Hoose, C., and Lohmann, U.: Classical nucleation theory of homogeneous freezing of water: thermodynamic and kinetic parameters, *Phys Chem Chem Phys*, 17, 5514-5537, 2015.

Inada, T., Zhang, X., Yabe, A., and Kozawa, Y.: Active control of phase change from supercooled water to ice by ultrasonic vibration 1. Control of freezing temperature, *International Journal of Heat and Mass Transfer*, 44, 4523-4531, 2001.

Irish, V. E., Elizondo, P., Chen, J., Chou, C., Charette, J., Lizotte, M., Ladino, L. A., Wilson, T. W., Gosselin, M., Murray, B. J., Polishchuk, E., Abbatt, J. P. D., Miller, L. A., and Bertram, A. K.: Ice-nucleating particles in Canadian Arctic sea-surface microlayer and bulk seawater, *Atmos. Chem. Phys.*, 17, 10583-10595, 2017.

Jiang, B., Li, W., Stewart, S., Ou, W., Liu, B., Comizzoli, P., and He, X.: Sand-mediated ice seeding enables serum-free low-cryoprotectant cryopreservation of human induced pluripotent stem cells, *Bioactive Materials*, 6, 4377-4388, 2021.

Kanji, Z. A., Ladino, L. A., Wex, H., Boose, Y., Burkert-Kohn, M., Cziczo, D. J., and Krämer, M.: Overview of Ice Nucleating Particles, *Meteorological Monographs*, 58, 1.1-1.33, 2017.

Kobayashi, A., Horikawa, M., Kirschvink, J. L., and Golash, H. N.: Magnetic control of heterogeneous ice nucleation with nanophase magnetite: Biophysical and agricultural implications, *Proceedings of the National Academy of Sciences*, 115, 5383, 2018.

Koop, T., Luo, B., Tsias, A., and Peter, T.: Water activity as the determinant for homogeneous ice nucleation in aqueous solutions, *Nature*, 406, 611-614, 2000.

Koop, T. and Murray, B. J.: A physically constrained classical description of the homogeneous nucleation of ice in water, *The Journal of Chemical Physics*, 145, 211915, 2016.

Kunert, A. T., Lamneck, M., Helleis, F., Pöschl, U., Pöhlker, M. L., and Fröhlich-Nowoisky, J.: Twin-plate Ice Nucleation Assay (TINA) with infrared detection for high-throughput droplet freezing experiments with biological ice nuclei in laboratory and field samples, *Atmos. Meas. Tech.*, 11, 6327-6337, 2018.

- Lupi, L., Hudait, A., Peters, B., Grünwald, M., Gotchy Mullen, R., Nguyen, A. H., and Molinero, V.: Role of stacking disorder in ice nucleation, *Nature*, 551, 218-222, 2017.
- Maeda, N.: Brief Overview of Ice Nucleation, *Molecules*, 26, 2021.
- Malkin, T. L., Murray, B. J., Brukhno, A. V., Anwar, J., and Salzmann, C. G.: Structure of ice crystallized from supercooled water, *Proceedings of the National Academy of Sciences*, 109, 1041, 2012.
- Malkin, T. L., Murray, B. J., Salzmann, C. G., Molinero, V., Pickering, S. J., and Whale, T. F.: Stacking disorder in ice I, *Physical Chemistry Chemical Physics*, 17, 60-76, 2015.
- Marcolli, C.: Deposition nucleation viewed as homogeneous or immersion freezing in pores and cavities, *Atmospheric Chemistry and Physics*, 14, 2071-2104, 2014.
- Marcolli, C., Gedamke, S., Peter, T., and Zobrist, B.: Efficiency of immersion mode ice nucleation on surrogates of mineral dust, *Atmos. Chem. Phys.*, 7, 5081-5091, 2007.
- Morris, G. J. and Acton, E.: Controlled ice nucleation in cryopreservation--a review, *Cryobiology*, 66, 85-92, 2013.
- Murray, B. J., Broadley, S. L., Wilson, T. W., Bull, S. J., Wills, R. H., Christenson, H. K., and Murray, E. J.: Kinetics of the homogeneous freezing of water, *Physical Chemistry Chemical Physics*, 12, 10380-10387, 2010.
- Murray, B. J., Knopf, D. A., and Bertram, A. K.: The formation of cubic ice under conditions relevant to Earth's atmosphere, *Nature*, 434, 202-205, 2005.
- Murray, B. J., O'Sullivan, D., Atkinson, J. D., and Webb, M. E.: Ice nucleation by particles immersed in supercooled cloud droplets, *Chem Soc Rev*, 41, 6519-6554, 2012.
- Peckhaus, A., Kiselev, A., Hiron, T., Ebert, M., and Leisner, T.: A comparative study of K-rich and Na/Ca-rich feldspar ice-nucleating particles in a nanoliter droplet freezing assay, *Atmospheric Chemistry and Physics*, 16, 11477-11496, 2016.
- Polen, M., Brubaker, T., Somers, J., and Sullivan, R. C.: Cleaning up our water: reducing interferences from nonhomogeneous freezing of "pure" water in droplet freezing assays of ice-nucleating particles, *Atmos. Meas. Tech.*, 11, 5315-5334, 2018.
- Pruppacher, H. R. and Klett, J. D.: *Microphysics of Clouds and Precipitation*, Springer Netherlands, 1997.
- Riikonen, M., Sillanpää, M., Virta, L., Sullivan, D., Moilanen, J., and Luukkonen, I.: Halo observations provide evidence of airborne cubic ice in the Earth's atmosphere, *Appl. Opt.*, 39, 6080-6085, 2000.
- Salzmann, C. G., Radaelli, P. G., Slater, B., and Finney, J. L.: The polymorphism of ice: five unresolved questions, *Physical Chemistry Chemical Physics*, 13, 18468-18480, 2011.

Tarn, M. D., Sikora, S. N. F., Porter, G. C. E., O'Sullivan, D., Adams, M., Whale, T. F., Harrison, A. D., Vergara-Temprado, J., Wilson, T. W., Shim, J.-u., and Murray, B. J.: The study of atmospheric ice-nucleating particles via microfluidically generated droplets, *Microfluidics and Nanofluidics*, 22, 52, 2018.

Tarn, M. D., Sikora, S. N. F., Porter, G. C. E., Shim, J.-u., and Murray, B. J.: Homogeneous Freezing of Water Using Microfluidics, *Micromachines*, 12, 2021.

Tobo, Y.: An improved approach for measuring immersion freezing in large droplets over a wide temperature range, *Scientific Reports*, 6, 32930, 2016.

Vali, G.: Freezing Rate Due to Heterogeneous Nucleation, *Journal of Atmospheric Sciences*, 51, 1843-1856, 1994.

Vali, G., DeMott, P. J., Möhler, O., and Whale, T. F.: Technical Note: A proposal for ice nucleation terminology, *Atmos. Chem. Phys.*, 15, 10263-10270, 2015.

Welti, A., Lüönd, F., Stetzer, O., and Lohmann, U.: Influence of particle size on the ice nucleating ability of mineral dusts, *Atmos. Chem. Phys.*, 9, 6705-6715, 2009.

Weng, L., Tessier, S. N., Smith, K., Edd, J. F., Stott, S. L., and Toner, M.: Bacterial Ice Nucleation in Monodisperse D<sub>2</sub>O and H<sub>2</sub>O-in-Oil Emulsions, *Langmuir*, 32, 9229-9236, 2016.

Whale, T. F., Murray, B. J., O'Sullivan, D., Wilson, T. W., Umo, N. S., Baustian, K. J., Atkinson, J. D., Workneh, D. A., and Morris, G. J.: A technique for quantifying heterogeneous ice nucleation in microlitre supercooled water droplets, *Atmos. Meas. Tech.*, 8, 2437-2447, 2015.

Widehem, P. and Cochet, N.: *Pseudomonas syringae* as an ice nucleator—application to freeze-concentration, *Process Biochemistry*, 39, 405-410, 2003.

Wragg, N. M., Tampakis, D., and Stolzing, A.: Cryopreservation of Mesenchymal Stem Cells Using Medical Grade Ice Nucleation Inducer, *International Journal of Molecular Sciences*, 21, 2020.

Yadav, S., Venezia, R. E., Paerl, R. W., and Petters, M. D.: Characterization of Ice-Nucleating Particles Over Northern India, *Journal of Geophysical Research: Atmospheres*, 124, 10467-10482, 2019.

Zolles, T., Burkart, J., Hausler, T., Pummer, B., Hitzenberger, R., and Grothe, H.: Identification of ice nucleation active sites on feldspar dust particles, *J Phys Chem A*, 119, 2692-2700, 2015.

## 1.2 Measurement of ice-nucleating materials in immersion mode

### 1.2.1 Experimental methods

Many different substances act as heterogeneous ice-nucleators with a wide variety of relative ice nucleating abilities (INA) (Kanji et al., 2017; Murray et al., 2012). For the INA of a particular substance or sample to be characterised in a standardised way it must be normalised to an attribute of the substance being tested, such as surface area data. There are a range of techniques for quantifying materials' heterogeneous ice-nucleating ability, generally suitable for testing both 'pure' materials and natural variable materials such as atmospheric aerosol. These can be divided into two broad classes of techniques – wet-dispersion and dry-dispersion – which refer to how the particles enter the instrument before being immersed in a water droplet that is subsequently supercooled (DeMott et al., 2018; Hiranuma et al., 2015). Microscopy and imaging techniques, while primarily used to physically and chemically characterise the material being tested, can also be used to locate the inferred location of nucleation sites (Gurganus et al., 2011; Holden et al., 2019).

#### 1.2.1.1 Ice nucleation event detection

##### *Wet-dispersion methods*

The majority of wet-dispersion methods used in atmospheric research are based on the droplet freezing assay technique (DFA). This involves dividing an aqueous suspension containing IN material into an array of droplets of known volume which then are cooled at a prescribed rate to produce a spectrum of freezing temperatures (Miller et al., 2021; Vali, 1995; Whale et al., 2015) (e.g., Fig. 1.5). Alternatively, pure water droplets of known footprint can be deposited directly onto an IN material's surface (Sosso et al., 2018). DFAs have been used for quantifying IN for several decades and hold the advantage that they can be performed with relatively rudimentary equipment, for example an array of sessile droplets, test tubes or even petri dishes (Suzuki et al., 2017) immersed in a cooling bath. DFA set-ups can take a range of different formats droplet volumes, and methods of droplet freezing temperature detection and also ways of supporting droplets (e.g. on a substrate or immersed in oil) (Miller et al., 2021). Recently, several purpose-built instruments intended for high-throughput testing have been developed, mainly for the processing of environmental samples such as rain,

seawater and aerosol (Beall et al., 2017; David et al., 2019; Harrison et al., 2018; Kunert et al., 2018).

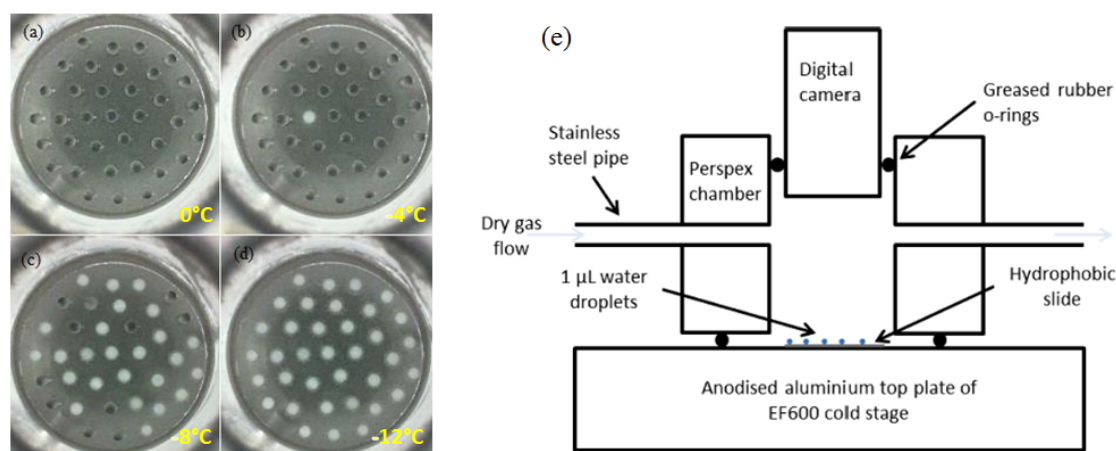


**Figure 1.5: Droplet freezing assay demonstration. a)-d) Glass slide with microlitre droplet array at various stages of freezing assay on  $\mu\text{L-NIPI}$  apparatus (Whale et al., 2015). Droplets appear dark while liquid (supercooled) and turn bright upon nucleation and freezing. Field of view is approximately 3cm. e) Schematic of the  $\mu\text{L-NIPI}$  set-up, diagram taken from (Whale et al., 2015). EF600 refers to model number of cold stage.**

Larger droplets approaching mL-size contain more suspended particles compared with smaller ones and therefore are more likely to contain and detect rare but very active sites. These are, however, more difficult to keep free of contamination which limits their use in DFAs to warmer ( $> -20^\circ\text{C}$ ) temperature ranges (Polen et al., 2018). Smaller droplets in the nL and pL range, meanwhile, are more readily cooled to temperatures approaching homogeneous IN meaning lower temperature active sites can be resolved (Reicher et al., 2018; Tarn et al., 2018). Therefore, when arrays of differing droplet size regime are used in combination then the full range of ice-nucleating sites above homogeneous freezing temperatures for a substance can be accessed.

In DFAs the freezing temperature of droplets are recorded by detecting the moment of IN and logging the temperature at which this occurs. This event may be detected visually from a change in droplet appearance captured by a video recording (Creamean et al., 2018; Hill et al., 2014; Whale et al., 2015), with some instruments capable doing this automatically (Budke and Koop, 2015; David et al., 2019; Stopelli et al., 2014). Alternatively, sudden temperature increases driven by latent heat release can be used

to detect ice-nucleation, for example captured by infra-red camera (Harrison et al., 2018; Zaragotas et al., 2016). Thermocouples placed directly into suspensions have also been used to record for very large volume assays, although these risk artificially triggering IN (Kobayashi et al., 2018).

Methods for supporting and immobilising droplets are either based on placing droplets on a clean hydrophobic substrate or by emulsifying them inside an immiscible oil phase. Substrates for droplets include hydrophobic glass slides (Whale et al., 2015), a petroleum jelly coated surface (Tobo, 2016), multiwell plates (Harrison et al., 2018; Hill et al., 2014) or even directly on hydrophobic filters with aerosol samples (Price et al., 2018). Sessile droplet methods may suffer from droplet evaporation and raised backgrounds due to ice-nuclei being introduced by airborne contaminants or by the substrate itself. Emulsions of suspension droplets in oil stabilised by a surfactant (Pummer et al., 2012; Wright and Petters, 2013) are relatively simple to produce although may produce a polydisperse size distribution of droplets. Microfluidic chip devices produce pL-sized monodisperse droplets and set-ups which can sort or even allow individual droplets to be chemically analysed based on their freezing temperature have recently been developed (Reicher et al., 2018; Tarn et al., 2018; Tarn et al., 2020).

### *Dry dispersion*

Dry-dispersion methods for measuring immersion mode IN involve detection of the freezing of droplets that are suspended in air (or any carrier gas) rather than immobilised on a substrate (DeMott et al., 2018; Murray et al., 2012). Samples (ambient aerosol or aerosolised dust) are introduced to the instrument in dry form and then activated as droplets by manipulating the internal temperature and/or humidity. These droplets may then freeze depending on the INA of the sample and the ice particles are then counted on account of their large size compared to condensed water droplets. Two general classes of instrument are popularly used, these based on how droplets are activated. There are closed system expansion type chambers which activate particles by depressurisation leading to adiabatic cooling and increased relative humidity (e.g. AIDA, (Niemand et al., 2012), PINE (Möhler et al., 2021)) Then there are open systems, such as Continuous Flow Diffusion Chambers, which have a continuous flow of sample through regions of supersaturated relative humidity

created by, for example, ice-coated surfaces maintained at different temperature (Garimella et al., 2016; Kanji et al., 2013). There are two main advantages of dry methods over wet methods: firstly, they more accurately represent the processes by which ice-nucleation by particles occurs in a cloud and secondly, they can provide real-time or ‘online’ measurements of the INA of particles sampled in ambient air. They are, however, more complex and expensive compared to DFAs, although portable dry dispersion instruments have recently been deployed on field campaigns (Barry et al., 2021; Brasseur et al., 2021).

### *Imaging*

Micro-imaging techniques have recently been used to infer the location of ice-nucleation events on mineral surfaces by observing the appearance of ice crystals. For example, Kiselev et al. (2017) and Pach and Verdaguer (2019) both used a humidity and temperature-controlled scanning electron microscope (SEM) to observe both where on the surfaces of feldspar particles ice-crystals first appeared and the microscale surface features associated with them. High-speed video optical microscopy can be used to observe the location of origin of ice growth within a water droplet placed on a polished mineral section and cooled (Holden et al., 2019).

#### ***1.2.1.2 Surface area measurement***

As heterogeneous IN is a surface mediated process the surface area of a material needs to be known in order to quantify its INA on a surface area basis. Where macroscopic amounts (several g to kgs) of the material are available then the specific surface area (SSA,  $\text{m}^2\text{g}^{-1}$ ) can be directly measured using the Brunauer-Emmet-Teller (BET)  $\text{N}_2$  gas absorption method. This method has been widely used for determining the INA of ground mineral powders and also natural soil and desert dust samples (Atkinson et al., 2013; O’Sullivan et al., 2014; Paramonov et al., 2018). If however, for example in the case of ambient aerosol, the amounts of material are too small to measure by BET then surface area can be calculated from aerosol particle size distribution (PSD) measurements or by visual analysis of collected particles on, for example a filter, by SEM (Sanchez-Marroquin et al., 2019). These methods both tend to result in lower estimates of SSA than for the BET method (Broadley et al., 2012; Hiranuma et al., 2019) as they assume spherical particle geometry and neglect particle roughness or non-spherical particles such as clay minerals.

## 1.2.2 Quantitative description of immersion mode heterogeneous ice-nucleation

Early studies that surveyed the ice-nucleating abilities of minerals typically used onset temperatures – the warmest temperature at which freezing was seen – to characterise their relative IN abilities (Mason and Maybank, 1958). However, there was little agreement in results across different studies which utilised different techniques. Since then, the field has developed enable how potent a material is as an ice nucleator to be described in ways that are standardised and repeatable across different instruments. Ultimately the goal is to be able to predict at what temperature ice nucleation will occur in the presence of a particular material, however as natural materials are complex it is a case of finding best approach that fits experimental data.

### 1.2.2.1 Theoretical framework (*Stochastic and Singular models*)

There are two theoretical approaches for quantifying heterogeneous ice-nucleation: the stochastic approach and the singular approach (Kanji et al., 2017; Murray et al., 2012). The stochastic approach is based on CNT and has a time-dependent probabilistic approach. In its simplest form it assumes that an ice-nucleator surface possesses at a given temperature a single nucleation rate throughout (equation 1.7) with a characteristic contact angle which controls the nucleation rate (Murray et al., 2011). Under this condition an array of droplets containing uniform surface area of ice-nucleator held at a constant temperature would freeze with an exponential ‘decay’ rate. However, experiments have shown this behaviour is rare even with ‘pure’ mineral samples which suggests that natural materials acting as ice-nucleators are typically too heterogeneous for this approach (Broadley et al., 2012). As such, a number of multicomponent stochastic models have been proposed where the surfaces of an ice-nucleator exhibit a multitude of different nucleation rates (and thus contact angles) instead and the probabilities are summed up (Niedermeier et al., 2011). There are adaptations of this approach where IN particles possess facets with a number of discrete contact angles akin to the panels of a soccer ball (Niedermeier et al., 2011; Peckhaus et al., 2016) or a continuum of contact angles (Beydoun et al., 2017).

The singular or active site approach is an alternative, deterministic way of describing heterogeneous IN which neglects the stochasticity and therefore time dependence. Instead, the ice-nucleating material’s surface possesses a distribution of singular sites which instantly become active at a characteristic temperature with the implication that

cooling rate makes no difference (Vali, 2008; Vali and Stansbury, 1966). Therefore, under this framework the variation in droplet freezing temperatures seen in a DFA arises purely from the spectrum of sites present within the ice-nucleator rather than any stochasticity. In practice, the time (and cooling rate) dependence is non-negligible, and a Modified Singular Description has been proposed (Herbert et al., 2014) that factors in the dependence of freezing temperatures on cooling rates, although this is based on applying an empirically derived parameter unique to each nucleating material. Overall, the singular approach has advantages in terms of its simplicity for being implemented in model parameterisations representing IN in the atmosphere compared with the multicomponent stochastic methods. However, they may not be as accurate in situations with very low cooling rates where a minor stochastic component may become non-negligible.

### ***1.2.2.2 Active site density derivation from experimental data.***

Here we describe how data from droplet freezing assays (DFAs) can be used to quantify the INA of materials using the singular (active site) approach. From DFAs can easily be derived the spectra for fraction of droplets frozen ( $f_{ice}$ ) as a function of temperature ( $T$ ):

$$f_{ice}(T) = \frac{n_{ice}(T)}{n_{total}} \quad (1.9)$$

where  $n_{ice}(T)$  is the number of droplets frozen at temperature  $T$  and  $n_{total}$  is the total number of droplets. Fraction frozen curves from separate freezing runs can be compared using the median  $f_{ice}$  value (or any other percentile), commonly denoted as  $T_{50}$ . These are useful for simple comparison between runs, but they do not take into account factors such as droplet size and nucleant concentration and so are dependent on the method used, rather than being intrinsic to the substance being tested. Instead, the cumulative active sites per unit volume of water (or active site density) at a given temperature,  $K(T)$ , can be calculated (Vali, 1971). This assumes the droplets containing ice-nucleating material freeze at a characteristic temperature and do so independent of cooling rate:

$$K(T) = \frac{-\ln(1-f_{ice}(T))}{V} \quad (1.10)$$

where  $V$  is the volume of water per droplet in mL. With knowledge of the mass, surface area or particle density of material present in the water,  $K(T)$  spectra can be adapted

to derive normalised values that are intrinsic to the ice-nucleating substance. For example, active site density per unit mass,  $n_m(T)$ , can be calculated with knowledge of mass of material per droplet,  $M$  (kg):

$$n_m(T) = \frac{-\ln(1-f_{ice}(T))}{M} \quad (1.11)$$

Active site density per unit surface area,  $n_s(T)$ , can be calculated with knowledge of surface area per droplet,  $S$  ( $\text{m}^2\text{g}^{-1}$ ):

$$n_s(T) = \frac{-\ln(1-f_{ice}(T))}{S} \quad (1.12)$$

Surface area data can be obtained from experimentally derived specific surface area measurements using BET gas absorption or estimated from particle size data. Active site density per particle number,  $n_n(T)$ , can be calculated from number of particles,  $N$ , per droplet:

$$n_n(T) = \frac{-\ln(1-f_{ice}(T))}{N} \quad (1.13)$$

Which type of active site density is derived depends on the nature of the ice-nucleating material. For particulate materials such as mineral dust the surface area per mass can vary greatly according to mineral type and, as such,  $n_s(T)$  is an appropriate descriptor. Materials that are soluble or have poorly defined surface areas, such as macromolecules, are described using  $n_m(T)$  while  $n_n(T)$  may be appropriate for entities such as cells and pollen grains. Measuring ice-nucleating ambient aerosols collected from the atmosphere onto filters adapts the above approaches to derive concentration of ice-nucleating particles ( $[INP]$ ,  $\text{L}^{-1}$ ) per unit volume of air sampled:

$$[INP] = K(T) \times \frac{V_{wash}}{V_{air}} \quad (1.14)$$

Where  $V_{wash}$  is the volume of water used for washing off and collecting particles from the filter and  $V_{air}$  is the volume of air sampled through the filter. If the collected INP are dominated by a single particle type (for example, in desert dust (Price et al., 2018) or volcanic ash plumes (Sanchez-Marroquin et al., 2020)) the  $n_s(T)$  values can be derived for the INP using simultaneously collected aerosol particle size distribution data.

## References

- Atkinson, J. D., Murray, B. J., Woodhouse, M. T., Whale, T. F., Baustian, K. J., Carslaw, K. S., Dobbie, S., O'Sullivan, D., and Malkin, T. L.: The importance of feldspar for ice nucleation by mineral dust in mixed-phase clouds, *Nature*, 498, 355-358, 2013.
- Barry, K. R., Hill, T. C. J., Levin, E. J. T., Twohy, C. H., Moore, K. A., Weller, Z. D., Toohey, D. W., Reeves, M., Campos, T., Geiss, R., Schill, G. P., Fischer, E. V., Kreidenweis, S. M., and DeMott, P. J.: Observations of Ice Nucleating Particles in the Free Troposphere From Western US Wildfires, *Journal of Geophysical Research: Atmospheres*, 126, e2020JD033752, 2021.
- Beall, C. M., Stokes, M. D., Hill, T. C., DeMott, P. J., DeWald, J. T., and Prather, K. A.: Automation and heat transfer characterization of immersion mode spectroscopy for analysis of ice nucleating particles, *Atmos. Meas. Tech.*, 10, 2613-2626, 2017.
- Beydoun, H., Polen, M., and Sullivan, R. C.: A new multicomponent heterogeneous ice nucleation model and its application to Snomax bacterial particles and a Snomax-illite mineral particle mixture, *Atmospheric Chemistry and Physics*, 17, 13545-13557, 2017.
- Brasseur, Z., Castarède, D., Thomson, E. S., Adams, M. P., Drossaert van Dusseldorp, S., Heikkilä, P., Korhonen, K., Lampilahti, J., Paramonov, M., Schneider, J., Vogel, F., Wu, Y., Abbat, J. P. D., Atanasova, N. S., Bamford, D. H., Bertozzi, B., Boyer, M., Brus, D., Daily, M. I., Fösig, R., Gute, E., Harrison, A. D., Hietala, P., Höhler, K., Kanji, Z. A., Keskinen, J., Lacher, L., Lampimäki, M., Levula, J., Manninen, A., Nadolny, J., Peltola, M., Porter, G. C. E., Poutanen, P., Proske, U., Schorr, T., Silas Umo, N., Stenszky, J., Virtanen, A., Moisseev, D., Kulmala, M., Murray, B. J., Petäjä, T., Möhler, O., and Duplissy, J.: Measurement report: Introduction to the HyICE-2018 campaign for measurements of ice nucleating particles in the Hyytiälä boreal forest, *Atmos. Chem. Phys. Discuss.*, 2021, 1-46, 2021.
- Broadley, S. L., Murray, B. J., Herbert, R. J., Atkinson, J. D., Dobbie, S., Malkin, T. L., Condliffe, E., and Neve, L.: Immersion mode heterogeneous ice nucleation by an illite rich powder representative of atmospheric mineral dust, *Atmos. Chem. Phys.*, 12, 287-307, 2012.
- Budke, C. and Koop, T.: BINARY: an optical freezing array for assessing temperature and time dependence of heterogeneous ice nucleation, *Atmos. Meas. Tech.*, 8, 689-703, 2015.
- Creamean, J. M., Kirpes, R. M., Pratt, K. A., Spada, N. J., Maahn, M., de Boer, G., Schnell, R. C., and China, S.: Marine and terrestrial influences on ice nucleating particles during continuous springtime measurements in an Arctic oilfield location, *Atmospheric Chemistry and Physics*, 18, 18023-18042, 2018.
- David, R. O., Cascajo-Castresana, M., Brennan, K. P., Rösch, M., Els, N., Werz, J., Weichlinger, V., Boynton, L. S., Bogler, S., Borduas-Dedekind, N., Marcolli, C., and Kanji, Z. A.: Development of the DRoplet Ice Nuclei Counter Zurich (DRINCZ): validation and application to field-collected snow samples, *Atmos. Meas. Tech.*, 12, 6865-6888, 2019.

DeMott, P. J., Möhler, O., Cziczo, D. J., Hiranuma, N., Petters, M. D., Petters, S. S., Belosi, F., Bingemer, H. G., Brooks, S. D., Budke, C., Burkert-Kohn, M., Collier, K. N., Danielczok, A., Eppers, O., Felgitsch, L., Garimella, S., Grothe, H., Herenz, P., Hill, T. C. J., Höhler, K., Kanji, Z. A., Kiselev, A., Koop, T., Kristensen, T. B., Krüger, K., Kulkarni, G., Levin, E. J. T., Murray, B. J., Nicosia, A., O'Sullivan, D., Peckhaus, A., Polen, M. J., Price, H. C., Reicher, N., Rothenberg, D. A., Rudich, Y., Santachiara, G., Schiebel, T., Schrod, J., Seifried, T. M., Stratmann, F., Sullivan, R. C., Suski, K. J., Szakáll, M., Taylor, H. P., Ullrich, R., Vergara-Temprado, J., Wagner, R., Whale, T. F., Weber, D., Welti, A., Wilson, T. W., Wolf, M. J., and Zenker, J.: The Fifth International Workshop on Ice Nucleation phase 2 (FIN-02): laboratory intercomparison of ice nucleation measurements, *Atmos. Meas. Tech.*, 11, 6231-6257, 2018.

Garimella, S., Kristensen, T. B., Ignatius, K., Welti, A., Voigtländer, J., Kulkarni, G. R., Sagan, F., Kok, G. L., Dorsey, J., Nichman, L., Rothenberg, D. A., Rösch, M., Kirchgäßner, A. C. R., Ladkin, R., Wex, H., Wilson, T. W., Ladino, L. A., Abbatt, J. P. D., Stetzer, O., Lohmann, U., Stratmann, F., and Cziczo, D. J.: The SPectrometer for Ice Nuclei (SPIN): an instrument to investigate ice nucleation, *Atmos. Meas. Tech.*, 9, 2781-2795, 2016.

Gurganus, C., Kostinski, A. B., and Shaw, R. A.: Fast Imaging of Freezing Drops: No Preference for Nucleation at the Contact Line, *The Journal of Physical Chemistry Letters*, 2, 1449-1454, 2011.

Harrison, A. D., Whale, T. F., Rutledge, R., Lamb, S., Tarn, M. D., Porter, G. C. E., Adams, M. P., McQuaid, J. B., Morris, G. J., and Murray, B. J.: An instrument for quantifying heterogeneous ice nucleation in multiwell plates using infrared emissions to detect freezing, *Atmos. Meas. Tech.*, 11, 5629-5641, 2018.

Herbert, R. J., Murray, B. J., Whale, T. F., Dobbie, S. J., and Atkinson, J. D.: Representing time-dependent freezing behaviour in immersion mode ice nucleation, *Atmospheric Chemistry and Physics*, 14, 8501-8520, 2014.

Hill, T. C. J., Moffett, B. F., Demott, P. J., Georgakopoulos, D. G., Stump, W. L., and Franc, G. D.: Measurement of ice nucleation-active bacteria on plants and in precipitation by quantitative PCR, *Applied and environmental microbiology*, 80, 1256-1267, 2014.

Hiranuma, N., Adachi, K., Bell, D. M., Belosi, F., Beydoun, H., Bhaduri, B., Bingemer, H., Budke, C., Clemen, H. C., Conen, F., Cory, K. M., Curtius, J., DeMott, P. J., Eppers, O., Grawe, S., Hartmann, S., Hoffmann, N., Höhler, K., Jantsch, E., Kiselev, A., Koop, T., Kulkarni, G., Mayer, A., Murakami, M., Murray, B. J., Nicosia, A., Petters, M. D., Piazza, M., Polen, M., Reicher, N., Rudich, Y., Saito, A., Santachiara, G., Schiebel, T., Schill, G. P., Schneider, J., Segev, L., Stopelli, E., Sullivan, R. C., Suski, K., Szakáll, M., Tajiri, T., Taylor, H., Tobo, Y., Ullrich, R., Weber, D., Wex, H., Whale, T. F., Whiteside, C. L., Yamashita, K., Zelenyuk, A., and Möhler, O.: A comprehensive characterization of ice nucleation by three different types of cellulose particles immersed in water, *Atmos. Chem. Phys.*, 19, 4823-4849, 2019.

Hiranuma, N., Augustin-Bauditz, S., Bingemer, H., Budke, C., Curtius, J., Danielczok, A., Diehl, K., Dreischmeier, K., Ebert, M., Frank, F., Hoffmann, N., Kandler, K., Kiselev, A., Koop, T., Leisner, T., Möhler, O., Nillius, B., Peckhaus,

- A., Rose, D., Weinbruch, S., Wex, H., Boose, Y., DeMott, P. J., Hader, J. D., Hill, T. C. J., Kanji, Z. A., Kulkarni, G., Levin, E. J. T., McCluskey, C. S., Murakami, M., Murray, B. J., Niedermeier, D., Petters, M. D., O'Sullivan, D., Saito, A., Schill, G. P., Tajiri, T., Tolbert, M. A., Welti, A., Whale, T. F., Wright, T. P., and Yamashita, K.: A comprehensive laboratory study on the immersion freezing behavior of illite NX particles: a comparison of 17 ice nucleation measurement techniques, *Atmos. Chem. Phys.*, 15, 2489-2518, 2015.
- Holden, M. A., Whale, T. F., Tarn, M. D., O'Sullivan, D., Walshaw, R. D., Murray, B. J., Meldrum, F. C., and Christenson, H. K.: High-speed imaging of ice nucleation in water proves the existence of active sites, *Sci Adv*, 5, eaav4316, 2019.
- Kanji, Z. A., Ladino, L. A., Wex, H., Boose, Y., Burkert-Kohn, M., Cziczo, D. J., and Krämer, M.: Overview of Ice Nucleating Particles, *Meteorological Monographs*, 58, 1.1-1.33, 2017.
- Kanji, Z. A., Welti, A., Chou, C., Stetzer, O., and Lohmann, U.: Laboratory studies of immersion and deposition mode ice nucleation of ozone aged mineral dust particles, *Atmospheric Chemistry and Physics*, 13, 9097-9118, 2013.
- Kiselev, A., Bachmann, F., Pedevilla, P., Cox, S. J., Michaelides, A., Gerthsen, D., and Leisner, T.: Active sites in heterogeneous ice nucleation-the example of K-rich feldspars, *Science*, 355, 367-371, 2017.
- Kobayashi, A., Horikawa, M., Kirschvink, J. L., and Golash, H. N.: Magnetic control of heterogeneous ice nucleation with nanophase magnetite: Biophysical and agricultural implications, *Proceedings of the National Academy of Sciences*, 115, 5383, 2018.
- Kunert, A. T., Lamneck, M., Helleis, F., Pöschl, U., Pöhlker, M. L., and Fröhlich-Nowoisky, J.: Twin-plate Ice Nucleation Assay (TINA) with infrared detection for high-throughput droplet freezing experiments with biological ice nuclei in laboratory and field samples, *Atmos. Meas. Tech.*, 11, 6327-6337, 2018.
- Mason, B. J. and Maybank, J.: Ice-nucleating properties of some natural mineral dusts, *Quarterly Journal of the Royal Meteorological Society*, 84, 235-241, 1958.
- Miller, A. J., Brennan, K. P., Mignani, C., Wieder, J., David, R. O., and Borduas-Dedekind, N.: Development of the drop Freezing Ice Nuclei Counter (FINC), intercomparison of droplet freezing techniques, and use of soluble lignin as an atmospheric ice nucleation standard, *Atmos. Meas. Tech.*, 14, 3131-3151, 2021.
- Möhler, O., Adams, M., Lacher, L., Vogel, F., Nadolny, J., Ullrich, R., Boffo, C., Pfeuffer, T., Hobl, A., Weiß, M., Vepuri, H. S. K., Hiranuma, N., and Murray, B. J.: The Portable Ice Nucleation Experiment (PINE): a new online instrument for laboratory studies and automated long-term field observations of ice-nucleating particles, *Atmos. Meas. Tech.*, 14, 1143-1166, 2021.
- Murray, B. J., Broadley, S. L., Wilson, T. W., Atkinson, J. D., and Wills, R. H.: Heterogeneous freezing of water droplets containing kaolinite particles, *Atmos. Chem. Phys.*, 11, 4191-4207, 2011.
- Murray, B. J., O'Sullivan, D., Atkinson, J. D., and Webb, M. E.: Ice nucleation by particles immersed in supercooled cloud droplets, *Chem Soc Rev*, 41, 6519-6554, 2012.

- Niedermeier, D., Shaw, R. A., Hartmann, S., Wex, H., Clauss, T., Voigtländer, J., and Stratmann, F.: Heterogeneous ice nucleation: exploring the transition from stochastic to singular freezing behavior, *Atmos. Chem. Phys.*, 11, 8767-8775, 2011.
- Niemand, M., Möhler, O., Vogel, B., Vogel, H., Hoose, C., Connolly, P., Klein, H., Bingemer, H., DeMott, P., Skrotzki, J., and Leisner, T.: A Particle-Surface-Area-Based Parameterization of Immersion Freezing on Desert Dust Particles, *Journal of the Atmospheric Sciences*, 69, 3077-3092, 2012.
- O'Sullivan, D., Murray, B. J., Malkin, T. L., Whale, T. F., Umo, N. S., Atkinson, J. D., Price, H. C., Baustian, K. J., Browse, J., and Webb, M. E.: Ice nucleation by fertile soil dusts: relative importance of mineral and biogenic components, *Atmos. Chem. Phys.*, 14, 1853-1867, 2014.
- Pach, E. and Verdaguer, A.: Pores Dominate Ice Nucleation on Feldspars, *The Journal of Physical Chemistry C*, 123, 20998-21004, 2019.
- Paramonov, M., David, R. O., Kretzschmar, R., and Kanji, Z. A.: A laboratory investigation of the ice nucleation efficiency of three types of mineral and soil dust, *Atmospheric Chemistry and Physics*, 18, 16515-16536, 2018.
- Peckhaus, A., Kiselev, A., Hiron, T., Ebert, M., and Leisner, T.: A comparative study of K-rich and Na/Ca-rich feldspar ice-nucleating particles in a nanoliter droplet freezing assay, *Atmospheric Chemistry and Physics*, 16, 11477-11496, 2016.
- Polen, M., Brubaker, T., Somers, J., and Sullivan, R. C.: Cleaning up our water: reducing interferences from nonhomogeneous freezing of “pure” water in droplet freezing assays of ice-nucleating particles, *Atmos. Meas. Tech.*, 11, 5315-5334, 2018.
- Price, H. C., Baustian, K. J., McQuaid, J. B., Blyth, A., Bower, K. N., Choulaton, T., Cotton, R. J., Cui, Z., Field, P. R., Gallagher, M., Hawker, R., Merrington, A., Miltenberger, A., Neely Iii, R. R., Parker, S. T., Rosenberg, P. D., Taylor, J. W., Trembath, J., Vergara-Temprado, J., Whale, T. F., Wilson, T. W., Young, G., and Murray, B. J.: Atmospheric Ice-Nucleating Particles in the Dusty Tropical Atlantic, *Journal of Geophysical Research: Atmospheres*, 123, 2175-2193, 2018.
- Pummer, B. G., Bauer, H., Bernardi, J., Bleicher, S., and Grothe, H.: Suspendable macromolecules are responsible for ice nucleation activity of birch and conifer pollen, *Atmos. Chem. Phys.*, 12, 2541-2550, 2012.
- Reicher, N., Segev, L., and Rudich, Y.: The Weizmann Supercooled Droplets Observation on a Microarray (WISDOM) and application for ambient dust, *Atmos. Meas. Tech.*, 11, 233-248, 2018.
- Sanchez-Marroquin, A., Arnalds, O., Baustian-Dorsi, K. J., Browse, J., Dagsson-Waldhauserova, P., Harrison, A. D., Maters, E. C., Pringle, K. J., Vergara-Temprado, J., Burke, I. T., McQuaid, J. B., Carslaw, K. S., and Murray, B. J.: Iceland is an episodic source of atmospheric ice-nucleating particles relevant for mixed-phase clouds, *Science Advances*, 6, eaba8137, 2020.
- Sanchez-Marroquin, A., Hedges, D. H. P., Hiscock, M., Parker, S. T., Rosenberg, P. D., Trembath, J., Walshaw, R., Burke, I. T., McQuaid, J. B., and Murray, B. J.: Characterisation of the filter inlet system on the FAAM BAe-146 research aircraft

and its use for size-resolved aerosol composition measurements, *Atmos. Meas. Tech.*, 12, 5741-5763, 2019.

Sosso, G. C., Whale, T. F., Holden, M. A., Pedevilla, P., Murray, B. J., and Michaelides, A.: Unravelling the origins of ice nucleation on organic crystals, *Chemical Science*, 9, 8077-8088, 2018.

Stopelli, E., Conen, F., Zimmermann, L., Alewell, C., and Morris, C. E.: Freezing nucleation apparatus puts new slant on study of biological ice nucleators in precipitation, *Atmos. Meas. Tech.*, 7, 129-134, 2014.

Suzuki, S., Fukuda, S., Fukushi, Y., and Arakawa, K.: Screening of plant resources with anti-ice nucleation activity for frost damage prevention, *Bioscience, Biotechnology, and Biochemistry*, 81, 2090-2097, 2017.

Tarn, M. D., Sikora, S. N. F., Porter, G. C. E., O'Sullivan, D., Adams, M., Whale, T. F., Harrison, A. D., Vergara-Temprado, J., Wilson, T. W., Shim, J.-u., and Murray, B. J.: The study of atmospheric ice-nucleating particles via microfluidically generated droplets, *Microfluidics and Nanofluidics*, 22, 52, 2018.

Tarn, M. D., Sikora, S. N. F., Porter, G. C. E., Wyld, B. V., Alayof, M., Reicher, N., Harrison, A. D., Rudich, Y., Shim, J.-u., and Murray, B. J.: On-chip analysis of atmospheric ice-nucleating particles in continuous flow, *Lab on a Chip*, 20, 2889-2910, 2020.

Tobo, Y.: An improved approach for measuring immersion freezing in large droplets over a wide temperature range, *Scientific Reports*, 6, 32930, 2016.

Vali, G.: Principles of Ice Nucleation. In: *Biological Ice Nucleation and its Applications*, Lee, R. E., Warren, G. J., and Gusta, L. V. (Eds.), APS Press, 1995.

Vali, G.: Quantitative Evaluation of Experimental Results on the Heterogeneous Freezing Nucleation of Supercooled Liquids, *Journal of Atmospheric Sciences*, 28, 402-409, 1971.

Vali, G.: Repeatability and randomness in heterogeneous freezing nucleation, *Atmos. Chem. Phys.*, 8, 5017-5031, 2008.

Vali, G. and Stansbury, E. J.: Time-dependent characteristics of the heterogeneous nucleation of ice, *Canadian Journal of Physics*, 44, 477, 1966.

Whale, T. F., Murray, B. J., O'Sullivan, D., Wilson, T. W., Umo, N. S., Baustian, K. J., Atkinson, J. D., Workneh, D. A., and Morris, G. J.: A technique for quantifying heterogeneous ice nucleation in microlitre supercooled water droplets, *Atmos. Meas. Tech.*, 8, 2437-2447, 2015.

Wright, T. P. and Petters, M. D.: The role of time in heterogeneous freezing nucleation, *Journal of Geophysical Research: Atmospheres*, 118, 3731-3743, 2013.

Zarogotas, D., Liolios, N. T., and Anastassopoulos, E.: Supercooling, ice nucleation and crystal growth: a systematic study in plant samples, *Cryobiology*, 72, 239-243, 2016.

## **1.3 Ice-nucleation in Cryobiology**

### **1.3.1 Introduction to cryopreservation**

Biological material, such as cells and tissues, can be cooled to cryogenic ( -100 °C and below) temperatures cold enough to enter a state of suspended animation, then thawed when desired to a viable and functional state in a process known as cryopreservation. In biological material cooled below its glass transition temperature metabolic, chemical and enzymatic activity is paused and water is effectively immobilised, thus biological activity is effectively paused (Clarke et al., 2013). This has established itself as a crucial tool in many applications since the first successful cryopreservation of mammalian sperm in 1949 (Polge et al., 1949). Gametes, (oocytes, embryos, and sperm, both human and animal) have been for many years routinely cryopreserved and recovered and used for in-vitro fertilisation (Fuller and Paynter, 2004) and cryoconservation (Glenister and Thornton, 2000). Cryopreserved animal and human cells are widely for use in biomedicine research where hepatocytes are used in-vitro for drug toxicology screening (Watson et al., 2016), as are stem cells for the emerging fields of regenerative medicine and cell therapy (Hunt, 2019; Meneghel et al., 2020). As well as serving as convenient storage for these materials, cryopreservation can prevent biological ‘drift’, preventing genetic changes that occur as cells reproduce (Steponkus et al., 1990) and reduce the demand for animals that need to be sacrificed to source the biological material (Takeo and Nakagata, 2020).

### **1.3.2 Approaches to animal cell cryopreservation**

Water makes up most of the mass in a biological system and therefore ice formation plays a crucial role in any cryopreservation process because the material must take a journey below and back again above water’s melting point. Ice formation, either inside cells or outside in the surrounding medium, is involved in several hazards posed to cells and tissues during the cooling cycle that takes place between the melting point of the cryopreservation medium and cryogenic temperatures of storage. Intracellular ice-formation (IIF), the instance where ice crystals nucleate and grow inside of the cell membrane, disrupts the internal organelles, can rupture the membrane and is usually lethal to cells (Lee et al., 1995). Extracellular ice-formation is not inevitably fatal but can mechanically damage cells by crushing and piercing and also, because growing ice crystals exclude solutes, can damage cells by causing them to excessively

dehydrate in response and cause osmotic injury by concentrating (or diluting at the thawing stage) solutes (Mazur, 1984; Mazur et al., 2005). Therefore, optimum recovery can be achieved by managing extracellular ice-formation and allowing cells to reach a glassy state by a technique known as controlled rate freezing (also known as slow freezing), illustrated in Fig 1.6. This technique is based on the 'two-factor hypothesis' of cell injury proposed by Mazur et al. (1972) which proposes that cooling too quickly means cells cannot dehydrate fast enough which results in IIF, but cooling too slowly means that cells are exposed to osmotic injury. These competing effects result in an optimum cooling rate (Fig. 1.7) which can vary from cell type to cell type although  $1\text{ }^{\circ}\text{C min}^{-1}$  is sufficient for a wide range of cell types (Bahsoun et al., 2019; Meneghel et al., 2020). Apparatus, such as programmable controlled rate freezers or isopropanol-based cooling devices, are usually needed to ensure that the sample endures a constant cooling rate from around physiological temperature to cryogenic storage temperature. An alternative approach to controlled rate freezing is vitrification (Fahy et al., 1984), where ice crystal formation is avoided altogether by cooling the sample at a rate so fast ( $> 1000\text{ }^{\circ}\text{C min}^{-1}$ ) that the glass transition temperature is reached before ice crystals can begin to nucleate and grow. During the thawing phase damage can occur to cells by ice-recrystallization and by the osmotic stress caused by melting ice with the former being particularly problematic for vitrified samples (Seki and Mazur, 2008). When cooling is complete, samples are typically stored at  $-196\text{ }^{\circ}\text{C}$  in liquid nitrogen where metabolic activity is minimal, or alternatively in freezers at  $-135\text{ }^{\circ}\text{C}$  or  $-80\text{ }^{\circ}\text{C}$  for medium term storage or where cryogenics (liquid nitrogen) are unavailable. Finally, the success of the cryopreservation process can be measured at various levels of detail by comparing various metrics to non-frozen control samples at various time points post-thaw. At the most basic level is cell viability (number or percentage) which can be measured with membrane integrity tests such as trypan blue or vital dye uptake assays such as Neutral Red. Further tests indicating if recovered cells are viable but damaged can be done at multiple timepoints, such as metabolic

assays, enzymatic assays or functionality assays specific to the cell being preserved - urea production by hepatocytes for example.

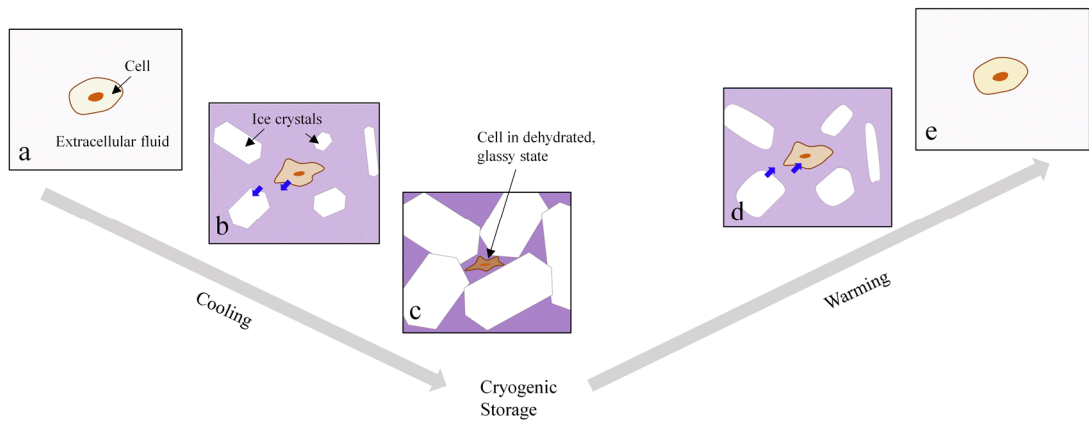


**Figure 1.6: Idealised example of slow freezing cell cryopreservation, adapted from Hunt (2019). Shade of extracellular fluid represents solute concentration; blue arrows represent water migration. a) Cell before cooling, b) Ice crystals nucleate at some point while below the melting point of the extracellular fluid, this increases the extracellular solute concentration and cell begins to dehydrate in response. c) Cell is contained in glassy, highly concentrated solution interstitial to ice crystals d) Warming begins and ice crystals begin to melt and cell re-hydrates. e) System warmed back above melting temperature and cell is fully rehydrated in a viable state.**

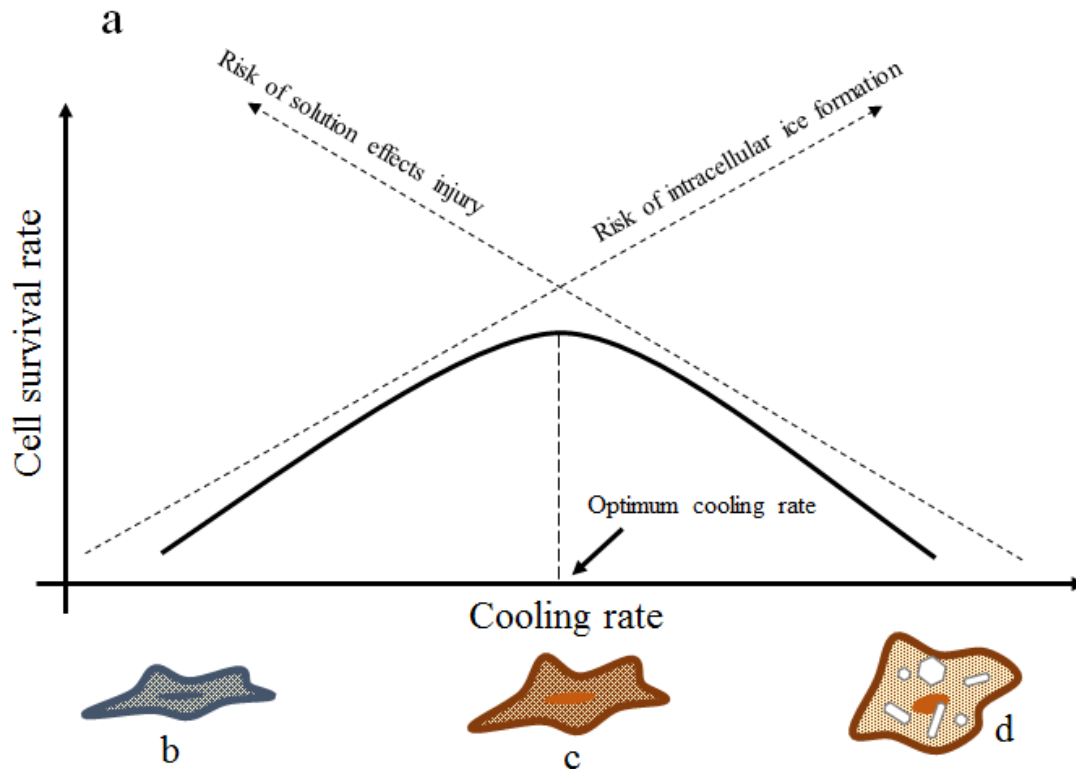


**Figure 1.7: Schematic of two-factor hypothesis of cell injury during controlled rate cell cryopreservation (Mazur, 1972). a) Plot of cell survival rate versus cooling rate. b) Cell injured by high solute content due to cooling too slowly. c) Cell avoids injury. d) Cell injured by intracellular ice formation due to cooling too quickly.**

### 1.3.3 Cryoprotectants

Cryoprotectants (CPAs) are soluble substances added to a cryopreservation system that act to significantly increase recovery and they are universally required in all conventional applications (Elliott et al., 2017). While a wide variety of compounds have been demonstrated to have cryoprotective effects they fall under two categories – penetrating and non-penetrating – and are often used in combination. Penetrating CPAs are typically low molecular weight, non-polar compounds which can penetrate cell membranes. The principal types are dimethyl sulphoxide (DMSO), glycerol, propylene glycol and ethylene glycol and their cryoprotective actions are thought to arise from various mechanisms. For example, by replacing intracellular water, increasing viscosity and by their ability to hydrogen bond with water molecules (Nash, 1962) the likelihood of IIF is reduced at any given temperature (Towey et al., 2012).

They also can act at osmotic ‘buffers,’ retarding the flow of water in and out of the cell when extracellular ice grows and when it melts (Fuller, 2004). Non-penetrating CPAs are higher molecular weight molecules which interact with and stabilise the cell membrane, and these include sugars such as trehalose and glucose and polymers such as polyethylene glycol and polyvinyl pyrrolidone (Elliott et al., 2017). The toxicity of CPAs to cells is an obstacle, particularly in the case of penetrating CPAs. For controlled rate freezing CPAs need to be used in concentrations of several percent and at even higher concentrations with vitrification (Best, 2015) for them to be effective. This means that CPAs must be added and removed from a sample in a way that minimises their toxic effects which increase with exposure time, temperature, and concentration. Another category of cryoprotectants is emerging which serve to modulate ice crystal growth by binding to ice crystals rather than interacting with cells directly (Carpenter and Hansen, 1992; Naing and Kim, 2019). These are inspired by naturally occurring antifreeze proteins (AFPs) found in fish, insects and frogs which create thermal hysteresis and delay ice-nucleation without significantly lowering the melting point. The benefits of AFPs include reducing the amount of toxic penetrating CPA needed for recovery and by preventing the hazardous re-crystallisation of ice during the thawing stage.

### **1.3.4 Role of controlled ice-nucleation in cryopreservation**

#### ***1.3.4.1 Benefits of controlled ice nucleation in cryopreservation***

Of all the parameters involved in cryopreservation processes, ice-nucleation is the least controlled due to its stochastic nature, even in heterogeneous mode (Morris and Acton, 2013). Uncontrolled ice-nucleation risks both deep supercooling and unacceptably large variability from sample to sample, this being most prevalent where small volumes are used as the potential for supercooling tends to be higher, as illustrated in Fig. 1.4. Where the relationship between ice-nucleation temperature and cryopreservation recovery has been investigated, for a wide variety of cell types controlling ice-nucleation usually (but not always) has a beneficial effect on recovery (Huang et al., 2021; Lauterboeck et al., 2016; Massie et al., 2014; Morris and Acton, 2013; Whittincham, 1977). Deep supercooling during controlled-rate cell cryopreservation is thought to pose a number of specific hazards. For example, IIF becomes more likely if cells have become deeply supercooled before having been dehydrated by the appearance of extracellular ice (Mazur et al., 2005). Other hazards

are related to the physical effects resulting from the faster rate of latent heat release occurring when ice-nucleates and grows from deeper supercooling. This causes severe thermal fluctuations that mechanically stress cells and also result in cooling rates that deviate from those intended after thermal re-equilibration (Hunt, 2019). Also, the structure and shape of the ice crystal matrix can be greatly affected by ice-nucleation temperature. For example, nucleation after deeper supercooling results in ice crystals growing in a dendritic manner increasing the risk of mechanical damage (Saragusty et al., 2009). Finally, the extracellular ice matrix that forms after nucleation is finer grained after deeper supercooling (Morris and Acton, 2013) and this has been shown to increase the risk of hazardous ice-recrystallization upon thawing (Huang et al., 2017).

#### ***1.3.4.2 Container types and liquid volumes***

A number of types of specialised containers are used for cell cryopreservation with capacities appropriate to their end uses and these include straws (> 0.5 mL), cryovials (2 mL to 10 mL) and cryobags (up to 200 mL). As discussed in Section 1.1.4, sample aliquot size has a significant effect on the expected ice-nucleation temperature of any aqueous sample with smaller volumes tending to supercool more. In cryopreservation applications the cleanliness and sterility requirements may serve to exacerbate this by removing contaminants acting as incidental nucleation sites.

Straws are routinely used for freezing sperm, oocytes and embryos for fertility applications while cryovials are the standard commercial delivery format for cryopreserved cells used in research. In these smaller containers supercooling of more than 10 °C is inevitable (Morris and Acton, 2013) and ice-nucleation usually needs to be controlled or bypassed in the case of straws by means of vitrification. Cryobags are sterile, flexible plastic vessels used where the preservation of larger volumes of cell suspension is needed, for example, in blood product freezing and cell therapy applications. Due to the larger volumes involved (100s of mL, for example) their contents tend to supercool much less than vials and straws. Also, unlike straws and vials, protective equipment such as metal cassettes or overwaps are needed when cooling cryobags to ensure homogenous cooling and protection from breakage (Meneghel et al., 2020).

Multiwell plates are plastic arrays of 6, 12, 24, 48, 96, 384 or 1536 wells within which multiple experiments or screenings can be carried out simultaneously and autonomously. Freezing of cells in multiwell plates has been reported in the literature (Campbell and Brockbank, 2014, 2007; Corsini et al., 2002; Wragg et al., 2020) but this is not a format that cells for research purposes are commercially delivered frozen in. Instead, to obtain cells in multiwell plates, cells need to be thawed from cryovials then transferred to and cultured up in multiwell plates over several days. The working volumes of the wells become small enough in 96-well plates (200  $\mu\text{L}$ ) that severe supercooling below  $-20\text{ }^{\circ}\text{C}$  is likely (Harrison et al., 2018; Zaragotas et al., 2016). Cryopreserving cells in this format this level of supercooling not only would overall viability reduce for the reasons outlined in the previous section, but random incidental nucleation events could also result in huge well to well variability, thus causing unacceptable sample-to-sample variability (Hunt, 2019). Figure 1.8 illustrates the problem.

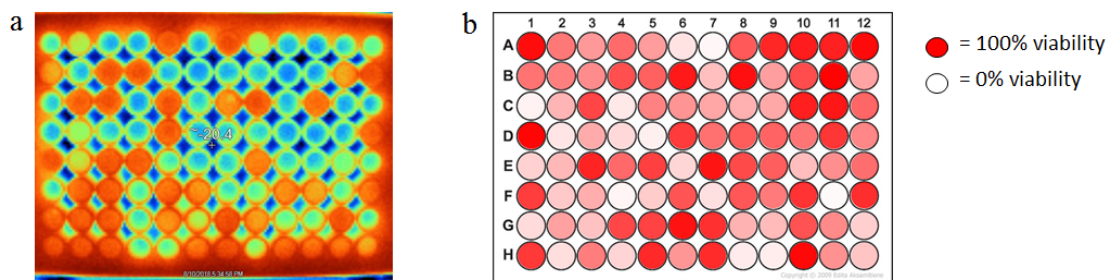


**Figure 1.8: Supercooling of liquid within 96-well plates and expected effect on post-thaw cell viability. a) Infra-red image (unpublished) of 96-well plate with each well containing 200  $\mu\text{L}$  of deionised filtered water at approximately  $-15\text{ }^{\circ}\text{C}$ . Wells showing as orange have recently nucleated and released latent heat while wells showing as blue are still supercooled – this demonstrates the randomness of ice-nucleation in this format. b) Expected distribution of cell viability levels resulting from chaotic supercooling seen in a).**

#### 1.3.4.3 Ice-nucleation control techniques

A variety of methods have been developed for controlling IN in cryopreservation scenarios (Morris and Acton, 2013). While each have their pros and cons (Table 1), they all have common goal of reliably inducing IN at warm temperatures and in a way that does not physically interfere with or contaminate the sample. Manual seeding, is

a traditional method where the external wall of the container is touched with a liquid nitrogen cooled tool to induce a cold spot where ice-nucleation occurs in the sample (Kilbride and Meneghel, 2021; Leibo et al., 1970). Seeding, in other contexts, may also refer to inducing nucleation in supercooled liquid by introducing a seed crystal, such as ice in the case of water. Due to contamination risks, this is not generally employed in cryopreservation. Shock or ramp cooling involves rapidly increasing the cooling rate to induce ice nucleation then increasing to compensate for the latent heat release (Diener et al., 1993). Special apparatus can induce ice nucleation by electric fields (Petersen et al., 2006), ultrasound (Kiani et al., 2012), magnetic fields (Kobayashi et al., 2018) and depressurisation to produce ice mist (Geidobler and Winter, 2013). Finally, substances that act as heterogeneous ice-nucleating agents can be added to the sample to passively induce ice-nucleation (Morris and Acton, 2013). Substances with potent ice-nucleating abilities such as Snomax (Teixeira et al., 2017), silver iodide (Kojima et al., 1988) and cholesterol (Massie et al., 2011) all have been demonstrated to improve cell recovery. However, the biocompatibility requirements for these substances to be compliant with Good Manufacturing Practice (GMP) to be used in clinical settings are strict and so use of these substances is still confined to research activities (Morris and Acton, 2013).

**Table 1.1. Comparison of methods for controlling ice-nucleation in cryopreservation applications**

<b>Ice-nucleation technique</b>	<b>Advantages</b>	<b>Disadvantages</b>
Manual seeding	<ul style="list-style-type: none"> <li>- Requires no specialist equipment</li> <li>- Control over ice-nucleation temperature</li> </ul>	<ul style="list-style-type: none"> <li>- Requires cryogens</li> <li>- Impractical for considerable number of vessels</li> </ul>
Shock / cooling ramp manipulation	<ul style="list-style-type: none"> <li>- Require no operator intervention</li> </ul>	<ul style="list-style-type: none"> <li>- Requires programmable freezer</li> <li>- Ice-nucleation depends on variability of sample containers</li> </ul>

(Continued overleaf...)

Mechanical and energy source (ultrasound, electric, magnetic) apparatus	<ul style="list-style-type: none"> <li>- Control over ice-nucleation temperature</li> </ul>	<ul style="list-style-type: none"> <li>- Difficult to standardise and integrate with freezing equipment</li> <li>- Expense and reliability of equipment</li> </ul>
Passive ice-nucleating substances	<ul style="list-style-type: none"> <li>- Requires no specialist equipment</li> <li>- Require no operator intervention</li> </ul>	<ul style="list-style-type: none"> <li>- Introduction to and removal from sample without contamination</li> <li>- Variability and stability of materials' ice-nucleation ability</li> <li>- Strict biocompatibility requirements</li> </ul>

#### ***1.3.4.4 Ice nucleation in aqueous solutions***

In cryopreservation systems, and to a certain extent in cloud droplets, IN events occur in aqueous solutions rather than pure water. The presence of solutes strongly influences the temperature of ice-nucleation and, in nearly all cases, reduces it compared to what it would be in pure water. In the case of homogeneous IN, the nucleation temperature is shifted lower according to the 'water activity criterion' which is determined simply by the reduction in water activity and not by the nature of the solute (Koop et al., 2000; Koop and Zobrist, 2009; Zobrist et al., 2008). In other words, the shift in IN temperature is the same as the melting point depression of the solution, akin to the colligative properties of water. In the case of heterogeneous IN in aqueous solutions the water activity criterion always applies but two other types of interactions can also occur, although to what extent depends heavily on the nature of the solute. Firstly, low concentrations of solutes can interact with nucleator surfaces in a way that reduces (or in rare cases increases) the ice-nucleation temperature by far more than would be expected by their water activity criterion alone (Kumar et al., 2018; Kumar et al., 2019a, b; Whale et al., 2018). This effect has been best demonstrated using milli-molar concentrations of inorganic salts and mineral ice-nucleators which can shift IN temperatures on mineral particles down by several degrees. An exceptional case is ammonium salts which shift ice-nucleation temperatures up by several degrees (Whale et al., 2018). This solute surface effect appears to diminish as the concentrations are increased to the point where the water

activity criterion effect begins to dominate (Kumar et al., 2018). Secondly, ice-nucleator surfaces and their active sites can be irreversibly degraded by solutes, for example acids on mineral surfaces (Sullivan et al., 2010), or by substances used to digest biological ice-nucleators such as enzymes or chemical denaturants (Kieft and Ruscetti, 1990; Maki et al., 1974; Pummer et al., 2012). These three types of scenarios are illustrated in Fig 1.9.

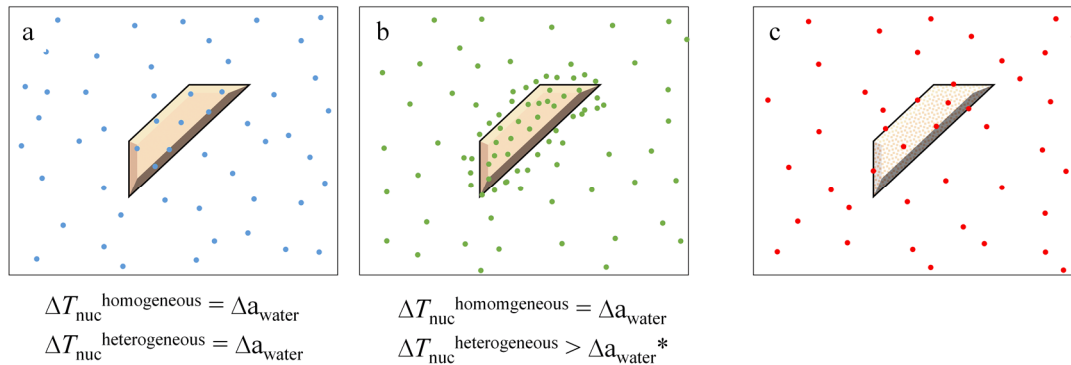


**Figure 1.9: Three different concepts on the effects of solutes on heterogeneous ice-nucleation temperatures. Dots represent hypothetical solutes which interact with ice-nucleating surface in distinct ways. a) Solute does not interact with surface and ice-nucleation temperatures decrease proportional to decrease in water activity. b) Solute interacts with surface and ice-nucleation temperature decreases more than expected for decrease in water activity. c) Solute attacks surface and destroys active sites**

## References

- Bahsoun, S., Coopman, K., and Akam, E. C.: The impact of cryopreservation on bone marrow-derived mesenchymal stem cells: a systematic review, *Journal of Translational Medicine*, 17, 397, 2019.
- Best, B. P.: Cryoprotectant Toxicity: Facts, Issues, and Questions, *Rejuvenation Res*, 18, 422-436, 2015.
- Campbell, L. H. and Brockbank, K. G. M.: Cryopreservation of Adherent Cells on a Fixed Substrate, *IntechOpen*, doi: 10.5772/58618, 2014. 2014.
- Campbell, L. H. and Brockbank, K. G. M.: Serum-free solutions for cryopreservation of cells, *In Vitro Cellular & Developmental Biology - Animal*, 43, 269-275, 2007.

- Carpenter, J. F. and Hansen, T. N.: Antifreeze protein modulates cell survival during cryopreservation: mediation through influence on ice crystal growth, *Proceedings of the National Academy of Sciences*, 89, 8953, 1992.
- Clarke, A., Morris, G. J., Fonseca, F., Murray, B. J., Acton, E., and Price, H. C.: A Low Temperature Limit for Life on Earth, *PLOS ONE*, 8, e66207, 2013.
- Corsini, J., Maxwell, F., and Maxwell, I. H.: Storage of various cell lines at -70 degrees C or -80 degrees C in multi-well plates while attached to the substratum, *Biotechniques*, 33, 42, 44, 46, 2002.
- Diener, B., Utesch, D., Beer, N., Dürk, H., and Oesch, F.: A Method for the Cryopreservation of Liver Parenchymal Cells for Studies of Xenobiotics, *Cryobiology*, 30, 116-127, 1993.
- Elliott, G. D., Wang, S. P., and Fuller, B. J.: Cryoprotectants: A review of the actions and applications of cryoprotective solutes that modulate cell recovery from ultra-low temperatures, *CRYOBIOLOGY*, 76, 74-91, 2017.
- Fahy, G. M., MacFarlane, D. R., Angell, C. A., and Meryman, H. T.: Vitrification as an approach to cryopreservation, *Cryobiology*, 21, 407-426, 1984.
- Fuller, B. and Paynter, S.: Fundamentals of cryobiology in reproductive medicine, *Reprod Biomed Online*, 9, 680-691, 2004.
- Fuller, B. J.: Cryoprotectants: The essential antifreezes to protect life in the frozen state, *CRYOLETTERS*, 25, 375-388, 2004.
- Geidobler, R. and Winter, G.: Controlled ice nucleation in the field of freeze-drying: Fundamentals and technology review, *European Journal of Pharmaceutics and Biopharmaceutics*, 85, 214-222, 2013.
- Glenister, P. H. and Thornton, C. E.: Cryoconservation - archiving for the future, *MAMMALIAN GENOME*, 11, 565-571, 2000.
- Harrison, A. D., Whale, T. F., Rutledge, R., Lamb, S., Tarn, M. D., Porter, G. C. E., Adams, M. P., McQuaid, J. B., Morris, G. J., and Murray, B. J.: An instrument for quantifying heterogeneous ice nucleation in multiwell plates using infrared emissions to detect freezing, *Atmos. Meas. Tech.*, 11, 5629-5641, 2018.
- Huang, H., Zhao, G., Zhang, Y., Xu, J., Toth, T. L., and He, X.: Predehydration and Ice Seeding in the Presence of Trehalose Enable Cell Cryopreservation, *ACS Biomater Sci Eng*, 3, 1758-1768, 2017.
- Huang, Z. Y., Liu, W., Liu, B. L., He, X. W., Guo, H., Xue, S. X., Yan, X. J., and Jaganathan, G. K.: Cryopreservation of human T lymphocytes under fast cooling with controlled ice nucleation in cryoprotective solutions of low toxicity, *CRYOBIOLOGY*, 103, 92-100, 2021.
- Hunt, C. J.: Technical Considerations in the Freezing, Low-Temperature Storage and Thawing of Stem Cells for Cellular Therapies, *Transfusion Medicine and Hemotherapy*, 46, 134-150, 2019.
- Kiani, H., Sun, D.-W., Delgado, A., and Zhang, Z.: Investigation of the effect of power ultrasound on the nucleation of water during freezing of agar gel samples in tubing vials, *Ultrasonics Sonochemistry*, 19, 576-581, 2012.

- Kieft, T. L. and Ruscetti, T.: Characterization of biological ice nuclei from a lichen, *J Bacteriol*, 172, 3519-3523, 1990.
- Kilbride, P. and Meneghel, J.: Freezing Technology: Control of Freezing, Thawing, and Ice Nucleation. In: *Cryopreservation and Freeze-Drying Protocols*, Wolkers, W. F. and Oldenhof, H. (Eds.), Springer US, New York, NY, 2021.
- Kobayashi, A., Horikawa, M., Kirschvink, J. L., and Golash, H. N.: Magnetic control of heterogeneous ice nucleation with nanophase magnetite: Biophysical and agricultural implications, *Proceedings of the National Academy of Sciences*, 115, 5383, 2018.
- Kojima, T., Soma, T., and Oguri, N.: Effect of ice nucleation by droplet of immobilized silver iodide on freezing of rabbit and bovine embryos, *Theriogenology*, 30, 1199-1207, 1988.
- Koop, T., Luo, B., Tsias, A., and Peter, T.: Water activity as the determinant for homogeneous ice nucleation in aqueous solutions, *Nature*, 406, 611-614, 2000.
- Koop, T. and Zobrist, B.: Parameterizations for ice nucleation in biological and atmospheric systems, *Phys Chem Chem Phys*, 11, 10839-10850, 2009.
- Kumar, A., Marcolli, C., Luo, B., and Peter, T.: Ice nucleation activity of silicates and aluminosilicates in pure water and aqueous solutions – Part 1: The K-feldspar microcline, *Atmos. Chem. Phys.*, 18, 7057-7079, 2018.
- Kumar, A., Marcolli, C., and Peter, T.: Ice nucleation activity of silicates and aluminosilicates in pure water and aqueous solutions – Part 2: Quartz and amorphous silica, *Atmos. Chem. Phys.*, 19, 6035-6058, 2019a.
- Kumar, A., Marcolli, C., and Peter, T.: Ice nucleation activity of silicates and aluminosilicates in pure water and aqueous solutions – Part 3: Aluminosilicates, *Atmos. Chem. Phys.*, 19, 6059-6084, 2019b.
- Lauterboeck, L., Gryshkov, O., Hofmann, N., and Glasmacher, B.: Importance of controlled ice formation for efficient cell biobanking, 2016, 84-90.
- Lee, R. E., Warren, G. J., and Gusta, L. V.: *Biological ice nucleation and its applications.*, 1995. 1995.
- Leibo, S. P., Farrant, J., Mazur, P., Hanna, M. G., and Smith, L. H.: Effects of preezing on marrow stem cell suspensions: Interactions of cooling and warming rates in the presence of pvp, sucrose, or glycerol, *Cryobiology*, 6, 315-332, 1970.
- Maki, L. R., Galyan, E. L., Chang-Chien, M. M., and Caldwell, D. R.: Ice nucleation induced by *pseudomonas syringae*, *Appl Microbiol*, 28, 456-459, 1974.
- Massie, I., Selden, C., Hodgson, H., and Fuller, B.: Cryopreservation of Encapsulated Liver Spheroids for a Bioartificial Liver: Reducing Latent Cryoinjury Using an Ice Nucleating Agent, *Tissue Engineering Part C: Methods*, 17, 765-774, 2011.
- Massie, I., Selden, C., Hodgson, H., Fuller, B., Gibbons, S., and Morris, G. J.: GMP Cryopreservation of Large Volumes of Cells for Regenerative Medicine: Active Control of the Freezing Process, *Tissue Engineering Part C: Methods*, 20, 693-702, 2014.

Mazur, P.: Freezing of living cells: mechanisms and implications, *American Journal of Physiology-Cell Physiology*, 247, C125-C142, 1984.

Mazur, P., Leibo, S. P., and Chu, E. H.: A two-factor hypothesis of freezing injury. Evidence from Chinese hamster tissue-culture cells, *Exp Cell Res*, 71, 345-355, 1972.

Mazur, P., Seki, S., Pinn, I. L., Kleinhans, F. W., and Edashige, K.: Extra- and intracellular ice formation in mouse oocytes, *Cryobiology*, 51, 29-53, 2005.

Meneghel, J., Kilbride, P., and Morris, G. J.: Cryopreservation as a Key Element in the Successful Delivery of Cell-Based Therapies—A Review, *Frontiers in Medicine*, 7, 2020.

Morris, G. J. and Acton, E.: Controlled ice nucleation in cryopreservation--a review, *Cryobiology*, 66, 85-92, 2013.

Naing, A. H. and Kim, C. K.: A brief review of applications of antifreeze proteins in cryopreservation and metabolic genetic engineering, *3 Biotech*, 9, 329, 2019.

Nash, T.: The chemical constitution of compounds which protect erythrocytes against freezing damage, *The Journal of general physiology*, 46, 167-175, 1962.

Petersen, A., Schneider, H., Rau, G., and Glasmacher, B.: A new approach for freezing of aqueous solutions under active control of the nucleation temperature, *Cryobiology*, 53, 248-257, 2006.

Polge, C., Smith, A. U., and Parkes, A. S.: Revival of Spermatozoa after Vitrification and Dehydration at Low Temperatures, *Nature*, 164, 666-666, 1949.

Pummer, B. G., Bauer, H., Bernardi, J., Bleicher, S., and Grothe, H.: Suspendable macromolecules are responsible for ice nucleation activity of birch and conifer pollen, *Atmos. Chem. Phys.*, 12, 2541-2550, 2012.

Saragusty, J., Gacitua, H., Rozenboim, I., and Arav, A.: Do physical forces contribute to cryodamage?, *Biotechnology and Bioengineering*, 104, 719-728, 2009.

Seki, S. and Mazur, P.: Effect of warming rate on the survival of vitrified mouse oocytes and on the recrystallization of intracellular ice, *Biol Reprod*, 79, 727-737, 2008.

Steponkus, P. L., Myers, S. P., Lynch, D. V., Gardner, L., Bronshteyn, V., Leibo, S. P., Rall, W. F., Pitt, R. E., Lin, T. T., and MacIntyre, R. J.: Cryopreservation of *Drosophila melanogaster* embryos, *Nature*, 345, 170-172, 1990.

Sullivan, R. C., Petters, M. D., DeMott, P. J., Kreidenweis, S. M., Wex, H., Niedermeier, D., Hartmann, S., Clauss, T., Stratmann, F., Reitz, P., Schneider, J., and Sierau, B.: Irreversible loss of ice nucleation active sites in mineral dust particles caused by sulphuric acid condensation, *Atmospheric Chemistry and Physics*, 10, 11471-11487, 2010.

Takeo, T. and Nakagata, N.: Cryobanking and Recovery of Genetically Modified Mice. In: *Transgenic Mouse: Methods and Protocols*, Larson, M. A. (Ed.), Springer US, New York, NY, 2020.

- Teixeira, M., Buff, S., Desnos, H., Loiseau, C., Bruyère, P., Joly, T., and Commin, L.: Ice nucleating agents allow embryo freezing without manual seeding, *Theriogenology*, 104, 173-178, 2017.
- Towey, J. J., Soper, A. K., and Dougan, L.: Molecular Insight Into the Hydrogen Bonding and Micro-Segregation of a Cryoprotectant Molecule, *The Journal of Physical Chemistry B*, 116, 13898-13904, 2012.
- Watson, C. Y., Damiani, F., Ram-Mohan, S., Rodrigues, S., de Moura Queiroz, P., Donaghey, T. C., Rosenblum Lichtenstein, J. H., Brain, J. D., Krishnan, R., and Molina, R. M.: Screening for Chemical Toxicity Using Cryopreserved Precision Cut Lung Slices, *Toxicol Sci*, 150, 225-233, 2016.
- Whale, T. F., Holden, M. A., Wilson, Theodore W., O'Sullivan, D., and Murray, B. J.: The enhancement and suppression of immersion mode heterogeneous ice-nucleation by solutes, *Chemical Science*, 9, 4142-4151, 2018.
- Whittincham, D. G.: Some Factors Affecting Embryo Storage in Laboratory Animals, *Ciba Foundation Symposium 52 - The Freezing of Mammalian Embryos*, doi: doi:10.1002/9780470720332.ch610.1002/9780470720332.ch6, 1977. 97-127, 1977.
- Wragg, N. M., Tampakis, D., and Stolzing, A.: Cryopreservation of Mesenchymal Stem Cells Using Medical Grade Ice Nucleation Inducer, *International Journal of Molecular Sciences*, 21, 2020.
- Zarogotas, D., Liolios, N. T., and Anastassopoulos, E.: Supercooling, ice nucleation and crystal growth: a systematic study in plant samples, *Cryobiology*, 72, 239-243, 2016.
- Zobrist, B., Marcolli, C., Peter, T., and Koop, T.: Heterogeneous Ice Nucleation in Aqueous Solutions: the Role of Water Activity, *The Journal of Physical Chemistry A*, 112, 3965-3975, 2008.

## 1.4 Ice-nucleation in Earth's atmosphere

### 1.4.1 Importance of ice-nucleation in clouds

Clouds play a key role in regulating the climate through controlling radiative balance and in the hydrological cycle with the formation of ice being crucial (Forster et al., 2021) for triggering precipitation. At temperatures below 0 °C in the Earth's troposphere water clouds potentially comprise of either a mixture of water droplets and ice crystals – Mixed Phase Clouds (MPCs) - or ice crystals only above temperatures below -38°C in the case of cirrus clouds. Ice-nucleating particles (INPs) are required to trigger ice formation via heterogeneous IN in clouds at temperatures above where homogeneous freezing becomes significant at -33°C and below (Herbert et al., 2015; Koop and Murray, 2016). The extent of supercooling in MPCs has been measured remotely with lidar and found that averaged globally, 50% of clouds are supercooled at -20 °C but with considerable spatial variability of +/- 20% (Choi et al., 2010).

The dominant modes of heterogeneous freezing in clouds are immersion freezing for MPCs (Ansmann et al., 2008; de Boer et al., 2011) and deposition for cirrus clouds (Cziczo et al., 2013) where it is too cold for droplet activation to take place. Condensation freezing and contact freezing (collision of INPs with supercooled droplets) are two other proposed liquid phase modes of ice-nucleation, although the former may be indistinguishable from immersion freezing (Hiranuma et al., 2019; Vali et al., 2015). Deposition mode freezing may actually occur via a pathway known as pore condensation and freezing rather than nucleation directly from vapour (Campbell et al., 2017; Christenson, 2013; Marcolli, 2014). Here, microscopic pores and cavities on an INP surface locally reduce the saturation  $RH_w$  due an 'inverse Kelvin' effect and cause water to condense and freeze homogeneously above the expected homogeneous freezing temperatures (-33 °C to -38 °C) and then seed ice crystal growth.

The albedo of clouds in certain meteorological settings have been demonstrated to be particularly sensitive to their ice content (Murray et al., 2021) where replacing water droplets with ice crystals through ice-nucleation in MPC lowers the albedo allowing more incoming shortwave radiation to reach the surface (Storelvmo, 2017). This lowering of albedo occurs via the Wegener-Bergeron-Findeisen process (Fig. 1.10), where ice crystals grow at the expense of co-existing supercooled water droplets due

to ice's lower equilibrium vapour pressure compared to supercooled water at the same temperature (Storelvmo and Tan, 2015). This can also lead to precipitation initiation where by the growing ice-crystals begin to fall out and collide with other droplets below, facilitating the droplet collision and coalescence process essential for rainfall. Fallstreak clouds (Fig. 1.11), formed by passing aircraft that artificially trigger ice-nucleation, are striking albeit rare example of this process in action. On a synoptic scale the ice content of MPC has significant effects on radiative balance, for example, the modelled incident shortwave radiation under low stratiform MFC in the cold sector of mid-latitude cyclones can vary by 100s of  $\text{W m}^{-2}$  depending on cloud INP content (Vergara-Temprado et al., 2018) (Figure 1.12).

Complicating matters are that ice-crystal number concentrations in warm ( $-10\text{ }^{\circ}\text{C}$  and above) MPCs are often observed to be orders of magnitude higher than the purported INP concentrations (Lloyd et al., 2020; Mossop and Ono, 1969; Yang et al., 2020) It has been therefore been proposed that ice crystal concentration are be further enhanced by several orders after the initial appearance of ice by secondary ice production (SIP) processes (Field et al., 2017). The best studied is the Hallett-Mossop or 'rime splintering' process (Hallett and Mossop, 1974) which is most efficient at relatively warm temperatures ( $-3\text{ }^{\circ}\text{C}$  to  $-8\text{ }^{\circ}\text{C}$ ).

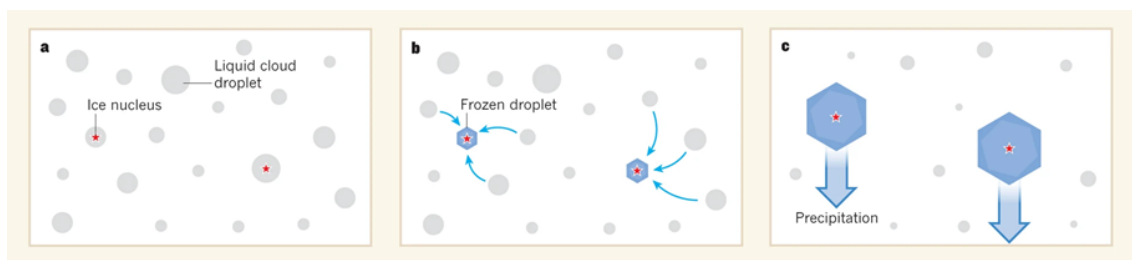


**Figure 1.10: Wegener-Bergeron-Findeisen process, diagram from Koop and Mahowald (2013)**



**Figure 1.11: Fallstreak or ‘hole-punch’ cloud photographed within an altostratus cloud layer on 18<sup>th</sup> January 2022, Leeds, UK. Two wispy features are visible just below the centre of the hole, these are patches of falling ice-crystals.**

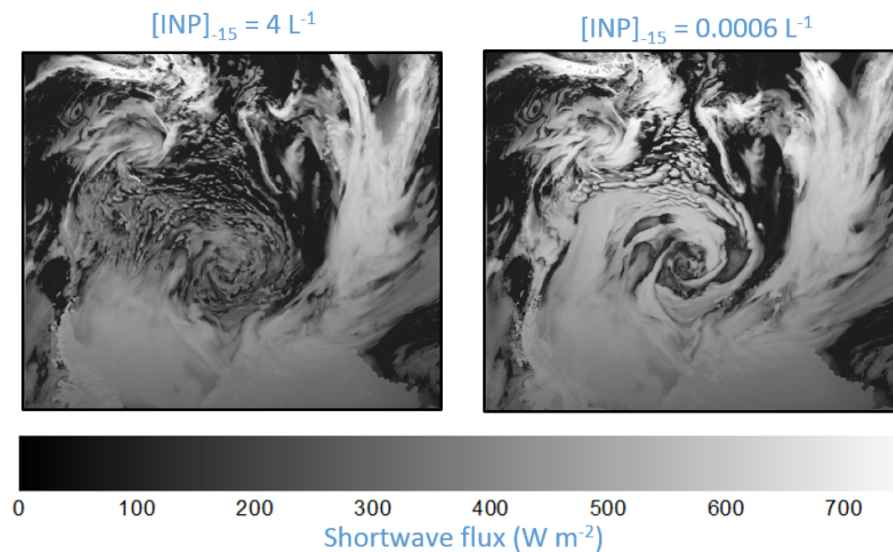


**Figure 1.12: Cloud model output showing effect of INP concentration on clouds in the cold-sector of mid-latitude cyclone over the Southern Ocean, a figure from Murray et al., (2021) which was adapted from Vergara-Temprado et al., (2018). This demonstrates how in this particular setting the shortwave radiation reaching the surface can differ by 100s of  $\text{W m}^{-2}$  according to the amount of primary ice production.**

### 1.4.2 Atmospheric aerosol and ice-nucleating particles

Atmospheric aerosol, of which INP are subset, are solid particles or liquid droplets suspended in the atmosphere. Broad classes include primary particles such as mineral and soil dust, volcanic ash, sea salt, combustion products such as smoke and soot, bioaerosols. Secondary particles, formed within the atmosphere from gas-phase reactions, include concentrated solution droplets of sulphate, nitrate and ammonium salts and secondary organic particles formed from volatile organic compounds. Without aerosols acting as cloud condensation nuclei (CCN), clouds would not be able to form as surfaces are needed for the droplets to condense on in water-supersaturated air. They are crucial components in the climate system, both from their direct radiative effects and indirect effects via cloud droplet interaction. Direct effects involve the direct absorption and scattering of incoming solar radiation while indirect effects refer to their interaction with clouds. Increased CCN from, for example pollution, lead to more numerous and smaller cloud droplets with constant liquid water path and this leads to increased light scattering and albedo as well as increased lifetime (Hartmann et al., 1992; Lohmann and Feichter, 2005). The degree of indirect effects depends on aerosol composition and size distribution as well as particle number, with larger and more hygroscopic particles more likely to act as CCN at a given water supersaturation.

INPs are aerosol particles which have the ability to induce ice-nucleation above the homogeneous freezing temperatures or ice supersaturation (Kanji et al., 2017; Murray et al., 2012). However only a small proportion - often between 1 in  $10^3$  and  $10^6$  - of aerosol particles can act as INP (DeMott et al., 2010; Murray et al., 2012) at MPC temperatures. Also, the necessary properties that make efficient CCN are different to those that make efficient INP with those for INP being much less well understood. All the types of atmospheric aerosol particle listed above can potentially act as INP to some extent (Kanji et al., 2017), except for inorganic solution droplets which instead play a role in cirrus cloud formation by freezing homogeneously (Heymsfield et al., 2017). The uncertainty about the magnitude of climate forcing through cloud-aerosol interactions has driven intense recent research into the nature, global abundances and sources of INP. This has greatly expanded knowledge, but much is still not understood about them due to their relative scarcity and diverse nature. For example, field campaigns have collected data on atmospheric INP concentrations in a variety of geographical settings as well as collecting and analysing INPs themselves in residuals

in ice-crystals or precipitation. Moreover, laboratory studies focused on certain types of INP have determined the relative potency of INP types in immersion and deposition mode. The end goal of understanding INPs in the atmosphere is to be able to accurately represent and predict cloud ice-formation in models. As this is a microphysical process occurring on a scale smaller than the resolution of cloud models it must be represented by a parameterisation, for example the number concentration of INP per litre of air ( $[INP] \text{ L}^{-1}$ ) as a function of temperature (DeMott et al., 2010; Harrison et al., 2019; Hoose et al., 2010b; Niemand et al., 2012). The parameterisations can be tested against INP concentration measurements collected in the field.

In the past decade field campaigns have built up a picture of the concentration and types of INPs in different environmental settings (Fig 1.13). Measurements, however, are episodic and sparse compared to those of aerosol particles for example. In areas with terrestrial influence mineral dust and biogenic INP are considered the two most important classes of INP by virtue of their relatively high combined abundance and ice-nucleating activity (Vergara-Temprado et al., 2017). Mineral dust only has significant ice-nucleating activity below  $-15 \text{ }^{\circ}\text{C}$  (Murray et al., 2012; Niemand et al., 2012) yet is emitted into the troposphere in huge quantities (up to 3,000 Tg per year), mainly from low latitude deserts such as the Sahara but also from agricultural land. Dust carried aloft in plumes can travel thousands of kilometres across oceans and has been detected in cirrus cloud ice-residuals (Cziczo et al., 2013). Laboratory studies have shown that the common mineral components of desert dust - quartz, feldspars, carbonates and clays - have a wide variety of ice-nucleating abilities and of these the potassium (K) variety of feldspar has the highest (Atkinson et al., 2013; Harrison et al., 2016; Kaufmann et al., 2016; Yakobi-Hancock et al., 2013), followed by plagioclase feldspars and quartz (Harrison et al., 2019; Zolles et al., 2015). Therefore, while K-feldspar typically makes up only a minor component (1-10%) of any mineral dust, its high activity will dominate and therefore control (and can be used to predict) the ice-nucleating ability of the dust as a whole (Atkinson et al., 2013). Biological material shown to act as INP include primary particles such as bacteria (Henderson-Begg et al., 2009), pollen (Augustin et al., 2013), viruses (Adams et al., 2021), and fungal material (Fröhlich-Nowoisky et al., 2015), biogenic ice-nucleating macromolecules (Pummer et al., 2012) and also biogenic but inert substances such as cellulose (Hiranuma et al., 2019) and lignin (Bogler and Borduas-Dedekind, 2020).

Based on laboratory experiments, ambient ice-nucleating activity above  $-10\text{ }^{\circ}\text{C}$  is generally thought to originate from biological INP, specifically proteinaceous material which include bacteria (*Pseudomonas syringae*) and fungi (*Fusarium sp.*) capable of nucleating ice as warmer than  $-5\text{ }^{\circ}\text{C}$  (Joly et al., 2013; Maki et al., 1974; Pouleur et al., 1992). Despite their higher activity it is not yet clear whether the influence of biological INP on clouds competes with that of mineral dust on a global scale (Hoose et al., 2010a; Spracklen and Heald, 2014). In remote ocean settings far from terrestrial sources of dust and biogenic material, sea-spray aerosol containing organic material, thought to originate from planktonic organisms becomes the principal INP source (Creamean et al., 2013; Wilson et al., 2015). These general regimes of terrestrial INP and remote oceanic INP dominating the northern and southern hemispheres respectively is evident from in-situ collection of INPs (Murray et al., 2021; Welte et al., 2020), modelling (Vergara-Temprado et al., 2017) and remote sensing of supercooled water content (Choi et al., 2010; Kanitz et al., 2011). Observed INP concentrations for a given temperature do, however, vary over several orders of magnitude, partly due to poorly understood natural variability and partly due to differences in the collection and measurement techniques used (Murray et al., 2021).

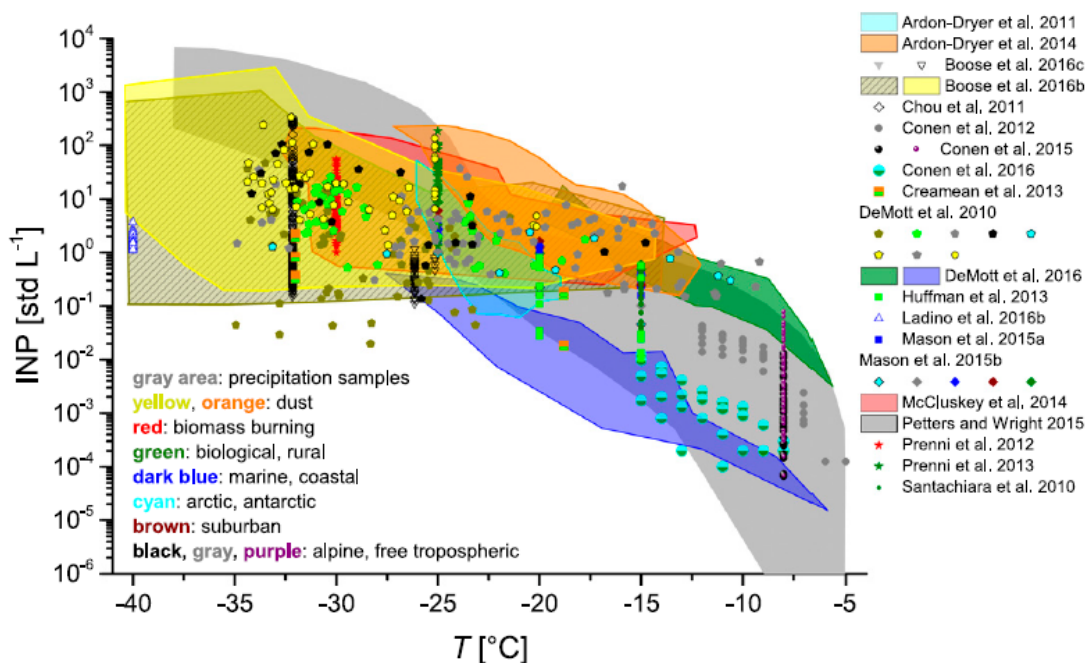


**Figure 1.13: Summary of INP measurements taken globally from Kanji et al., (2017).**

To add to the complexity, atmospheric INPs may be degraded by or coated with other atmospheric components (Knopf et al., 2018; Kulkarni, 2018), be subject to seasonal cycles (Conen et al., 2015; Schneider et al., 2021) or released by human activity such as agriculture (Garcia et al., 2012; Suski et al., 2018). Also, INP populations are likely to be mixed, for example externally within an aerosol assemblage or internally if biological INP are attached to soil dust particles (O'Sullivan et al., 2014; O'Sullivan et al., 2016). For analysis of samples offline this can make it difficult to assign the source of the ice-nucleating activity observed, for example, to mineral dust or biological content. Heating a sample to denature biological material present while assuming that preserving inorganic is a widely used method to do this (Christner et al., 2008; Conen et al., 2011), and is often combined with further analysis (chemical, biological, imaging) of the sample content (Baloh et al., 2019; Hill et al., 2014; Tobo et al., 2019).

### **1.4.3 Climate change feedbacks controlled by ice-nucleation in clouds**

As well as being able to accurately model the ice content of clouds in the present day we need to understand how the role of ice nucleation in mixed phase clouds will change in response to warmer global temperatures (Murray et al., 2021). Feedbacks are processes that dampen or accelerate warming in response to a climate forcing such as increased CO<sub>2</sub>. Feedbacks are built into Equilibrium Climate Sensitivity, defined as the amount of warming resulting from a doubling of atmospheric CO<sub>2</sub> after Earth returns to equilibrium (Forster et al., 2021). The sign of feedback from clouds as a whole is thought to be positive, mainly due to the removal of reflective low stratus clouds over the tropical oceans (Ceppi et al., 2017). A warming world could, however, also change the proportion of ice formed in MPCs and alter emissions of INPs, both potentially resulting in feedbacks (Fig. 1.14). The cloud-phase feedback (Murray et al., 2021) purports that in a warmer world with an unchanged INP population, less ice nucleates in mixed clouds at any given height (temperature) resulting in more liquid droplets, increased albedo, thus causing negative feedback. This feedback contributes to the IPCC report's estimate of ECS; however, the latest generation of models show less strong feedback, meaning higher estimates of ECS are more accurate and more warming is likely. The treatment of cloud-phase and ECS correlates most strongly with mid to high latitude MPCs over oceans, therefore they are a particularly important

regime to be correctly represented in models in terms of cloud ice production (Vergara-Temprado et al., 2018).

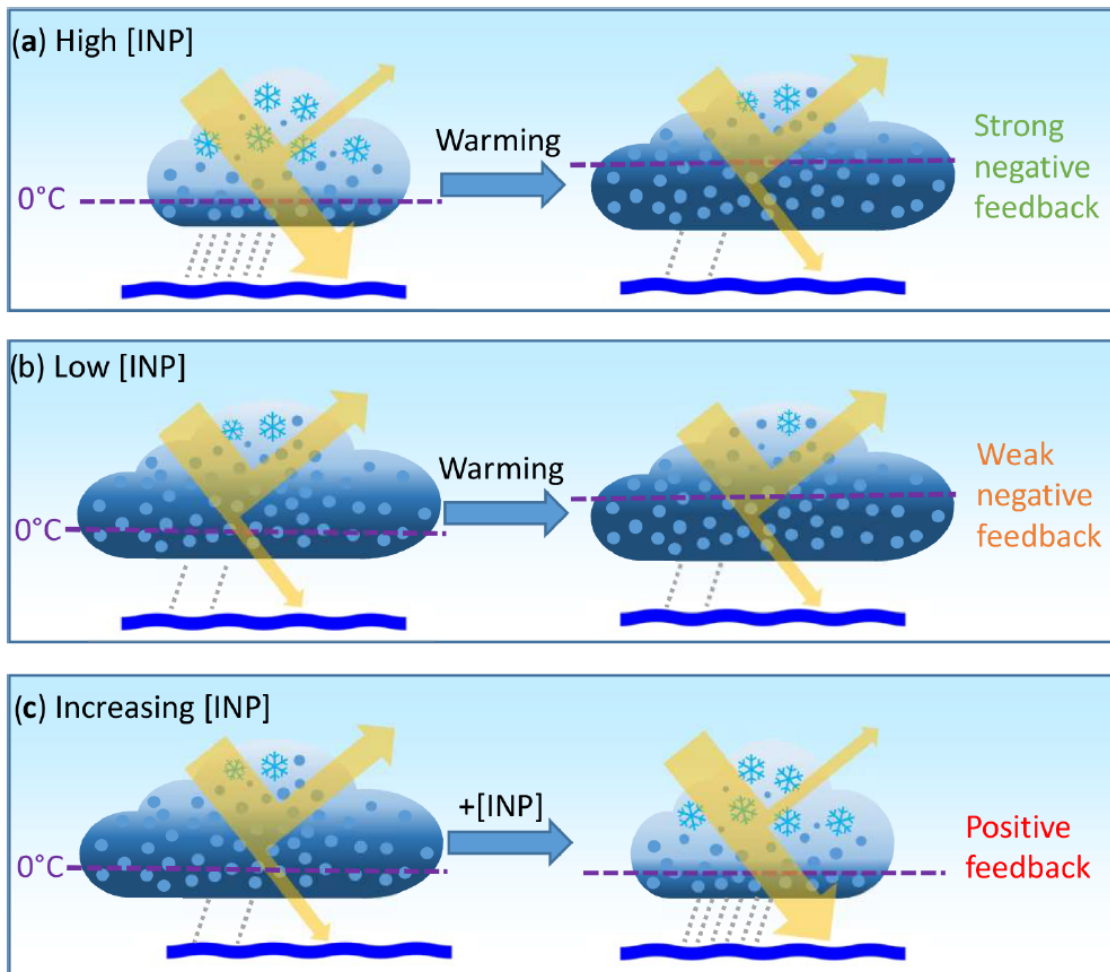


**Figure 1.14: Mixed phase clouds' possible responses to climate change, taken from Murray et al. (2021). a) Warming resulting in lifting of isotherm (purple line) in scenario with high INP. b) Warming in scenario with low INP. c) Scenario where temperature does not change but INPs increase.**

Changes to the abundance and to the nature of the INP supply would result in a separate feedback regardless of temperature change, where increasing INP would increase ice production and lower albedo resulting in positive feedback, and vice-versa (Fig 1.14c). Several possible changes to INP sources resulting from a warming planet have been hypothesised, yet they are difficult to prove due to a sparse record of global INP measurements. For example, new sources of INP may emerge from melting permafrost (Creamean et al., 2020) and previously glaciated land in high latitudes (particularly in the northern hemisphere such as Greenland), which may also harbour

biological INP that benefit from increased productivity (Sanchez-Marroquin et al., 2020; Tobo et al., 2019).

## References

- Adams, M. P., Atanasova, N. S., Sofieva, S., Ravantti, J., Heikkinen, A., Brasseur, Z., Duplissy, J., Bamford, D. H., and Murray, B. J.: Ice nucleation by viruses and their potential for cloud glaciation, *Biogeosciences*, 18, 4431-4444, 2021.
- Ansmann, A., Tesche, M., Althausen, D., Müller, D., Seifert, P., Freudenthaler, V., Heese, B., Wiegner, M., Pisani, G., Knippertz, P., and Dubovik, O.: Influence of Saharan dust on cloud glaciation in southern Morocco during the Saharan Mineral Dust Experiment, *Journal of Geophysical Research: Atmospheres*, 113, 2008.
- Atkinson, J. D., Murray, B. J., Woodhouse, M. T., Whale, T. F., Baustian, K. J., Carslaw, K. S., Dobbie, S., O'Sullivan, D., and Malkin, T. L.: The importance of feldspar for ice nucleation by mineral dust in mixed-phase clouds, *Nature*, 498, 355-358, 2013.
- Augustin, S., Wex, H., Niedermeier, D., Pummer, B., Grothe, H., Hartmann, S., Tomsche, L., Clauss, T., Voigtländer, J., Ignatius, K., and Stratmann, F.: Immersion freezing of birch pollen washing water, *Atmos. Chem. Phys.*, 13, 10989-11003, 2013.
- Baloh, P., Els, N., David, R. O., Larose, C., Whitmore, K., Sattler, B., and Grothe, H.: Assessment of Artificial and Natural Transport Mechanisms of Ice Nucleating Particles in an Alpine Ski Resort in Obergurgl, Austria, *Frontiers in Microbiology*, 10, 2278, 2019.
- Bogler, S. and Borduas-Dedekind, N.: Lignin's ability to nucleate ice via immersion freezing and its stability towards physicochemical treatments and atmospheric processing, *Atmos. Chem. Phys.*, 20, 14509-14522, 2020.
- Campbell, J. M., Meldrum, F. C., and Christenson, H. K.: Observing the formation of ice and organic crystals in active sites, *Proceedings of the National Academy of Sciences*, 114, 810, 2017.
- Ceppi, P., Brient, F., Zelinka, M. D., and Hartmann, D. L.: Cloud feedback mechanisms and their representation in global climate models, *WIREs Climate Change*, 8, e465, 2017.
- Choi, Y.-S., Lindzen, R. S., Ho, C.-H., and Kim, J.: Space observations of cold-cloud phase change, *Proceedings of the National Academy of Sciences*, 107, 11211, 2010.
- Christenson, H. K.: Two-step crystal nucleation via capillary condensation, *CrystEngComm*, 15, 2030-2039, 2013.
- Christner, B. C., Cai, R., Morris, C. E., McCarter, K. S., Foreman, C. M., Skidmore, M. L., Montross, S. N., and Sands, D. C.: Geographic, seasonal, and precipitation chemistry influence on the abundance and activity of biological ice nucleators in rain and snow, *Proc Natl Acad Sci U S A*, 105, 18854-18859, 2008.

Conen, F., Morris, C. E., Leifeld, J., Yakutin, M. V., and Alewell, C.: Biological residues define the ice nucleation properties of soil dust, *Atmospheric Chemistry and Physics*, 11, 9643-9648, 2011.

Conen, F., Rodríguez, S., Hülin, C., Henne, S., Herrmann, E., Bukowiecki, N., and Alewell, C.: Atmospheric ice nuclei at the high-altitude observatory Jungfraujoch, Switzerland, *Tellus B: Chemical and Physical Meteorology*, 67, 25014, 2015.

Creamean, J. M., Hill, T. C. J., DeMott, P. J., Uetake, J., Kreidenweis, S., and Douglas, T. A.: Thawing permafrost: an overlooked source of seeds for Arctic cloud formation, *Environmental Research Letters*, 15, 084022, 2020.

Creamean, J. M., Suski, K. J., Rosenfeld, D., Cazorla, A., DeMott, P. J., Sullivan, R. C., White, A. B., Ralph, F. M., Minnis, P., Comstock, J. M., Tomlinson, J. M., and Prather, K. A.: Dust and Biological Aerosols from the Sahara and Asia Influence Precipitation in the Western U.S, *Science*, 339, 1572, 2013.

Cziczo, D. J., Froyd, K. D., Hoose, C., Jensen, E. J., Diao, M., Zondlo, M. A., Smith, J. B., Twohy, C. H., and Murphy, D. M.: Clarifying the Dominant Sources and Mechanisms of Cirrus Cloud Formation, *Science*, 340, 1320-1324, 2013.

de Boer, G., Morrison, H., Shupe, M. D., and Hildner, R.: Evidence of liquid dependent ice nucleation in high-latitude stratiform clouds from surface remote sensors, *Geophysical Research Letters*, 38, 2011.

DeMott, P. J., Prenni, A. J., Liu, X., Kreidenweis, S. M., Petters, M. D., Twohy, C. H., Richardson, M. S., Eidhammer, T., and Rogers, D. C.: Predicting global atmospheric ice nuclei distributions and their impacts on climate, *Proceedings of the National Academy of Sciences*, 107, 11217, 2010.

Field, P. R., Lawson, R. P., Brown, P. R. A., Lloyd, G., Westbrook, C., Moisseev, D., Miltenberger, A., Nenes, A., Blyth, A., Choulaton, T., Connolly, P., Buehl, J., Crosier, J., Cui, Z., Dearden, C., DeMott, P., Flossmann, A., Heymsfield, A., Huang, Y., Kalesse, H., Kanji, Z. A., Korolev, A., Kirchgaessner, A., Lasher-Trapp, S., Leisner, T., McFarquhar, G., Phillips, V., Stith, J., and Sullivan, S.: Secondary Ice Production: Current State of the Science and Recommendations for the Future, *Meteorological Monographs*, 58, 7.1-7.20, 2017.

Fröhlich-Nowoisky, J., Hill, T. C. J., Pummer, B. G., Yordanova, P., Franc, G. D., and Pöschl, U.: Ice nucleation activity in the widespread soil fungus *Mortierella alpina*, *Biogeosciences*, 12, 1057-1071, 2015.

Garcia, E., Hill, T. C. J., Prenni, A. J., DeMott, P. J., Franc, G. D., and Kreidenweis, S. M.: Biogenic ice nuclei in boundary layer air over two U.S. High Plains agricultural regions, *Journal of Geophysical Research: Atmospheres*, 117, n/a-n/a, 2012.

Hallett, J. and Mossop, S. C.: Production of secondary ice particles during the riming process, *Nature*, 249, 26-28, 1974.

Harrison, A. D., Lever, K., Sanchez-Marroquin, A., Holden, M. A., Whale, T. F., Tarn, M. D., McQuaid, J. B., and Murray, B. J.: The ice-nucleating ability of quartz immersed in water and its atmospheric importance compared to K-feldspar, *Atmos. Chem. Phys.*, 19, 11343-11361, 2019.

Harrison, A. D., Whale, T. F., Carpenter, M. A., Holden, M. A., Neve, L., and Sullivan, D., Vergara Temprado, J., and Murray, B. J.: Not all feldspars are equal: a survey of ice nucleating properties

across the feldspar group of minerals, *Atmospheric Chemistry and Physics*, 16, 10927-10940, 2016.

Hartmann, D. L., Ockert-Bell, M. E., and Michelsen, M. L.: The Effect of Cloud Type on Earth's Energy Balance: Global Analysis, *Journal of Climate*, 5, 1281-1304, 1992.

Henderson-Begg, S. K., Hill, T., Thyrrhaug, R., Khan, M., and Moffett, B. F.: Terrestrial and airborne non-bacterial ice nuclei, *Atmospheric Science Letters*, 10, 215-219, 2009.

Herbert, R. J., Murray, B. J., Dobbie, S. J., and Koop, T.: Sensitivity of liquid clouds to homogenous freezing parameterizations, *Geophysical Research Letters*, 42, 1599-1605, 2015.

Heymsfield, A. J., Krämer, M., Luebke, A., Brown, P., Cziczo, D. J., Franklin, C., Lawson, P., Lohmann, U., McFarquhar, G., Ulanowski, Z., and Van Tricht, K.: Cirrus Clouds, *Meteorological Monographs*, 58, 2.1-2.26, 2017.

Hill, T. C. J., Moffett, B. F., Demott, P. J., Georgakopoulos, D. G., Stump, W. L., and Franc, G. D.: Measurement of ice nucleation-active bacteria on plants and in precipitation by quantitative PCR, *Applied and environmental microbiology*, 80, 1256-1267, 2014.

Hiranuma, N., Adachi, K., Bell, D. M., Belosi, F., Beydoun, H., Bhaduri, B., Bingemer, H., Budke, C., Clemen, H. C., Conen, F., Cory, K. M., Curtius, J., DeMott, P. J., Eppers, O., Grawe, S., Hartmann, S., Hoffmann, N., Höhler, K., Jantsch, E., Kiselev, A., Koop, T., Kulkarni, G., Mayer, A., Murakami, M., Murray, B. J., Nicosia, A., Petters, M. D., Piazza, M., Polen, M., Reicher, N., Rudich, Y., Saito, A., Santachiara, G., Schiebel, T., Schill, G. P., Schneider, J., Segev, L., Stopelli, E., Sullivan, R. C., Suski, K., Szakáll, M., Tajiri, T., Taylor, H., Tobo, Y., Ullrich, R., Weber, D., Wex, H., Whale, T. F., Whiteside, C. L., Yamashita, K., Zelenyuk, A., and Möhler, O.: A comprehensive characterization of ice nucleation by three different types of cellulose particles immersed in water, *Atmos. Chem. Phys.*, 19, 4823-4849, 2019.

Hoose, C., Kristjánsson, J. E., and Burrows, S. M.: How important is biological ice nucleation in clouds on a global scale?, *Environmental Research Letters*, 5, 024009, 2010a.

Hoose, C., Kristjánsson, J. E., Chen, J.-P., and Hazra, A.: A Classical-Theory-Based Parameterization of Heterogeneous Ice Nucleation by Mineral Dust, Soot, and Biological Particles in a Global Climate Model, *Journal of the Atmospheric Sciences*, 67, 2483-2503, 2010b.

Joly, M., Attard, E., Sancelme, M., Deguillaume, L., Guilbaud, C., Morris, C. E., Amato, P., and Delort, A.-M.: Ice nucleation activity of bacteria isolated from cloud water, *Atmospheric Environment*, 70, 392-400, 2013.

Kanitz, T., Seifert, P., Ansmann, A., Engelmann, R., Althausen, D., Casiccia, C., and Rohwer, E. G.: Contrasting the impact of aerosols at northern and southern

- midlatitudes on heterogeneous ice formation, *Geophysical Research Letters*, 38, 2011.
- Kanji, Z. A., Ladino, L. A., Wex, H., Boose, Y., Burkert-Kohn, M., Cziczo, D. J., and Krämer, M.: Overview of Ice Nucleating Particles, *Meteorological Monographs*, 58, 1.1-1.33, 2017.
- Kaufmann, L., Marcolli, C., Hofer, J., Pinti, V., Hoyle, C. R., and Peter, T.: Ice nucleation efficiency of natural dust samples in the immersion mode, *Atmospheric Chemistry and Physics*, 16, 11177-11206, 2016.
- Knopf, D. A., Alpert, P. A., and Wang, B.: The Role of Organic Aerosol in Atmospheric Ice Nucleation: A Review, *ACS Earth and Space Chemistry*, 2, 168-202, 2018.
- Koop, T. and Murray, B. J.: A physically constrained classical description of the homogeneous nucleation of ice in water, *The Journal of Chemical Physics*, 145, 211915, 2016.
- Kulkarni, G.: Immersion Freezing of Total Ambient Aerosols and Ice Residuals, *Atmosphere*, 9, 55, 2018.
- Lloyd, G., Choularton, T., Bower, K., Crosier, J., Gallagher, M., Flynn, M., Dorsey, J., Liu, D., Taylor, J. W., Schlenczek, O., Fugal, J., Borrmann, S., Cotton, R., Field, P., and Blyth, A.: Small ice particles at slightly supercooled temperatures in tropical maritime convection, *Atmos. Chem. Phys.*, 20, 3895-3904, 2020.
- Lohmann, U. and Feichter, J.: Global indirect aerosol effects: a review, *Atmos. Chem. Phys.*, 5, 715-737, 2005.
- Maki, L. R., Galyan, E. L., Chang-Chien, M. M., and Caldwell, D. R.: Ice nucleation induced by *Pseudomonas syringae*, *Appl Microbiol*, 28, 456-459, 1974.
- Marcolli, C.: Deposition nucleation viewed as homogeneous or immersion freezing in pores and cavities, *Atmospheric Chemistry and Physics*, 14, 2071-2104, 2014.
- Mossop, S. C. and Ono, A.: Measurements of Ice Crystal Concentration in Clouds, *Journal of Atmospheric Sciences*, 26, 130-137, 1969.
- Murray, B. J., Carslaw, K. S., and Field, P. R.: Opinion: Cloud-phase climate feedback and the importance of ice-nucleating particles, *Atmos. Chem. Phys.*, 21, 665-679, 2021.
- Murray, B. J., O'Sullivan, D., Atkinson, J. D., and Webb, M. E.: Ice nucleation by particles immersed in supercooled cloud droplets, *Chem Soc Rev*, 41, 6519-6554, 2012.
- Niemand, M., Möhler, O., Vogel, B., Vogel, H., Hoose, C., Connolly, P., Klein, H., Bingemer, H., DeMott, P., Skrotzki, J., and Leisner, T.: A Particle-Surface-Area-Based Parameterization of Immersion Freezing on Desert Dust Particles, *Journal of the Atmospheric Sciences*, 69, 3077-3092, 2012.
- O'Sullivan, D., Murray, B. J., Malkin, T. L., Whale, T. F., Umo, N. S., Atkinson, J. D., Price, H. C., Baustian, K. J., Browse, J., and Webb, M. E.: Ice nucleation by fertile soil dusts: relative importance of mineral and biogenic components, *Atmos. Chem. Phys.*, 14, 1853-1867, 2014.

O'Sullivan, D., Murray, B. J., Ross, J. F., and Webb, M. E.: The adsorption of fungal ice-nucleating proteins on mineral dusts: a terrestrial reservoir of atmospheric ice-nucleating particles, *Atmos. Chem. Phys.*, 16, 7879-7887, 2016.

Pouleur, S., Richard, C., Martin, J. G., and Antoun, H.: Ice Nucleation Activity in *Fusarium acuminatum* and *Fusarium avenaceum*, *Applied and environmental microbiology*, 58, 2960-2964, 1992.

Pummer, B. G., Bauer, H., Bernardi, J., Bleicher, S., and Grothe, H.: Suspendable macromolecules are responsible for ice nucleation activity of birch and conifer pollen, *Atmos. Chem. Phys.*, 12, 2541-2550, 2012.

Sanchez-Marroquin, A., Arnalds, O., Baustian-Dorsi, K. J., Browse, J., Dagsson-Waldhauserova, P., Harrison, A. D., Maters, E. C., Pringle, K. J., Vergara-Temprado, J., Burke, I. T., McQuaid, J. B., Carslaw, K. S., and Murray, B. J.: Iceland is an episodic source of atmospheric ice-nucleating particles relevant for mixed-phase clouds, *Science Advances*, 6, eaba8137, 2020.

Schneider, J., Höhler, K., Heikkilä, P., Keskinen, J., Bertozzi, B., Bogert, P., Schorr, T., Umo, N. S., Vogel, F., Brasseur, Z., Wu, Y., Hakala, S., Duplissy, J., Moisseev, D., Kulmala, M., Adams, M. P., Murray, B. J., Korhonen, K., Hao, L., Thomson, E. S., Castarède, D., Leisner, T., Petäjä, T., and Möhler, O.: The seasonal cycle of ice-nucleating particles linked to the abundance of biogenic aerosol in boreal forests, *Atmos. Chem. Phys.*, 21, 3899-3918, 2021.

Spracklen, D. V. and Heald, C. L.: The contribution of fungal spores and bacteria to regional and global aerosol number and ice nucleation immersion freezing rates, *Atmos. Chem. Phys.*, 14, 9051-9059, 2014.

Storelvmo, T.: Aerosol Effects on Climate via Mixed-Phase and Ice Clouds, *Annual Review of Earth and Planetary Sciences*, 45, 199-222, 2017.

Storelvmo, T. and Tan, I.: The Wegener-Bergeron-Findeisen process - Its discovery and vital importance for weather and climate, *Meteorologische Zeitschrift*, 24, 455-461, 2015.

Suski, K. J., Hill, T. C. J., Levin, E. J. T., Miller, A., DeMott, P. J., and Kreidenweis, S. M.: Agricultural harvesting emissions of ice nucleating particles, *Atmospheric Chemistry and Physics Discussions*, doi: 10.5194/acp-2018-348, 2018. 1-30, 2018.

Tobo, Y., Adachi, K., DeMott, P. J., Hill, T. C. J., Hamilton, D. S., Mahowald, N. M., Nagatsuka, N., Ohata, S., Uetake, J., Kondo, Y., and Koike, M.: Glacially sourced dust as a potentially significant source of ice nucleating particles, *Nature Geoscience*, 12, 253-258, 2019.

Vali, G., DeMott, P. J., Möhler, O., and Whale, T. F.: Technical Note: A proposal for ice nucleation terminology, *Atmos. Chem. Phys.*, 15, 10263-10270, 2015.

Vergara-Temprado, J., Miltenberger, A. K., Furtado, K., Grosvenor, D. P., Shipway, B. J., Hill, A. A., Wilkinson, J. M., Field, P. R., Murray, B. J., and Carslaw, K. S.: Strong control of Southern Ocean cloud reflectivity by ice-nucleating particles, *Proc Natl Acad Sci U S A*, 115, 2687-2692, 2018.

Vergara-Temprado, J., Murray, B. J., Wilson, T. W., amp, apos, Sullivan, D., Browse, J., Pringle, K. J., Ardon-Dryer, K., Bertram, A. K., Burrows, S. M.,

Ceburnis, D., DeMott, P. J., Mason, R. H., and Dowd, C. D., Rinaldi, M., and Carslaw, K. S.: Contribution of feldspar and marine organic aerosols to global ice nucleating particle concentrations, *Atmospheric Chemistry and Physics*, 17, 3637-3658, 2017.

Welti, A., Bigg, E. K., DeMott, P. J., Gong, X., Hartmann, M., Harvey, M., Henning, S., Herenz, P., Hill, T. C. J., Hornblow, B., Leck, C., Löffler, M., McCluskey, C. S., Rauker, A. M., Schmale, J., Tatzelt, C., van Pinxteren, M., and Stratmann, F.: Ship-based measurements of ice nuclei concentrations over the Arctic, Atlantic, Pacific and Southern oceans, *Atmos. Chem. Phys.*, 20, 15191-15206, 2020.

Wilson, T. W., Ladino, L. A., Alpert, P. A., Breckels, M. N., Brooks, I. M., Browse, J., Burrows, S. M., Carslaw, K. S., Huffman, J. A., Judd, C., Kilthau, W. P., Mason, R. H., McFiggans, G., Miller, L. A., Najera, J. J., Polishchuk, E., Rae, S., Schiller, C. L., Si, M., Temprado, J. V., Whale, T. F., Wong, J. P., Wurl, O., Yakobi-Hancock, J. D., Abbatt, J. P., Aller, J. Y., Bertram, A. K., Knopf, D. A., and Murray, B. J.: A marine biogenic source of atmospheric ice-nucleating particles, *Nature*, 525, 234-238, 2015.

Yakobi-Hancock, J. D., Ladino, L. A., and Abbatt, J. P. D.: Feldspar minerals as efficient deposition ice nuclei, *Atmospheric Chemistry and Physics*, 13, 11175-11185, 2013.

Yang, J., Wang, Z., Heymsfield, A. J., DeMott, P. J., Twohy, C. H., Suski, K. J., and Toohey, D. W.: High ice concentration observed in tropical maritime stratiform mixed-phase clouds with top temperatures warmer than  $-8^{\circ}\text{C}$ , *Atmospheric Research*, 233, 104719, 2020.

Zolles, T., Burkart, J., Hausler, T., Pummer, B., Hitzenberger, R., and Grothe, H.: Identification of ice nucleation active sites on feldspar dust particles, *J Phys Chem A*, 119, 2692-2700, 2015.

## 1.5 Ice-nucleating materials

There is no single universal property that makes a material an effective ice-nucleator and this is underlined by the fact that the most active ice-nucleating substances known are incredibly diverse in terms of their composition. For example, the most active reported substances include bacteria, organic molecules, minerals and silver iodide (AgI), all capable of nucleating ice at warm as  $-2\text{ }^{\circ}\text{C}$ . Here we briefly discuss some fundamental properties that lead to high INA and then fully introduce known substances that act as particularly active heterogeneous ice-nucleators. These have been divided into two broad classes, insoluble and soluble.

### 1.5.1 Fundamental prerequisites for ice-nucleating materials

According to CNT a heterogeneous ice-nucleator is a substrate that arranges and orders water molecules to form an embryo of critical size to become a nucleus. As the size of the critical radius required increases exponentially as the temperature approaches  $0\text{ }^{\circ}\text{C}$  this becomes increasingly unlikely. Therefore, the materials with the highest ice-nucleating activities will have some physical or chemical configuration (or most likely a combination of these) that is highly effective at arranging water molecules into an ice-like state (Kanji et al., 2017; Maeda, 2021). A list of five prerequisites was proposed by (Pruppacher and Klett, 1997) for atmospheric particles to have at least some ice-nucleating activity:

1. Insolubility: Providing a surface or interface for water molecules to interact
2. Active sites: Based on early observations that nucleation occurs at discrete points such as surface defects (Fukuta and Mason, 1963)
3. Size: Particles must be large enough to contain an active site and be at least as large as the size of the critical ice nucleus
4. Lattice matching: Substances with similar crystal configurations to those of ice have a templating effect facilitating ice-nucleation by epitaxial growth. AgI is a classic early discovery of this (Vonnegut, 1947).
5. Chemical bonding: The surface must be favourable for bonding with or orientating water molecules.

Of these requirements, insolubility and size are now the most challenged due to the discovery of a plethora of biogenic ice-nucleating macromolecules which induce ice-nucleation in a dissolved form (Huang et al., 2021; Kanji et al., 2017; Pummer et al.,

2015), although the activity of macromolecules does seem to scale with their size (Pummer et al., 2015). A challenge to the lattice-matching requirement comes from the fact that there are examples of substances with good ice lattice-matches which do not nucleate ice strongly - BaF<sub>2</sub> for example (Conrad et al., 2005)- and substances with poor lattice-match that do nucleate ice strongly, such as cholesterol (Sosso et al., 2018). This has also been challenged with computer simulation studies that suggest lattice-match is not a sole requisite for ice-nucleation on mineral surfaces (Fitzner et al., 2015; Pedevilla et al., 2017). Degree of crystallinity has, however, been shown to correlate with higher ice-nucleating activity in the case of volcanic ash (Maters et al., 2019) and mineral samples that had been melted into glass and reground (Cook et al., 2020). Chemical bonding aspects such as hydrophobicity (Cox et al., 2015; Lupi and Molinero, 2014), hydroxyl group density (Kumar et al., 2019; Pedevilla et al., 2017) and interfacial water (Kumar et al., 2021) may also play roles. Also, experiments have shown how the addition of electrolytes can change the apparent ice-nucleating ability of substances and this can be ‘tuned’ by changing the species of the ion (He et al., 2016; Kumar et al., 2018; Whale et al., 2018). Microscopic surface features such as cracks, steps, dislocations and pores may create conditions conducive to ice-nucleation on otherwise chemically homogeneous substrates (Campbell et al., 2017; Hiranuma et al., 2014). Direct evidence for these discrete sites has been identified experimentally as active sites on mineral samples (Holden et al., 2019; Kiselev et al., 2017). Enhancement of IN sites by changing topography may be dependent on the material however, for example silicon surfaces scratched with diamond powder of a range of sizes did not enhance its ice-nucleating activity (Campbell et al., 2015). Overall, this underlines the complexity of heterogeneous IN and the difficulty of predicting the activity of a substance or even designing bespoke ice-nucleation substances which has not yet been done to date.

### **1.5.2 Insoluble or particulate ice-nucleating materials**

AgI is one of the earliest discovered (Vonnegut, 1947) substances to have ice-nucleating properties and has received much investigation (Marcolli et al., 2016) due to its role in cloud seeding for artificial enhancement of rainfall (French et al., 2018). Ice-nucleation temperatures of up to -3 °C have been reported and related compounds – AgCl-AgI solid solution (Palanisamy et al., 1986) and 3AgI·NH<sub>4</sub>I·H<sub>2</sub>O (Davis et al., 1975) – with slightly better lattice matches to ice have been reported to nucleate ice at

-1 °C (Marcolli et al., 2016). Cholesterol, a crystalline organic lipid compound of the steroid family, has also been known as a strong ice-nucleator with temperatures of up to -4 °C reported (Head, 1961; Sosso et al., 2018). Its high INA has been attributed to a favourable combination of topographic sites and surface structure allowing unusual hydrogen bonded cages of water to form (Sosso et al., 2018).

The INA of minerals received relatively little attention until the importance of understanding the role ice-nucleation in the climate system became clear by the 21<sup>st</sup> Century. Clay minerals, such as kaolinite, were originally thought of as being active ice-nucleating minerals and are often still referred to in the literature as such. This has since been superseded by the discovery that feldspar minerals are the most active on a surface active-site density basis (Atkinson et al., 2013; Zolles et al., 2015) with quartz (Harrison et al., 2019) and pyroxenes (Jahn et al., 2019) and some volcanic ashes (Maters et al., 2019) also having reported activities approaching -5 °C.

Feldspars are a group of framework silicate minerals that constitute the most abundant mineral in the Earth's crust, are ubiquitous in igneous, metamorphic and some sedimentary rocks and also in atmospheric mineral dusts. Compositions of feldspar can be plotted on a ternary diagram (Fig. 1a) and fall along two continuous series – plagioclase feldspars and alkali feldspars – with three endmembers, anorthite ( $\text{CaAl}_2\text{Si}_2\text{O}_8$ ), Albite ( $\text{NaAlSi}_3\text{O}_8$ ) and K-feldspar ( $\text{KAlSi}_3\text{O}_8$ ). Microcline, orthoclase and sanidine are polymorphs of K-feldspar rich feldspars, each with increasing degrees of disorder of  $\text{Si}^{4+}$  and  $\text{Al}^{3+}$  in their crystal structures. Solid solution along the two series takes place with  $\text{Na}^+$  substituting for  $\text{Ca}^{2+}$  in plagioclases and for  $\text{K}^+$  with the alkali feldspars meaning feldspars can crystallise with compositions anywhere along these series. However, alkali feldspar solid solutions are thermodynamically unstable at lower (below 700 °C for the most unstable mixture) temperatures and will slowly undergo exsolution (solid state un-mixing). Therefore, a common feature of K-rich feldspars (commonly referred to simply as K-feldspars here) is exsolution microtexture or perthitic texture, where unmixed regions of Na-rich and K-rich feldspars are visible (Figs 1b and c).

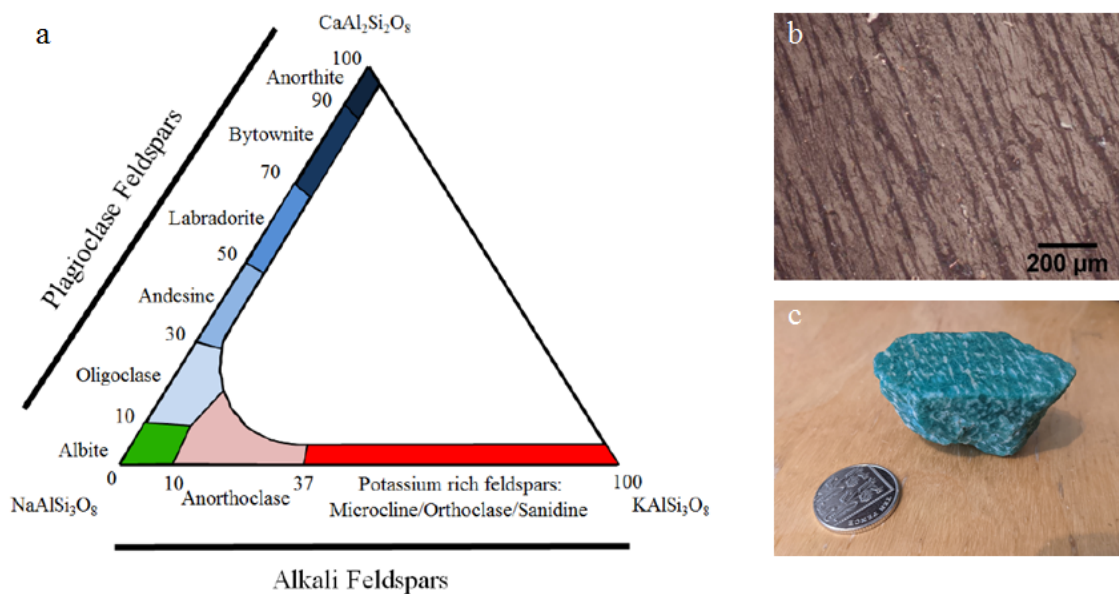


**Figure 1.15: a) Feldspar group compositions plotted on ternary diagram (taken from Harrison et al (2016)). b) Thin section of perthitic orthoclase under crossed polarised light showing exsolution microtexture lamellae. c) Specimen of amazonite, a green variant of microcline, showing exsolution microtexture on a larger scale. White lamellae of albite are visible with a preferred orientation.**

Of the many varieties of feldspar, K-feldspars, and particularly the microcline polymorph, have the highest ice-nucleating abilities (Fig. 1.16a) with some samples having reported activities of  $-2^{\circ}\text{C}$  (Harrison et al., 2016; Peckhaus et al., 2016; Welti et al., 2019). Plagioclase feldspars are the next most active class with albite (Na rich) compositions tending to have higher activities than anorthite (Ca rich) samples (Harrison et al., 2016). The propensity of K-rich feldspars for being more ice-active than plagioclases has been correlated with the presence of exsolution microtexture, where the strain leads to nanoscale topographical features such as pull-aparts and nanotunnels which are hypothesised to harbour active sites (Whale et al., 2017). Imaging using environmental SEM (E-SEM) of ice crystals nucleating from water vapour in on surfaces of microcline aligned along the (100) plane suggests exsolution exposes a surface that is very favourable for arranging water molecules into ice embryos (Kiselev et al., 2017; Kiselev et al., 2021). However, the same technique also showed that sites of nucleation appeared to associate with micropores (Holden et al., 2019; Pach and Verdaguer, 2019). Micropores are microscopic cavities created during the formation of the crystal or after formation by annealing of cracks and are often

associated with hydrothermal alteration (Wilkinson, 2001). Some varieties of feldspar, for example Amelia Albite, USA and Mt Malosa Microcline, Malawi, have extremely high activity (above  $-5\text{ }^{\circ}\text{C}$  and up to  $-2\text{ }^{\circ}\text{C}$ ) compared to equivalent samples of the same polymorphs for reasons that yet remain unclear.

### 1.5.3 Soluble or non-particulate ice-nucleating materials

Examples of soluble species with high INA are mainly of biological origin (Huang et al., 2021) with an exception being long-chain alcohol monolayers, which have been reported to nucleate ice at temperatures approaching  $0\text{ }^{\circ}\text{C}$  (Gavish et al., 1990). Whole biological structures such as bacteria (Maki et al., 1974) and fungal material (Pouleur et al., 1992) have been known to be efficient ice-nucleators but the sources of their activity have eventually been isolated as ice-nucleating macromolecules (INM) composed of proteins or polysaccharides (Govindarajan and Lindow, 1988; Pummer et al., 2015). Bacterial ice-nucleating INMs are proteins that contain beta sheets (Garnham et al., 2011) with alternating hydrophobic and hydrophilic patterns that interact with water molecules via  $-\text{OH}$  and  $-\text{NH}_2$  groups, templating water into an ice-like configuration (Davies, 2014). Encoded by the *ina* gene (Warren, 1987), they are thought to have evolved as a tool for plant pathogen bacteria to induce frost damage in their hosts. They are also the source of Snomax, a proteinaceous extract from *Pseudomonas syringae* which can nucleate ice as warm as  $-2\text{ }^{\circ}\text{C}$ . Snomax was originally developed for artificial snow production but has since become an important proxy for proteinaceous INMs in ice-nucleation research and also has been investigated as an ice-nucleating agent in cryopreservation (Teixeira et al., 2017). Fungal spores and pollen grains also release INMs with ice-nucleating temperatures reaching as warm as  $-4\text{ }^{\circ}\text{C}$  and  $-5\text{ }^{\circ}\text{C}$  respectively (Kunert et al., 2018; Pouleur et al., 1992; Tong et al., 2015), though in general pollen INMs are less active than fungi or bacterial INMs (Fig. 2b) and differ by being made of polysaccharides rather than proteinaceous (Dreischmeier et al., 2017; Pummer et al., 2012). As a result, they are resistant to heat, and enzymatic attack compared to proteinaceous INMs (Pummer et al., 2012) which are mostly denatured by heating above  $60\text{ }^{\circ}\text{C}$  (Kieft and Ruscetti, 1990; Pouleur et al., 1992).

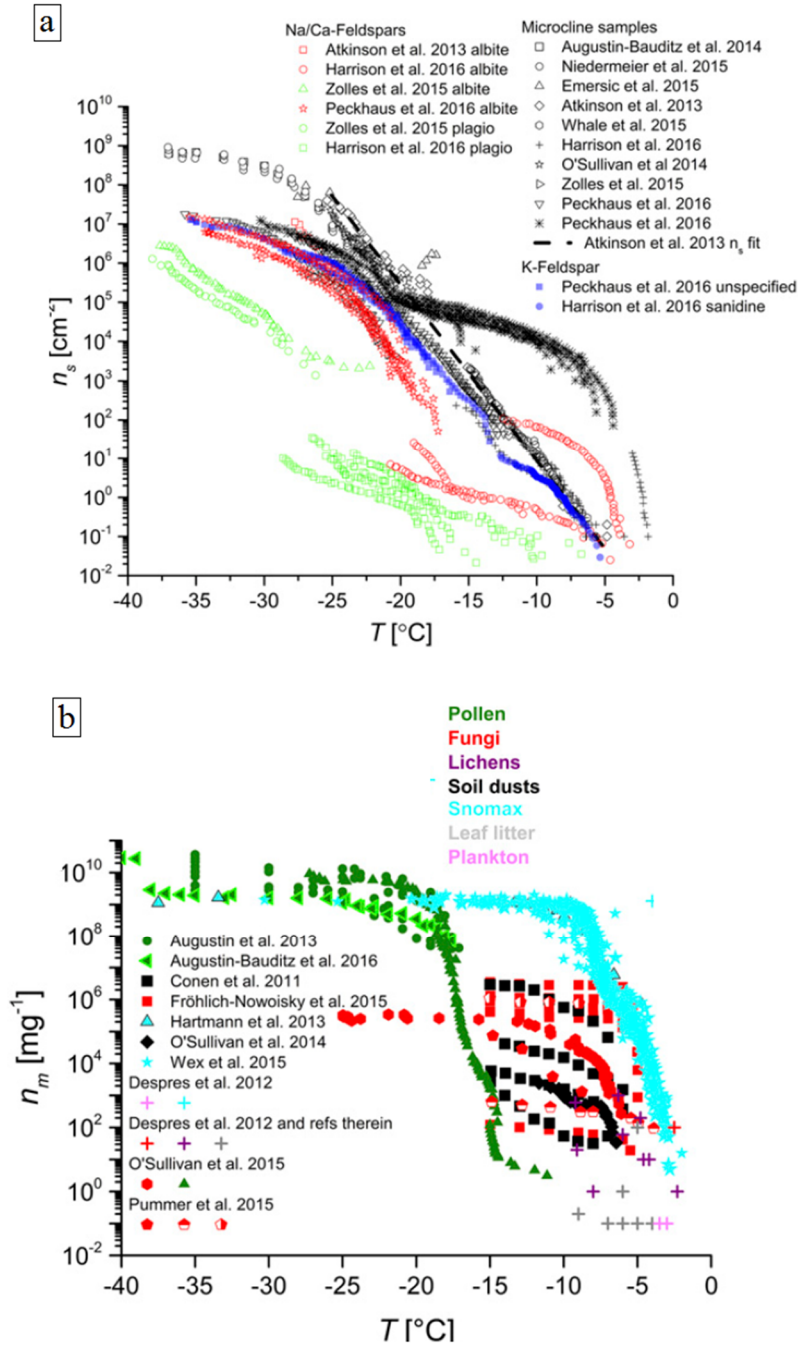


**Figure 1.16: Compilation of literature data taken from Kanji et al. (2017) showing relative ice-nucleating active site densities of biological INP (a) and feldspar variants (b).**

## References

Atkinson, J. D., Murray, B. J., Woodhouse, M. T., Whale, T. F., Baustian, K. J., Carslaw, K. S., Dobbie, S., O'Sullivan, D., and Malkin, T. L.: The importance of

feldspar for ice nucleation by mineral dust in mixed-phase clouds, *Nature*, 498, 355-358, 2013.

Campbell, J. M., Meldrum, F. C., and Christenson, H. K.: Is Ice Nucleation from Supercooled Water Insensitive to Surface Roughness?, *The Journal of Physical Chemistry C*, 119, 1164-1169, 2015.

Campbell, J. M., Meldrum, F. C., and Christenson, H. K.: Observing the formation of ice and organic crystals in active sites, *Proceedings of the National Academy of Sciences*, 114, 810, 2017.

Conrad, P., Ewing, G. E., Karlinsey, R. L., and Sadtchenko, V.: Ice nucleation on BaF<sub>2</sub>(111), *The Journal of Chemical Physics*, 122, 064709, 2005.

Cook, F., Lord, R., Sitbon, G., Stephens, A., Rust, A., and Schwarzacher, W.: A pyroelectric thermal sensor for automated ice nucleation detection, *Atmos. Meas. Tech.*, 13, 2785-2795, 2020.

Cox, S. J., Kathmann, S. M., Slater, B., and Michaelides, A.: Molecular simulations of heterogeneous ice nucleation. I. Controlling ice nucleation through surface hydrophilicity, *The Journal of Chemical Physics*, 142, 184704, 2015.

Davies, P. L.: Ice-binding proteins: a remarkable diversity of structures for stopping and starting ice growth, *Trends in Biochemical Sciences*, 39, 548-555, 2014.

Davis, B. L., Johnson, L. R., and Moeng, F. J.: An Explanation for the Unusual Nucleating Ability of Aerosols Produced from the AgI-NH<sub>4</sub>I-Acetone System, *Journal of Applied Meteorology and Climatology*, 14, 891-896, 1975.

Dreichmeier, K., Budke, C., Wiehemeier, L., Kottke, T., and Koop, T.: Boreal pollen contain ice-nucleating as well as ice-binding 'antifreeze' polysaccharides, *Sci Rep*, 7, 41890, 2017.

Fitzner, M., Sosso, G. C., Cox, S. J., and Michaelides, A.: The Many Faces of Heterogeneous Ice Nucleation: Interplay Between Surface Morphology and Hydrophobicity, *J Am Chem Soc*, 137, 13658-13669, 2015.

French, J. R., Friedrich, K., Tessorf, S. A., Rauber, R. M., Geerts, B., Rasmussen, R. M., Xue, L., Kunkel, M. L., and Blestrud, D. R.: Precipitation formation from orographic cloud seeding, *Proceedings of the National Academy of Sciences*, 115, 1168, 2018.

Fukuta, N. and Mason, B. J.: Epitaxial growth of ice on organic crystals, *Journal of Physics and Chemistry of Solids*, 24, 715-718, 1963.

Garnham, C. P., Campbell, R. L., Walker, V. K., and Davies, P. L.: Novel dimeric  $\beta$ -helical model of an ice nucleation protein with bridged active sites, *BMC Struct Biol*, 11, 36-36, 2011.

Gavish, M., Popovitz-Biro, R., Lahav, M., and Leiserowitz, L.: Ice Nucleation by Alcohols Arranged in Monolayers at the Surface of Water Drops, *Science*, 250, 973, 1990.

Govindarajan, A. G. and Lindow, S. E.: Size of bacterial ice-nucleation sites measured *in situ* by radiation inactivation analysis, *Proceedings of the National Academy of Sciences*, 85, 1334, 1988.

- Harrison, A. D., Lever, K., Sanchez-Marroquin, A., Holden, M. A., Whale, T. F., Tarn, M. D., McQuaid, J. B., and Murray, B. J.: The ice-nucleating ability of quartz immersed in water and its atmospheric importance compared to K-feldspar, *Atmos. Chem. Phys.*, 19, 11343-11361, 2019.
- Harrison, A. D., Whale, T. F., Carpenter, M. A., Holden, M. A., Neve, L., and Sullivan, D., Vergara Temprado, J., and Murray, B. J.: Not all feldspars are equal: a survey of ice nucleating properties across the feldspar group of minerals, *Atmospheric Chemistry and Physics*, 16, 10927-10940, 2016.
- He, Z., Xie Wen, J., Liu, Z., Liu, G., Wang, Z., Gao Yi, Q., and Wang, J.: Tuning ice nucleation with counterions on polyelectrolyte brush surfaces, *Science Advances*, 2, e1600345, 2016.
- Head, R. B.: Steroids as Ice Nucleators, *Nature*, 191, 1058-1059, 1961.
- Hiranuma, N., Hoffmann, N., Kiselev, A., Dreyer, A., Zhang, K., Kulkarni, G., Koop, T., and Möhler, O.: Influence of surface morphology on the immersion mode ice nucleation efficiency of hematite particles, *Atmospheric Chemistry and Physics*, 14, 2315-2324, 2014.
- Holden, M. A., Whale, T. F., Tarn, M. D., O'Sullivan, D., Walshaw, R. D., Murray, B. J., Meldrum, F. C., and Christenson, H. K.: High-speed imaging of ice nucleation in water proves the existence of active sites, *Sci Adv*, 5, eaav4316, 2019.
- Huang, S., Hu, W., Chen, J., Wu, Z., Zhang, D., and Fu, P.: Overview of biological ice nucleating particles in the atmosphere, *Environment International*, 146, 106197, 2021.
- Jahn, L. G., Fahy, W. D., Williams, D. B., and Sullivan, R. C.: Role of Feldspar and Pyroxene Minerals in the Ice Nucleating Ability of Three Volcanic Ashes, *ACS Earth and Space Chemistry*, 3, 626-636, 2019.
- Kanji, Z. A., Ladino, L. A., Wex, H., Boose, Y., Burkert-Kohn, M., Cziczo, D. J., and Krämer, M.: Overview of Ice Nucleating Particles, *Meteorological Monographs*, 58, 1.1-1.33, 2017.
- Kieft, T. L. and Ruscetti, T.: Characterization of biological ice nuclei from a lichen, *J Bacteriol*, 172, 3519-3523, 1990.
- Kiselev, A., Bachmann, F., Pedevilla, P., Cox, S. J., Michaelides, A., Gerthsen, D., and Leisner, T.: Active sites in heterogeneous ice nucleation-the example of K-rich feldspars, *Science*, 355, 367-371, 2017.
- Kiselev, A. A., Keinert, A., Gaedeke, T., Leisner, T., Sutter, C., Petrishcheva, E., and Abart, R.: Effect of chemically induced fracturing on the ice nucleation activity of alkali feldspar, *Atmos. Chem. Phys.*, 21, 11801-11814, 2021.
- Kumar, A., Bertram, A. K., and Patey, G. N.: Molecular Simulations of Feldspar Surfaces Interacting with Aqueous Inorganic Solutions: Interfacial Water/Ion Structure and Implications for Ice Nucleation, *ACS Earth and Space Chemistry*, 5, 2169-2183, 2021.
- Kumar, A., Marcolli, C., Luo, B., and Peter, T.: Ice nucleation activity of silicates and aluminosilicates in pure water and aqueous solutions – Part 1: The K-feldspar microcline, *Atmos. Chem. Phys.*, 18, 7057-7079, 2018.

- Kumar, A., Marcolli, C., and Peter, T.: Ice nucleation activity of silicates and aluminosilicates in pure water and aqueous solutions – Part 2: Quartz and amorphous silica, *Atmos. Chem. Phys.*, 19, 6035-6058, 2019.
- Kunert, A. T., Lamneck, M., Helleis, F., Pöschl, U., Pöhlker, M. L., and Fröhlich-Nowoisky, J.: Twin-plate Ice Nucleation Assay (TINA) with infrared detection for high-throughput droplet freezing experiments with biological ice nuclei in laboratory and field samples, *Atmos. Meas. Tech.*, 11, 6327-6337, 2018.
- Lupi, L. and Molinero, V.: Does Hydrophilicity of Carbon Particles Improve Their Ice Nucleation Ability?, *The Journal of Physical Chemistry A*, 118, 7330-7337, 2014.
- Maeda, N.: Brief Overview of Ice Nucleation, *Molecules*, 26, 2021.
- Maki, L. R., Galyan, E. L., Chang-Chien, M. M., and Caldwell, D. R.: Ice nucleation induced by *Pseudomonas syringae*, *Appl Microbiol*, 28, 456-459, 1974.
- Marcolli, C., Nagare, B., Welti, A., and Lohmann, U.: Ice nucleation efficiency of AgI: review and new insights, *Atmos. Chem. Phys.*, 16, 8915-8937, 2016.
- Maters, E. C., Dingwell, D. B., Cimarelli, C., Müller, D., Whale, T. F., and Murray, B. J.: The importance of crystalline phases in ice nucleation by volcanic ash, *Atmos. Chem. Phys.*, 19, 5451-5465, 2019.
- Pach, E. and Verdaguer, A.: Pores Dominate Ice Nucleation on Feldspars, *The Journal of Physical Chemistry C*, 123, 20998-21004, 2019.
- Palanisamy, M., Thangaraj, K., Gobinathan, R., and Ramasamy, P.: Effect of Particle Size on the Ice Nucleating Ability of AgI□AgBr□CuI System, *Crystal Research and Technology*, 21, 853-857, 1986.
- Peckhaus, A., Kiselev, A., Hiron, T., Ebert, M., and Leisner, T.: A comparative study of K-rich and Na/Ca-rich feldspar ice-nucleating particles in a nanoliter droplet freezing assay, *Atmospheric Chemistry and Physics*, 16, 11477-11496, 2016.
- Pedevilla, P., Fitzner, M., and Michaelides, A.: What makes a good descriptor for heterogeneous ice nucleation on OH-patterned surfaces, *Physical Review B*, 96, 2017.
- Pouleur, S., Richard, C., Martin, J. G., and Antoun, H.: Ice Nucleation Activity in *Fusarium acuminatum* and *Fusarium avenaceum*, *Applied and environmental microbiology*, 58, 2960-2964, 1992.
- Pruppacher, H. R. and Klett, J. D.: *Microphysics of Clouds and Precipitation*, Springer Netherlands, 1997.
- Pummer, B. G., Bauer, H., Bernardi, J., Bleicher, S., and Grothe, H.: Suspendable macromolecules are responsible for ice nucleation activity of birch and conifer pollen, *Atmos. Chem. Phys.*, 12, 2541-2550, 2012.
- Pummer, B. G., Budke, C., Augustin-Bauditz, S., Niedermeier, D., Felgitsch, L., Kampf, C. J., Huber, R. G., Liedl, K. R., Loerting, T., Moschen, T., Schauerperl, M., Tollinger, M., Morris, C. E., Wex, H., Grothe, H., Pöschl, U., Koop, T., and Fröhlich-Nowoisky, J.: Ice nucleation by water-soluble macromolecules, *Atmos. Chem. Phys.*, 15, 4077-4091, 2015.

- Sosso, G. C., Whale, T. F., Holden, M. A., Pedevilla, P., Murray, B. J., and Michaelides, A.: Unravelling the origins of ice nucleation on organic crystals, *Chemical Science*, 9, 8077-8088, 2018.
- Teixeira, M., Buff, S., Desnos, H., Loiseau, C., Bruyère, P., Joly, T., and Commin, L.: Ice nucleating agents allow embryo freezing without manual seeding, *Teriogenology*, 104, 173-178, 2017.
- Tong, H. J., Ouyang, B., Nikolovski, N., Lienhard, D. M., Pope, F. D., and Kalberer, M.: A new electrodynamic balance (EDB) design for low-temperature studies: application to immersion freezing of pollen extract bioaerosols, *Atmos. Meas. Tech.*, 8, 1183-1195, 2015.
- Vonnegut, B.: The Nucleation of Ice Formation by Silver Iodide, *Journal of Applied Physics*, 18, 593-595, 1947.
- Warren, G. J.: Bacterial Ice Nucleation: Molecular Biology and Applications, *Biotechnology and Genetic Engineering Reviews*, 5, 107-136, 1987.
- Welti, A., Lohmann, U., and Kanji, Z. A.: Ice nucleation properties of K-feldspar polymorphs and plagioclase feldspars, *Atmospheric Chemistry and Physics Discussions*, doi: 10.5194/acp-2018-1271, 2019. 1-25, 2019.
- Whale, T. F., Holden, M. A., Kulak, A. N., Kim, Y. Y., Meldrum, F. C., Christenson, H. K., and Murray, B. J.: The role of phase separation and related topography in the exceptional ice-nucleating ability of alkali feldspars, *Phys Chem Chem Phys*, 19, 31186-31193, 2017.
- Whale, T. F., Holden, M. A., Wilson, Theodore W., O'Sullivan, D., and Murray, B. J.: The enhancement and suppression of immersion mode heterogeneous ice-nucleation by solutes, *Chemical Science*, 9, 4142-4151, 2018.
- Wilkinson, J. J.: Fluid inclusions in hydrothermal ore deposits, *Lithos*, 55, 229-272, 2001.
- Zolles, T., Burkart, J., Hausler, T., Pummer, B., Hitzenberger, R., and Grothe, H.: Identification of ice nucleation active sites on feldspar dust particles, *J Phys Chem A*, 119, 2692-2700, 2015.

## 1.6 Project objectives

At the core of this project is the synergy between the understanding of cryopreservation and ice formation in clouds. Both fields, while being very different in their applications and objectives have a requirement for an understanding of the process of ice nucleation. Hence, the aim of this project is to apply discoveries made in the field of atmospheric sciences on the ice-nucleating properties of minerals to improving cryopreservation processes and also to feed what we learnt in cryopreservation back into the atmospheric sciences.

This PhD is a CASE (Collaborative Awards in Science and Engineering) in partnership with Asymptote Ltd (now part of Cytiva) who are specialists in cryochain technology: the sequence of equipment and materials needed for successful and consistent cryopreservation. Part of this sequence includes control of IN and the discovery of feldspar's exceptional ice-nucleating ability (Atkinson et al., 2013; Harrison et al., 2016; Peckhaus et al., 2016) is the basis of a product in development called IceStart™ (Morris and Lamb, 2018). These are disposable plastic devices containing a chemical ice-nucleating agent that are to be inserted into a cryobiological container, for example a 96-well plate, in a sterile manner (Fig. 1) before cryopreservation and removed upon thawing. The high ice nucleating ability, low cost and chemical inertness of feldspar make it ideal for controlling ice-nucleation in small liquid volumes such as those used in multiwell plates, which are standard platform for high-throughput screening assays for drug discovery (Michelini et al., 2010). Cultures of primary cells, such as primary rat hepatocytes, can be purchased in fresh form and used as in-vitro for toxicology screening (not previously frozen) but cost several hundred pounds each. If these could be purchased in cryopreserved format this would reduce costs, increase the volume and consistency of cells available for testing and expedite the discovery of new drugs and therapies.

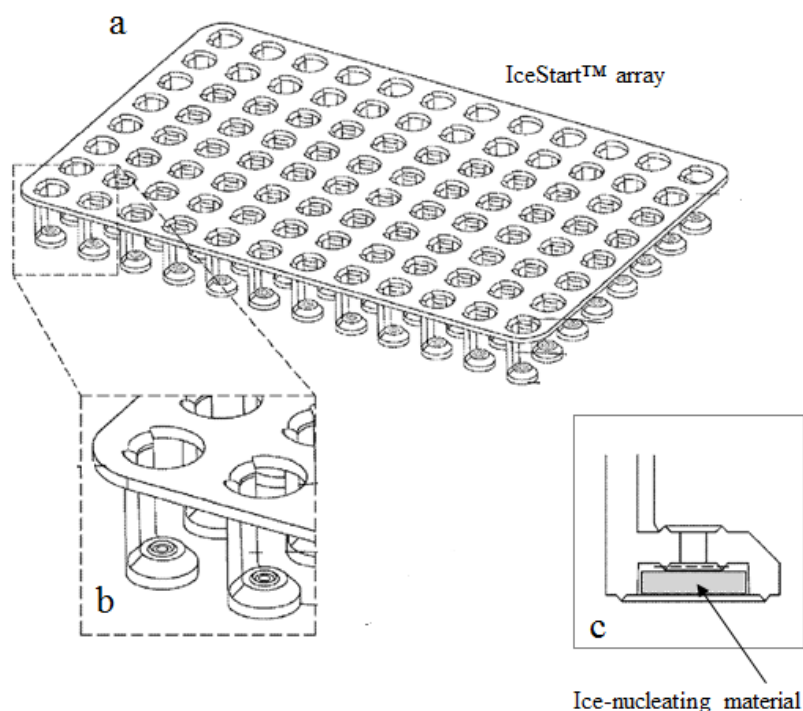


**Figure 1.17: Schematic of IceStart array for 96-well plate, adapted from Morris and Lamb, 2018. a) Full array to be inserted into standard 96-well microplate of dimensions 127.1 mm x 85.4 mm x 14.1 mm. b) Close-up of array ‘feet’ which are placed into wells without disturbing cells or other biological material on the well surface. c) Cross section of ‘foot’ showing a charge of ice-nucleating material and sealed with a semipermeable membrane**

Three specific objectives of the project are defined below:

### **1.6.1 Demonstrate importance of controlling ice-nucleating in 96-well plates and the effectiveness of IceStart™ for cryopreserving cells**

We hypothesise that excessive supercooling causing low post-thaw cell viability is the reason cells are not commercially frozen in microplate format, but these have not been previously linked directly. To do this we must be able to measure supercooling of both water and cryoprotectant (CPA) in multiwell plates in a non-invasive way in order to characterise ice-nucleation temperature in controlled and non-controlled settings. This can be done using the IR-NIPI instrument (Harrison et al., 2018), an instrument developed for atmospheric INP research. Also, we must perform cell culture cryopreservation trials in 96-well plates with ice-nucleation temperature as the

controlled variable, assess post-thaw recovery, and then determine if a causal link can be found.

### **1.6.2 Optimise performance of mineral ice-nucleator**

Use of chemical ice-nucleating agents is the strategy of ice-nucleation control on which IceStart™ is based and mineral nucleators have highest potential for biocompatibility compared to other potent nucleators such as AgI and Snomax®. IceStart™ arrays can be loaded with any ice nucleant and it is advantageous for it to have the highest INA per mass possible. As well as limiting supercooling and variability, this also reduces the amount of material needed. Although the most active of minerals, K-feldspar has a huge variety in INA sample to sample (Harrison et al., 2016; Welti et al., 2019) due to natural mineralogical variability. Aided by droplet freezing assays, a formulation should be found that is very highly active, non-toxic to cells, can be sterilised without losing activity and is easily sourced.

### **1.6.3 Investigate stability of mineral ice-nucleators and compare with biological ice-nucleators**

Mineral ice-nucleators can be deactivated by acids (Sullivan et al., 2010), electrolytes (Kumar et al., 2019; Whale et al., 2018) or even by ageing in pure water (Harrison et al., 2019; Perkins et al., 2020). Their use in biological applications may need knowledge about their what their response is to storage in cryoprotectants and to sterilisation methods such as heating. Of these, response to heat has a crucial role in determining the relative contributions of mineral dust and biological INP in internally or externally mixed environmental samples such as aerosol (Brasseur et al., 2021), precipitation (Christner et al., 2008) and soils (Conen et al., 2011). Investigating this through droplet freezing assays before and after heat treatments will aid interpretation of this widely used methodology. This may also give insights into the nature of the active sites on minerals (Holden et al., 2021; Kiselev et al., 2017) which are still poorly understood.

## **References**

Atkinson, J. D., Murray, B. J., Woodhouse, M. T., Whale, T. F., Baustian, K. J., Carslaw, K. S., Dobbie, S., O'Sullivan, D., and Malkin, T. L.: The importance of

feldspar for ice nucleation by mineral dust in mixed-phase clouds, *Nature*, 498, 355-358, 2013.

Brasseur, Z., Castarède, D., Thomson, E. S., Adams, M. P., Drossaert van Dusseldorp, S., Heikkilä, P., Korhonen, K., Lampilahti, J., Paramonov, M., Schneider, J., Vogel, F., Wu, Y., Abbat, J. P. D., Atanasova, N. S., Bamford, D. H., Bertozzi, B., Boyer, M., Brus, D., Daily, M. I., Fösig, R., Gute, E., Harrison, A. D., Hietala, P., Höhler, K., Kanji, Z. A., Keskinen, J., Lacher, L., Lampimäki, M., Levula, J., Manninen, A., Nadolny, J., Peltola, M., Porter, G. C. E., Poutanen, P., Proske, U., Schorr, T., Silas Umo, N., Stenszky, J., Virtanen, A., Moisseev, D., Kulmala, M., Murray, B. J., Petäjä, T., Möhler, O., and Duplissy, J.: Measurement report: Introduction to the HyICE-2018 campaign for measurements of ice nucleating particles in the Hyytiälä boreal forest, *Atmos. Chem. Phys. Discuss.*, 2021, 1-46, 2021.

Christner, B. C., Morris, C. E., Foreman, C. M., Cai, R., and Sands, D. C.: Ubiquity of Biological Ice Nucleators in Snowfall, *Science*, 319, 1214, 2008.

Conen, F., Morris, C. E., Leifeld, J., Yakutin, M. V., and Alewell, C.: Biological residues define the ice nucleation properties of soil dust, *Atmospheric Chemistry and Physics*, 11, 9643-9648, 2011.

Harrison, A. D., Lever, K., Sanchez-Marroquin, A., Holden, M. A., Whale, T. F., Tarn, M. D., McQuaid, J. B., and Murray, B. J.: The ice-nucleating ability of quartz immersed in water and its atmospheric importance compared to K-feldspar, *Atmos. Chem. Phys.*, 19, 11343-11361, 2019.

Harrison, A. D., Whale, T. F., Carpenter, M. A., Holden, M. A., Neve, L., and Sullivan, D., Vergara Temprado, J., and Murray, B. J.: Not all feldspars are equal: a survey of ice nucleating properties across the feldspar group of minerals, *Atmospheric Chemistry and Physics*, 16, 10927-10940, 2016.

Harrison, A. D., Whale, T. F., Rutledge, R., Lamb, S., Tarn, M. D., Porter, G. C. E., Adams, M. P., McQuaid, J. B., Morris, G. J., and Murray, B. J.: An instrument for quantifying heterogeneous ice nucleation in multiwell plates using infrared emissions to detect freezing, *Atmos. Meas. Tech.*, 11, 5629-5641, 2018.

Holden, M. A., Campbell, J. M., Meldrum, F. C., Murray, B. J., and Christenson, H. K.: Active sites for ice nucleation differ depending on nucleation mode, *Proceedings of the National Academy of Sciences*, 118, e2022859118, 2021.

Kiselev, A., Bachmann, F., Pedevilla, P., Cox, S. J., Michaelides, A., Gerthsen, D., and Leisner, T.: Active sites in heterogeneous ice nucleation-the example of K-rich feldspars, *Science*, 355, 367-371, 2017.

Kumar, A., Marcolli, C., and Peter, T.: Ice nucleation activity of silicates and aluminosilicates in pure water and aqueous solutions – Part 3: Aluminosilicates, *Atmos. Chem. Phys.*, 19, 6059-6084, 2019.

Michellini, E., Cevenini, L., Mezzanotte, L., Coppa, A., and Roda, A.: Cell-based assays: fuelling drug discovery, *Analytical and Bioanalytical Chemistry*, 398, 227-238, 2010.

Morris, G. J. and Lamb, S.: Improved Methods for Cryopreservation of Biological Material. (GB), A. L. (Ed.), 15/557320, 2018.

Peckhaus, A., Kiselev, A., Hiron, T., Ebert, M., and Leisner, T.: A comparative study of K-rich and Na/Ca-rich feldspar ice-nucleating particles in a nanoliter droplet freezing assay, *Atmospheric Chemistry and Physics*, 16, 11477-11496, 2016.

Perkins, R. J., Gillette, S. M., Hill, T. C. J., and DeMott, P. J.: The Labile Nature of Ice Nucleation by Arizona Test Dust, *ACS Earth and Space Chemistry*, 4, 133-141, 2020.

Sullivan, R. C., Petters, M. D., DeMott, P. J., Kreidenweis, S. M., Wex, H., Niedermeier, D., Hartmann, S., Clauss, T., Stratmann, F., Reitz, P., Schneider, J., and Sierau, B.: Irreversible loss of ice nucleation active sites in mineral dust particles caused by sulphuric acid condensation, *Atmospheric Chemistry and Physics*, 10, 11471-11487, 2010.

Welti, A., Lohmann, U., and Kanji, Z. A.: Ice nucleation properties of K-feldspar polymorphs and plagioclase feldspars, *Atmospheric Chemistry and Physics Discussions*, doi: 10.5194/acp-2018-1271, 2019. 1-25, 2019.

Whale, T. F., Holden, M. A., Wilson, Theodore, W., O'Sullivan, D., and Murray, B. J.: The enhancement and suppression of immersion mode heterogeneous ice-nucleation by solutes, *Chemical Science*, 9, 4142-4151, 2018.

## 1.7 Thesis Overview

The body of this thesis contains three research papers driven and authored by myself during the course of the PhD project. *Chapter Two* was published in *Cryobiology* in February 2020, *Chapter Three* is a final draft of a paper and *Chapter Four* was accepted for publication (subject to minor revisions) in *Atmospheric Measurement Techniques* in February 2022.

*Chapter Two: Cryopreservation of primary cultures of somatic cells in 96-well plates benefits from control of ice nucleation.* This chapter demonstrates that primary cells can be cryopreserved in monolayers in 96-well plates and controlling ice-nucleation using a manual seeding method is essential for acceptable survival. This is significant as primary cells when used *in-vitro* are more representative of biological systems than cell lines and less convenient to source. The link between liquid aliquot volume and uncontrolled ice-nucleation temperature is also explored and an empirical relation derived from it which can be used to predict ranges of ice-nucleation temperature if aliquot volume is known.

*Chapter Three: A highly active mineral ice nucleating agent supports in-situ high throughput cell cryopreservation.* This chapter builds on the findings of Chapter two and demonstrates how IceStart system, optimised with a hyperactive form of ice-nucleating feldspar, enables cryopreservation of a cell line in 96-well plates. The two significant highlights of this chapter are showing how hyperactive feldspar practically eliminates all supercooling and directly relating ice nucleation temperature to cell survival on a well-by-well basis in a 96-well plate with partly controlled ice-nucleation.

*Chapter Four: An evaluation of the heat test for the ice-nucleating ability of minerals and biological material:* The ‘heat test’ refers to a widely used treatment used to treat samples of environmental media that are being analysed for INP content – decreases in ice-nucleating activity after heat treatment are interpreted as indication of biological INP being present. The absolute heat stability of mineral INP is assumed yet has never been systematically tested despite evidence of degradation in room temperature water. A wide selection of mineral samples were heated both in water and in air to test this assumption and it was found that quartz, ubiquitous in airborne mineral dust is heat

sensitive in water. Improvements to the protocol of the heat test are suggested as well as discussions as to reasons for deactivations.

Chapter Five: Here the objectives are addressed and we draw overall conclusions on the wide range of work presented here and future work to build on the findings.

## **2 Cryopreservation of primary cultures of mammalian somatic cells in 96-well plates benefits from control of ice nucleation.**

This Chapter has been published in *Cryobiology* as:

**Martin I. Daily, Thomas F. Whale, Riitta Partanen, Alexander D. Harrison, Peter Kilbride, Stephen Lamb, G. John Morris, Helen M. Picton, Benjamin J. Murray: ‘Cryopreservation of primary cultures of mammalian somatic cells in 96-well plates benefits from control of ice nucleation’, *Cryobiology*, 93, 62-69, <https://doi.org/10.1016/j.cryobiol.2020.02.008>, 2020.**

### **Chapter Abstract**

Cryopreservation of mammalian cells has, to date, typically been conducted in cryovials, but there are applications where cryopreservation of primary cells in multiwell plates would be advantageous. However excessive supercooling in the small volumes of liquid in each well of the multiwell plates is inevitable without intervention and tends to result in high and variable cell mortality. Here, we describe a technique for cryopreservation of adhered primary bovine granulosa cells in 96-well plates by controlled rate freezing using controlled nucleation. Inducing ice nucleation at warm supercooled temperatures (less than 5 °C below the melting point) during cryopreservation using a manual seeding technique significantly improved post-thaw recovery from 29.6% (SD = 8.3%) where nucleation was left uncontrolled to 57.7% (9.3%) when averaged over 8 replicate cultures ( $p < 0.001$ ). Detachment of thawed cells was qualitatively observed to be more prevalent in wells which did not have ice nucleation control which suggests cryopreserved cell monolayer detachment may be a consequence of deep supercooling. Using an infra-red thermography technique we showed that many aliquots of cryoprotectant solution in 96-well plates can supercool to temperatures below  $-20$  °C when nucleation is not controlled, and also that the freezing temperatures observed are highly variable despite stringent attempts to remove contaminants acting as nucleation sites. We conclude that successful cryopreservation of cells in 96-well plates, or any sub-mL volume format, benefits from control of ice nucleation.

## 2.1 Introduction

A range of cells are routinely cryopreserved in millilitre volumes of aqueous cell suspensions, but successfully cryopreserving cells using a controlled rate freezing method in smaller volumes such as those used in 96-well microplates is, in comparison, more challenging. This is in part because small volumes of water and aqueous solutions tend to supercool by many degrees below the melting point before the onset of ice-nucleation and subsequent ice growth (Hobbs and Hobbs, 1974; Pruppacher and Klett, 1997). It is well established that inducing extracellular ice formation at relatively warm supercooled temperatures during controlled rate freezing is beneficial to the post-thaw viability of many cell types (Lauterboeck et al., 2016; Lauterboeck et al., 2015; Massie et al., 2014; Petersen et al., 2006; Prickett et al., 2015; Wolkers et al., 2007). However this is still a significant uncontrolled variable during many cell and tissue cryopreservation procedures (Morris and Acton, 2013).

The efficacy of controlled rate freezing is often qualitatively understood by the two-factor hypothesis (Mazur et al., 1972). This hypothesis states that cooling must be sufficiently slow for cells to dehydrate and avoid intracellular ice formation, but quick enough to avoid other detrimental impacts of low temperature on cells. When ice nucleation is controlled (i.e. extracellular ice crystals are actively nucleated) during cryopreservation, pure water migrates to and is locked away in ice crystals, resulting in the inter-crystal channels where cells reside becoming increasingly concentrated in solutes. This osmotic imbalance drives cellular dehydration (Mazur, 1963). Dehydration reduces the water activity of intracellular solutions which lowers the freezing point of the cytoplasm and thus favours solidification of the cytoplasm in a survivable, non-crystalline state (Clarke et al., 2013; Mazur, 1990; Meneghel et al., 2019). In contrast, without controlled extracellular ice formation, cells dehydrate less, increasing the chance of intracellular ice formation, which is usually fatal (Lee et al., 1995).

Another factor to consider is the sudden rise in temperature resulting in a 'thermal shock' from the release of latent heat of crystallisation followed by a rapid cooling as the system comes back to equilibrium with its surroundings. The magnitude of this thermal shock increases with the depth of supercooling. Finally, there is evidence that following ice nucleation at warm supercooled temperatures cell membranes of

mammalian somatic cell lines (Balasubramanian et al., 2009; Wolkers et al., 2007) and horse spermatozoa (Oldenhof et al., 2010) undergo a dehydration induced phase transition, which is absent when ice forms at colder temperatures and it is possible that this lyotropic phase transition is beneficial for cell survival. In earlier work on the topic, samples were seeded with ice at warm supercooled temperatures to ensure crystallisation (Mazur et al., 1972). However the practice of controlling ice nucleation is to date prevalent only in only a few areas, notably oocyte and embryo cryopreservation for reproductive biology where failure to control ice nucleation is clearly detrimental (Fuller and Paynter, 2004).

While the cryovial is the standard vessel used for the shipping of cryopreserved cells and for the long-term storage of complex human tissues with clinical therapeutic application the routine cryopreservation of mammalian cells in 96-well culture plates would be beneficial as many somatic cell bioassays require this format. Ice nucleation however tends to occur both at lower temperatures and with greater variability within the sub-millilitre volumes of liquid used in multiwell plates than in millilitre volume vials (Morris and Acton, 2013). This poses the problem of both poor and variable post-thaw cell viability which would be an unacceptable baseline condition in plates used, for example, for cytotoxicity assays. A great deal of standard analytical equipment is built around the multiwell plate format allowing, for example, standard *in-vitro* pharmacological experiments to be rapidly performed on large numbers of samples. Specifically, routine cryopreservation in 96-well plates would facilitate ADME (adsorption, distribution, metabolism, excretion) and toxicology screening of drug compounds against new drug molecules by allowing large, homogeneous batches of relevant cell types to be frozen and shipped to toxicology labs and stored for use over extended time periods. Despite these advantages commercial suppliers of cells for scientific research may at present offer only plated cells shipped fresh or cryopreserved cells shipped in cryovial format for subsequent thawing and seeding into plates (Morris and Lamb, 2018). The former format raises logistical challenges resulting in high shipping costs while the thawing and re-plating associated with the latter is inefficient and incurs additional time and labour. Overall both these delivery formats increase the cost and reduce the effectiveness of toxicology assays for the end user.

Whilst not currently available ‘off the shelf’, demonstrations of cell cryopreservation in microplated monolayer format do exist in the literature. Protocols have been devised for freezing of immortalised cell lines (Campbell and Brockbank, 2014, 2012, 2007; Halwani et al., 2014; Katkov et al., 2011), embryonic stem cells (Nagy et al., 2006) and hybridomas (Wells and Price, 1983). A frequently observed issue when attempting to freeze cells in this way is post-thaw detachment of cells from the substrate. Campbell *et. al.* (Campbell et al., 2003) devised a controlled warming methodology upon thawing to prevent cell detachment, attributing this phenomenon to thermal expansion stresses within the plate upon rapid warming. The use of immortalised and previously cryopreserved cell lines means that many studies are conducted with cells that are relatively resistant to the damage caused by cryopreservation, which may distort the true effect of the nucleation control in practically relevant primary cell types. More recent advances have, however, demonstrated freezing and good recovery of primary cells under small volumes of liquid cryoprotectant. Eskandari *et. al.* (Eskandari et al., 2018) were able to successfully recover porcine endothelial corneal cells by selecting a monolayer substrate with similar thermal expansion properties to that of ice. Also, Töpfer *et. al.* (Töpfer et al., 2019) demonstrated cryopreservation of bovine colonic cell in 3-D organoid format within 96-well plates was successful in terms of post thaw viability and cytotoxic response compared to a control. The influence of ice nucleation temperature in these studies received relatively little attention and has not been investigated at all in the case of primary cells. A possible reason for this is the practical difficulty of simultaneously inducing ice nucleation in each and every well of a 96-plate at a discrete temperature in a way that does not disturb or contaminate the cells within. Campbell *et. al.* (Campbell and Brockbank, 2014) studied the effect of ice nucleation control during the cryopreservation of plated rat aorta and bovine corneal cell lines by separately using Snomax (a commercial ice nucleating agent made from non-viable *Pseudomonas syringae* bacteria) and also a cryogenically cooled manifold device to control ice nucleation. While they saw some evidence of improvement in both the post-thaw cell viability and attachment rates when ice nucleation was controlled they were unable to induce ice nucleation across plates in a sufficiently uniform manner using these techniques.

Here we demonstrate, using cultures of primary bovine granulosa cells and a non-invasive method of inducing ice nucleation, that active control of the ice nucleation step is required for both successful and consistent cryopreservation of monolayers of primary mammalian cells in generic polypropylene 96-well plates. Granulosa cells surround and support oocyte growth and development in mammalian ovarian follicles, and they are the subject of intense research in their own right (Picton et al., 1999; Wrathall and Knight, 1993). We used granulosa cells as a convenient primary cell model as these cells can be rapidly harvested from abattoir-derived ovarian tissues without the need for any enzymatic digestion to demonstrate proof of concept of the efficacy of our approach for in-plate somatic cell cryopreservation. We show that inducing ice nucleation in individual wells at high supercooled temperatures (less than 5 °C of supercooling) is vital for achieving good levels of cell viability. Since our hypothesis is that the degree of supercooling is very important for high post-thaw cell recovery, we have gone to some effort to characterise freezing temperatures when nucleation is controlled and uncontrolled. We then discuss the reasons for this by reviewing observations of the supercooling behaviour of purified water over a wide range of aliquot volumes and why this has hindered the efficient cryopreservation of cells within 96-well plates from being conducted on a larger scale.

## **2.2 Materials and methods**

### **2.2.1 Controlled and uncontrolled ice nucleation temperatures within 96-well plates**

To quantify the variability of temperatures of controlled and uncontrolled freezing in the multiwell plates used in this study we have used the IR-NIPI (Infra-Red – Immersion by Immersed Particle Instrument) to determine the range of ice nucleation temperatures that occur when sub-mL volumes of ultrapure water and of cryoprotectant solution are slow-cooled ( $1\text{ °C min}^{-1}$ ) to cryogenic temperatures. The IR-NIPI comprises a controlled rate freezer (Asymptote ViaFreeze Research) and an integrated IR camera (Fluke Ti9) which is used to observe the temperatures of individual wells within a multiwell plate mounted upon the cooling plate. This system avoids the use of thermocouples in direct contact with the liquid in the wells which may themselves trigger nucleation. Temperatures of individual wells are logged every 15 seconds using the IR camera and nucleation events are captured by the rapid release

of latent heat which occurs when the contents of the wells freeze. The nucleation temperature for a well is taken as the temperature immediately before sharp temperature increase. A full description of the IR-NIPI apparatus is detailed in Harrison *et al.* (Harrison *et al.*, 2018).

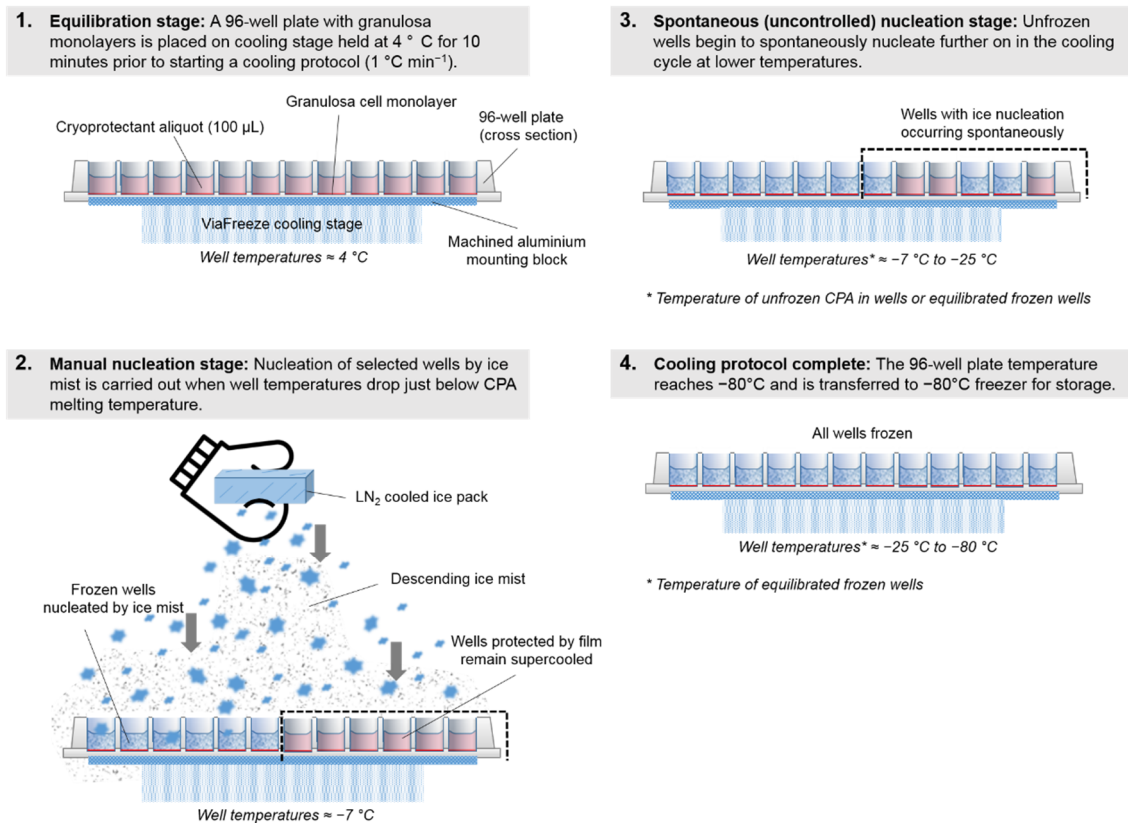


**Figure 2.1: Description of 96-plate cryopreservation procedure and manual ice nucleation technique.**

### 2.2.2 Bovine granulosa cell cultures

Bovine granulosa cells were cultured after Wrathall and Knight (Wrathall and Knight, 1993) and Picton *et al.* (Picton *et al.*, 1999). Bovine ovaries were transported to the laboratory at ambient temperature from the local abattoir (JC Penny and Sons, Rawdon, Leeds, UK), and were cut from the reproductive tract as received and washed very briefly in 70% (v/v) ethanol to remove unwanted detritus. The ovaries were then decanted and washed in room temperature phosphate buffered saline (PBS) containing 100 kIU L<sup>-1</sup> penicillin and 0.1 µg L<sup>-1</sup> streptomycin at 39 °C. Granulosa cells were extracted from the ovaries by needle aspiration from individual follicles using a 10 mL syringe fitted with a 19G needle. The follicle aspiration media (AM) was made

up of M199 media containing 10 mM HEPES, 100 kIU L<sup>-1</sup> penicillin, 0.1 µg L<sup>-1</sup> streptomycin, 1 mg L<sup>-1</sup> amphotericin and 3000 IU heparin L<sup>-1</sup>, pre-equilibrated to 39 °C. A small amount of media was taken up into the syringe before the follicles were gently punctured and aspirated up and down after gently scraping the walls of the follicles to dislodge the granulosa cells. Cells were then decanted into a 50 mL polypropylene tube. This process was repeated with multiple ovaries (typically 5 to 8) to obtain a stock with a sufficient number of cells to seed a set of plates for each freezing experiment. When cell extraction was complete the cells were washed by centrifugation for 10 minutes at 250 x g at room temperature. After washing the cells were re-suspended in 5 mL of pre-equilibrated culture media (CM) at 39 °C, consisting of McCoy's 5a medium supplemented with 20 mM HEPES, 100 kIU L<sup>-1</sup> penicillin, 0.1 µg L<sup>-1</sup> streptomycin, 3 mM L<sup>-1</sup> L-glutamine, 10 µg L<sup>-1</sup> bovine insulin, 2.5 mg L<sup>-1</sup> transferrin, 4 µg L<sup>-1</sup> sodium selenite and 10% v/v foetal calf serum. In order to break up cell aggregates the cells were repeatedly, gently aspirated through two stacked pipette tips. The cell stock concentration was determined by trypan blue dry exclusion and counting with a haemocytometer and subsequently diluted with CM to achieve a plating density of 10<sup>5</sup> viable cells per well in 250 µl of CM in sterile polypropylene flat bottom 96-well plates (Thermo Scientific Nunclon™ Delta Surface Cat. No. 167008). Cells were cultured for 72 hours at 39 °C in a 5% CO<sub>2</sub> humidified atmosphere with complete media changes conducted after 48 hours of culture. All media and additives were purchased from Sigma-Aldrich (Poole Dorset, UK).

### **2.2.3 Cryopreservation of 96-well plates**

After culturing for 72 hours the cells in the 96-well plates consistently formed confluent fibroblastic monolayers. To prepare for freezing, the 96-well plates with confluent granulosa cells were cooled to approximately 4 °C by placing them on an ice-cooled aluminium mounting block specially machined for maximum thermal contact with the underside of the plate. Once equilibrated the CM was removed from each well and replaced with 100 µL of cryoprotectant (CPA) media consisting of CM with 10% (v/v) dimethyl sulfoxide and 0.1 M trehalose. The CPA was chilled to 4 °C in a refrigerator prior to use to minimise toxicity and after addition of CPA the plates were left to equilibrate at 4 °C for 10 minutes. Then the plates along with mounting block were placed on the cooling stage of a controlled rate freezer (Asymptote

ViaFreeze Duo, Asymptote Ltd, Cambridge, UK) and a protocol was initiated which cooled the plates from 4 °C to -80 °C at a rate of -1 °C min<sup>-1</sup>. Ice nucleation treatments were applied and once the cooling protocol was complete plates were transferred immediately to a -80 °C chest freezer for storage. An illustration of the controlled rate freezing process and ice nucleation steps is provided in Fig. 2.1.

#### **2.2.4 Manual induction of ice-nucleation in 96-well plates**

Ice nucleation was simultaneously induced by manual nucleation and left uncontrolled to occur spontaneously in subsets of wells within the same plate used for controlled rate cooling. Manual ice nucleation was achieved by exposing wells to ice mist descending from a very cold-object held just above the exposed plate (Fig. 2.1, panel 2). The object we used here was a gel ice-pack for domestic freezers, one end of which had been submerged in liquid nitrogen for ten seconds and was then, while still cold, held around 15cm directly above an exposed 96-well plate mounted on the cold plate of the VIA Freeze. From this ice pack a stream of mist containing microscopic airborne ice crystals - which formed from moisture in the cooled air around the cold ice pack condensing and freezing - fell down onto the exposed 96-well plate. The falling ice crystals in the mist acted as seed crystals and, upon contact, instantly triggered ice nucleation to occur across all wells of the plate, this visually confirmed by a sudden change of appearance of the well liquid from clear to translucent. The well nucleation temperatures using this method and CPA melting temperature were determined by infra-red thermometry to be approximately -7 °C ± 1 °C ( $n = 24$ ) and -4 °C ± 1 °C ( $n = 15$ ) respectively. This confirmed that the wells across a plate typically froze in a very narrow range of temperatures and that this method was capable of inducing ice-nucleation close to (within 5 °C) of the melting point of the CPA. Also, this method of manual nucleation used for 96-plate freezing is less invasive than a previously reported mechanical protocol which required physical intervention (Campbell and Brockbank, 2014). Where ice nucleation was intended to occur uncontrolled during cooling, subsets of wells were covered with laboratory film to prevent exposure to the falling ice mist during manual nucleation (Fig.2.1, panels 2 and 3). In the spontaneously nucleating wells, ice-nucleation events were consistently observed at a much later time points (and correspondingly lower temperatures) during the cooling protocol qualitatively confirming the greater degree of supercooling in these wells. Further details of well freezing temperature measurement is provided in Section 2.3.1.

### **2.2.5 Thawing of cryopreserved 96-well plates**

After 3 to 4 days of storage, 96-well plates were removed from the  $-80\text{ }^{\circ}\text{C}$  freezer and placed into an incubator held at a temperature of  $39\text{ }^{\circ}\text{C}$ . Aluminium plates shaped to fit to the top and bottom of the 96-well plate and pre-heated to a temperature of  $39\text{ }^{\circ}\text{C}$  were attached to either side of the plate in the hotbox. After 10 minutes the plates were removed from the incubator and the CPA media removed as rapidly and thoroughly as possible with a multichannel micropipette.  $200\text{ }\mu\text{L}$  of CM containing  $50\text{ }\mu\text{g mL}^{-1}$  vital dye neutral red was then added to each well and the plates placed in the incubator at  $39\text{ }^{\circ}\text{C}$  in a  $5\%$   $\text{CO}_2$  atmosphere for 3 hours. At this point the dye uptake was complete and the plate was ready for viable cell counting.

### **2.2.6 Neutral Red assessment of cell number and viability**

A viable cell counting assay based on the uptake of neutral red by only living cells (Borenfreund and Puerner, 1985) allowed rapid assessment of the number of live granulosa cells present in individual wells and was used to determine viable cell numbers per well of cryopreserved plates upon thawing and also of non-frozen control plates. The 96-well plates containing granulosa cultures were, as mentioned above, incubated for 3 hours in  $50\text{ }\mu\text{g mL}^{-1}$  neutral red dye in CM.  $200\text{ }\mu\text{L}$  of a washing solution (WS) containing  $4\%$  formaldehyde and  $1\%$   $\text{CaCl}_2$  in distilled water was then added to each well and left to stand for 3 minutes. The wash solution was then carefully removed and  $200\text{ }\mu\text{L}$  of fixing solution (FS) containing  $1\%$  (v/v) glacial acetic acid and  $25\%$  (v/v) ethanol was added to release the dye retained by viable cells. The plates were then left to stand for 30 minutes before the absorbance of each well (dye concentration) was measured at  $540\text{ nm}$  using a microplate reader (Thermo Scientific Multiskan GO) with analysis software (Thermo Scientific SkanIt™ Software v. 4.1). To translate dye concentration into viable cell number per well in the frozen-thawed plates the absorbance of cells in test wells were compared to a standard curve. The standard curve was derived from a dilution series of a known quantity of neutral red stained and lysed granulosa cells (typically in the range of  $4 \times 10^3$  to  $4 \times 10^5$  cells per well) and measured in triplicate at  $540\text{ nm}$ .

### **2.2.7 Assessment of cell morphology**

The visual appearance of the cell monolayers *in vitro* was recorded before and after freezing using a Nikon Eclipse Ti inverted microscope at  $250\times$  magnification fitted

with a digital camera and processed with RI Viewer Imaging Software. The cells were incubated with neutral red dye before imaging as previously described above.

### **2.2.8 Cryoprotectant toxicity testing**

In order to determine the cytotoxic impact of the CPA on the granulosa cells separately from the impact of freezing, 100  $\mu$ L of CPA at 4 °C was added to plates containing granulosa at the 72 hour time point and left in contact for a time period identical to the cell exposures used during the cryopreservation protocol. The CPA was then removed with a multichannel micropipette, replaced with the CM-neutral red solution before returning to the incubator for 3 hours. Finally viable cell number in the plate was quantified using the neutral red assay as detailed above.

### **2.2.9 Experimental design and statistical analysis of post-thaw cell viability**

Eight, independent, replicate bovine granulosa cell cultures (*a-h*) were conducted and each were seeded into separate 96-well plates. In each plate equal subsets were designated for a range of ‘treatments’ after culturing. These comprised a subset not subject to any addition of CPA or freezing treatment and used as a control (‘Baseline’); a subset subject to addition of CPA and cryopreservation using manually controlled nucleation (‘Controlled Nucleation’); a subset subject to addition of CPA and cryopreservation with uncontrolled ice nucleation (‘Uncontrolled Nucleation’); and a subset subject to addition of CPA without freezing as an indicator of CPA toxicity (‘CPA Treatment Only’).

A two-sample T-test of the viable cell number means of Baseline and CPA Treatment only tests from all 8 culture replicates showed no significant difference between the groups ( $p = 0.835$ ). This confirmed that the addition of CPA *per se* had no significant toxic impact on the viability of cultured granulosa cells, accordingly this variable was disregarded during the statistical comparisons of the Baseline, Controlled Nucleation and Uncontrolled Nucleation data subsets. The differences in mean viable cell numbers between the Baseline, Controlled Nucleation and Uncontrolled Nucleation wells for each culture replicate were analysed by Welch’s one-way ANOVA with a Games-Howell post-hoc test to determine differences of means. These tests were selected as they assumed non-equivalent variances between the groups which arises from the fact that uncontrolled nucleation results in a very wide range of freezing temperatures compared with that of the manual seeding method. Finally to establish

relative cell viability for each group (i.e. % survival) after cryopreservation the mean cell number for the treated plates was divided by the cell number measured in the Baseline (unfrozen) plate.

## **2.3 Results**

### **2.3.1 Freezing temperatures with controlled and uncontrolled nucleation**

The freezing temperatures where nucleation was not controlled for 100  $\mu\text{L}$  volumes of water and CPA in 96-well plates from the IR-NIPI instrument alongside previous data for 50  $\mu\text{L}$  MilliQ are shown in Fig. 2.2. Generally, the freezing occurred at much lower temperatures and over a wider range of temperatures when uncontrolled compared with when it was controlled with the ice mist method. Also, the freezing temperature of the 100  $\mu\text{L}$  volumes was generally warmer than the freezing temperatures in the 50  $\mu\text{L}$  volumes; this was expected, since the probability of freezing generally increases with volume (Bigg, 1953). The plates containing water were prepared either aseptically in a laminar flow hood with a washing step or simply in an ambient laboratory setting to determine the effect of potential airborne contamination on freezing temperatures. This tentatively showed that the effect of sterile preparation and washing was to lower the variability and slightly lower the overall freezing temperatures. Nevertheless, the freezing temperatures were generally much lower and far more variable than those which result from manual nucleation. The freezing temperatures for the CPA loaded plates show a comparable level of variability while median nucleation temperatures are about 4  $^{\circ}\text{C}$  lower. This would be expected due to the colligative effect of solutes on heterogeneous ice nucleation. Tests with CPA in the wells, with and without granulosa cells showed that the presence of a cell monolayer had no apparent effect on freezing temperatures.

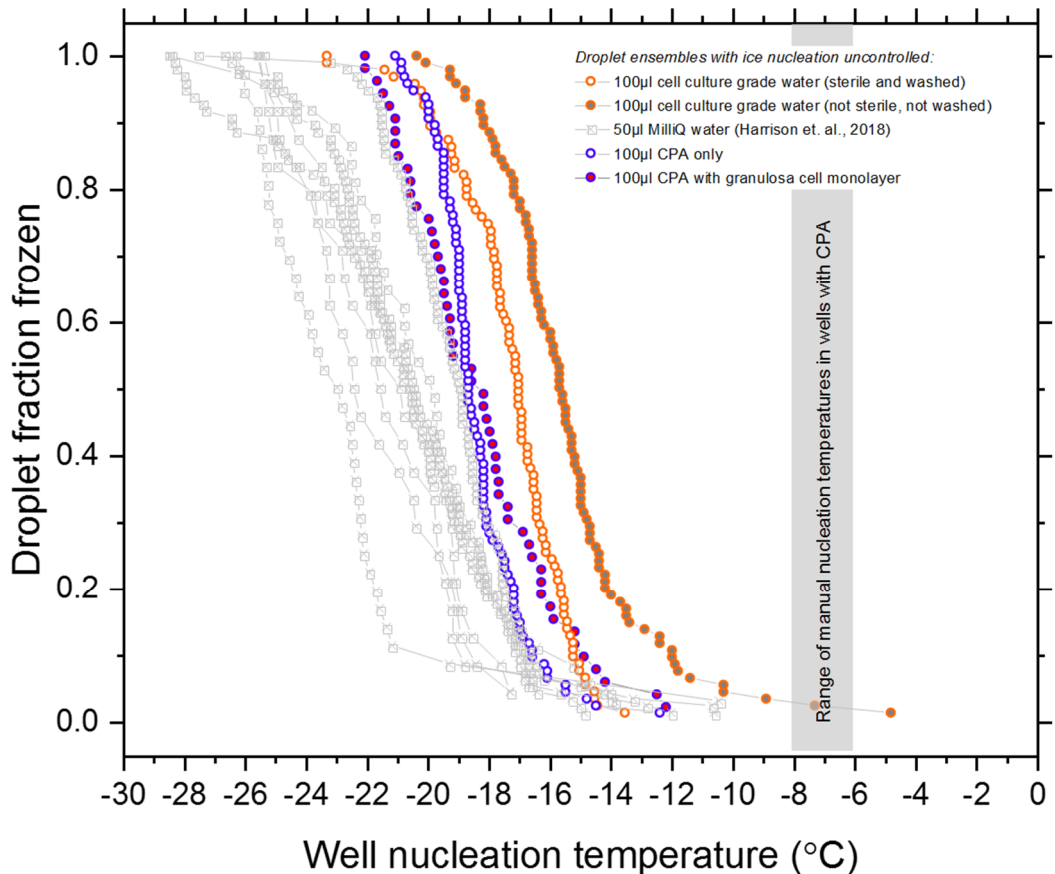


**Figure 2.2: Droplet fraction frozen against well ice nucleation temperature for ensembles of 100  $\mu$ L droplets of water prepared in different conditions of sterility and of CPA with and without a cell monolayer in polypropylene 96-well plates. This variability of freezing temperature is representative of uncontrolled freezing while the expected range of freezing temperatures induced by ice-mist manual nucleation method is depicted for reference. The temperature uncertainty of the IR-NIPI used is  $\pm 0.9$   $^{\circ}$ C.**

We also used the IR-NIPI instrument to record the temperature of each well during cooling in order to quantify the temperature profile of the wells as they heated up during freezing and then cooled down again after freezing (see Fig. 2.3). This was done by loading a 96-plate with 50  $\mu$ L aliquots of CPA, where we controlled nucleation for half of the plate and left it uncontrolled in the other half ( $n = 15$  wells for each group). Alternate wells were left empty to avoid artefacts caused by latent heat release being transferred to adjacent wells upon freezing. Figure 2.3 shows that controlling nucleation manually resulted in a very narrow range of nucleation

temperatures all at higher temperatures (approximately  $-7.0\text{ }^{\circ}\text{C}$ ; a supercooling of about  $3\text{ }^{\circ}\text{C}$ ) compared with those wells where nucleation occurred uncontrolled ( $-12.9\text{ }^{\circ}\text{C}$  to  $-22.5\text{ }^{\circ}\text{C}$ , median  $-20.5\text{ }^{\circ}\text{C}$ ). As the manual nucleation procedure required temporary disabling of the IR camera for 45 seconds it was not possible to observe temperatures treated this way at the exact point of nucleation. However, nucleation was visually observed to be uniform and instantaneous across these wells and any variation in nucleation temperatures across this group was probably due to a small ( $\pm 1\text{ }^{\circ}\text{C}$ ) cross-plate temperature gradient. Also apparent from Figure 2.3 is that uncontrolled nucleation results in much greater cooling rates after nucleation (up to  $10.3\text{ }^{\circ}\text{C min}^{-1}$ ), whilst those wells nucleated manually displayed a cooling rate of up to  $3.5\text{ }^{\circ}\text{C min}^{-1}$ , much closer to the nominal plate cooling rate of  $1\text{ }^{\circ}\text{C min}^{-1}$ . A more modest cooling rate is thought to be advantageous for cell survival, hence this is another reason for controlling freezing.

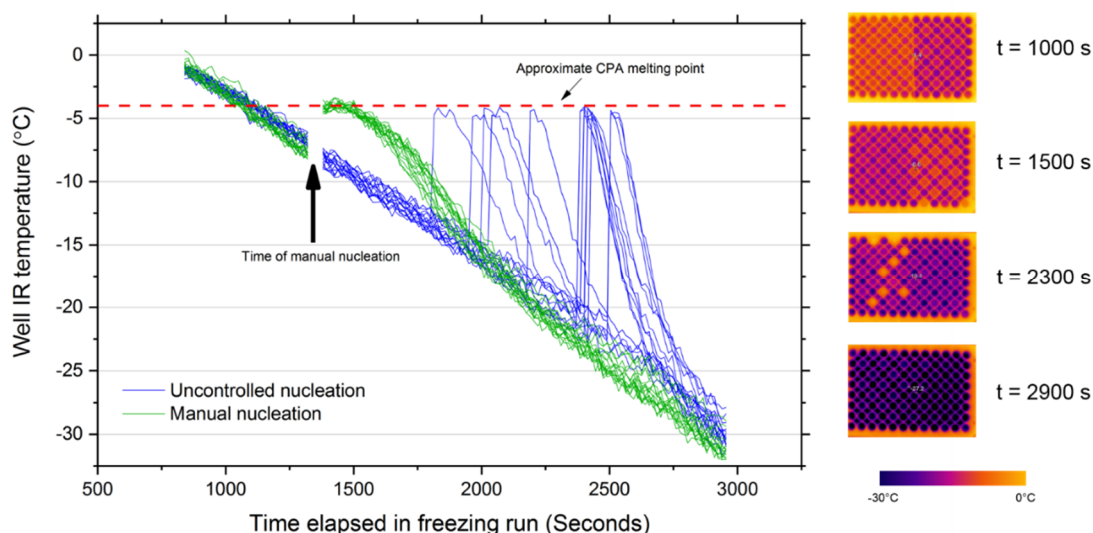


**Figure 2.3: (Left): IR NIPI temperature log of 96-well plate loaded with 50  $\mu$ L aliquots of CPA where half of the wells were nucleated manually with ice mist (green lines) and half left to nucleate without control (blue lines). The data gap at around 1300 s is due to the apparatus being disabled to allow the manual nucleation procedure. Right: IR colour map images of the plate undergoing cooling at progressing time points – manually nucleated wells are on the right half of the plate, uncontrolled on the left. Recently frozen wells having released latent heat appear yellow (temperature-colour scale below is approximate). A plastic film covering the left side of the plate appears as an orange region in the image taken at 1000s. This was placed to protect the wells on this side of the plate from the nucleation inducing ice mist. After manual nucleation was done the film was removed so is no longer visible by the next image at 1500 s.**

Overall, these tests show that controlling freezing with an ice mist dramatically reduces the supercooling experienced by the cells, reduces the variability in supercooling and also reduces the cooling rate that they experience.

### 2.3.2 The effect of controlling nucleation on post thaw cell viability

The number of cells per well determined by the Neutral Red assay for the Baseline and post-freezing treatments for culture replicates *a-h* are presented in the box plots in Fig. 4A. Qualitatively, there is clearly a trend, with the number of viable cells being generally higher when nucleation was controlled than when it was uncontrolled.

However, there is also a great deal of variability, both across plates and batches. ANOVA analysis found the differences between mean cell viability for each treatment (controlled and uncontrolled freezing) are significant ( $p < 0.01$ ) across all granulosa culture batches. Furthermore post-hoc analysis between the Controlled and Uncontrolled Nucleation treatments showed that the Controlled Nucleation treatment resulted in significantly higher post-thaw viabilities in the case of all batches ( $p < 0.05$ ).

The overall survival rates for Controlled and Uncontrolled Nucleation are shown in Fig 2.4B. Across all batches a mean post-thaw recovery rate of 57.7% (Standard error of mean (SEM) = 8.3%) was observed when ice nucleation was controlled compared to a mean post-thaw recovery of 29.6% (SEM = 9.3%) when ice nucleation was left uncontrolled. A 2-sample T-test found the difference of 28.1% to be statistically significant ( $p < 0.001$ ) (Fig. 2.4B). It was therefore evident that controlling and restricting ice nucleation to high temperatures ( $1\text{ }^{\circ}\text{C} \pm 1\text{ }^{\circ}\text{C}$  of supercooling) during controlled rate freezing of 96-well plates significantly increased the proportion of bovine granulosa cells which survived cryopreservation.

### **2.3.3 Effect of cryopreservation on cell morphology**

Micrographs shown in Fig. 2.4C-E contrast the representative morphologies of the granulosa cells before and after cryopreservation and thawing, illustrating the effects of nucleation control. Non-frozen cells (Fig. 2.4C) show a homogeneously adherent monolayer whilst thawed cells (Figs. 2.4D and 2.4E) are more clumped and appear attached to the well bottom by cellular processes. The viable (indicated by red staining) adherent cells are, however, more abundant in the manually nucleated plate (Fig. 2.4D) compared to the uncontrolled nucleation plate (Fig. 2.4E) where several non-viable, unstained cells are visible. A loss of cell layer coverage indicative of post-thaw detachment is also apparent in the frozen plates, the degree of which appeared most severe in the uncontrolled plate (Fig. 2.4E). These observations are qualitatively consistent with the viability analysis detailed in the previous section.

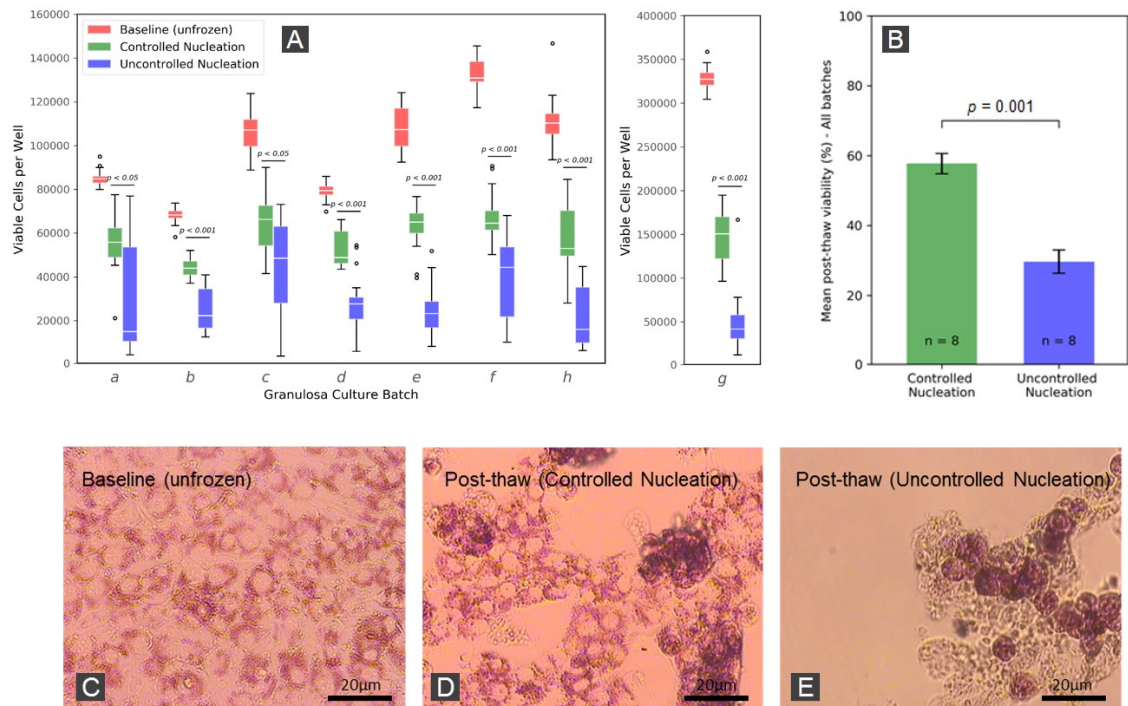


**Figure 2.4: (A) Boxplots of viable granulosa cell number pre- and post-cryopreservation as determined by Neutral Red assays. All treatments within all groups are shown to be significantly distinct by ANOVA post-hoc tests with results of post-hoc analyses between Controlled and Uncontrolled Nucleation treatments for each cell batch shown as p values. Batch g is shown in separate pane with its own y-axis because the cell density was 2-3 times higher than the other batches. n = 24 for each Baseline group and n = 16 for each Controlled Nucleation and Uncontrolled Nucleation group. (B): Cell viability post-thawing relative to Baseline averaged across all cell batches with result of two sample t-test. Values plotted are means  $\pm$  SEM for the number of replicates shown. (C-E): Micrographs of adhered bovine granulosa cells stained with Neutral Red dye. Panel C shows cells in the non-cryopreserved control plate at the end of the 72 h incubation period. Panels D and E depict representative morphologies of thawed cells immediately after cryopreservation with and without ice nucleation control respectively.**

## 2.4 Discussion

In our experiments controlling ice nucleation by seeding with an ice mist improved cell viability from only 29.6% when ice nucleation was uncontrolled to 57.7% ( $p < 0.001$ ). These cell viability results are consistent with previous work which demonstrates that induction of ice nucleation at high temperatures improves cryopreservation results (C. Prickett et al., 2015; Kilbride et al., 2019; Lauterboeck et al., 2016; Lauterboeck et al., 2015; Massie et al., 2014; Morris and Acton, 2013; Petersen et al., 2006; Wolkers et al., 2007) and are consistent with the classic two-factor picture of freezing injury (expanded on below) (Mazur et al., 1972; Morris and Acton, 2013). The poor post-thaw cell viability when ice nucleation is uncontrolled is most likely related to the high degree, and variable nature, of supercooling of the small aliquot volumes (100s of  $\mu\text{L}$ ) typically used in 96-well plates. This unpredictable variability in well ice nucleation temperatures compared with where ice nucleation was controlled was confirmed by our IR thermometry measurements as were much more severe temperature fluctuations.

The enhanced cell survival with controlled freezing can be rationalised through an understanding of the fundamental processes that occur in the freezing process. For example, one factor mitigated by reducing the degree of supercooling is the rapid cooling after crystal growth experienced by cells when freezing occurs at deep supercooling (see Fig. 2.3). Also, water diffusion is slowed by increasing the component of initially formed ice volume as a result of more supercooling (Morris and Acton, 2013; Whittincham, 1977). This, coupled with faster than intended cooling rates, can result in cells not being able to dehydrate quickly enough and increasing the chance of lethal intracellular ice formation. Furthermore cells frozen in monolayer form have previously been found to have a higher susceptibility to intracellular ice formation compared to equivalent cells in suspension which is related to intercellular ice formation travelling from cell to cell through the monolayer (Acker et al., 1999). Further work is needed to supplement findings on immediate post-thaw viability and confirm that granulosa cell functionality is retained post thaw. This could be done, for example, by extended culture and measurement of specific granulosa cell steroidogenic function (Picton et al., 1999).

We sometimes observed that adherent cells would detach from the base of the wells upon thawing. This observation is consistent with previous work by others (Campbell and Brockbank, 2014; Corsini et al., 2002; Ebertz and McGann, 2004) attempting to cryopreserve cell monolayers either in multiwell plates or on other substrates. However from visual inspection the degree of detachment was found to be more severe in wells which experienced deeper supercooling which has not previously been reported. The cells that detached in our experiments may have simply been the ones that did not survive the freezing and/or thawing processes. Adherent cells, however, having become rigid at cryogenic temperatures may have also become mechanically separated from the substrate during the freezing and thawing cycle while remaining viable (Ebertz and McGann, 2004).

Campbell *et. al.* (Campbell and Brockbank, 2007) attributed cell detachment to thermal expansion of the plate if warmed too rapidly. Having warmed all our plates by the same method and therefore at the same rate we cannot solely attribute the degree of detachment to warming rate. Moreover, Eskandari *et. al.* (Eskandari et al., 2018) and Rutt *et. al.* (Rutt et al., 2019) recently tackled the mechanical detachment of cell monolayers by freezing cells on substrate with a similar coefficient of linear expansion to that of ice. They hypothesised that by eliminating differential expansion of ice and substrate the buckling or splitting of the cell monolayer over the course of a cooling and thawing cycle culminating in detachment. In our case as we used the same plate type for each freezing run we did not vary the ice-substrate thermal mismatch. However controlling (increasing) the ice nucleation temperatures did result in much less severe temperature fluctuations during the cooling cycle which may have led to less severe thermal stresses, protecting the integrity of the monolayer.

Detachment of cells from the substrate post thaw presents a technical obstacle for producing frozen plated cells on a commercial basis since detached cells would be lost during the CPA removal and washing steps. These observations of cell detachment in our thawed granulosa cultures adds the importance of controlling ice nucleation to list of factors identified by previous workers, such as substrate composition and controlled warming, for plated cell monolayer cryopreservation protocols. Further work quantifying the degree of cell detachment, viability of detached cells and trialling plates with different compositions would confirm this.

Since ice nucleation temperature is clearly an important consideration in the cryopreservation of cells, we will now discuss freezing in typical cryopreservation containers with a range of volumes. We summarise literature data and some new data for freezing temperatures for vessels with a range of volumes in Fig. 2.5. Truly pure liquid water, containing no contaminating particles and in contact with no surface, can nucleate via homogeneous nucleation which can be described with Classical Nucleation Theory (CNT) (Koop and Murray, 2016). Homogeneous ice nucleation is practically possible to achieve only in very small droplets and is readily accessed in droplets of around a nanolitre in volume or smaller (Atkinson et al., 2013; Tarn et al., 2018). However all the freezing events in vessels of volumes relevant to cryopreservation applications (multiwell plates, vials, straws etc.) tend to occur at temperatures clearly too warm to be homogeneous, yet apparently occur ‘randomly’ within a predictable range of values correlated with the aliquot volume (Fig. 2.5). Stringent efforts to eradicate heterogeneous ice nucleating contaminants in the liquids or ambient atmosphere by washing and preparing in a laminar flow hood made only a minor difference to the well freezing temperatures. Nevertheless it is apparent larger aliquot volume or substrate surface area increases the chances of one of these sites being present. Indeed, successful cryopreservation in large volumes such as bags may not require control of nucleation because they freeze spontaneously at these high temperatures. In contrast, multiwell plates containing 10s of  $\mu\text{L}$ s are highly susceptible to supercooling. Hence, in order to achieve successful cryopreservation in multiwell plates, the control of ice nucleation is needed.

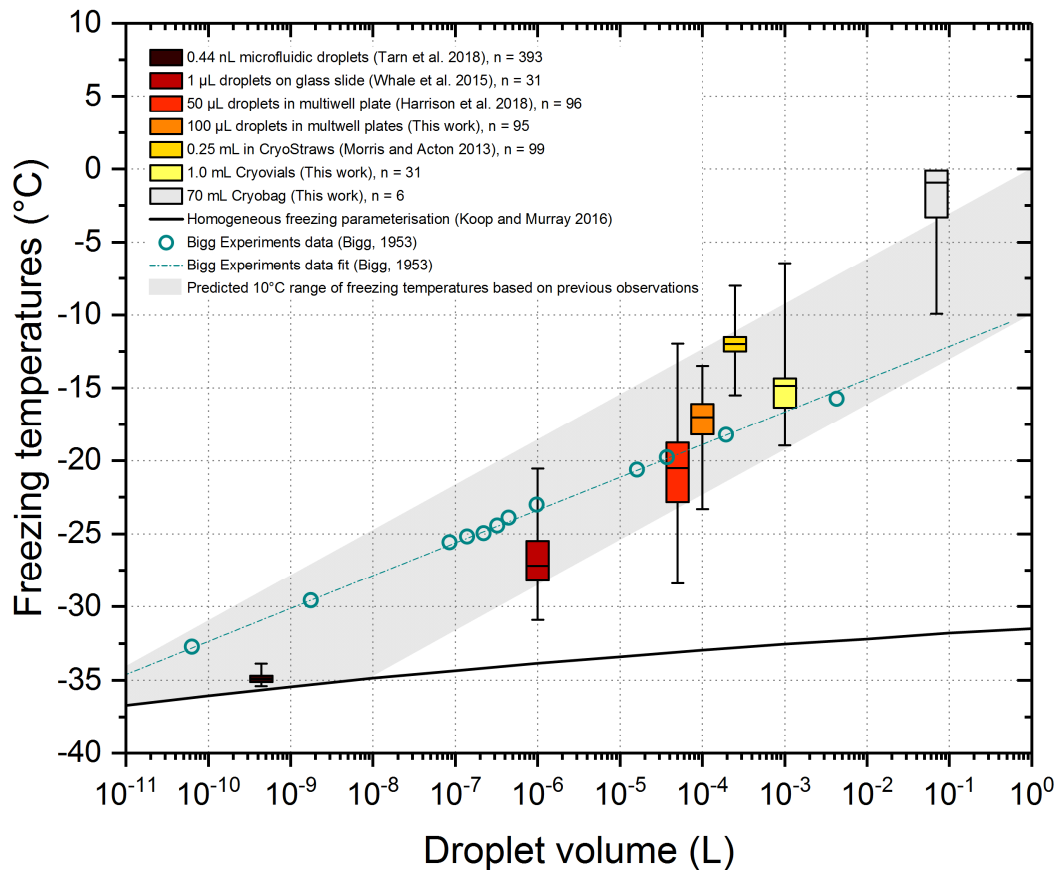


**Figure 2.5: Freezing temperatures of purified water droplet ensembles at a range of volumes with an empirical trend Boxes denote 25th – 75th percentiles, bars denote medians and whiskers denote range of values. We have plotted literature data [4; 5; 13; 25; 34; 37] of ice nucleation temperatures of pure water aliquots in various containers and spanning volumes from sub-pL to tens of mL along with a homogenous freezing parameterisation [16]. We also show new data for 100  $\mu$ L droplets (from Fig. 2.2) and data for 1.0 ml in cryovials (Corning 2.0 mL capacity, Cat No. 430488) and 70 ml in cryobags (Milenyi CD250). We used Hyclone cell culture water. The cryovials assay was performed using the IR-NIPI as previously described (n=31); while for the cryobags the ice nucleation temperatures (n=31) were determined using a thermocouple as the bags were cooled while inside aluminium cassettes.**

## 2.5 Conclusions

We have demonstrated that primary bovine granulosa cells can be successfully cryopreserved in monolayers in a generic 96-well culture plate format using controlled-rate freezing with a non-invasive manual nucleation technique. Using a

remote IR thermometry technique we quantified, for the first time remotely, the supercooling behaviour of aliquots of cryoprotectant in a 96-well plate. The granulosa cell culture freezing survival rates coupled with the IR measurement of freezing temperatures in multiwell plates indicate a first order link between higher nucleation temperatures and better rates of post-thaw survival. We also describe for the first time a qualitative link between higher ice nucleation temperatures and a reduction in the degree of post-thaw cell detachment which is known to be a problem when freezing cells in monolayer form. Optimal conditions such as cryoprotectant formulation, thermal expansion properties of the substrate, cooling rate and thawing method are likely to differ when cryopreserving differing cell types in multiwell plates. Controlling ice nucleation at high temperatures should now also be considered as standard protocol as we also have shown that deep and variable supercooling occurs when sub-mL aliquots of cryoprotectant are cooled to cryogenic temperatures in 96-well plates. This finding should prove useful for the development of high throughput screening of cryobiological procedures, facilitating quick testing of new cryoprotectants and treatments in a primary cell system. Additionally, there are applications where cryopreservation of cells directly in 96-well plates will be of use, notably testing of drug molecules on, for example, primary hepatocytes and cardiomyocytes. This work indicates that control of ice nucleation will likely be critical for the success of any such application. Therefore further work is proposed to cryopreserve a wider range cell types, expand performance metrics to cell functionality as well as viability and assess methods of controlling ice nucleation in 96-well plates in a potentially cGMP compliant manner.

.

## References

- Acker, J. P., Larese, A., Yang, H., Petrenko, A., and McGann, L. E.: Intracellular Ice Formation Is Affected by Cell Interactions, *Cryobiology*, 38, 363-371, 1999.
- Atkinson, J. D., Murray, B. J., Woodhouse, M. T., Whale, T. F., Baustian, K. J., Carslaw, K. S., Dobbie, S., O'Sullivan, D., and Malkin, T. L.: The importance of feldspar for ice nucleation by mineral dust in mixed-phase clouds, *Nature*, 498, 355-358, 2013.
- Balasubramanian, S. K., Wolkers, W. F., and Bischof, J. C.: Membrane hydration correlates to cellular biophysics during freezing in mammalian cells, *Biochim Biophys Acta*, 1788, 945-953, 2009.
- Bigg, E. K.: The Supercooling of Water, *Proceedings of the Physical Society. Section B*, 66, 688-694, 1953.
- Borenfreund, E. and Puerner, J. A.: A simple quantitative procedure using monolayer cultures for cytotoxicity assays (HTD/NR-90), *Journal of tissue culture methods*, 9, 7-9, 1985.
- C. Prickett, R., A. Marquez-Curtis, L., A.W. Elliott, J., and McGann, L.: Effect of supercooling and cell volume on intracellular ice formation, 2015.
- Campbell, L. H. and Brockbank, K. G. M.: Cryopreservation of Adherent Cells on a Fixed Substrate, *IntechOpen*, doi: 10.5772/58618, 2014. 2014.
- Campbell, L. H. and Brockbank, K. G. M.: Culturing with trehalose produces viable endothelial cells after cryopreservation, *Cryobiology*, 64, 240-244, 2012.
- Campbell, L. H. and Brockbank, K. G. M.: Serum-free solutions for cryopreservation of cells, *In Vitro Cellular & Developmental Biology - Animal*, 43, 269-275, 2007.
- Campbell, L. H., Brockbank, K. G. M., and Taylor, M. J.: Two stage method for thawing cryopreserved cells. Inc, L. S. (Ed.), US6596531B2, 2003.
- Clarke, A., Morris, G. J., Fonseca, F., Murray, B. J., Acton, E., and Price, H. C.: A Low Temperature Limit for Life on Earth, *PLOS ONE*, 8, e66207, 2013.
- Corsini, J., Maxwell, F., and Maxwell, I. H.: Storage of various cell lines at -70 degrees C or -80 degrees C in multi-well plates while attached to the substratum, *Biotechniques*, 33, 42, 44, 46, 2002.
- Ebertz, S. L. and McGann, L. E.: Cryoinjury in endothelial cell monolayers, *Cryobiology*, 49, 37-44, 2004.
- Eskandari, N., Marquez-Curtis, L. A., McGann, L. E., and Elliott, J. A. W.: Cryopreservation of human umbilical vein and porcine corneal endothelial cell monolayers, *Cryobiology*, 85, 63-72, 2018.
- Fuller, B. and Paynter, S.: Fundamentals of cryobiology in reproductive medicine, *Reprod Biomed Online*, 9, 680-691, 2004.
- Halwani, D. O., Brockbank, K. G. M., Duman, J. G., and Campbell, L. H.: Recombinant *Dendroides canadensis* antifreeze proteins as potential ingredients in cryopreservation solutions, *Cryobiology*, 68, 411-418, 2014.

Harrison, A. D., Whale, T. F., Rutledge, R., Lamb, S., Tarn, M. D., Porter, G. C. E., Adams, M. P., McQuaid, J. B., Morris, G. J., and Murray, B. J.: An instrument for quantifying heterogeneous ice nucleation in multiwell plates using infrared emissions to detect freezing, *Atmos. Meas. Tech.*, 11, 5629-5641, 2018.

Hobbs, C. A. and Hobbs, P. V.: *Ice Physics*, Clarendon Press, 1974.

Katkov, I. I., Kan, N. G., Cimadamore, F., Nelson, B., Snyder, E. Y., and Terskikh, A. V.: DMSO-Free Programmed Cryopreservation of Fully Dissociated and Adherent Human Induced Pluripotent Stem Cells, *Stem Cells Int*, 2011, 981606-981606, 2011.

Kilbride, P., Meneghel, J., Lamb, S., Morris, J., Pouzet, J., Jurgielewicz, M., Leonforte, C., Gibson, D., and Madrigal, A.: Recovery and Post-Thaw Assessment of Human Umbilical Cord Blood Cryopreserved as Quality Control Segments and Bulk Samples, *Biology of Blood and Marrow Transplantation*, 25, 2447-2453, 2019.

Koop, T. and Murray, B. J.: A physically constrained classical description of the homogeneous nucleation of ice in water, *The Journal of Chemical Physics*, 145, 211915, 2016.

Lauterboeck, L., Gryshkov, O., Hofmann, N., and Glasmacher, B.: Importance of controlled ice formation for efficient cell biobanking, 2016, 84-90.

Lauterboeck, L., Hofmann, N., Mueller, T., and Glasmacher, B.: Active control of the nucleation temperature enhances freezing survival of multipotent mesenchymal stromal cells, *Cryobiology*, 71, 384-390, 2015.

Lee, R. E., Warren, G. J., and Gusta, L. V.: *Biological ice nucleation and its applications.*, 1995. 1995.

Massie, I., Selden, C., Hodgson, H., Fuller, B., Gibbons, S., and Morris, G. J.: GMP Cryopreservation of Large Volumes of Cells for Regenerative Medicine: Active Control of the Freezing Process, *Tissue Engineering Part C: Methods*, 20, 693-702, 2014.

Mazur, P.: Equilibrium, quasi-equilibrium, and nonequilibrium freezing of mammalian embryos, *Cell Biophysics*, 17, 53-92, 1990.

Mazur, P.: Kinetics of Water Loss from Cells at Subzero Temperatures and the Likelihood of Intracellular Freezing, *The Journal of General Physiology*, 47, 347, 1963.

Mazur, P., Leibo, S. P., and Chu, E. H.: A two-factor hypothesis of freezing injury. Evidence from Chinese hamster tissue-culture cells, *Exp Cell Res*, 71, 345-355, 1972.

Meneghel, J., Kilbride, P., Morris, J. G., and Fonseca, F.: Physical events occurring during the cryopreservation of immortalized human T cells, *PLOS ONE*, 14, e0217304, 2019.

Morris, G. J. and Acton, E.: Controlled ice nucleation in cryopreservation--a review, *Cryobiology*, 66, 85-92, 2013.

Morris, G. J. and Lamb, S.: Improved Methods for Cryopreservation of Biological Material. (GB), A. L. (Ed.), 15/557320, 2018.

- Nagy, A., Gertsenstein, M., Vintersten, K., and Behringer, R.: Freezing Embryonic Stem (ES) Cells in 96-Well Plates, *CSH Protoc*, 2006, 2006.
- Oldenhof, H., Friedel, K., Sieme, H., Glasmacher, B., and Wolkers, W. F.: Membrane permeability parameters for freezing of stallion sperm as determined by Fourier transform infrared spectroscopy, *Cryobiology*, 61, 115-122, 2010.
- Petersen, A., Schneider, H., Rau, G., and Glasmacher, B.: A new approach for freezing of aqueous solutions under active control of the nucleation temperature, *Cryobiology*, 53, 248-257, 2006.
- Picton, H. M., Campbell, B. K., and Hunter, M. G.: Maintenance of oestradiol production and expression of cytochrome P450 aromatase enzyme mRNA in long-term serum-free cultures of pig granulosa cells, *J Reprod Fertil*, 115, 67-77, 1999.
- Prickett, R. C., Marquez-Curtis, L. A., Elliott, J. A. W., and McGann, L. E.: Effect of supercooling and cell volume on intracellular ice formation, *Cryobiology*, 70, 156-163, 2015.
- Pruppacher, H. R. and Klett, J. D.: *Microphysics of Clouds and Precipitation*, Springer Netherlands, 1997.
- Rutt, T., Eskandari, N., Zhurova, M., Elliott, J. A. W., McGann, L. E., Acker, J. P., and Nychka, J. A.: Thermal expansion of substrate may affect adhesion of Chinese hamster fibroblasts to surfaces during freezing, *Cryobiology*, 86, 134-139, 2019.
- Tarn, M. D., Sikora, S. N. F., Porter, G. C. E., O'Sullivan, D., Adams, M., Whale, T. F., Harrison, A. D., Vergara-Temprado, J., Wilson, T. W., Shim, J.-u., and Murray, B. J.: The study of atmospheric ice-nucleating particles via microfluidically generated droplets, *Microfluidics and Nanofluidics*, 22, 52, 2018.
- Töpfer, E., Pasotti, A., Telopoulou, A., Italiani, P., Boraschi, D., Ewart, M.-A., and Wilde, C.: Bovine colon organoids: From 3D bioprinting to cryopreserved multi-well screening platforms, *Toxicology in Vitro*, 61, 104606, 2019.
- Wells, D. E. and Price, P. J.: Simple rapid methods for freezing hybridomas in 96-well microculture plates, *J Immunol Methods*, 59, 49-52, 1983.
- Whittinham, D. G.: Some Factors Affecting Embryo Storage in Laboratory Animals, *Ciba Foundation Symposium 52 - The Freezing of Mammalian Embryos*, doi: doi:10.1002/9780470720332.ch610.1002/9780470720332.ch6, 1977. 97-127, 1977.
- Wolkers, W. F., Balasubramanian, S. K., Ongstad, E. L., Zec, H. C., and Bischof, J. C.: Effects of freezing on membranes and proteins in LNCaP prostate tumor cells, *Biochim Biophys Acta*, 1768, 728-736, 2007.
- Wrathall, J. H. and Knight, P. G.: Production of immunoactive inhibin by bovine granulosa cells in serum-free culture: effects of exogenous steroids and FSH, *Domest Anim Endocrinol*, 10, 289-304, 1993.

### **3 A highly active mineral ice nucleating agent supports in-situ high throughput cell cryopreservation**

#### **Chapter abstract**

Cryopreservation of biological matter in microliter volumes of liquid would be enormously useful for a range of applications, however it is hampered by the propensity of microlitre volumes to supercool. Deep supercooling is known to lead to poor post thaw viability. Here we show that a newly discovered mineral ice nucleator can almost eliminate supercooling in 100 microlitre aliquots in multiwell plates. This elimination of supercooling greatly enhances cell viability relative to uncontrolled nucleation. Using infrared thermography, we demonstrate a direct relationship between extent of supercooling and cell viability. Using a mineral nucleator delivery system we open the door to the routine cryopreservation of mammalian cells in multiwell plates for applications such as high throughput toxicology testing of pharmaceutical products.

#### **3.1 Introduction**

Cryopreservation is the process of cooling biological materials to low temperatures to allow long term storage of the biological material (Mazur, 1984; Mazur et al., 1972). If left uncontrolled, ice nucleation is an unpredictable variable in cryopreservation procedures as aqueous solutions typically supercool well below their equilibrium melting points (Daily et al., 2020; Hunt, 2019; Morris and Acton, 2013). When uncontrolled the ice-nucleation temperature ( $T_{nuc}$ ) is determined by the presence (or absence) of heterogeneous ice nucleating sites in the form of impurities within the sample media or features on walls of the vessel (Morris and Acton, 2013). This becomes increasingly problematic when the vessel volume is small (<1 mL) as heterogeneous ice nucleating sites are less likely to be present, meaning deep supercooling of aqueous solutions can occur (Daily et al., 2020). This deep supercooling can reduce viability by increasing the likelihood of lethal intracellular ice formation during the cooling step (Acker et al., 1999; Clarke et al., 2013; Lauterboeck et al., 2016; Massie et al., 2011). The irregular presence of ice nucleation (IN) sites within cryopreservation vessels means the degree of supercooling is

unpredictable (Daily et al., 2020; Morris and Acton, 2013). This often leads poor and inconsistent post-thaw recovery and function of the preserved cells or tissue. The ability to reliably cryopreserve plated cell monolayers in situ in a high throughput multiwell plate format would be highly beneficial in the field of drug discovery and toxicity screening. There are also other emerging fields in biomedicine and cryobiology where controlled ice nucleation would be advantageous such as complex tissue banking (Meneghel et al., 2020; Taylor et al., 2019), and regenerative medicine (Sun et al., 2016). However, the typical volume of liquid aliquots in 96-well plates of around 100  $\mu\text{L}$  will supercool by up to 25  $^{\circ}\text{C}$  when IN is uncontrolled (Daily et al., 2020; Harrison et al., 2018). Isolated cells must be preserved in suspension format before thawing, transferred to multiwell plates and cultured onto confluent monolayers over several days before meaningful diagnostic assays or manipulations can be performed.

Customary practice in cryopreservation for inducing ice-nucleation is ‘manual’ nucleation, where touching the outside of the vessel with a very cold object locally cools the contents enough to trigger freezing (Kilbride and Meneghel, 2021; Mazur et al., 1972; Whittincham, 1977). While achievable for vessels such as straws, cryovials and cryobags, it is far less practical for multiwell plates which would require ice-nucleation in each individual well to be induced simultaneously. A solution to this where ice-mist falling from a cryogenically cooled object into exposed supercooled liquid in a 96-well plate has been demonstrated (Daily et al., 2020). While this method reliably and non-invasively triggered ice-nucleation at warm ( $< 5$   $^{\circ}\text{C}$  supercooling) temperatures, having sample contents exposed to air creates sterility issues and scaling up would require challenging of automation.

An alternative method of controlling IN is by introducing ice-nucleating materials to the cryopreservation medium in a manner where they do not interfere with the specimen and can be easily removed after thawing (Morris and Acton, 2013). Ice-nucleating materials are substances which possess sites which substantially raise the temperature at which heterogeneous IN occurs in both supercooled water (Murray et al., 2012) and aqueous solutions (Whale et al., 2018). Ice-nucleating materials tested to date include insoluble substances such as silver iodide (AgI) (Atig et al., 2018; DeMott, 1995; Herbert et al.) and cholesterol (Head, 1961; Sosso et al., 2018) and dispersible substances of biological origin such as Snomax® (Beydoun et al., 2017;

Desnos et al., 2018; Roy et al., 2021; Wex et al., 2015) and pollen washings (Augustin et al., 2013; Dreischmeier et al., 2017; O'Sullivan et al.; Pummer et al., 2012). Several studies have shown how these ice-nucleating materials can be applied to cryopreservation (Jiang et al., 2021; Kojima et al., 1988; Massie et al., 2014; Missous et al., 2007; Teixeira et al., 2017), although they ultimately may be difficult to make compliant with cGMP (current Good Manufacturing Practice) applications (Morris and Acton, 2013). Also, few of these studies involved 96-well plates (Campbell and Brockbank, 2014; Wragg et al., 2020), which pose some specific challenges for this application. Firstly, smaller aliquot volumes limit the mass of ice-nucleating materials that can be deployed, reducing the probability of having one of the rare ice-nucleating sites that are capable of inducing freezing at warm temperatures in any one aliquot. Secondly, measuring the temperature ice nucleating temperatures that occur in each well using, for example thermocouples, is problematic. Doing this would enable confirmation that the ice-nucleating materials deployed are successfully controlling ice-nucleation and even enable the relationship between  $T_{\text{nuc}}$  and post-thaw survival to be quantified.

We report a formulation based on a 'hyperactive' variety of potassium- (K-) feldspar, 'LDH1', as a novel passive IN material with biocompatibility potential for use with cryopreserving cultured cells in a small volume, *in situ* in a high throughput, multiwell plate format. Mineral powders are emerging as a type of IN material that could be used for cryopreservation applications (Jiang et al., 2021; Wragg et al., 2020). They potentially offer advantages over biologically derived ice-nucleating materials in terms of their biocompatibility with the samples being preserved and their stability. For instance, the ice-nucleating proteins in Snomax lose their ice-nucleating ability after moderate heat treatment (Pummer et al., 2015) (Daily et al., 2021) or after several months' storage (Polen et al., 2016). The ice-nucleating ability of minerals has been intensely studied (Atkinson et al., 2013; Harrison et al., 2019; Yakobi-Hancock et al., 2013) due their potential role as ice-nucleating particles in atmospheric mineral dust from deserts and their resultant role in modulating the radiative properties of clouds (Murray et al., 2021; Storelvmo and Tan, 2015). Although clay minerals such as kaolinite were long considered to be efficient ice-nucleators (Mason and Maybank, 1958) (and are sometimes still referred to as such (Sosso et al., 2016; Zielke et al., 2016)), K-feldspar, plagioclase feldspars and quartz have since been shown to be far

more effective nucleators (Atkinson et al., 2013; Harrison et al., 2019; Kaufmann et al., 2016; Yakobi-Hancock et al., 2013; Zolles et al., 2015). The IN activity of individual samples of the same mineral can still vary substantially and as such some hyperactive varieties of K-feldspar have been identified which can nucleate ice at temperatures as warm as  $-2\text{ }^{\circ}\text{C}$  (Harrison et al., 2016; Peckhaus et al., 2016). While the physical reasons for their hyperactivity remain unclear, their active sites have been imaged concentrated on microscopic steps, cracks and pores (Kiselev et al., 2017; Pach and Verdaguer, 2019). These sites are unlikely to be proteinaceous IN material contaminants due to their heat resistance (Daily et al., 2021; Peckhaus et al., 2016).

In this study we characterise the exceptional ice nucleating ability of LDH1 in sub-mL aliquots of both pure water and cryoprotectant (CPA) solution in 96 well plates so to quantitatively compare its INA with other ice-nucleating substances applied to this format. We then go on to demonstrate how LDH1 can aid cell cryopreservation *in situ* within multiwell plates using monolayer cultures of immortalised human hepatocytes under small aliquots of cryoprotectant. We do this firstly by directly linking  $T_{\text{nuc}}$  in a 96-well plate to the post-thaw cell recovery rate on an individual well by well basis with remote temperature measurements using infra-red- (IR) thermography. Secondly, we trial the high throughput cell freezing and recovery performance in several 96-well plates frozen with IN controlled by LDH1 delivered in IceStart™ arrays (Morris and Lamb, 2018; Wragg et al., 2020).

## 3.2 Results

### 3.2.1 The ice-nucleating ability of LDH1

To assess the ability of LDH1 to control IN in relative to other materials we performed droplet freezing assays of both single microlitre (pipetted on to a hydrophobic glass slide (Whale et al., 2015)) and 50  $\mu\text{L}$  sized droplets (pipetted into flat-bottomed polypropylene 96-well plates (Harrison et al., 2018)) of varyingly concentrated suspensions of ice-nucleating materials in pure water and cooled at a rate of  $1^\circ\text{C min}^{-1}$ . These included particulate samples LDH1, BCS-376 microcline, quartz, cholesterol monohydrate crystals and suspendable biologically derived ice-nucleating materials in the form of birch pollen washings and Snomax®.

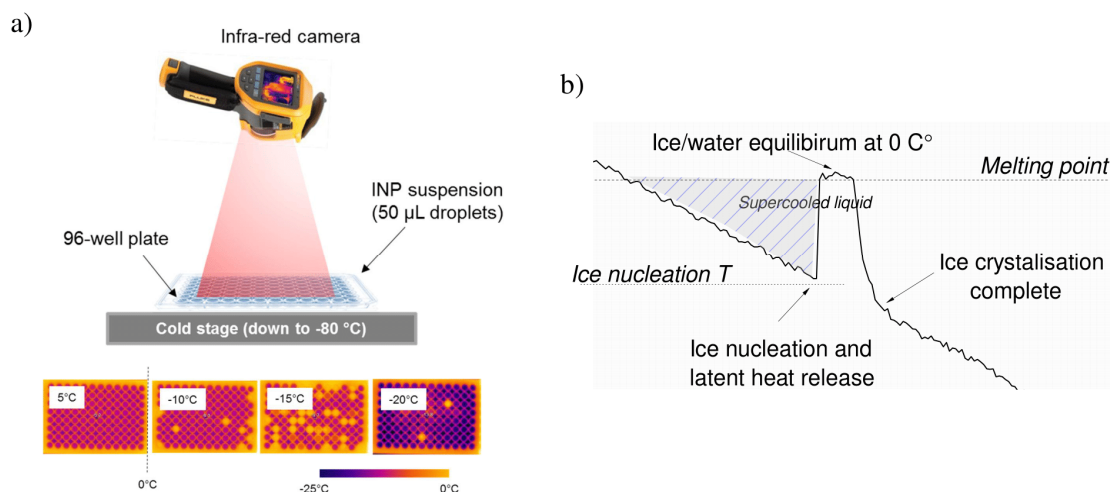


**Figure 3.1: Nucleation characteristics of a range of ice nucleating materials including the hyperactive K-feldspar (LDH1). a) Cartoon of IR-NIPI instrument with example IR images of 96-well plate and well ice-nucleation events used to obtain all the data in this figure. b) Demonstration of thermal history of well and determination of  $T_{\text{nuc}}$**

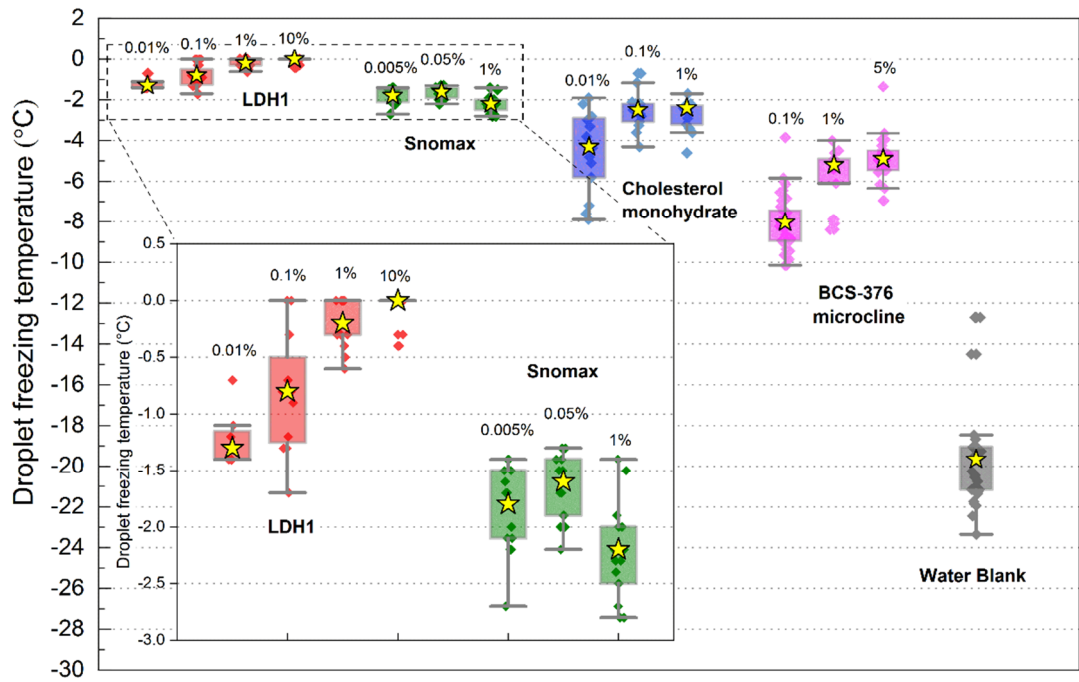


**Figure 3.2: Boxplot showing IR-NIPI results of droplet freezing assays for 50  $\mu$ L droplets of suspensions of several ice-nucleating materials in water at different concentrations. Boxes depict 25-75<sup>th</sup> percentile and yellow stars depict median droplet freezing temperatures.**

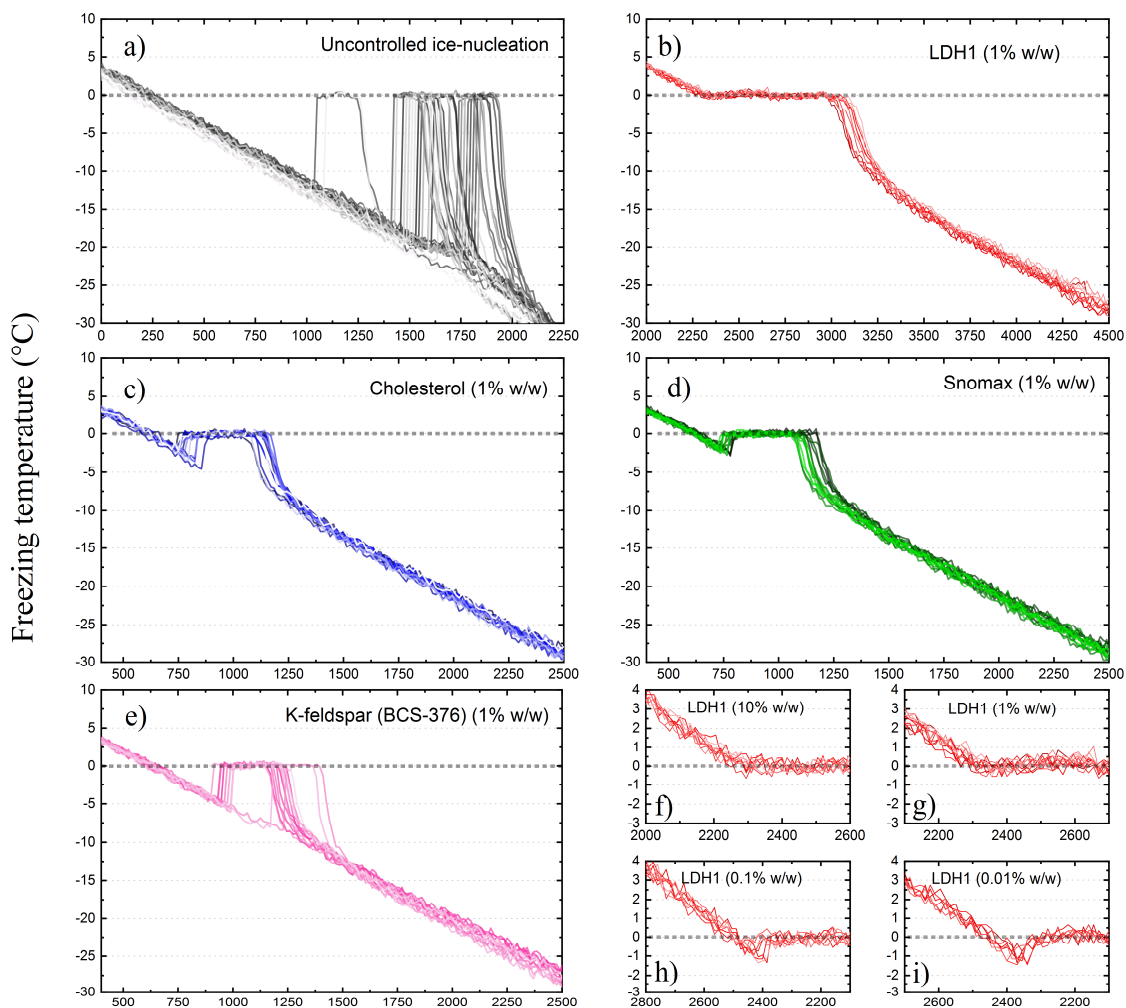


**Figure 3.3: a-e) Thermal history traces of droplet freezing assays shown in c) at concentrations of 1% w/w. f-i) Detailed thermal history of LDH1 runs at all concentrations illustrating the apparent elimination of supercooling. For plots in d-k) numbers indicate droplet temperature ( $^{\circ}\text{C}$ ) on  $x$ -axis and time into freezing run (s) on  $y$ -axis.**

The droplet freezing temperatures for 50  $\mu\text{L}$  droplets of ice-nucleating materials at various concentrations in 96-well plates, using IR-NIPI (Fig. 3.1a, b), are shown as boxplots in Fig. 3.2 as a simple comparison of freezing temperatures. For LDH1, the freezing temperatures are greater than any other ice-nucleating materials and increase with increasing concentration of nucleator (inset in Fig. 3.2). The IR-NIPI derived thermal history of individual wells in 96-well plates containing 50  $\mu\text{L}$  suspension droplets of LDH1 and the other ice-nucleating materials, as well as a blank run with pure water, are shown in Figs. 3.3. In the blank runs, the aliquots of water supercool by more than  $15^{\circ}\text{C}$  before nucleation occurred. The subsequent release of latent heat

caused the aliquot to warm to the melting point where crystal growth was limited by the loss of heat to the environment (Harrison et al., 2018). The temperature then returned to the temperature of its immediate surroundings once crystallisation was complete. The degree of supercooling is clearly much smaller when heterogeneous ice-nucleating materials are present. Strikingly, for wells with LDH1 at suspension concentrations above 1% none of the well temperatures noticeably dip below 0°C. Instead, they plateau at around 0°C before cooling again after crystallisation was complete. This observation implies that no measurable supercooling occurred and IN took place close to the melting point. Realistically our instrument cannot reliably detect supercooling of less than its nominal precision level of  $\pm 1$  °C (Harrison et al., 2018).

Using the data from Fig. 3.3, in combination with our microlitre droplet freezing assays data and literature data, we plot the number of active IN sites per unit mass of material as a function of temperature -  $n_m(T)$  (Fig. 3.4). This is an intrinsic measure of a specific material's ability to nucleate ice normalised to mass and can be used for comparison with other ice-nucleating materials. The results, shown in Fig. 3.4 show new  $n_m(T)$  fits for LDH1 and cholesterol plotted alongside existing  $n_m(T)$  parameterisations for K-feldspar (non-hyperactive), quartz, birch pollen and Snomax®. We found that LDH1 is more ice-active on a mass-by-mass basis than any other mineral, cholesterol or AgI and is comparable to Snomax®. Moreover, median freezing temperatures  $<1.5$ °C of the melting point of ice were seen for  $<0.1\%$  LDH1 (0.05 mg of LDH1 per well) suspension droplets in 96-well plates.

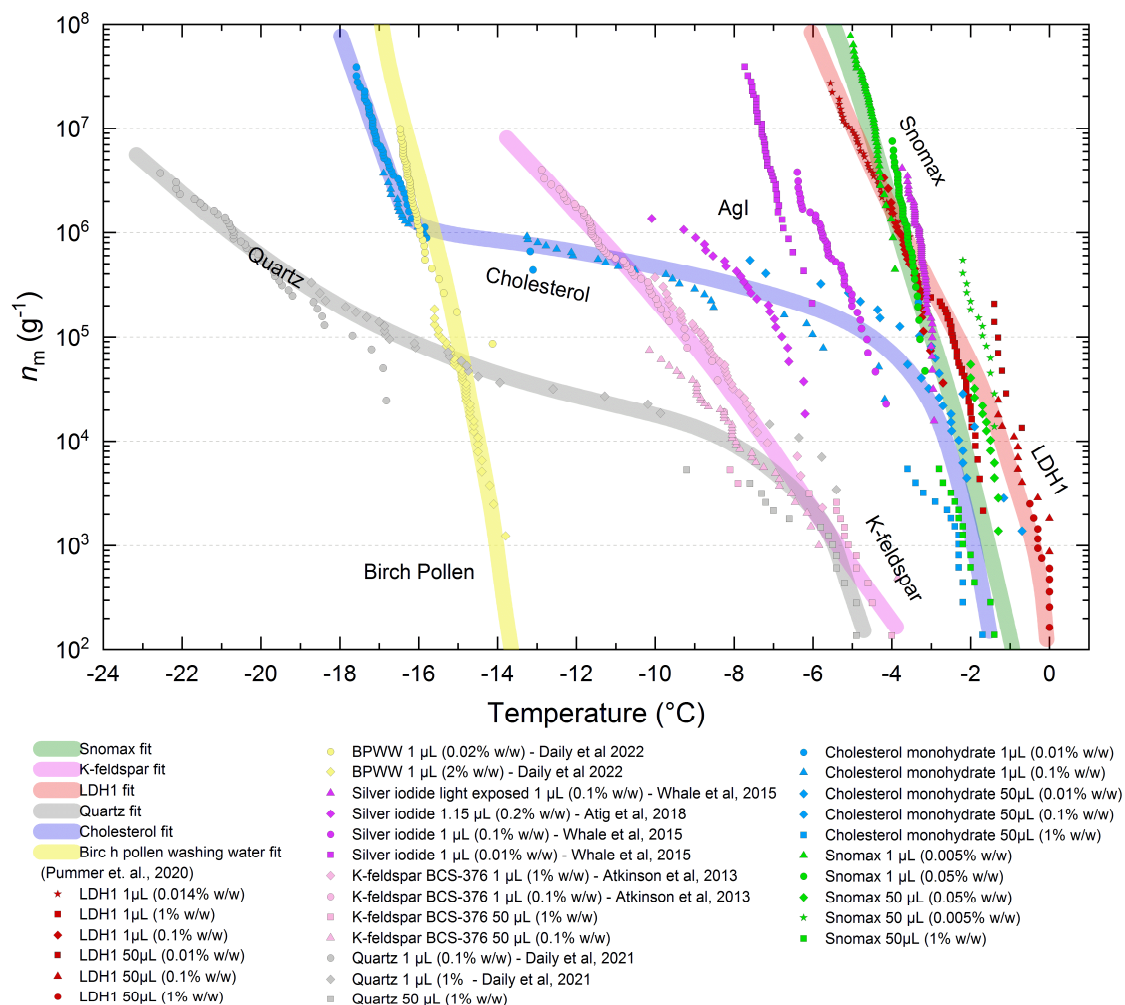


**Figure 3.4: Number of active sites per unit mass of LDH1 and other strong ice-nucleators as a function of temperature ( $n_m(T)$ ). Data points derived using equation (3.1) using data from droplet freezing assays either in 1  $\mu\text{L}$  or 50  $\mu\text{L}$  droplets. Fits for each material were plotted apart from birch pollen which is a parameterisation from Pummer et al. 2012. No fit was plotted for AgI due to the spread of data points.**

That LDH1 was able to virtually eliminate supercooling in 50  $\mu\text{L}$  droplets at concentrations as low as 0.1 wt. % (0.05 mg of material) implies that it contains sites able to nucleate ice close to the equilibrium melting point. The only other material recorded to induce IN at the melting point of water are long chain aliphatic alcohol monolayers (Gavish et al., 1990). This has not previously been seen in any mineral samples, although compared to other methods such as smaller volume droplet freezing assays (Harrison et al., 2016; Zolles et al., 2015) and differential scanning calorimetry (Kaufmann et al., 2016; Kumar et al., 2019) our experiment used a relatively large

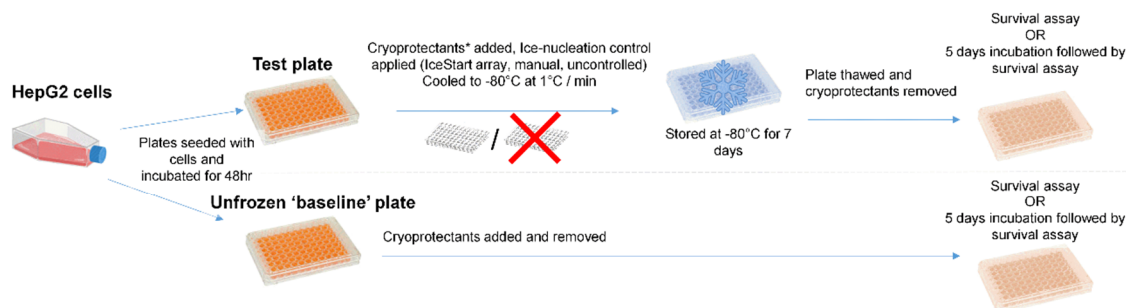
amount of material in each droplet. Natural mineral samples possess a range of chemical and crystallographic variations that could influence INA (Welti et al., 2019; Whale et al., 2017) and as such the reason for the exceptional INA of LHD1 compared to similar K-feldspar samples has yet to be elucidated (Kiselev et al., 2017; Peckhaus et al., 2016). Snomax®, in contrast with LDH1, is an exceptionally potent ice-nucleating material that does not appear to possess sites that can nucleate ice within 1 °C of the ice melting point. Our data shows 50 µL droplets appeared to reach a maximum IN temperature of around -1 °C at a concentration of 0.05% with a more concentrated suspension not increasing the IN temperature. This was previously seen with both Snomax® (Desnos et al., 2018; Wex et al., 2015) and its raw bacterial form *Pseudomonas syringae* (Lindow et al., 1989; Maki et al., 1974; Schnell and Vali, 1976). For example, maximum IN temperatures were around -2 °C and increasing the concentration from 0.1% to 1% did not result in significantly warmer IN temperatures (Wex et al., 2015) indicating that the Snomax® particles interacted in a manner where ice nucleating proteins were disrupted or occluded due to aggregation. We also found that the IN activity of LDH1 did not change significantly after three month storage in water at 4 °C (see Fig. 3.13 in the Supplementary Information (SI)). Also, its IN temperatures in 10% DMSO (dimethyl sulphoxide) solution are reduced by around 4 °C which is close to the melting point depression of the CPA formulation we used. This indicates that LDH1 is stable in water in terms of IN activity and is not affected by DMSO more than would be expected because of a reduction in water activity (Koop et al., 2000; Whale et al., 2018).

### **3.2.2 Link between aliquot ice-nucleation temperature and post-thaw survival rates of cryopreserved cells**

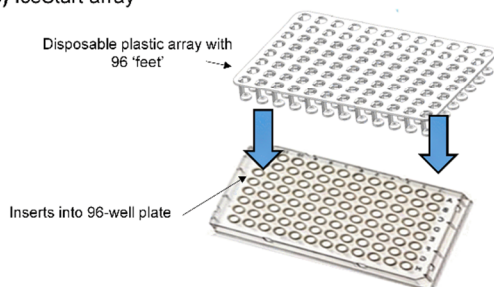
While it is known that ice formation at severe supercooling is likely to be hazardous to cells undergoing cryopreservation it is not quantitatively clear from the literature whether inducing ice nucleation at the melting point has significant benefits (Morris and Acton, 2013). To examine this, we took a 96-well plate containing HepG2 monolayer cultures and, using the IR-NIPI instrument, we simultaneously cryopreserved the cells and recorded the thermal history and IN temperature that occurred in each individual well of the plate. Doing this required a broad range of IN temperatures to occur across the 96-well plate and this would be impractical to induce by manual nucleation methods. Instead, we achieved this by spiking a small number

of wells with a few grains of LDH1 powder to nucleate ice close to the melting point and allowing the remaining wells to nucleate in an uncontrolled manner at much lower temperatures.

a) Plate cryopreservation experiment design



b) IceStart array



c) Well cross section

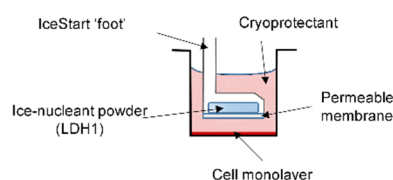


**Figure 3.5: Schematics for a) HepG2 plate cryopreservation protocol; b) and c) IceStart™ arrays. Note that IceStart™ arrays were only used for the high-throughput trials in results Section 3.2.3.**

The cell culture and cryopreservation protocols and cell viability assay are described in detail in Section 3.4.2.2 and outlined in Fig. 3.5. Briefly, a set of 96-well plates were seeded with HepG2 cells and cultured for 48hr until confluent monolayers formed. A subset of plates was designated for freezing and another for non-frozen controls. HepG2 cells are an immortalised human hepatocyte carcinoma cell line which can be cultured as 2D epithelial monolayers and are used as *in vitro* models for drug metabolism and liver cell toxicity studies (Donato et al., 2015; Massie et al., 2011; Stokich et al., 2014). Cryopreservation of confluent HepG2 cells *in situ* within the culture plates consisted of firstly replacing the culture medium with cryoprotectant solution. The plates were then transferred to the cooling plate of a controlled rate freezer (IR-NIPI or Asymptote ViaFreeze Duo) which cooled the plates at  $1\text{ }^{\circ}\text{C min}^{-1}$  to  $-80\text{ }^{\circ}\text{C}$  and then transferred to a  $-80\text{ }^{\circ}\text{C}$  freezer for storage. Plates were thawed in two stages (Campbell and Brockbank, 2014) to prevent thermal stresses – in a  $-20\text{ }^{\circ}\text{C}$

freezer for 20 minutes followed by warming to 37 °C using aluminium warming blocks to complete thawing in under 2 minutes. Post-thaw cell viability (PTV) was determined immediately by addition of the vital dye Neutral Red to the cell monolayer, with dye uptake limited to viable and metabolising cells only followed by lysing of the cells and measuring dye concentration by visible light absorbance on a microplate reader (Daily et al., 2020; Picton et al., 1999; Repetto et al., 2008).

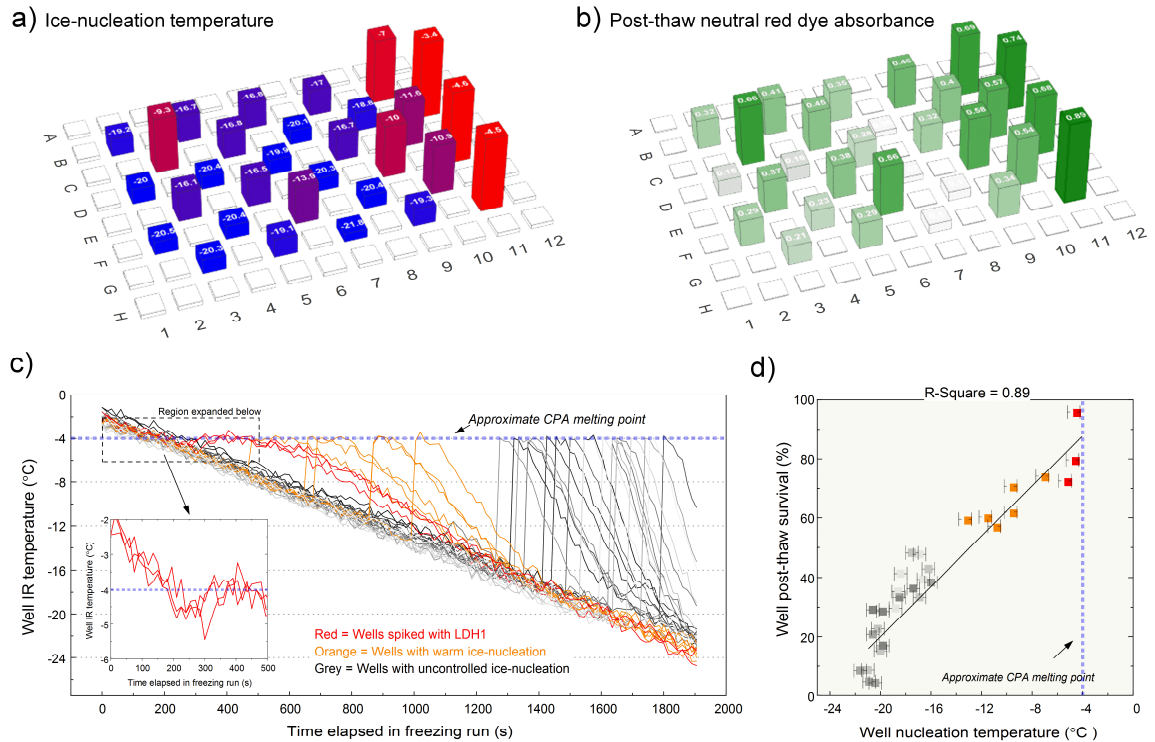


**Figure 3.6: Results for a 96-well plate with HepG2 culture cryopreserved with IR-NIPI instrument: a) Individual well  $T_{nuc}$ ; b) Individual well post-thaw neutral red dye absorbance; c) Thermal history of wells with detail for wells spiked with LDH1 d). Correlation plot of data from a) and b)**

Using a combination of uncontrolled IN of wells and spiking with LDH1 powder we were able to produce well  $T_{nuc}$  values ranging from -21.8 °C to -3.4 °C in the plate (Fig 3.6a) and these clearly correspond to the distribution of plate PTV values. Indeed, the scatter plot of well PTV and  $T_{nuc}$ , shown in Fig 3.6d, show that well IN temperature and PTV is strongly positively correlated ( $R^2 = 0.89$ ) and appear to show a linear dependence. The thermal histories for each well, shown in Fig 3.6c, contrast the temperature fluctuations that occur in wells with IN controlled at warm temperature with those with IN occurring at colder temperature. These fluctuations comprise a very

rapid jump in temperature due to latent heat release when ice-nucleation and crystallisation occur and, once all the available water has crystallised, followed by a drop in temperature as the fully frozen well equilibrates with the bulk of the plate (Daily et al., 2020). The total latent heat released from each well after is the same regardless of  $T_{\text{nuc}}$  as this only depends on the mass of ice crystallised. The severity of the temperature fluctuations, however, increases with the degree of supercooling because the rate of release of latent heat from ice crystal growth depends on how readily the heat can be dissipated to surroundings. If there is a significant temperature difference between the melting point of the well liquid and the bulk plate temperature when IN occurs (i.e., deep supercooling) this will drive faster ice crystallisation and thus faster latent heat release. A consequence of this is not only that wells may experience rapid rises in temperature but also cool at rates far faster than intended after ice-nucleation occurs. Figure 3.6c illustrates how the maximum rate of cooling of wells after the ice crystallisation phase is far higher for wells with low (uncontrolled)  $T_{\text{nuc}}$  ( $\sim 7 \text{ }^\circ\text{C min}^{-1}$ ) than those with  $T_{\text{nuc}}$  near the melting point ( $3 \text{ }^\circ\text{C min}^{-1}$ ). The rate of warming upon ice-nucleation was far faster than the 15 s time interval we used for temperature measurements apart from when nucleation occurred close (within  $1 \text{ }^\circ\text{C}$ ) to the melting point. For wells nucleating below  $-10 \text{ }^\circ\text{C}$  the rise to melting point appeared instantaneous implying warming rates of 100s of  $^\circ\text{C}$  per minute. Overall, it is clear that warmer well IN temperatures and corresponding smaller rates of change of temperature are conducive to cell survival.

### **3.2.3 High-throughput cryopreservation of HepG2 cell monolayers in situ within 96-well plate with LDH1 delivered via IceStart™ arrays**

We then tested our method of 96-well plate cell cryopreservation with controlled IN using IceStart™ arrays as vehicle for delivery of LDH1 (Morris and Lamb, 2018; Wragg et al., 2020). This strategy enabled us to determine whether LHD1 significantly improved cryopreservation performance using a protocol that could be scaled up. IceStart™ arrays (Fig. 3.5a, see also Fig 1.17) are disposable plastic devices, containing a mineral nucleator (in this case LDH1), that can be inserted into a 96-well plate containing adherent cells prior to undergoing freezing and then removed after thawing without contacting the cells. They contain ‘feet’ each of which is loaded with approximately 25 mg of IN material and which fit into each well of the 96-well plate and trigger IN in the CPA in each well when the temperature at which the INM

becomes active. We were unable to measure IN temperatures for the 96-well plates cryopreserved in this section, however in ‘blank’ plate freezing runs without cells we observed using the IR-NIPI that indeed no supercooling was detected when IceStart™ arrays loaded with LDH1 were applied to 96-well plate wells with either 100 µL of water and CPA. Each foot of the IceStart array contains 25mg of LDH and this amount deployed per well is considerably higher the amounts that reliably eliminated supercoolings of more than 1 °C, with 1mg per well for 1% w/v and 10mg for 10% w/v, as demonstrated in Fig 3.3. Therefore, we can assume that IN was initiated close to the CPA melting point wherever IceStart™ arrays were applied to cryopreserved 96-well plates.

We performed two 96-well plate freezing trials, each consisting of eight identical plates of HepG2 monolayer cultures cryopreserved with varying methods of IN control. Post-thaw cell viability (PTV, number of viable cells) was assessed immediately upon thawing and compared them to a non-frozen control 96-well plate culture to determine acute cell post-thaw survival rates (PTS, %). The first trial determined PTV immediately upon thawing while for the second trial the cryopreserved plates were cultured for a further five days after thawing to determine longer term cell viability and performance. Plates were frozen with portions divided into varying methods of IN control: IceStart™ arrays loaded with LDH1 powder, uncontrolled nucleation as a negative control and manual nucleation as a positive control (see Fig 3.7a). The manual nucleation method used ice mist falling from a cold object and has been previously demonstrated to induce IN uniformly at moderately low supercooling (at most 5 °C) in 96-well plates (Daily et al., 2020). However, as this method involves exposing the plate to ambient air under non-sterile conditions these plates were unsuitable for inclusion in the 5-day post-thaw culture trial.

The results of the freezing trials for both immediate post-thaw and 5-day post thaw along with statistical significance testing (one way ANOVA for the immediate post-thaw trial and two sample t-test for the 5-day post thaw trial) are shown in Fig. 3.7. For the immediate post-thaw viability assessment, all eight plates’ wells with IceStart™ applied had significantly higher PTV cell counts than where IN was uncontrolled ( $p < 0.05$ ). Differences were seen in individual plates between IceStart™ and Manual nucleation wells, however overall neither nucleation method resulted in constantly higher or lower results. The overall immediate post-thaw recovery rate of

the eight replicates were 51.0 %, 47.0 % and 19.1 % for IceStart™, Manual nucleation and Uncontrolled nucleation respectively meaning both IceStart™ and Manual nucleation resulted in significantly higher PTS than uncontrolled nucleation and there was no significant difference between either method (one way ANOVA,  $p < 0.05$ ). For the 5-day post-thaw trial, where only IceStart™ and Uncontrolled nucleation methods of IN were used, all eight replicate plates showed significantly higher PTV cell number. Overall PTS over all plates averaged: 80.5 % vs 53.1 % respectively (two sample t-test  $p < 0.05$ ). In contrast to the immediate post-thaw viability trial, when the cryopreserved plates were cultured for a further 5 days after thawing the data was far more variable. For example, the uncontrolled nucleation datasets included clusters of ‘dead’ wells and ‘recovered’ wells within plates: this is clearest in Plate#10, #14 and #15 (Fig. 3.7e). In contrast, the LDH1 nucleated wells have a much greater and less variable PTV.

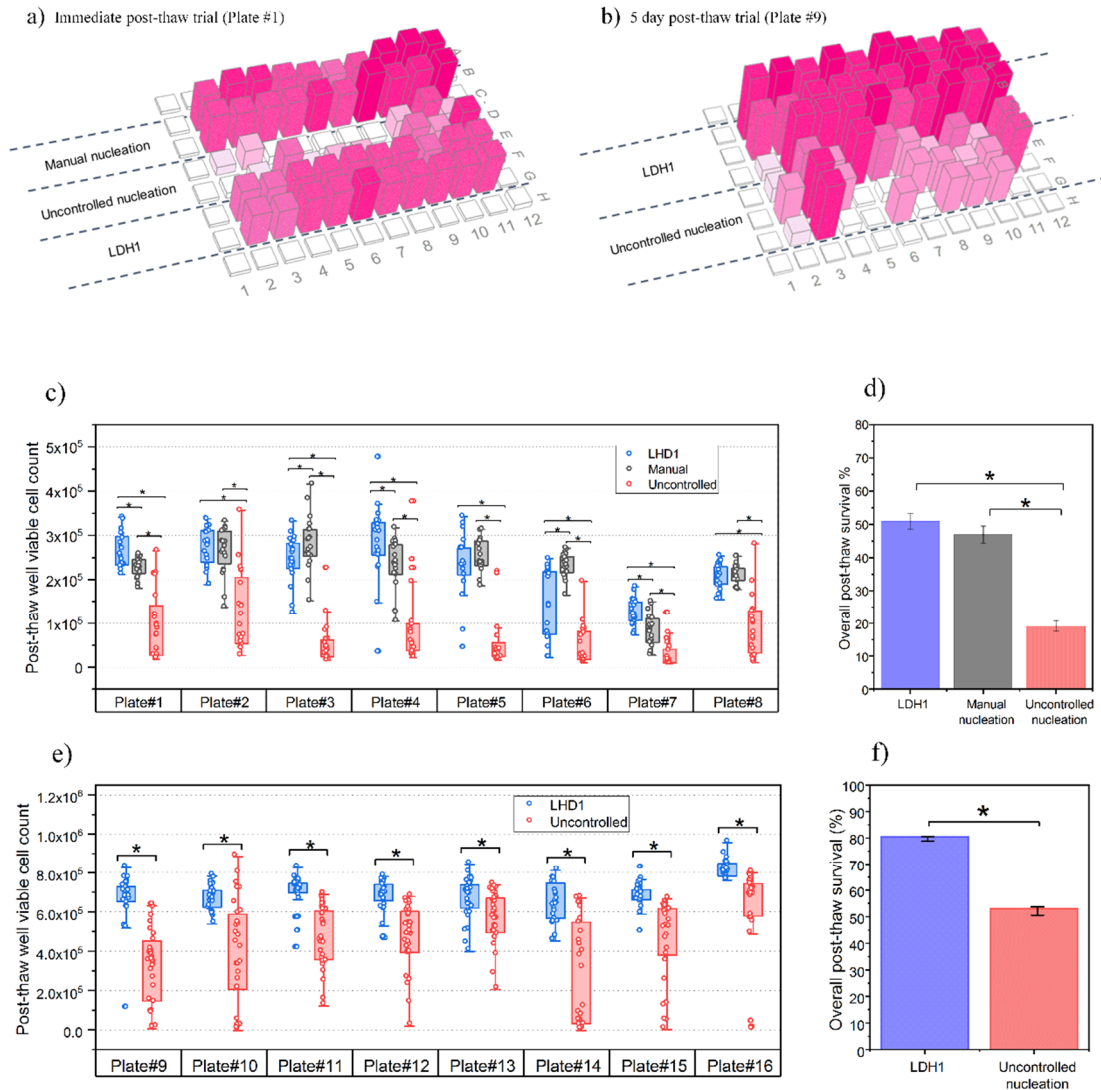


**Figure 3.7: Results for high-throughput trials of HepG2 cells cryopreserved in 96-well plate with and without controlled ice-nucleation with viability assays performed immediately post-thaw (a, c, d) and 5 days post-thaw (b, e, f). Example results for individual plates within the groups are shown in a) and b) with bar height and colour strength indicating post-thaw viability. Boxplots and ANOVA results for individual freezing runs are shown in c) and e). Overall post-thaw survival rates averaged over all 8 runs shown as d) and f). Note that manual nucleation was not used in the 5-day trial as this technique could not be executed in sterile conditions. Error bars indicate standard error of mean; bars and asterisk (\*) indicate significance between groups were  $p < 0.05$ .**

Using an optical microscope, we visually inspected the cell monolayers within the 96-well plates of non-frozen control cultures compared with those after thawing at the

point where neutral red dye had stained all the viable cells. Lower magnification images detailing the condition of the monolayers and higher magnification images resolving individual cells are shown in Fig. 3.8. Analysis revealed that the HepG2 monolayer detached from the culture plate surface when IN was not controlled, although the degree of detachment was variable and rarely complete. This detachment was almost absent when IceStart™ or Manual nucleation was used. In the former cases, where the cell layer had detached there were cells still visibly stained by the dye and therefore still viable. Closer inspection of the monolayer where still *in-situ* at the immediate post-thaw stage (Fig 3.8) revealed a network of spherical viable cells which had lost their epithelial morphology and were clumped together in places together with dead (unstained) cells. The proportion of viable cells to dead cells was qualitatively lower where ice-nucleation was uncontrolled compared to controlled, either by ice-mist or IceStart arrays. Re-examination after 5-days of culturing showed the surviving cells had re-attached and started proliferating once again, consistent with the general higher cell viability seen for all treatment groups compared with Immediate post-thaw. The manner of proliferation in wells frozen with controlled versus uncontrolled ice-nucleation was, however, distinct and reflected the variable amount of initial post-thaw monolayer detachment where well cultures grew as confluent monolayers compared with irregular masses.

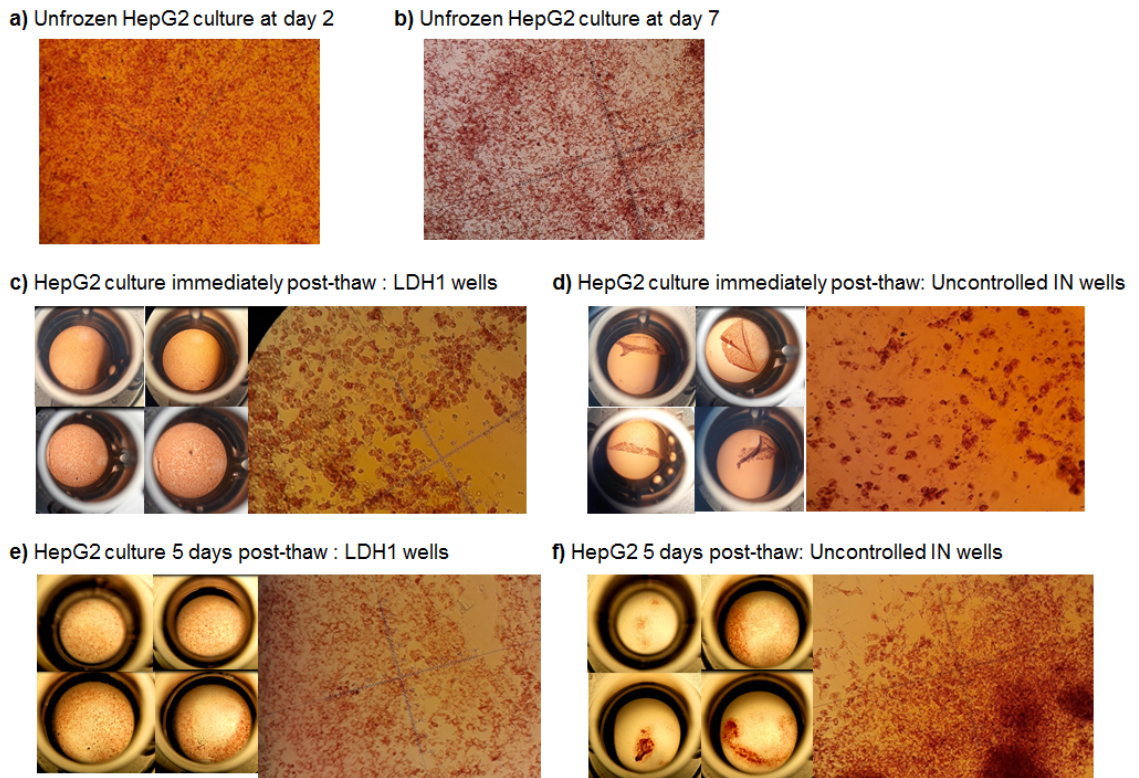


**Figure 3.8: Microscope images of cell monolayers after neutral red staining illustrating differences in cell morphology dependent on ice-nucleation control. Low magnification images illustrate condition of monolayer. Well diameter is 6.4mm. d-f) Same as above but for 5-day post-thaw trial. Note that manual nucleation was not used in this trial due to lack of sterility.**

Overall, we suggest that a combination of monolayer detachment and cell death contributed to the reduction in cell viability after our 96-well plate cultures were cryopreserved and thawed and these factors, particularly monolayer detachment are mitigated by the control of ice-nucleation.

### 3.3 Discussion

The exceptional ice-nucleating activity of LDH1 we reported allows us to use very small amounts (1mg) of it to almost eliminate supercooling. Also, the uniformity of the warm freezing temperatures also greatly reduces the randomness of heterogeneous ice-nucleation occurring – as little as 0.05 mg per well ensured no more than 1 °C of supercooling in any of the wells. Thus, with this substance we can control ice nucleation to a narrow range of warm temperatures and at small volume scales such

as 96-well (or even 384-well multiplates) in which supercooling of aqueous liquids at their working volumes is severe (10s of °C) and inevitable if left uncontrolled. Our freezing trials where plate cultures with HepG2 monolayers with IceStart™ arrays to control ice-nucleation at the CPA melting point clearly showed improved survival compared to uncontrolled ice-nucleation. Moreover, when we froze a plate culture with a broad range of well  $T_{\text{nuc}}$  we found a simple relationship existed where the warmer nucleation temperature correlated with post-thaw recovery rate. This simple relationship between well  $T_{\text{nuc}}$  we found is notable as it has been previously thought that mere prevention of severe supercooling is adequate for successful cell cryopreserving (Morris and Acton, 2013), but our results indicate that any degree of supercooling is detrimental.

Our observations quantitatively support the generally accepted theory that for slow-freezing cryopreservation of cells, preventing severe supercooling is required for good cell post-thaw recovery (C. Prickett et al., 2015; Lauterboeck et al., 2016; Lauterboeck et al., 2015; Massie et al., 2014) and is also linked to improved cell functionality. The nucleation and growth of extracellular ice enables migration of water from the cell, raising the glass transition temperature of the unfrozen cell contents. This allows the cell interior to vitrify, thus preventing intracellular ice formation (Clarke et al., 2013). Without extracellular ice present, intracellular ice formation is more likely to occur due to higher water content of the cells (Mazur et al., 1972). The configuration of cells in this case - monolayers attached to a substrate – is prone to ice propagation through cell-to-cell contact making them especially sensitive to incidence of IIF (Acker et al., 1999). Another possible protective mechanism from warm ice-nucleation temperature is the prevention of IIF occurring during thawing. The degree of supercooling affects the ice crystal structure that results after freezing with deeper supercooling leading to a finer-grained network (Morris and Acton, 2013). Smaller crystals higher interfacial free energy which can drive ice-recrystallization ultimately leading to IIF. Warmer ice-nucleation resulting in a coarser-grained ice crystal network has, however, been demonstrated to prevent this (Huang et al., 2017).

Detachment of the HepG2 cell monolayer from the surface of culture plate appeared to result in low post-thaw viability and mostly only occurred when ice-nucleation was left uncontrolled (Fig. 3.8.). Monolayer detachment is a known issue from previous attempts to cryopreserve cells in this format in multiwell plates. When using a similar

protocol to cryopreserve primary cultures of bovine granulosa in 96-well plate using manual versus uncontrolled IN a comparable situation was seen with cell layer detachment being more apparent in the latter (Daily et al., 2020). This prevention of monolayer detachment may be related to controlling IN in the well liquid at close to the melting point as it prevents the severe temperature fluctuations that would otherwise occur inside the well following the ice crystallisation process. In the case where a plate culture was cryopreserved coincident with IR temperature measurements (Fig. 3.6) we calculated that the maximum cooling rates experienced in the warmest nucleating wells during thermal equilibration after latent heat release were around  $3\text{ }^{\circ}\text{C min}^{-1}$  compared with up to  $7\text{ }^{\circ}\text{C min}^{-1}$  in the most deeply supercooled wells. This resulted in an effective cooling rate much higher than the nominal  $1\text{ }^{\circ}\text{C min}^{-1}$  defined by the cooling programme on the controlled rate freezer. Not only does higher than optimum cooling rates after extracellular ice formation mean that cells cannot dehydrate fast enough to avoid intracellular ice formation (Mazur et al., 1972), but also, that frozen cell monolayer and substrate thermally contract at different rates causing the cells to lose adhesion to the surface (Eskandari et al., 2018; Rutt et al., 2019). Those authors were able to prevent monolayers of various cell types detaching after cryopreservation by using as a substrate rinzl, a type of PVC plastic, which has a close thermal expansion coefficient to that of ice. Alternatively, the cell layer may have been mechanically overstressed and detached by differential expansion caused by the latent heat release at the point of ice-nucleation rather than the cooling and contraction during the equilibration step. Ice-nucleation at deeper levels of supercooling results in correspondingly higher effective rates of heating and cooling (Daily et al., 2020) but, as pointed out in Section 3.2, the increase in heating rates with  $T_{\text{nuc}}$  are far more extreme than those of the cooling rates. In summary, severe temperature fluctuations following ice-nucleation events are a plausible reason for the cell monolayer detachments and were minimised by controlling ice-nucleation at the melting point with IceStart arrays. This may negate the need for a using thermally matched substrate materials for cell monolayer freezing.

Overall, we have demonstrated how the survival of cell monolayers frozen within multiwell plates is directly related to the temperature of ice nucleation and it can be significantly improved with the aid of a mineral based agent. A passive, sterilisable device inserted into the 96-well plate reliably induces ice-nucleation at close to the

melting point of the host cryoprotectant, thus avoiding severe thermal stresses caused by latent heat release. While factors other than  $T_{\text{nuc}}$  will certainly have significant influence on cryopreservation success (such as CPA formulation, thawing protocols etc.) it can be also the most difficult to control in a repeatable way because of the inherent randomness of IN (Morris and Acton, 2013). In the literature it has been stated (Morris and Acton, 2013) that the downside to using chemical ice-nucleating agents is not being able to control the temperature of ice-nucleation reliably and precisely since nucleation is inherently a probabilistic process (Pruppacher and Klett, 1997). If, however, a chemical agent is active enough to eliminate supercooling, then by definition there is no variation in ice-nucleation temperature so this hurdle is overcome. As this is the case with LDH1 this work is a significant advance in this respect. Our method for quantifying the relationship between  $T_{\text{nuc}}$  and cell viability described in this work could be adapted to other cell or tissue types and biological markers as well as other multiwell plate formats (e.g., 386-well plates). This will enable the responses to diverse types of cells cryopreserved in multiwell plates, or any other biological specimens for that matter, to ice-nucleation to be explored further. This might enable existing cryopreservation protocols to be suitably tailored. Further research is needed to identify the nature of the hyperactive ice-nucleating sites found in mineral specimens such as LDH1 to enable further sources of this material to be identified, or even manufactured. More detailed studies are required to determine improved delivery methods for LDH1 (or similar mineral nucleating agents), such as encapsulation or integration into vessel surfaces, all in a manner that can meet the stringent biocompatibility requirements required of current good manufacturing practices (cGMP) (Meneghel et al., 2020). Moreover, the exceptional INA of hyperactive ice nucleating minerals such as LDH1 means that ice-nucleation can potentially be controlled at even smaller scales such as 384 well plates or in microfluidic droplets (Tarn et al., 2018; Zhao and Fu, 2017). This possibility creates new scope for even higher throughput sample cryopreservation in new applications in which IN can be controlled

## 3.4 Materials and Methods

### 3.4.1 Sourcing and preparation of LDH1 and other ice-nucleating materials

A sample of the ice-nucleating mineral sample LDH1 was sourced along with four additional materials (two mineral-based and two non-mineral-based) selected based on being already known as being highly active ice-nucleating activities and also easily dispersible in water. LDH1 was obtained from a sample of potassium feldspar obtained from the University of Leeds mineral collection (see Section 3.5.1). The mineral phase has been previously confirmed as microcline, a polymorph of K-feldspar by X-ray diffraction by (Harrison et al., 2016). Ground samples of K-feldspar from the same as geological locality as LDH1 that exhibit similarly hyperactive INA have previously been investigated (Harrison et al., 2016; Kiselev et al., 2017; Peckhaus et al., 2016). The raw sample was a large crystal of grey-white K-feldspar with unidentified rusty-brown coating and inclusions of smaller prismatic black crystals (Fig. 3.9 to 3.11). To obtain as 'pure' as possible sample for our experiments we broke up the crystal, which split easily along cleavage planes, and selected fragments from inside the bulk of the K-feldspar crystal taking care not to include impurities. This reduced the chance of the hyperactive IN sites being of a result of biological contamination. The fragments were then ground into a fine powder using an agate pestle and mortar followed by being dry sieved to remove particles above 63  $\mu\text{m}$  in diameter. Separate analysis of these parts of the sample confirmed that the bulk of the sample exhibited high ice-nucleating activity (Fig. 3.12). The two other mineral samples we used were purchased in ready ground form. These included BCS-376 microcline, a sample of the same mineral phase as LDH1 but without hyperactive ice-nucleating sites (Bureau of Analysed Standards, Middlesbrough, UK) and Quartz powder (Honeywell Fluka, Cat No. 83340, purchased from Fischer Scientific, Loughborough, UK). All three mineral samples were sufficiently fine grained to be able to suspend evenly in water during the droplet pipetting step. The BCS-376 microcline and Quartz samples mean spherical equivalent grain diameter have previously estimated to be around 0.5 to 1.0 based on measurements of specific surface area (Atkinson et al., 2013; Harrison et al., 2019). Although we did not measure the specific surface area of the LDH1 sample when mineral samples have been ground using the same procedure here, they resulted in powders with very similar estimated mean spherical equivalent grain diameters. Visual inspection of the powders with optical microscope confirmed the powders were

dominated by particles less than 10 $\mu\text{m}$  in diameter while particles larger than 100  $\mu\text{m}$  in diameter were rare in the LDH1 powder and absent in the BCS-367 microcline and Quartz. Cholesterol monohydrate crystals were produced by dissolving reagent-grade cholesterol (Sigma Aldrich, Gillingham, UK) in ethanol and recrystallizing as per Sosso et. al. (Sosso et al., 2018), then grinding the resultant plates into a much finer suspendable powder. Snomax® was obtained from York Snow. Inc., USA and is a commercially available snow-inducer derived from bacteria (Roy et al., 2021; Wex et al., 2015). It takes the form of lyophilised protein pellets that readily disperse into a non-particulate suspension when mixed with water.

### **3.4.2 Droplet freezing assays and derivation of INA**

To quantify the INA of LDH1 and other ice nucleators we performed the well-established droplet freezing assay technique using a combination of two instruments (Harrison et al., 2019; Whale et al., 2015). The microlitre Nucleation by Immersed Particle Instrument ( $\mu\text{L}$  – NIPI) was used for smaller droplet sizes and Infra-Red Nucleation by Immersed Particle Instrument (IR-NIPI) for larger droplets on the scale of the working volume of 96-well plates (100  $\mu\text{L}$  and above). The design, operation and calibration of these instruments is described in detail in (Whale et al., 2015) and (Harrison et al., 2018). The two instruments differ in the sizes of droplets used and their method of droplet IN temperature detection, however used in combination they can derive IN site concentrations over several orders of magnitude. For the  $\mu\text{L}$ -NIPI experiments 30-50 microlitre sized droplets of IN material suspension were pipetted at room temperature onto a cleaned hydrophobic glass coverslip (Hampton Instruments, USA) resting on an aluminium cooling stage powered by a programmable sterling engine freezer (Asymptote EF600, UK). The stage was then enclosed by a Perspex cell through which dry  $\text{N}_2$  gas was flowed through to prevent frost formation on the coverslip. For each run the droplets were cooled at a rate of 1  $^{\circ}\text{C min}^{-1}$  until all droplets had frozen. Droplet freezing (nucleation) events were detected visually with a webcam its corresponding temperature obtained from the plate temperature thermocouple in the cooling plate. For the larger volume droplet freezing assays on the IR-NIPI instrument 50  $\mu\text{L}$  droplets of IN material suspension were pipetted into gamma-ray sterilised 96-well plates (Thermo Scientific Nunclon™ Delta Surface, Cat. No. 167008) and placed onto the cooling plate of a programmable sterling engine freezer (Asymptote ViaFreeze Research, Cambridge, UK) and were subjected to a

cooling protocol of 1 °C min<sup>-1</sup> until all droplets were frozen. An infra-red camera (Fluke Ti9, USA) mounted above the cooling plate collected images of the 96-well plate every 15 seconds during freezing runs with each pixel in the images comprising temperature data with the pixel at the centre of each well is defined as the droplet temperature. Using a Python processing script the temperature data contained in each image was used to construct a temperature time series for droplets in each individual well. Droplet ice-nucleation events in the 96-well plates are detected using the sudden rise in temperature captured by the IR camera resulting from the release of latent heat of crystallisation, thus the lowest temperature in the time series just before this ‘jump’ is observed is defined as the droplet IN temperature. The latent heat release of a freezing droplet can cause significant warming of droplets in neighbouring wells, so for each run every other well was left empty and filled in ‘chessboard pattern’ so to prevent such artefacts (Zaragotas et al., 2016). Following ice nucleation the droplet temperature will rise and plateau at what theoretically is the ice-liquid equilibrium of 0°C and this provides a point of calibration for each individual well (Harrison et al., 2018). This method was also used to determine the melting point of the CPA – approximately -4°C - from the temperature difference between the ice-liquid equilibrium ‘plateau’ for both water and CPA in wells in the same 96-well plate.

Both the  $\mu$ L-NIPI and IR-NIPI techniques produce data for fraction of droplets frozen as function of temperature -  $f_{ice}(T)$  - for a given INP suspension:

$$f_{ice} = \frac{n(T)}{N} \quad (3.1)$$

Where  $n(T)$  is the number of droplets frozen at temperature  $T$  and  $N$  is the total number of droplets in the assay. This is the basis for calculating the intrinsic IN ability of a material on a mass-by-mass basis. Combined with knowledge of the mass of ice-nucleator per droplet ( $m$ ) we can derive for any material the density of active sites per unit mass,  $n_m(T)$ , using the equation (Vali et al., 2015):

$$n_m(T) = \frac{(-\ln(1-f_{ice}(T)))}{m} \quad (3.2)$$

This assumes that sites contained within the material become active upon reaching a characteristic temperature without any significant time dependent component (Herbert et al., 2014). Using  $n_m(T)$  allows us to compare the intrinsic INA of particulate samples such as ground mineral powders, normally measured by active sites per INP surface

area,  $n_s(T)$ , with non-particulate ice-nucleating materials such as Snomax® and pollen washing water.

### **3.4.3 HepG2 cell culture and plate cryopreservation**

#### ***3.4.3.1 96-well plate culture protocol***

HepG2 cells, an immortalised human hepatocyte carcinoma cell line (Sigma Aldrich, Gillingham, UK), were used in all cryopreservation experiments (Stokich et al., 2014) and procedures were carried out aseptically in a laminar flow hood unless stated. Cells were cultured in a humidified incubator at 37 °C and 5% CO<sub>2</sub> in T75 flasks with culture medium (CM) comprised of RPMI 1640 supplemented with 10% FBS and 1% penicillin-streptomycin for 1 week before first passage. Upon each passage up to five (depending on cell yield) 96-well plates pre-coated with collagen solution (0.05 mg L<sup>-1</sup>, Roche) were seeded with cells at a density of 50,000 per well under 200 µL per well of CM and cultured for 48 hr by which time confluent monolayers were achieved. For the culture plates that were to be cryopreserved with simultaneous thermal measurements (Fig 3.6) every other well was left empty and not seeded to avoid latent heat release from freezing wells interfering with neighbouring wells, similar to with the droplet freezing assays. Edge wells were left empty to avoid the edge effects that are a known source of variability in cell growth when culturing cells in 96-well plates (Lundholt et al., 2003; Mansoury et al., 2021). Of the set of plates cultured from each passage one plate was assigned as a non-freeze control ‘baseline’ plate while the remainder were prepared for cryopreservation.

#### ***3.4.3.2 Cryopreservation and ice-nucleation protocol***

Prior to cryopreservation culture media was replaced with 100 µL per well of cryoprotectant (CPA) consisting of CM with 10% (v/v) dimethyl sulphoxide (DMSO) and 0.015M trehalose. This CPA formulation was tested for cytotoxicity and cryopreservation performance against formulations with other penetrating CPAs including glycerol, propylene glycol and ethylene glycol (see Section 3.5.3 and Figs. 3.14 and 3.15). After addition of CPA the plates were placed on ice-cold aluminium blocks and the plates were then divided into areas to be subjected to different methods of ice nucleation control: IceStart™ arrays, manual nucleation or uncontrolled nucleation. Cell that had undergone manual nucleation were unsuitable for evaluation in 5-day post thaw cultures as this method of IN was incompatible with the

maintenance of a sterile culture environment. First, the sections for manual nucleation (if used) and uncontrolled nucleation were covered with sterile plastic strips to prevent contamination from IceStart™ arrays. IceStart™ arrays loaded with LDH1 powder pre-cut into suitably sized portions and were wet sterilised immersion in 70% (v/v) ethanol which was then allowed to fully evaporate before the arrays were inserted into their section of the plate. A simple toxicity test confirmed no apparent detrimental effect from IceStart array insertion to unfrozen cells at 37 °C (Fig. 3.16). The plates were sealed and then placed on a controlled rate freezer (Asymptote Via Freeze Duo) set to a cooling protocol of 1°C min<sup>-1</sup> from +4 to -80 °C. Manual nucleation was performed when the plate temperature had dipped below the CPA melting point which corresponded to a freezer temperature of around -15 °C. The plate was unsealed, the cover strips removed from the section to be nucleated and then a deep cooled object was held above the plate with the falling ice mist triggering ice nucleation in the exposed wells. The technique is described in detail in Daily et al 2020 (Daily et al., 2020). The plate was then resealed, and the cooling protocol allowed to complete, during which time uncontrolled nucleation would proceed in the remaining plate section. The plate was then transferred to a -80 °C freezer and stored for 7 days.

#### **3.4.3.3 Thawing**

Cryopreserved culture plates were removed from the -80 °C freezer and transferred to a -20 °C freezer and held for 20 mins to minimise the thermal expansion experienced by the plate upon warming (Campbell et al., 2003). The plates were then moved into a laminar flow hood, unsealed and placed on aluminium mounting blocks warmed to 37 °C. 100 µL of warm CM was added dropwise to the wells until the IceStart™ arrays were removed once all ice had melted - this procedure typically took no more than 2 minutes. The CPA was then carefully aspirated away and replaced with 200 µL of CM. Plates used for the acute post-thaw cell viability trial were then subject to the neutral red viability assay while those used for the 5-day post-thaw culture trial were transferred to a humidified incubator for culture at 37 °C in an atmosphere of 5% CO<sub>2</sub> over 5 days with media changes performed after 48 or 72 hours.

#### **3.4.3.4 Viability assay**

Viable cell counts were performed using the neutral red dye uptake assay (Daily et al., 2020; Picton et al., 1999; Repetto et al., 2008) either immediately after thawing or after 5 days of culture post-thaw. Cell viability was assessed in a non-frozen control

plate after culture for 2 days or 7 days to provide equivalent time points to the immediate post-thaw and 5-day post thaw viability assays, respectively. Neutral Red dye was added to culture wells at a concentration of  $50 \mu\text{g L}^{-1}$  and allowed to equilibrate at  $37^\circ\text{C}$  for 2 hours during which time the dye was taken-up by viable cells only. The dye solution was then removed from the wells and replaced with a wash-fix solution of 10% (w/v) calcium chloride and 1% (v/v) formaldehyde solution followed by a releasing solution (50% (v/v) ethanol acidified with 1% (v/v) acetic acid). Dye concentration per well was quantified by measuring optical absorbance at 540 nm using a microplate reader (Thermo Scientific Multiskan GO). The absorbance values were translated to cell numbers using a standard curve constructed from neutral red absorbance values for a series of known HepG2 cell concentrations (typically in the range of  $10^3$  to  $10^6$  cells per well) sampled from each passage.

#### **3.4.3.5 Statistical analysis**

Two separate plate cryopreservation experiments were performed each consisting of 8 replicates of plates frozen with varying methods of ice-nucleation control and tested for post-thaw cell viability either immediately post-thaw or after 5-day of post-thaw culture. The acute post-thaw experimental series included 3 ice-nucleation ‘treatments’ – IceStart™, Manual nucleation and uncontrolled nucleation. The differences in post-thaw viable cell counts between these groups were analysed by one-way ANOVA with a Games Howell post-hoc test which is required when comparing groups with unequal variances. As the 5-day trial included only two treatments, IceStart™ and uncontrolled nucleation, comparisons were conducted using a two-sample t-test. All significance tests were performed using Minitab v17.20.2 and the results of the analyses are shown in Fig. 3.7c-f. We previously performed preliminary toxicity experiments which showed, using two-sample t-tests, neither treatment of the cells with CPA or IceStart™ array installation had a significant effect on cell viability (data not shown). These activities were not there regarded as additional treatments. Viable cell numbers were converted to post thaw recovery rates (or % survival compared to unfrozen controls) by normalising data to mean viable cell numbers of unfrozen plate cultures from the same passage. This was averaged over 8 replicate plates for both experimental series.

### 3.5 Supplementary Information (SI)

#### 3.5.1 Source of LDH1 and ice-nucleating ability of its components

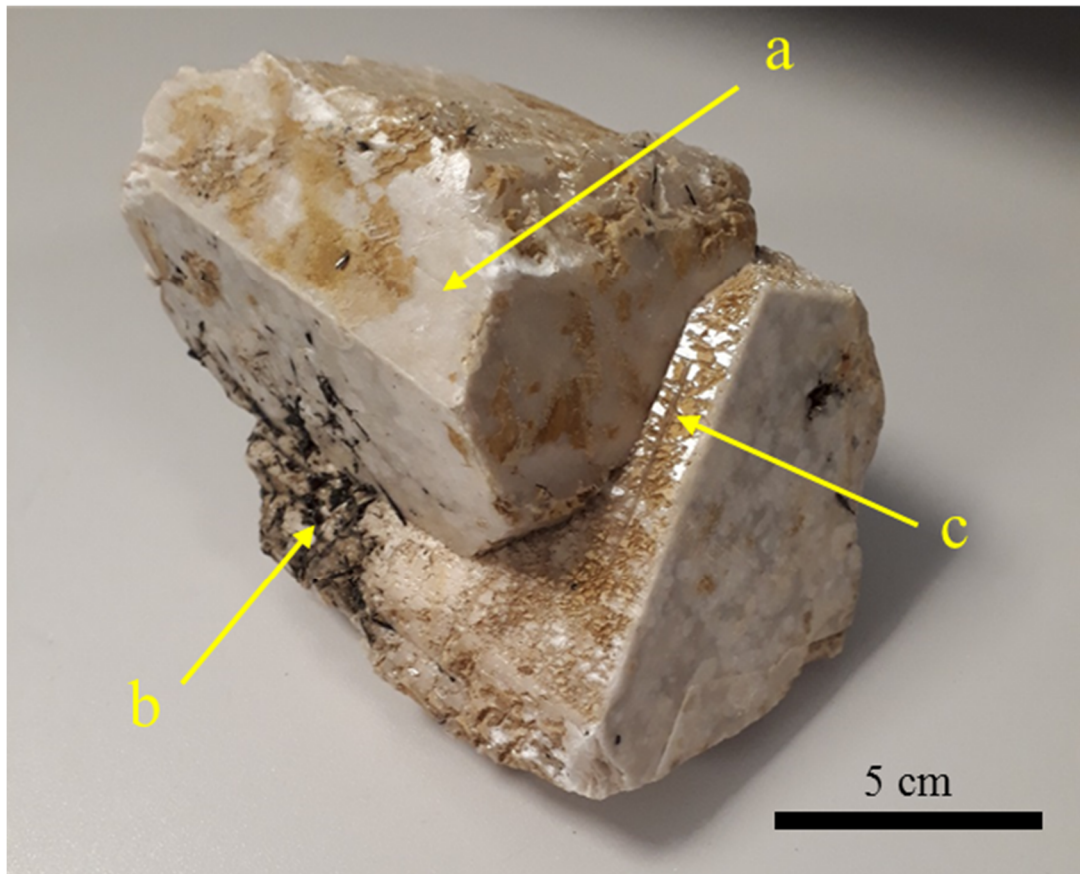


**Figure 3.9** Source material for LDH1. a) Euhedral microcline crystal (light grey) forming bulk of sample. b) Cluster of unidentified dark prismatic crystal inclusions, 5mm – 10mm in length. c) Unidentified brown material covering parts of sample surface.

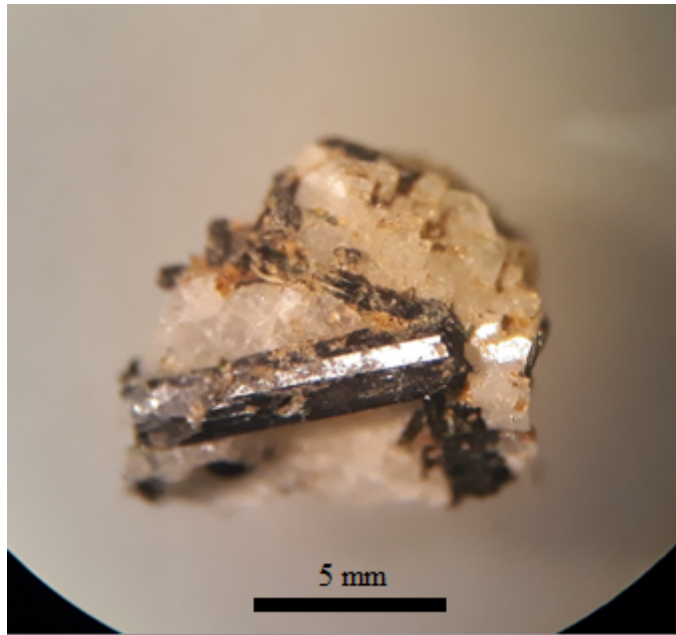


**Figure 3.10: Close up of dark inclusion crystal under stereomicroscope at 4x magnification.**



**Figure 3.11: Fragment of sample shown in Fig. S1 broken along cleavage plane showing interior.**

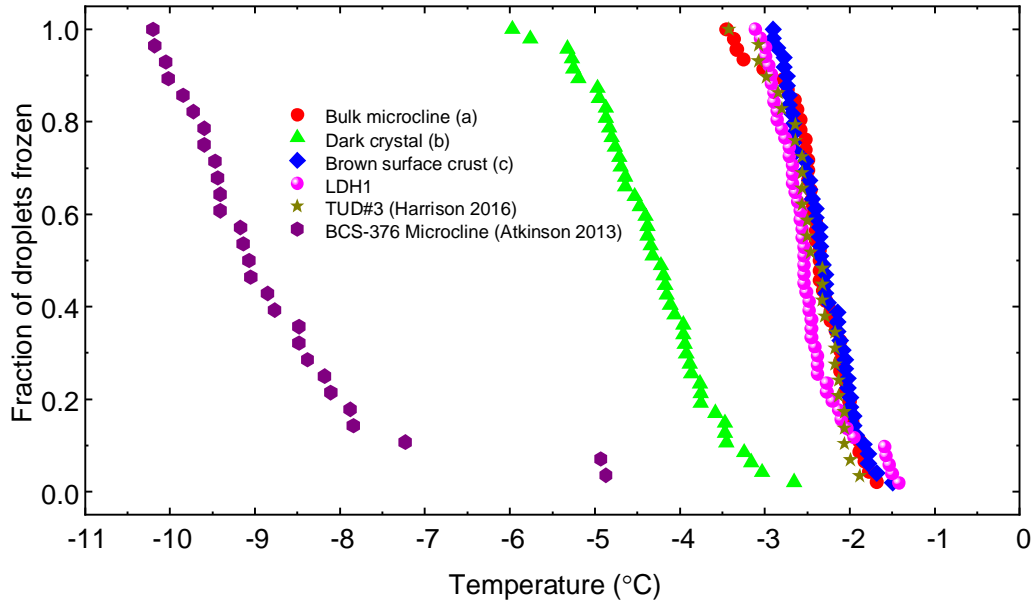


**Figure 3.12: Plot of  $f_{ice}$  for microlitre droplets of suspensions of ground constituents of sample shown in Fig. S1. Data collected using the  $\mu\text{L-NIPI}$ , all suspensions shown were 1% w/w. The material used in the IceStart arrays and all experimental data in the main text is shown for comparison and denoted as ‘LDH1’. BCS-376 Microcline, a non-hyperactive variety of K-feldspar, is shown for comparison.**

### 3.5.2 Long term stability of LDH1 in water and DMSO solution

The ice-nucleating activity of K-feldspar can slowly degrade in pure water (Harrison et al., 2016). Also, aqueous solutions can change the activity of heterogeneous ice- by reducing water activity (Zobrist et al., 2008), interacting with surfaces (Kumar et al., 2018; Whale et al., 2018) or a combination of these factors, depending on the nature of the solute. Ageing experiments were carried with LDH1 and BCS-376 microcline (as comparison with a non-hyperactive K-feldspar variant) in deionised water and in a 10% DMSO solution kept at 4°C for up to 3 months to simulate storage in cryoprotectant.

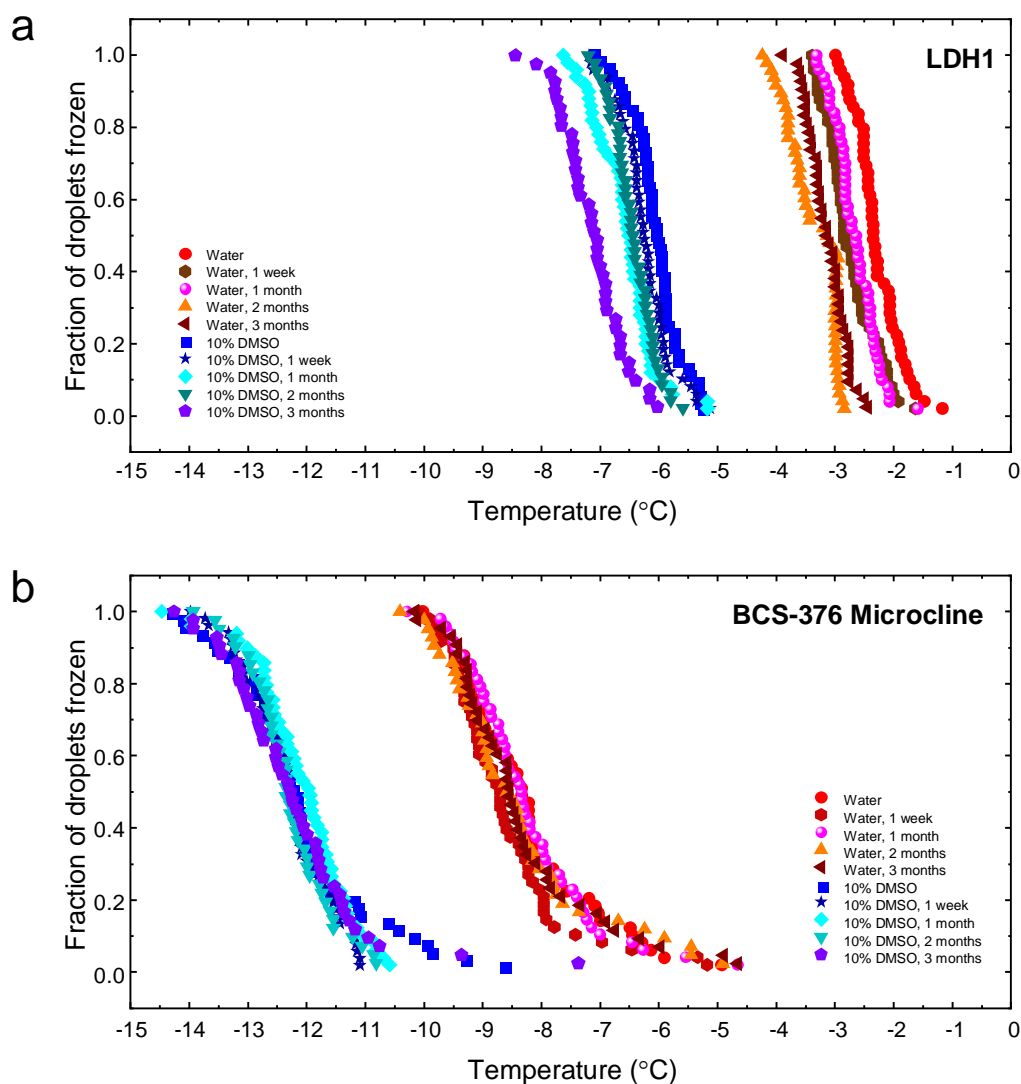


**Figure 3.13 Stability of LDH1 (a) and BCS-376 Microcline (b) in water and 10% DMSO solution. Data collected on  $\mu\text{L-NIPI}$  with microlitre droplets of 1% w/v suspensions**

The results, shown in Fig. 3.13 indicate that in both water and 10% DMSO LDH1 the median freezing temperature gradually drops by  $1^{\circ}\text{C}$  -  $2^{\circ}\text{C}$  indicating a slight sensitivity. BCS-376 in comparison lost activity above  $-11^{\circ}\text{C}$  in 10% DMSO, but otherwise showed almost no change. Interestingly the behaviour was identical in water and 10% DMSO except for a temperature shift downwards of  $4^{\circ}\text{C}$ . This suggests that the reduction in activity in 10% DMSO is purely due to the reduction in water activity rather than any degradation of active sites on either feldspar sample. If the reduction in homogeneous freezing temperature of 10% DMSO droplets was identical to this shift then this would confirm this, however the background freezing temperatures on

the  $\mu\text{L-NIPI}$  are too high ( $-20^{\circ}\text{C}$  -  $-30^{\circ}\text{C}$ ) to achieve this. It should be noted that CPA used for the cryopreservation experiments contained other components as well as 10% DMSO, however the temperature shift here is consistent with the CPA melting point depression inferred from the IR (Infra-Red) camera experiments in Sections 3.2.2. Overall this suggests that LDH1 is largely stable in water in terms of ice-nucleating activity and its active sites are not degraded by the presence of 10% DMSO, a standard cryoprotectant.

### **3.5.3 Optimisation of cryoprotectant and toxicity trials**

The plots below (Fig 3.14 and Fig. 3.15) detail the optimisation of CPA formulation and toxicity testing which were carried out on 96-well plate cultures of HepG2 cells prepared as described in the main text and cultured for 48 h. Plates were divided into sections of wells with  $n = 6$  wells for each section. CPA preparations containing culture medium, 0.02M trehalose and four different penetrating CPAs – DMSO, glycerol, propylene glycol and ethylene glycol at concentrations of 5% and 10% were trialed as well as a section containing culture medium without CPA as a control. Unfrozen toxicity testing (Fig 3.14) involved replacing culture medium with 100  $\mu\text{L}$  aliquots of CPA to wells and incubating at  $37^{\circ}\text{C}$  for 15 minutes, then removing and immediately performing neutral red viability assays. CPA performance testing (Fig 3.15) involved cryopreservation of plate cultures as described in the main text using the different CPAs in sections of a plate. Ice-nucleation induced in all wells using the manual nucleation (ice-mist) technique during the cryopreservation protocol. It was found that while none of the formulations of CPAs seemed to have significant toxicity on unfrozen cells compared to a control group, only 10% DMSO showed acceptable performance with frozen cells.

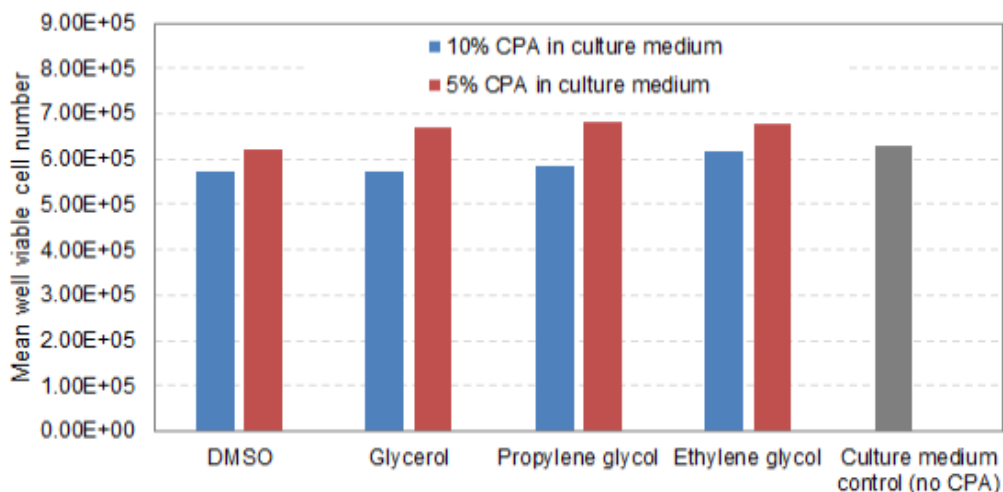


**Figure 3.14: Toxicity effect of different penetrating CPA formulations after 15 min exposure at 37 °C on unfrozen HepG2 cell viability.** Percentages in legend refer to weight concentration of each penetrating CPA in culture medium used.

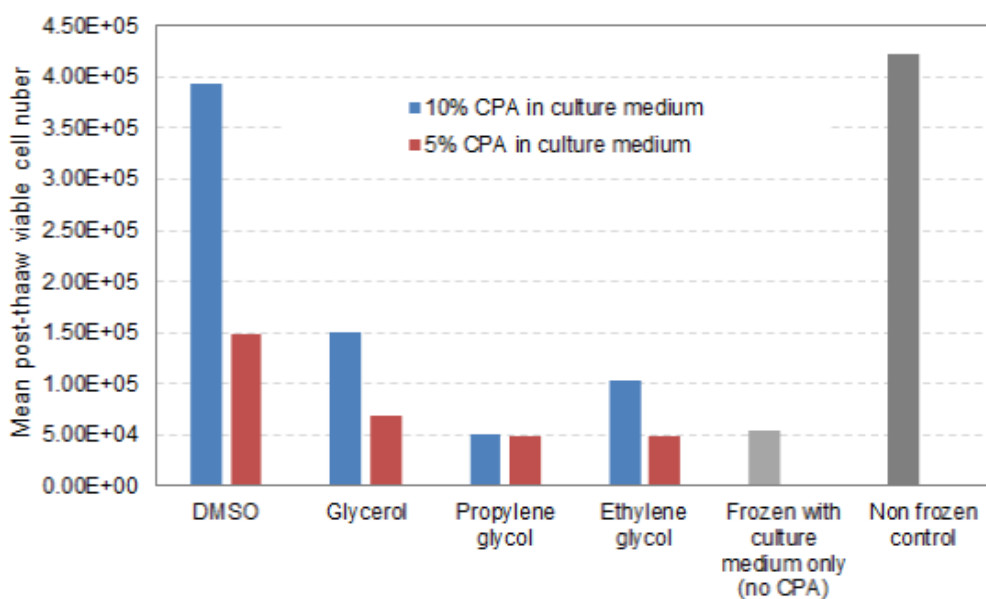


**Figure 3.15: Performance of different penetrating CPA formulations on cryopreserved HepG2 post-thaw viability.**

For the IceStart toxicity test, (Fig. 3.16) a portion of IceStart array was pre-sterilised by soaking in 70% ethanol, allowed to dry, then was inserted into a section of a plate

culture of HepG2 cells (n = 16 wells), incubated at 37 °C for 30 minutes, then removed. The other section of the culture plate was used as a control (n = 40 wells) and did not have an IceStart array inserted. A viability assay was then carried out and the result compared with a two-sample t-test which showed no significant difference between the groups ( $p < 0.01$ ) indicating the IceStart arrays with LDH1 have no detrimental effect on the cells independent of the cryopreservation process.

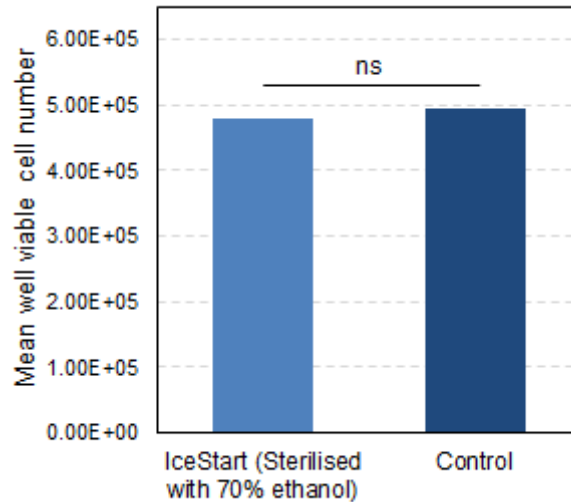


**Figure 3.16: Toxicity effect of sterilised IceStart arrays on unfrozen HepG2 cells.** 'ns' denotes no significant difference between the two groups.

### 3.5.4 Tabulated values of HepG2 viability assay data

**Table 3.1 HepG2 cell count data obtained by neutral red viability assay for plate cryopreservation trials shown in Fig 3.7. Each number represents cell number for an individual well. IN = ice-nucleation; SD = standard deviation.**

	<i>Plate#1</i>				<i>Plate#2</i>		
	<b>IceStart (+LDH1)</b>	<b>Manual IN</b>	<b>Uncontrolled IN</b>		<b>IceStart (+LDH1)</b>	<b>Manual IN</b>	<b>Uncontrolled IN</b>
	305509	99750	251891		340119	359556	287171
	343712	218380	253902		288512	146424	289182
	307520	115835	215699		284490	143072	287841
	239827	22003	245189		235564	222829	313310
	215699	28706	227763		257011	30474	287841
	233795	25355	253902		314651	257011	334757
	256583	30716	221731		248968	224840	320683
	274679	43451	219050		265724	142402	277788
	285403	123208	184198		217468	74709	263713
	235806	44121	204975		226851	55943	216797
	316903	268647	255913		232213	53262	161169
	296126	165432	230444		324704	76050	261703
	272668	215699	244519		339449	59964	318002
	339021	30716	233795		311970	194010	313980
	225082	91037	224412		290522	46560	254330
	260604	97069	260604		309959	45890	311970
	237146	74951	239827		322693	98837	268405
	238487	213688	231784		308619	68677	224170
	233125	76962	192241		279799	230872	222159
	248540	23344	206986		191999	123636	140392
<i>Mean</i>	268312	100453	229941	<i>Mean</i>	279564	132751	267768
<i>SD</i>	38713	77329	21636	<i>SD</i>	43250	89477	52374

Table 3.1 cont...

	<i>Plate#3</i>				<i>Plate#4</i>		
	<b>IceStart (+LDH1)</b>	<b>Manual IN</b>	<b>Uncontrolled IN</b>		<b>IceStart (+LDH1)</b>	<b>Manual IN</b>	<b>Uncontrolled IN</b>
	233516	130301	242229		230649	378099	130785
	264346	57246	344103		311746	29581	240032
	272389	23735	385657		334534	33602	293650
	234186	31107	297187		372737	87220	236681
	216090	33788	292496		258798	33602	213893
	240888	40490	314613		328502	98614	244053
	224803	49203	262336		322470	247404	287618
	248931	47863	315954		326491	198478	275554
	141695	19713	327348		478633	59741	282926
	184589	41831	269708		313757	62422	319789
	126950	19043	199334		290299	55720	107997
	241559	86066	418499		274214	55049	256788
	297858	92098	256304		350619	99284	226627
	293836	49203	258984		258128	80518	234000
	269038	25075	234186		36953	25559	128774
	248931	66629	275070		150892	46336	216574
	309922	228154	315284		335874	38294	244724
	289145	65289	295177		234000	227298	195127
	281102	25075	155099		318449	106657	288959
	334720	37810			266841	46336	280916
<i>Mean</i>	247725	58486	287346	<i>Mean</i>	289729	100491	235273
<i>SD</i>	52344	48732	61086	<i>SD</i>	88473	92182	57928
	<i>Plate#5</i>				<i>Plate#6</i>		
	<b>IceStart (+LDH1)</b>	<b>Manual IN</b>	<b>Uncontrolled IN</b>		<b>IceStart (+LDH1)</b>	<b>Manual IN</b>	<b>Uncontrolled IN</b>
	273135	44587	283188		78099	80109	198069
	320721	32523	295252		100886	31853	264422
	330104	19789	314689		221527	89493	259730
	238283	41907	314019		218846	14427	243645
	225549	26491	258390		250347	16438	234932
	236272	23810	282518		234932	21800	239623
	198069	39226	241634		216166	59332	230911
	167909	35204	234262		146462	17108	271124
	47268	21800	236272		142441	21129	219517
	86812	23810	200080		70056	20459	205442
	291231	73407	241634		208123	108929	168579
	345519	30513	242975		228230	25821	257049
	274475	220857	316700		143781	25821	252358
	274475	33864	289891		228230	88822	244315
	242975	43917	289891		82790	94184	273805
	273805	216166	271124		48609	31853	226219
	214155	32523	241634		215495	74077	219517
		73407	231581		25821	30513	235602
		92844	225549		25821	198740	212144
		31183	189356			32523	222868
<i>Mean</i>	237692	57891	260032	<i>Mean</i>	151930	54172	233994
<i>SD</i>	79605	58126	37295	<i>SD</i>	78554	46071	26288

Table 3.1 cont...

<i>Plate#7</i>			<i>Plate#8</i>			
<b>IceStart (+LDH1)</b>	<b>Manual IN</b>	<b>Uncontrolled IN</b>	<b>IceStart (+LDH1)</b>	<b>Manual IN</b>	<b>Uncontrolled IN</b>	
98090	61898	14982	211901	210561	14854	
106133	50504	12971	238710	232008	132814	
149698	31067	12301	213912	201177	166996	
155059	93399	58547	214582	213242	26918	
113505	62568	11631	214582	183752	51047	
186560	71951	13642	256806	203188	103324	
118197	97420	15652	244072	223295	66462	
122889	113505	11631	223965	256136	81877	
157740	147017	67260	168336	180400	70483	
82675	116856	48493	158283	182411	130804	
100771	37770	15652	208550	225976	26248	
143666	57877	25706	192464	223965	18876	
178517	58547	12301	209890	200507	199167	
156400	86696	19003	179730	202518	283615	
150368	82675	126240	232678	208550	28929	
113505	97420	16993	189784	231338	134155	
117527	114176	81334	245412	240051	107346	
124899	98760	18333	232008	254796	116729	
134953	134953	41121	198497	201848	130804	
77313	153049	20344	193135	218603	43674	
<i>Mean</i>	<i>129423</i>	<i>88405</i>	<i>Mean</i>	<i>211365</i>	<i>214716</i>	<i>96756</i>
<i>SD</i>	<i>29937</i>	<i>34768</i>	<i>SD</i>	<i>26267</i>	<i>21655</i>	<i>68774</i>

Table 3.1 cont...

	<i>Plate#9</i>		<i>Plate#10</i>		<i>Plate#11</i>	
	<b>IceStart (+LDH1)</b>	<b>Uncontrolled IN</b>	<b>IceStart (+LDH1)</b>	<b>Uncontrolled IN</b>	<b>IceStart (+LDH1)</b>	<b>Uncontrolled IN</b>
	689419	555373	750409	501755	578241	406663
	750409	273878	795985	897189	752500	461621
	686738	464892	661269	32596	674753	137231
	741026	228973	608991	17851	769255	647274
	838879	405913	697461	13159	735744	471004
	666631	493712	674003	298006	757862	462962
	784591	631109	625747	543309	741776	165381
	680706	346262	584863	656577	763894	305458
	741026	518511	690089	340900	742446	450898
	713547	161280	713547	600949	422748	448887
	737005	587544	593576	265165	507867	259213
	760463	356986	727621	609662	771936	616444
	631109	312081	635800	536607	721669	701563
	782580	361678	696791	32596	838959	562155
	685397	397870	706844	544649	735074	629848
	664620	102300	658588	456180	786681	371141
	674003	25224	720919	29915	710946	476366
	653226	389827	759792	17181	710275	626497
	535937	643843	746388	340900	757862	593656
	530575	407923	606310	351624	729712	338299
	745718	21872	552022	221600	576230	385215
	730302	374412	707515	728292	692850	548081
	754431	331517	706174	553362	769926	677434
	635130	420658	696121	486340	737755	646604
	629098	99619	743037	754431	753170	618454
	741026	365699	781240	430041	729042	354385
	710196	26564	686738	810730	708935	665370
	686738	94927	706844	728292	725020	540038
	716898	644513	675344	221600	720329	597007
	119726	149886	598268	60075	751830	357736
<i>Mean</i>	680572	339828	683610	402718	710510	484096
<i>SD</i>	125079	188551	60962	267737	98675	152701

Table 3.1 cont...

	<i>Plate#12</i>		<i>Plate#13</i>		<i>Plate#14</i>	
	<b>IceStart (+LDH1)</b>	<b>Uncontrolled IN</b>	<b>IceStart (+LDH1)</b>	<b>Uncontrolled IN</b>	<b>IceStart (+LDH1)</b>	<b>Uncontrolled IN</b>
	773794	671249	647944	605050	569451	33940
	713473	438680	780649	573549	550015	653900
	730229	492969	714967	533336	661272	327499
	720846	550608	724350	636550	774541	17854
	752347	398467	715637	578911	780573	460874
	700739	614950	704914	661349	649208	409267
	754357	260400	749149	700222	642506	13163
	763070	588811	751159	725020	556717	653230
	676611	499671	760542	534006	622399	36621
	470181	34533	857725	707595	674007	632453
	620982	615620	584943	442185	773870	682720
	642429	406509	643923	219669	759796	552696
	726208	496320	778639	749819	778562	442778
	766421	460128	698211	729042	694113	570121
	759049	648461	749149	507867	824137	18525
	744304	543906	731053	495133	609665	678028
	791890	547257	764564	507197	465566	506450
	772453	659185	774617	735074	558057	96941
	625003	627684	812820	296075	757115	84207
	477554	240963	718988	608401	714890	127772
	704760	594173	450898	474356	590898	56057
	669238	531172	518591	658668	646527	58738
	700739	690686	601699	682126	702826	14503
	672590	656504	413365	391918	485003	387149
	686664	509054	643923	619795		
	699399	429967	513229	584943		
	720846	453425	602369	718988		
	688675	275145	700892	675424		
	631706	403829	668051	571538		
	541895	149813	632529	529984		
Mean	689948	483005	680316	581793	660071	313145
SD	80518	160973	105200	129357	99199	262904

Table 3.1 cont...

<i>Plate#15</i>		<i>Plate#16</i>	
<b>IceStart (+LDH1)</b>	<b>Uncontrolled IN</b>	<b>IceStart (+LDH1)</b>	<b>Uncontrolled IN</b>
725327	419033	852284	797325
699858	55770	884455	575480
704550	361394	863007	697461
740072	616080	825475	699472
776934	610718	809389	710866
744763	654283	861667	710866
508173	642889	833517	735664
723316	678411	818772	728962
738061	611388	818102	19192
833904	536993	802017	804698
669698	263540	826145	579501
694496	635516	814081	694110
674390	628814	795314	812740
705220	614739	788612	790623
717954	59791	777218	557384
717284	641548	779229	701483
697848	641548	773867	698131
602005	620771	909923	757111
756828	608037	968903	726281
763530	636857		722260
699858	15556		48682
671038	529621		592236
659645	488066		501755
678411	141559		774537
703209	592622		761133
685113	392894		763144
631495	132176		688078
668358	564472		749069
689135	475332		699472
680422	532301		13830
<i>Mean</i>	<i>698696</i>	<i>480091</i>	<i>831683</i>
<i>SD</i>	<i>57339</i>	<i>206364</i>	<i>49660</i>
			<i>637051</i>
			<i>220108</i>

## References

Acker, J. P., Larese, A., Yang, H., Petrenko, A., and McGann, L. E.: Intracellular Ice Formation Is Affected by Cell Interactions, *Cryobiology*, 38, 363-371, 1999.

Atig, D., Touil, A., Ildefonso, M., Marlin, L., Bouriat, P., and Broseta, D.: A droplet-based millifluidic method for studying ice and gas hydrate nucleation, *Chemical Engineering Science*, 192, 1189-1197, 2018.

Atkinson, J. D., Murray, B. J., Woodhouse, M. T., Whale, T. F., Baustian, K. J., Carslaw, K. S., Dobbie, S., O'Sullivan, D., and Malkin, T. L.: The importance of feldspar for ice nucleation by mineral dust in mixed-phase clouds, *Nature*, 498, 355-358, 2013.

Augustin, S., Wex, H., Niedermeier, D., Pummer, B., Grothe, H., Hartmann, S., Tomsche, L., Clauss, T., Voigtländer, J., Ignatius, K., and Stratmann, F.: Immersion

- freezing of birch pollen washing water, *Atmos. Chem. Phys.*, 13, 10989-11003, 2013.
- Beydoun, H., Polen, M., and Sullivan, R. C.: A new multicomponent heterogeneous ice nucleation model and its application to Snomax bacterial particles and a Snomax–illite mineral particle mixture, *Atmospheric Chemistry and Physics*, 17, 13545-13557, 2017.
- C. Prickett, R., A. Marquez-Curtis, L., A.W. Elliott, J., and McGann, L.: Effect of supercooling and cell volume on intracellular ice formation, 2015.
- Campbell, L. H. and Brockbank, K. G. M.: Cryopreservation of Adherent Cells on a Fixed Substrate, IntechOpen, doi: 10.5772/58618, 2014. 2014.
- Campbell, L. H., Brockbank, K. G. M., and Taylor, M. J.: Two stage method for thawing cryopreserved cells. Inc, L. S. (Ed.), US6596531B2, 2003.
- Clarke, A., Morris, G. J., Fonseca, F., Murray, B. J., Acton, E., and Price, H. C.: A Low Temperature Limit for Life on Earth, *PLOS ONE*, 8, e66207, 2013.
- Daily, M. I., Tarn, M. D., Whale, T. F., and Murray, B. J.: The sensitivity of the ice-nucleating ability of minerals to heat and the implications for the heat test for biological ice nucleators, *Atmos. Meas. Tech. Discuss.*, 2021, 1-40, 2021.
- Daily, M. I., Whale, T. F., Partanen, R., Harrison, A. D., Kilbride, P., Lamb, S., Morris, G. J., Picton, H. M., and Murray, B. J.: Cryopreservation of primary cultures of mammalian somatic cells in 96-well plates benefits from control of ice nucleation, *Cryobiology*, 93, 62-69, 2020.
- DeMott, P. J.: Quantitative descriptions of ice formation mechanisms of silver iodide-type aerosols, *Atmospheric Research*, 38, 63-99, 1995.
- Desnos, H., Baudot, A., Teixeira, M., Louis, G., Commin, L., Buff, S., and Bruyère, P.: Ice induction in DSC experiments with Snomax®, *Thermochimica Acta*, 667, 193-206, 2018.
- Donato, M. T., Tolosa, L., and Gómez-Lechón, M. J.: Culture and Functional Characterization of Human Hepatoma HepG2 Cells. In: *Protocols in In Vitro Hepatocyte Research*, Vinken, M. and Rogiers, V. (Eds.), Springer New York, New York, NY, 2015.
- Dreischmeier, K., Budke, C., Wiehemeier, L., Kottke, T., and Koop, T.: Boreal pollen contain ice-nucleating as well as ice-binding 'antifreeze' polysaccharides, *Sci Rep*, 7, 41890, 2017.
- Eskandari, N., Marquez-Curtis, L. A., McGann, L. E., and Elliott, J. A. W.: Cryopreservation of human umbilical vein and porcine corneal endothelial cell monolayers, *Cryobiology*, 85, 63-72, 2018.
- Gavish, M., Popovitz-Biro, R., Lahav, M., and Leiserowitz, L.: Ice Nucleation by Alcohols Arranged in Monolayers at the Surface of Water Drops, *Science*, 250, 973, 1990.
- Harrison, A. D., Lever, K., Sanchez-Marroquin, A., Holden, M. A., Whale, T. F., Tarn, M. D., McQuaid, J. B., and Murray, B. J.: The ice-nucleating ability of quartz

- immersed in water and its atmospheric importance compared to K-feldspar, *Atmos. Chem. Phys.*, 19, 11343-11361, 2019.
- Harrison, A. D., Whale, T. F., Carpenter, M. A., Holden, M. A., Neve, L., amp, apos, Sullivan, D., Vergara Temprado, J., and Murray, B. J.: Not all feldspars are equal: a survey of ice nucleating properties across the feldspar group of minerals, *Atmospheric Chemistry and Physics*, 16, 10927-10940, 2016.
- Harrison, A. D., Whale, T. F., Rutledge, R., Lamb, S., Tarn, M. D., Porter, G. C. E., Adams, M. P., McQuaid, J. B., Morris, G. J., and Murray, B. J.: An instrument for quantifying heterogeneous ice nucleation in multiwell plates using infrared emissions to detect freezing, *Atmos. Meas. Tech.*, 11, 5629-5641, 2018.
- Head, R. B.: Steroids as Ice Nucleators, *Nature*, 191, 1058-1059, 1961.
- Herbert, R. J., Murray, B. J., Whale, T. F., Dobbie, S. J., and Atkinson, J. D.: Representing time-dependent freezing behaviour in immersion mode ice nucleation, *Atmospheric Chemistry and Physics*, 14, 8501-8520, 2014.
- Huang, H., Zhao, G., Zhang, Y., Xu, J., Toth, T. L., and He, X.: Predehydration and Ice Seeding in the Presence of Trehalose Enable Cell Cryopreservation, *ACS Biomater Sci Eng*, 3, 1758-1768, 2017.
- Hunt, C. J.: Technical Considerations in the Freezing, Low-Temperature Storage and Thawing of Stem Cells for Cellular Therapies, *Transfusion Medicine and Hemotherapy*, 46, 134-150, 2019.
- Jiang, B., Li, W., Stewart, S., Ou, W., Liu, B., Comizzoli, P., and He, X.: Sand-mediated ice seeding enables serum-free low-cryoprotectant cryopreservation of human induced pluripotent stem cells, *Bioactive Materials*, 6, 4377-4388, 2021.
- Kaufmann, L., Marcolli, C., Hofer, J., Pinti, V., Hoyle, C. R., and Peter, T.: Ice nucleation efficiency of natural dust samples in the immersion mode, *Atmospheric Chemistry and Physics*, 16, 11177-11206, 2016.
- Kilbride, P. and Meneghel, J.: Freezing Technology: Control of Freezing, Thawing, and Ice Nucleation. In: *Cryopreservation and Freeze-Drying Protocols*, Wolkers, W. F. and Oldenhof, H. (Eds.), Springer US, New York, NY, 2021.
- Kiselev, A., Bachmann, F., Pedevilla, P., Cox, S. J., Michaelides, A., Gerthsen, D., and Leisner, T.: Active sites in heterogeneous ice nucleation-the example of K-rich feldspars, *Science*, 355, 367-371, 2017.
- Kojima, T., Soma, T., and Oguri, N.: Effect of ice nucleation by droplet of immobilized silver iodide on freezing of rabbit and bovine embryos, *Theriogenology*, 30, 1199-1207, 1988.
- Koop, T., Luo, B., Tsias, A., and Peter, T.: Water activity as the determinant for homogeneous ice nucleation in aqueous solutions, *Nature*, 406, 611-614, 2000.
- Kumar, A., Marcolli, C., Luo, B., and Peter, T.: Ice nucleation activity of silicates and aluminosilicates in pure water and aqueous solutions – Part 1: The K-feldspar microcline, *Atmos. Chem. Phys.*, 18, 7057-7079, 2018.

- Kumar, A., Marcolli, C., and Peter, T.: Ice nucleation activity of silicates and aluminosilicates in pure water and aqueous solutions – Part 3: Aluminosilicates, *Atmos. Chem. Phys.*, 19, 6059-6084, 2019.
- Lauterboeck, L., Gryshkov, O., Hofmann, N., and Glasmacher, B.: Importance of controlled ice formation for efficient cell biobanking, 2016, 84-90.
- Lauterboeck, L., Hofmann, N., Mueller, T., and Glasmacher, B.: Active control of the nucleation temperature enhances freezing survival of multipotent mesenchymal stromal cells, *Cryobiology*, 71, 384-390, 2015.
- Lindow, S. E., Lahue, E., Govindarajan, A. G., Panopoulos, N. J., and Gies, D.: Localization of ice nucleation activity and the iceC gene product in *Pseudomonas syringae* and *Escherichia coli*, *Mol Plant Microbe Interact*, 2, 262-272, 1989.
- Lundholt, B. K., Scudder, K. M., and Pagliaro, L.: A Simple Technique for Reducing Edge Effect in Cell-Based Assays, *Journal of Biomolecular Screening*, 8, 566-570, 2003.
- Maki, L. R., Galyan, E. L., Chang-Chien, M. M., and Caldwell, D. R.: Ice nucleation induced by *pseudomonas syringae*, *Appl Microbiol*, 28, 456-459, 1974.
- Mansoury, M., Hamed, M., Karmustaji, R., Al Hannan, F., and Safrany, S. T.: The edge effect: A global problem. The trouble with culturing cells in 96-well plates, *Biochemistry and Biophysics Reports*, 26, 100987, 2021.
- Mason, B. J. and Maybank, J.: Ice-nucleating properties of some natural mineral dusts, *Quarterly Journal of the Royal Meteorological Society*, 84, 235-241, 1958.
- Massie, I., Selden, C., Hodgson, H., and Fuller, B.: Cryopreservation of Encapsulated Liver Spheroids for a Bioartificial Liver: Reducing Latent Cryoinjury Using an Ice Nucleating Agent, *Tissue Engineering Part C: Methods*, 17, 765-774, 2011.
- Massie, I., Selden, C., Hodgson, H., Fuller, B., Gibbons, S., and Morris, G. J.: GMP Cryopreservation of Large Volumes of Cells for Regenerative Medicine: Active Control of the Freezing Process, *Tissue Engineering Part C: Methods*, 20, 693-702, 2014.
- Mazur, P.: Freezing of living cells: mechanisms and implications, *American Journal of Physiology-Cell Physiology*, 247, C125-C142, 1984.
- Mazur, P., Leibo, S. P., and Chu, E. H.: A two-factor hypothesis of freezing injury. Evidence from Chinese hamster tissue-culture cells, *Exp Cell Res*, 71, 345-355, 1972.
- Meneghel, J., Kilbride, P., and Morris, G. J.: Cryopreservation as a Key Element in the Successful Delivery of Cell-Based Therapies—A Review, *Frontiers in Medicine*, 7, 2020.
- Missous, G., Thammavongs, B., Dieuleveux, V., Guéguen, M., and Panoff, J. M.: Improvement of the cryopreservation of the fungal starter *Geotrichum candidum* by artificial nucleation and temperature downshift control, *Cryobiology*, 55, 66-71, 2007.

Morris, G. J. and Acton, E.: Controlled ice nucleation in cryopreservation--a review, *Cryobiology*, 66, 85-92, 2013.

Morris, G. J. and Lamb, S.: Improved Methods for Cryopreservation of Biological Material. (GB), A. L. (Ed.), 15/557320, 2018.

Murray, B. J., Carslaw, K. S., and Field, P. R.: Opinion: Cloud-phase climate feedback and the importance of ice-nucleating particles, *Atmos. Chem. Phys.*, 21, 665-679, 2021.

Murray, B. J., O'Sullivan, D., Atkinson, J. D., and Webb, M. E.: Ice nucleation by particles immersed in supercooled cloud droplets, *Chem Soc Rev*, 41, 6519-6554, 2012.

O'Sullivan, D., Murray, B. J., Ross, J. F., Whale, T. F., Price, H. C., Atkinson, J. D., Umo, N. S., and Webb, M. E.: The relevance of nanoscale biological fragments for ice nucleation in clouds, *Scientific Reports*, 5, 8082, 2015.

Pach, E. and Verdaguer, A.: Pores Dominate Ice Nucleation on Feldspars, *The Journal of Physical Chemistry C*, 123, 20998-21004, 2019.

Peckhaus, A., Kiselev, A., Hiron, T., Ebert, M., and Leisner, T.: A comparative study of K-rich and Na/Ca-rich feldspar ice-nucleating particles in a nanoliter droplet freezing assay, *Atmospheric Chemistry and Physics*, 16, 11477-11496, 2016.

Picton, H. M., Campbell, B. K., and Hunter, M. G.: Maintenance of oestradiol production and expression of cytochrome P450 aromatase enzyme mRNA in long-term serum-free cultures of pig granulosa cells, *J Reprod Fertil*, 115, 67-77, 1999.

Polen, M., Lawlis, E., and Sullivan, R. C.: The unstable ice nucleation properties of Snomax® bacterial particles, *Journal of Geophysical Research: Atmospheres*, 121, 11,666-611,678, 2016.

Pruppacher, H. R. and Klett, J. D.: *Microphysics of Clouds and Precipitation*, Springer Netherlands, 1997.

Pummer, B. G., Bauer, H., Bernardi, J., Bleicher, S., and Grothe, H.: Suspendable macromolecules are responsible for ice nucleation activity of birch and conifer pollen, *Atmos. Chem. Phys.*, 12, 2541-2550, 2012.

Pummer, B. G., Budke, C., Augustin-Bauditz, S., Niedermeier, D., Felgitsch, L., Kampf, C. J., Huber, R. G., Liedl, K. R., Loerting, T., Moschen, T., Schauer, M., Tollinger, M., Morris, C. E., Wex, H., Grothe, H., Pöschl, U., Koop, T., and Fröhlich-Nowoisky, J.: Ice nucleation by water-soluble macromolecules, *Atmos. Chem. Phys.*, 15, 4077-4091, 2015.

Repetto, G., del Peso, A., and Zurita, J. L.: Neutral red uptake assay for the estimation of cell viability/cytotoxicity, *Nature Protocols*, 3, 1125-1131, 2008.

Roy, P., House, M. L., and Dutcher, C. S.: A Microfluidic Device for Automated High Throughput Detection of Ice Nucleation of Snomax®, *Micromachines*, 12, 2021.

Rutt, T., Eskandari, N., Zhurova, M., Elliott, J. A. W., McGann, L. E., Acker, J. P., and Nychka, J. A.: Thermal expansion of substrate may affect adhesion of Chinese hamster fibroblasts to surfaces during freezing, *Cryobiology*, 86, 134-139, 2019.

- Schnell, R. C. and Vali, G.: Biogenic Ice Nuclei: Part I. Terrestrial and Marine Sources, *Journal of Atmospheric Sciences*, 33, 1554-1564, 1976.
- Sosso, G. C., Li, T., Donadio, D., Tribello, G. A., and Michaelides, A.: Microscopic Mechanism and Kinetics of Ice Formation at Complex Interfaces: Zooming in on Kaolinite, *The Journal of Physical Chemistry Letters*, 7, 2350-2355, 2016.
- Sosso, G. C., Whale, T. F., Holden, M. A., Pedevilla, P., Murray, B. J., and Michaelides, A.: Unravelling the origins of ice nucleation on organic crystals, *Chemical Science*, 9, 8077-8088, 2018.
- Stokich, B., Osgood, Q., Grimm, D., Moorthy, S., Chakraborty, N., and Menze, M. A.: Cryopreservation of hepatocyte (HepG2) cell monolayers: Impact of trehalose, *Cryobiology*, 69, 281-290, 2014.
- Storelvmo, T. and Tan, I.: The Wegener-Bergeron-Findeisen process - Its discovery and vital importance for weather and climate, *Meteorologische Zeitschrift*, 24, 455-461, 2015.
- Sun, C., Yue, J., He, N., Liu, Y., Zhang, X., and Zhang, Y.: Fundamental Principles of Stem Cell Banking. In: *Biobanking and Cryopreservation of Stem Cells*, Karimi-Busheri, F. and Weinfeld, M. (Eds.), Springer International Publishing, Cham, 2016.
- Tarn, M. D., Sikora, S. N. F., Porter, G. C. E., O'Sullivan, D., Adams, M., Whale, T. F., Harrison, A. D., Vergara-Temprado, J., Wilson, T. W., Shim, J.-u., and Murray, B. J.: The study of atmospheric ice-nucleating particles via microfluidically generated droplets, *Microfluidics and Nanofluidics*, 22, 52, 2018.
- Taylor, M. J., Weegman, B. P., Baicu, S. C., and Giwa, S. E.: New Approaches to Cryopreservation of Cells, Tissues, and Organs, *Transfusion Medicine and Hemotherapy*, 46, 197-215, 2019.
- Teixeira, M., Buff, S., Desnos, H., Loiseau, C., Bruyère, P., Joly, T., and Commin, L.: Ice nucleating agents allow embryo freezing without manual seeding, *Theriogenology*, 104, 173-178, 2017.
- Vali, G., DeMott, P. J., Möhler, O., and Whale, T. F.: Technical Note: A proposal for ice nucleation terminology, *Atmos. Chem. Phys.*, 15, 10263-10270, 2015.
- Welti, A., Lohmann, U., and Kanji, Z. A.: Ice nucleation properties of K-feldspar polymorphs and plagioclase feldspars, *Atmospheric Chemistry and Physics Discussions*, doi: 10.5194/acp-2018-1271, 2019. 1-25, 2019.
- Wex, H., Augustin-Bauditz, S., Boose, Y., Budke, C., Curtius, J., Diehl, K., Dreyer, A., Frank, F., Hartmann, S., Hiranuma, N., Jantsch, E., Kanji, Z. A., Kiselev, A., Koop, T., Möhler, O., Niedermeier, D., Nillius, B., Rösch, M., Rose, D., Schmidt, C., Steinke, I., and Stratmann, F.: Intercomparing different devices for the investigation of ice nucleating particles using Snomax<sup>®</sup> as test substance, *Atmos. Chem. Phys.*, 15, 1463-1485, 2015.
- Whale, T. F., Holden, M. A., Kulak, A. N., Kim, Y. Y., Meldrum, F. C., Christenson, H. K., and Murray, B. J.: The role of phase separation and related topography in the exceptional ice-nucleating ability of alkali feldspars, *Phys Chem Chem Phys*, 19, 31186-31193, 2017.

- Whale, T. F., Holden, M. A., Wilson, Theodore W., O'Sullivan, D., and Murray, B. J.: The enhancement and suppression of immersion mode heterogeneous ice-nucleation by solutes, *Chemical Science*, 9, 4142-4151, 2018.
- Whale, T. F., Murray, B. J., O'Sullivan, D., Wilson, T. W., Umo, N. S., Baustian, K. J., Atkinson, J. D., Workneh, D. A., and Morris, G. J.: A technique for quantifying heterogeneous ice nucleation in microlitre supercooled water droplets, *Atmos. Meas. Tech.*, 8, 2437-2447, 2015.
- Whittincham, D. G.: Some Factors Affecting Embryo Storage in Laboratory Animals, *Ciba Foundation Symposium 52 - The Freezing of Mammalian Embryos*, doi: doi:10.1002/9780470720332.ch610.1002/9780470720332.ch6, 1977. 97-127, 1977.
- Wragg, N. M., Tampakis, D., and Stolzing, A.: Cryopreservation of Mesenchymal Stem Cells Using Medical Grade Ice Nucleation Inducer, *International Journal of Molecular Sciences*, 21, 2020.
- Yakobi-Hancock, J. D., Ladino, L. A., and Abbatt, J. P. D.: Feldspar minerals as efficient deposition ice nuclei, *Atmospheric Chemistry and Physics*, 13, 11175-11185, 2013.
- Zarogotas, D., Liolios, N. T., and Anastassopoulos, E.: Supercooling, ice nucleation and crystal growth: a systematic study in plant samples, *Cryobiology*, 72, 239-243, 2016.
- Zhao, G. and Fu, J.: Microfluidics for cryopreservation, *Biotechnol Adv*, 35, 323-336, 2017.
- Zielke, S. A., Bertram, A. K., and Patey, G. N.: Simulations of Ice Nucleation by Kaolinite (001) with Rigid and Flexible Surfaces, *The Journal of Physical Chemistry B*, 120, 1726-1734, 2016.
- Zobrist, B., Marcolli, C., Peter, T., and Koop, T.: Heterogeneous Ice Nucleation in Aqueous Solutions: the Role of Water Activity, *The Journal of Physical Chemistry A*, 112, 3965-3975, 2008.
- Zolles, T., Burkart, J., Hausler, T., Pummer, B., Hitzenberger, R., and Grothe, H.: Identification of ice nucleation active sites on feldspar dust particles, *J Phys Chem A*, 119, 2692-2700, 2015.

## **4 An evaluation of the heat test for the ice-nucleating ability of minerals and biological material**

This Chapter has been accepted for publication with Atmospheric Measurement Techniques with minor revisions and is publically available on Atmospheric Measurement Techniques Discussions as: **Daily, M. I., Tarn, M.D., Whale, T.F., and Murray, B.J.** ‘An evaluation of the heat test for the ice-nucleating ability of minerals and biological material’ (February 2022)

**Chapter Abstract.** Ice-nucleating particles (INPs) are atmospheric aerosol particles that can strongly influence the radiative properties and precipitation onset in mixed-phase clouds by triggering ice formation in supercooled cloud water droplets. The ability to distinguish between INPs of mineral and biological origin in samples collected from the environment is needed to better understand their distribution and sources. A common method for assessing the relative contributions of mineral and biogenic INPs in samples collected from the environment (e.g., aerosol, rainwater, soil) is to determine the ice-nucleating ability (INA) before and after heating, where heat is expected to denature proteins associated with some biological ice nucleants. The key assumption is that the ice nucleation sites of biological origin are denatured by heat, while those associated with mineral surfaces remain unaffected; we test this assumption here. We exposed atmospherically relevant mineral samples to wet heat (INP suspensions warmed to above 90 °C) or dry heat (dry samples heated up to 250 °C) and assessed the effects on their immersion mode INA using a droplet freezing assay. K-feldspar, thought to be the dominant mineral-based atmospheric INP type where present, was not significantly affected by wet heating, while quartz, plagioclase feldspars and Arizona test Dust (ATD) lost INA when heated in this mode. We argue that these reductions in INA in the aqueous phase result from direct alteration of the mineral particle surfaces by heat treatment rather than from biological or organic contamination. We hypothesise that degradation of active sites by dissolution of mineral surfaces is the mechanism in all cases due to the correlation between mineral INA deactivation magnitudes and their dissolution rates. Dry heating produced minor but repeatable deactivations in K-feldspar particles but was generally less likely to

deactivate minerals compared to wet heating. We also heat tested proteinaceous and non-proteinaceous biogenic INP proxy materials and found that non-proteinaceous samples (cellulose and pollen) were relatively resistant to wet heat. In contrast, the proteinaceous ice-nucleating samples were highly sensitive to wet heat as expected, although their activity remained non-negligible after wet heating. Dry heating at 250 °C leads to deactivation of both proteinaceous and non-proteinaceous biogenic INPs. However, the use of dry heat at 250 °C for the detection of biological INPs is limited since K-feldspar's activity is also reduced under these conditions. Future work should focus on finding a set of dry heat conditions where all biological material is deactivated, but key mineral types are not. We conclude that, while wet INP heat tests at (>90°C) have the potential to produce false positives, i.e., deactivation of a mineral INA that could be misconstrued as the presence of biogenic INPs, they are still a valid method for qualitatively detecting proteinaceous biogenic INP in ambient samples if the mineral-based INA is controlled by K-feldspar.

#### **4.1 Introduction**

In the absence of nucleation sites, cloud water droplets can supercool to temperatures below around  $-35$  °C before freezing via homogeneous nucleation (Ickes et al., 2015; Herbert et al., 2015). However, a rare subset of atmospheric aerosol particles known as ice-nucleating particles (INPs) can elevate the temperature of ice formation (Murray et al., 2012; Hoose and Möhler, 2012; Kanji et al., 2017). INPs are important because newly formed ice crystals can grow at the expense of supercooled liquid droplets. This is a process that strongly modulates the radiative properties of shallow mixed-phase clouds (i.e., their albedo) (Storelvmo and Tan, 2015; Murray et al., 2021), can initiate precipitation by enhancing collision and coalescence processes (Vergara-Temprado et al., 2018; Rosenfeld et al., 2011) and can influence anvil cirrus properties in deep convective systems (Hawker et al., 2021).

To represent the impact of INPs on clouds in our models, we must improve our understanding of the global distribution and temporal variability of INPs. However, much uncertainty remains regarding the distribution, sources, and relative ice-nucleating ability (INA) of INPs throughout the Earth's atmosphere (Kanji et al., 2017; Huang et al., 2021; Murray et al., 2021). Two important general categories of INPs are mineral dust (Hoose et al., 2010; DeMott et al., 2003; Vergara-Temprado et al., 2017) and biogenic materials (Vergara-Temprado et al., 2017; Creamean et al., 2013).

Laboratory and field data indicate that mineral dusts often dominate the INP population relevant for mixed-phase clouds below around  $-15\text{ }^{\circ}\text{C}$  (O'Sullivan et al., 2014; Murray et al., 2012; Ansmann et al., 2008; Niemand et al., 2012; Ullrich et al., 2017). Potassium rich feldspars (K-feldspars) are considered to be the most important ice-nucleating mineral commonly present in airborne mineral dust (Atkinson et al., 2013; Harrison et al., 2019; Zolles et al., 2015; Augustin-Bauditz et al., 2014; Kaufmann et al., 2016), with immersion mode nucleation observed at temperatures warmer than  $-5\text{ }^{\circ}\text{C}$  in laboratory experiments (Harrison et al., 2016; Kaufmann et al., 2016; Whale et al., 2017). Quartz and the other feldspar varieties, plagioclase and albite, are thought to play a lesser role than K-feldspar in terms of mineral dust INA (Harrison et al., 2019; Harrison et al., 2016; Atkinson et al., 2013), with quartz being on average the more abundant of these in the atmosphere (Murray et al., 2012).

Biological INPs are capable of nucleating ice at much warmer temperatures than all but the most active minerals, and can include primary biological particles (PBAPs) such as bacteria, fungal spores, pollen grains, fragments of terrestrial organic material such as cellulose (Hiranuma et al., 2015b; Hiranuma et al., 2019) and macromolecules of marine biogenic origin (Schnell and Vali, 1976; Warren, 1987; Wilson et al., 2015; McCluskey et al., 2018a). Atmospheric concentrations of ice-active bacteria, fungal spores and pollen grains are much smaller than mineral dusts (Hoose et al., 2010). Estimates of the mass of PBAPs emitted to the atmosphere annually range from low hundreds to  $\sim 1000\text{ Tg}$  (Hoose et al., 2010; Jaenicke et al 2005) compared to  $1,000 - 3,000\text{ Tg}$  per year for mineral dust (Zender et al., 2004). However, the concentration of fragments of biogenic INPs may be much greater given the release of macromolecular INPs (Augustin et al., 2013; O'Sullivan et al., 2015) and their adsorption onto lofted soil dust (Schnell and Vali, 1976; O'Sullivan et al., 2016). Also the sources and atmospheric distribution of biogenic INPs are less well characterised compared to those of minerals dusts (Huang et al., 2021; Kanji et al., 2017), owing to the diversity of marine and terrestrial sources that may be subject to seasonal variations (Conen et al., 2015; Schneider et al., 2020; Šantl-Temkiv et al., 2019) or influenced by anthropogenic activities such as agricultural processes (Garcia et al., 2012; Suski et al., 2018; O'Sullivan et al., 2014).

Biological INPs tend to nucleate ice at temperatures where they may initiate secondary ice production processes (Morris et al., 2014; Field et al., 2017), thus amplifying their

effect in clouds. Biogenic INPs could also play an important role in feedback processes in the rapidly warming Arctic climate, as increasing surface temperatures may expose new terrestrial sources in thawing permafrost (Creamean et al., 2020), newly exposed glacial outwash sediments (Tobo et al., 2019) or reveal new marine reservoirs as the sea ice coverage is reduced (Hartmann et al., 2020). While the INA of mineral dust from various arid sources around the world is relatively similar (within around a factor of 10) (Niemand et al., 2012; Atkinson et al. 2013), the INA of biological material varies massively between the various sources, which makes predicting the INP population of biological material particularly challenging.

Much effort in the past decade has been put into not only collecting and identifying biogenic INPs or their markers in the environment, but also in determining their relative contributions to the total measured INP population (Huang et al., 2021). While techniques such as genomic sequencing (Garcia et al., 2012; Huffman et al., 2013; Hill et al., 2014; Christner et al., 2008) and microscopy (Huffman et al., 2013; Sanchez-Marroquin et al., 2021) can reveal the presence of biological species in an aerosol sample that has been found to contain INPs, it remains difficult to characterise the ice-nucleating ability of these species over other constituents (e.g. mineral dusts) when a sample's INA is analysed by, for example, a droplet freezing assay alone. To date, no high-throughput technique has been established that can directly identify both the composition and nucleation temperatures of a specific INP type within a sample. However, a widely used methodology for performing an indirect assessment of the contribution of mineral vs. biogenic INPs involves treating a collected aerosol sample (or other INP-containing media) with heat and comparing its INA spectrum before and after heating. Changes in INA can then be related to the presence and domination of biogenic INPs over inorganic INPs based on several assumptions, as discussed below. This heat treatment procedure has the advantages of being suitable for high-throughput offline sample analysis and does not require specialised equipment or the addition of reagents to selectively degrade biological material such as hydrogen peroxide (Suski et al., 2018; O'Sullivan et al., 2014; Tobo et al., 2019), lysozyme (Joyce et al., 2019; Henderson-Begg et al., 2009; Christner et al., 2008) or guanidinium hydrochloride (Conen and Yakutin, 2018). We have compiled a list of past studies which have employed heat tests to detect biological INP with the conditions and method of INP detection in Table 1.

**Table 4.1: List of past studies in which heat treatments were used to infer the presence of biological INPs in samples of various environmental media.**

Study	Sample media	Heat treatment method	Ice nucleation measurement method
Baloh et al., 2019	Snow and surface water	Wet: 95 °C for 20 min	DFA: 50 µL droplets in 96-well plates
Barry et al., 2021	Aerosol from wildfire smoke plume	Wet: 95 °C for 20 min	DFA: 50 µL droplets in 96-well plates
Boose et al., 2019	Desert dusts from nine worldwide locations	Dry: 300 °C for 10 h	Ice crystal counting by optical particle counter downstream of CFDC*
Christner et al., 2008a and b	Snow and rainwater	Wet: 95 °C for 10 min	DFA: 0.25 - 1 mL aliquots in test tubes
Conen et al., 2011	Soils with varying organic content	Wet: 100 °C for 10 min	DFA: 50 µL droplets in microfuge tubes
Conen et al., 2016	Aerosol and leaf litter suspension	Wet: 80 °C for 10 min	DFA: unstated volume in microfuge tubes
Conen et al., 2017	Aerosol sampled on hillside	Wet: 90 °C for 10 min	DFA: filter punches immersed in 100 µL droplets in microfuge tubes
Creamean et al., 2018	Bulk seawater and sea surface microlayer	Wet: 90 °C for 30 min	DFA: 2.5 µL droplets on cooling stage
Creamean et al., 2020	Permafrost soil and ice wedge	Wet: 95 °C for 20 min	DFA: 50 µL droplets in 96-well plates
D'Souza et al., 2013	Plankton sample from frozen lake	Wet: 45, 65 and 90 °C for 2 h	DFA: 80 µL aliquots in microcapillary tubes
Du et al., 2017	Rainwater	Wet: 100 °C for 10 min	DFA: 10 µL droplets on cooling stage
Garcia et al., 2012	Aerosol and surface dust collected on a farm	Wet: 98 °C for 20 min	DFA: 30 or 50 µL droplets in 96-well plates
Gong et al., 2020	Bulk seawater and sea surface microlayer, cloud water and aerosol	Wet: 95 °C for 1 h	DFA: 1 µL droplets on cooling stage and 50 µL droplets in 96-well plates
Hara et al., 2016a	Snow collected from ground	Wet: 40 °C and 90 °C for 1 h	DFA: filter punches immersed 0.5 mL in microfuge tubes

Hara et al., 2016b	Aerosol collected on building top	Wet: 90 °C for 1 h	DFA: filter punches immersed 0.5 mL in microfuge tubes
Hartmann et al., 2020	Bulk seawater, sea surface microlayer and fog water	Wet: 95 °C for 1 h	DFAs: 1 µL droplets on cooling stage and 50 µL droplets in 96-well plates
Henderson-Begg et al., 2009	Lichen samples and aerosol sample in urban location	Wet: 37, 60 and 90 °C for unspecified duration	Not stated
Hill et al., 2014	Vegetation washings and snow and hail from ground	Wet: 60 °C and 90 °C for 10 min	DFA: 50 µL droplets in 96-well plates
Hill et al., 2016	Topsoil	Wet: 60 °C and 105 °C for 20 min	DFA: 50 µL droplets in 96-well plates
Hiranuma et al., 2021	Aerosol and surface dust sampling on a cattle farm	Wet: 100 °C for 20 min	DFAs: 50 µL droplets in 96-well plates
Irish et al., 2017	Bulk seawater and surface microlayer	Wet: 100 °C for 1 h	DFA: 0.6 µL droplets on cooling stage
Iwata et al., 2019	Aerosol collected on building in forest	Dry: 150 °C for 10 min	Visual identification of ice growing on particles on cooling Si substrate
Joly et al., 2014	Cloud water	Wet: 95 °C for 10 min	DFA: 20 µL aliquots in microfuge tubes
Joyce et al., 2019	Rainwater, sleet and snow	Wet: 95 °C for 10 min	DFA: 200 µL droplets in 96-well plates
Knackstedt et al., 2018	River water and aerosolised river water	Wet: 95 °C for 20 min	DFA: 80 µL droplets in 96-well plates
Lu et al., 2016	Rainwater	Wet: 100 °C for 20 min	DFA: 10 µL droplets on cooling stage
Martin et al., 2019	Rainwater	Wet: 90 °C for 20 min	DFA: 50 µL droplets in 96-well plates
McCluskey et al., 2018a	Aerosol at coastal site	Wet: 95 °C for 20 min	DFA: 50 µL droplets in 96-well plates; CFDC*

McCluskey et al., 2018b	Sea spray aerosol, bulk seawater and sea surface microlayer	Wet: 95 °C for 20 min	DFA: 50 µL droplets in 96-well plates
Michaud et al., 2014	Hailstones	Wet: 95 °C for 10 min	DFA: 50 µL droplets in 96-well plates
Moffett et al., 2018	River water	Wet: 90 °C for 10 min	Differential scanning calorimetry of river water emulsion
Moffett et al., 2018	River water	Wet: 95 °C for 20 min	DFA: 80-100 µL droplets in 96-well plates
O'Sullivan et al., 2014	Agricultural soils	Wet: 90 °C for 10 min	DFA: 1 µL droplets on cooling stage
O'Sullivan et al., 2015	Woodland soils	Wet: 90 °C for 45 min	DFA: 1 µL droplets on cooling stage
O'Sullivan et al., 2018	Aerosol sampling on an arable farm	Wet: 95 °C for 1 hr	DFA: 1 µL droplets on cooling stage
Paramonov et al., 2018	Soil and desert dusts	Dry: 300 °C for 2 h	Ice crystal counting by optical particle counter downstream of CFDC*
Šantl-Temkiv et al., 2015	Snow and rainwater	Wet: 95 °C for 10 min	DFA: 240 - 300 µL droplets in 96-well plates
Šantl-Temkiv et al., 2019	Aerosol and snow samples	Wet: 100 °C for 10 min	DFA: 100 - 200 µL droplets for snow samples and filter punches immersed in 50 µL droplets in 96-well plates
Schneider et al., 2021	Aerosol collected from a boreal forest	Wet: 95 °C for 20 min	DFA: 50 µL droplets in 96-well plates
Schnell and Vali, 1976	Leaf litter collected from various locations worldwide and seawater	Wet: 60 – 100 °C for unspecified duration	DFA
Steinke et al., 2016	Agricultural soils	Dry: 110 °C for 1 h	Ice crystal concentration by optical particle counter in cloud chamber

Suski et al., 2018	Aerosol and surface dust sampling on an arable farm	Wet: 95°C for 20 min. Dry: 300 °C upstream of CFDC	DFA: 50 µL droplets in 96-well plates; ice crystal counting by optical particle counter downstream of CFDC*
Tobo et al., 2014	Agricultural soil dusts	Dry: 300 °C for 2 h	Ice crystal counting by optical particle counter downstream of CFDC*
Tobo et al., 2020	Aerosol collected from tall TV mast in Tokyo, Japan	Wet: 100°C for 1 h	DFA: 5 µL droplets on cooling stage
Tesson and Šantl-Temkiv, 2018	Snow	Wet: 100 °C for 10 min	DFA: droplets of unspecified volume on cooling stage
Wilson et al., 2015	Bulk seawater and sea surface microlayer	Wet: 8 temperatures between 20 °C and 100 °C for 10 min	DFA: 1 µL droplets on cooling stage
Yadav et al., 2019	Rainwater and desert dust from surface	Wet: 100 °C for 10 min	DFA: 1 µL droplets on cooling stage
Zinke et al., 2021	Cloud water	Wet: 100 °C for 30 min	DFA: 1 µL droplets on cooling stage

CFDC = Continuous Flow Diffusion Chamber

DFA = Droplet freezing assay

The identification of the presence of biogenic INPs using a heat test is based on the assumption that heat will inactivate biogenic (often but not always explicitly proteinaceous) INPs, yielding a reduction in ice nucleation temperatures following the treatment, while the INA of inorganic INPs (likely to be dominated by mineral dust) will remain unaffected (Conen et al., 2011). In addition to merely determining the presence of biogenic INPs, this method has also been used by some researchers to quantify the abundance of biogenic INPs in their samples by evaluating the magnitude of the INA reduction (Christner et al., 2008; Joly et al., 2014; Joyce et al., 2019). The assumption that protein-bearing biological INPs associated with bacteria and fungi can lose at least some of their INA when sufficiently heated (up to 100 °C) has been confirmed via many previous studies (Lundheim, 2002; Pummer et al., 2015; Roy et al., 2021) (see the review of Lundheim (2002) for an overview). However, non-

proteinaceous biogenic INPs, for example polysaccharides from pollen (Pummer et al., 2012; Pummer et al., 2015; Dreischmeier et al., 2017) and lignin (Bogler and Borduas-Dedekind, 2020), can retain their original INA when heated to temperatures over 200 °C. In contrast, the assumption that mineral particles acting as INPs cannot lose any INA when subjected to heat treatment has yet to be thoroughly tested, while the question of whether a mineral reacts differently to being heated while suspended in water or while heated in air has not been addressed at all. Zolles et al. (2015) measured the change in INA of feldspars, quartz, kaolinite and Arizona Test Dust (ATD) after dry heating to 250 °C for 4-5 h and observed only minor reductions within instrumental error. No similar surveys exist for wet heating, the more commonly used form of heat treatment of samples, although a small proportion of studies that employed the wet heat test for biological INP detection included control tests with mineral suspensions including K-feldspar (O'Sullivan et al., 2014), montmorillonite (Conen et al., 2011), kaolinite (Hara et al., 2016; Hill et al., 2016) and ATD (Yadav et al., 2019). No significant changes in INA were observed in these examples except for ATD by (Yadav et al., 2019), who attributed this to the removal of an unspecified organic ice-nucleating material from the surface of the mineral.

Finally, several studies have demonstrated the apparent lability of mineral INP kept in deionised water at room temperature over hours to days, wherein the immersion mode INA gradually decreased, which has been observed with samples of K-feldspar (Harrison et al., 2016; Peckhaus et al., 2016), quartz (Harrison et al., 2019; Kumar et al., 2019a) and ATD (Perkins et al., 2020). It is reasonable to predict that elevated temperatures could accelerate the 'ageing' behaviour seen with these minerals leading to an INA deactivation on the timescale of a biological INP heat test.

Overall, this highlights that the potential for the false positive 'detection' of biogenic INPs through the loss of mineral INA when using heat treatments has yet to be ruled out. Here, we aim to validate the heat test in its current form by fully characterising how mineral INPs respond to heating both in air and in water compared to biogenic INPs. We achieve this via a laboratory study in which we tested the immersion mode INA of a set of atmospherically relevant mineral samples before and after two types of heat treatment. We also performed equivalent tests on a set of biogenic INP

analogue samples for direct comparison to the mineral INP results and as a positive control to ensure that the heat treatments would reproduce the known heat sensitivity behaviour of biogenic INPs.

We employed two methods of heat treatment: (1) direct heating of the sample in aqueous suspension (wet heating), and (2) heating the sample while in dry powder form prior to immersion in water (dry heating). This enabled us to investigate whether the deactivation behaviour of a sample depends on the medium in which it is heated, as previous studies have either involved heating samples in the wet or dry modes but not both. Our rationale for this is that an INP sample's potential chemical or physical reactions to heating in water or air may differ as these are fundamentally different treatments. Where possible, we also characterise the heat sensitivity of the important subclasses of mineral INPs and then discuss how this could affect interpretations of biogenic INP heat test results and how this can inform us in the development of a more robust protocol. While our primary objective was to empirically evaluate commonly employed heat tests, we also discuss the physical reasons for the changes in INA found in our results, which may prove useful for future studies on the fundamental mechanisms of how mineral surfaces nucleate ice. This work may also be pertinent to emerging practical applications for mineral-based ice-nucleating agents in fields such as cell cryopreservation (Daily et al., 2020; Wragg et al., 2020; Morris and Lamb, 2018).

## **4.2 Materials and methods**

### **4.2.1 Sample selection**

A set of atmospherically relevant ice-nucleating materials was assembled into two broad classes of “mineral” and “biogenic” for heat treatment experiments. The mineral class comprised samples of ground minerals (either purchased from vendors in a milled form or milled in-house from a bulk mineral using a planetary ball mill) and commercially available dust proxies. Details of the identity, provenance and purity of each of these are provided in Tables 2 and 3 background information on each class of mineral and their significance as atmospheric INP is provided in Section 4.8 of the Supplementary Information (SI). Most emphasis was placed on the feldspar and silica classes of minerals as these have previously been shown to be the most ice-active mineral classes in immersion mode freezing experiments (Atkinson et al., 2013;

Harrison et al., 2019; Peckhaus et al., 2016) and therefore likely control the INA of a mineral dust assemblage of mixed mineralogy. Several of our samples have been analysed in the past using the same method and instrumentation as we employed here (Atkinson et al., 2013; Whale et al., 2017; Harrison et al., 2016; Harrison et al., 2019) and of these only Atkinson Quartz showed a deviation (slight loss in activity) in INA since they were last tested. This indicates that the INA of the mineral samples remains largely stable while in storage. The remaining mineral samples were clay-based samples, the dust surrogates NX Illite and ATD and, finally, calcite.

#### ***4.2.1.1 Mineral sample selection rationale***

We included five different samples of K-feldspar in our survey (see Fig. 4.2a) in order to represent the diversity of this group of minerals. These included: BCS-376 Microcline, which was studied previously (Atkinson et al., 2013) and is considered generally representative of the INA of standard K-feldspars (Harrison et al., 2016); Amazonite and TUD#3 Microcline, which are samples of microcline that show exceptionally high INA compared to typical variants of microcline and the other K-feldspar polymorphs for reasons that are still unclear (Harrison et al., 2016; Welte et al., 2019; Peckhaus et al., 2016); Eifel Sanidine, which exhibits much lower INA compared to the other samples due to a lack of features related to exsolution microtexture (Kiselev et al. 2021; Whale 2017}.

Three samples of plagioclase feldspar were included (see Fig. 4.3), two of which - BCS-375 Albite (Atkinson et al., 2013; Harrison et al., 2016) and TUD#2 Albite (Peckhaus et al., 2016) - are predominantly composed of the albite endmember, and Labradorite – a plagioclase that features a Ca composition between 50 % and 70 % that of anorthite. BCS-375 Abite contains quartz (4.0 %) and K-feldspar (16.7 %) impurities, while TUD#2 Albite contains at least 90 % plagioclase feldspar with the remaining 10 % of the content being unknown (based on X-ray diffraction (XRD) data (Atkinson et al., 2013; Peckhaus et al., 2016). The presence of K-feldspar in the former may mean that the observed activity is related to the presence of this component. No information is available on the mineral impurities present in the Labradorite sample. However, as plagioclase feldspar of labradorite composition is typically only found in basalts and gabbros, it is unlikely to coexist with quartz or K-feldspar since these rarely occur in these types of igneous rocks.

We included three samples of silica (see Fig. 4.4a): two  $\alpha$ -quartz samples - Atkinson Quartz and Fluka Quartz, and a sample of Fused Quartz, which is produced by melting quartz crystals then quenching to yield a glass (i.e. amorphous silica). We also included Bombay Chalcedony, which is composed of a cryptocrystalline intergrowth of quartz and moganite (another silica polymorph) and is notable as being the silica sample with the highest recorded INA (Harrison et al., 2019). We included this sample since its distinctly higher INA implies that the nature of the ice-active sites may be distinct from those of  $\alpha$ -quartz. Literature XRD data for our quartz samples indicate they are exceptionally pure in terms of mineralogy, with an  $\alpha$ -quartz content of at least 99.9 % (Harrison et al., 2019). Fused Quartz, as stated by the manufacturer, has a silica content of >99 %.

To represent clays we included samples that represent the main classes of clay minerals but also different samples of the same mineral to account for impurities which, due to the generally low INA of clays, may control the INA of the sample. Two samples of kaolinite (KGa-1b Kaolinite and Fluka Kaolinite), two samples of montmorillonite (SWy-2 Montmorillonite and Sigma Montmorillonite) and one sample of chlorite (Chlorite). An illite-rich sample (NX Illite) was included, but we classed this along with Arizona Test Dust (ATD) as a Mineral Dust Analogue – these being commercially available dusts of composite mineralogy which have been used in the past as representative e surrogates of atmospheric mineral dust. Finally, powder from a ground pure calcite crystal was used to represent the carbonates.

**Table.4.2: Sample information for mineral-based INP samples. Sources of data for purity and specific surface area (SSA) are detailed in the annotations.**

Sample name	Classification	Source	Purity (%)	SSA (m <sup>2</sup> g <sup>-1</sup> )
<b>BCS-376 Microcline</b>	K-feldspar	Bureau of Analysed Samples, UK	80.1 <sup>a</sup>	2.59
<b>TUD#3 Microcline</b>	K-feldspar	TU Darmstadt, Germany	80.0 <sup>b</sup>	2.94 <sup>b</sup>
<b>Amazonite Microcline</b>	K-feldspar	University of Leeds mineral collection	No data	No data
<b>Eifel Sanidine</b>	K-feldspar	University of Leeds mineral collection	No data	1.1 <sup>c</sup>

<b>Pakistan Orthoclase</b>	K-feldspar	University of Leeds mineral collection	No data	No data
<b>TUD#2 Albite</b>	Plagioclase feldspar	TU Darmstadt, Germany	90 <sup>b</sup>	1.92 <sup>b</sup>
<b>BCS-375 Albite</b>	Plagioclase feldspar	Bureau of Analysed Samples, UK	76.6 <sup>a</sup>	5.8 <sup>a</sup>
<b>Atkinson Quartz</b>	Quartz	University of Leeds mineral collection	99.9 <sup>d</sup>	4.2 <sup>d</sup>
<b>Fluka Quartz</b>	Quartz	Honeywell/Fluka (Cat No 83340), UK	99 <sup>d</sup>	0.9 <sup>d</sup>
<b>Fused Quartz</b>	Quartz	Goodfellow (Cat No. SI616010, 45 µm), UK	>99 <sup>*</sup>	No data
<b>Bombay Chalcedony</b>	Quartz	University of Leeds mineral collection	>99 <sup>d</sup>	1.23 <sup>d</sup>
<b>KGa-1b Kaolinite</b>	Clay based	Clay Minerals Society, USA (KGa-1b)	96 <sup>a</sup>	13.6 <sup>a</sup>
<b>Fluka Kaolinite</b>	Clay based	Fluka (Cat No. 03584)	82.7 <sup>a</sup>	No data
<b>Sigma Montmorillonite</b>	Clay based	Sigma Aldrich (Cat No. 69907), UK	57.0 <sup>a</sup>	No data
<b>SWy-2 Montmorillonite</b>	Clay based	Clay Minerals Society, USA	75 <sup>a</sup>	91.4 <sup>a</sup>
<b>Chlorite</b>	Clay based	University of Leeds mineral collection	99.6 <sup>a</sup>	25 <sup>a</sup>
<b>Arizona Test Dust (ATD)</b>	Dust surrogate	Powder Technology Inc., USA (A1 Ultra fine)	-	85 <sup>e</sup>
<b>NX Illite</b>	Dust surrogate	Arginotec, B+M Nottenkamper, Germany	-	104.2 <sup>f</sup>
<b>Calcite</b>	Carbonate	University of Leeds mineral collection	99.6 <sup>a</sup>	6 <sup>a</sup>

References: a. Atkinson et al. (2013), b. Peckhaus et al. (2016), c. Whale et al. (2017), d. Harrison et al. (2019), e. Bedjanian et al. (2013), f. Broadley et al. (2012), \* Data from manufacturer

#### **4.2.1.2 Biogenic sample selection rationale**

The biogenic class of samples tested here included examples of material in which proteins are responsible for ice nucleation (Snomax<sup>®</sup> as a non-viable form of *Pseudomonas syringae* bacteria, and lichen collected from trees in southern Finland) and non-proteinaceous material (microcrystalline cellulose (MCC) powder and silver birch pollen). The sources for each sample are provided in Table 3. Snomax<sup>®</sup> and lichen were used as representative of bacterial and fungal derived proteinaceous INP

respectively. Snomax<sup>®</sup> is a snow inducer product composed of lyophilised material derived from *Pseudomonas syringae* bacteria cultures and also used a surrogate for ice-nucleating bacteria (Wex et al., 2015; Polen et al., 2016). Lichens are symbiotic associations of fungi and algae and have been found to contain highly active INPs that are proteinaceous and likely originate from the fungal component (Moffett et al., 2015; Kieft and Ruscetti, 1990) so was therefore used a convenient source of fungal ice-nucleating material. Fungal INPs, have been found to have slightly higher heat resistance in wet mode compared to bacterial INPs, typically showing no reduction in INA with up to 60 °C of heating compared to 40 °C with bacterial INP but for both these it is eliminated by heating above 90 °C. (Pummer et al., 2015; Pouleur et al., 1992; Fröhlich-Nowoisky et al., 2015). Pollen and cellulose based INP were chosen to represent soluble and insoluble non-proteinaceous biological INP sources respectively where the INA is related to polysaccharide components and is much more heat resistant compared with proteinaceous INP (Pummer et al., 2012; Bogler et al., 2020). A sample of raw silver birch pollen (*Betula pendula*) was used to prepare an aqueous suspension of birch pollen washing water (BPWW). Pollen contains water-soluble ice-nucleating polysaccharide macromolecules (Pummer et al., 2012; Dreischmeier et al., 2017), which can be readily released into suspension with water (Augustin et al., 2013). Microcrystalline cellulose (MCC), a particulate polysaccharide reagent derived from wood pulp, was used as a surrogate for detrital plant material (Hiranuma et al., 2015b).

**Table.4.3: Sample information for biological-based INP samples**

Sample name	Classification	Source	SSA (m <sup>2</sup> g <sup>-1</sup> )
<b>Snomax<sup>®</sup> (freeze-dried, non-viable <i>Pseudomonas syringae</i> bacteria)</b>	Proteinaceous	York Snow, Inc., USA	Non-particulate
<b>Lichen (<i>Evernia prunastri</i>)</b>	Proteinaceous	Collected from trees around Hyytiälä Forestry Station, Finland	Non-particulate after 0.2 µm filtration
<b>Birch pollen (<i>Betula pendula</i>) washing water (BPWW)</b>	Non-proteinaceous	Pharmallerga, Czech Republic	Non-particulate after 0.2 µm filtration
<b>Microcrystalline cellulose (MCC)</b>	Non-proteinaceous	Sigma-Aldrich, UK (Cat. No. 435236)	0.068 <sup>a</sup>

#### 4.2.2 Sample preparation

All aqueous suspensions were prepared in 0.1 µm pre-filtered, cell culture-grade deionised water (HyClone™ HyPure, GE Lifesciences). A standard concentration of 1 % w/v was used for the mineral suspensions although additional aliquots with different concentrations were prepared for selected mineral samples (BCS-376 Microcline, Fluka Quartz, NX-Illite and ATD – see Appendix B). All mineral samples were stored in darkness at room temperature and suspensions of mineral samples were prepared by mixing 0.1 g of sample with 10 mL water in 20 mL borosilicate glass vials (Samco type T006/01, Surrey, UK), which had been pre-sterilised by dry heating at 175 °C for 2 h. The suspensions were thoroughly dispersed on a vortexer for 10 seconds after mixing and were gently inverted by hand several times to ensure even mixing before each drawing of the suspension via an electronic pipette. Glass vessels, rather than polypropylene centrifuge tubes, were used for all experiments unless stated due to their higher thermal conductivity when placed in a water bath (see Appendix A) and resistance to oven heating. The biogenic samples were stored cold (Snomax® at –20 °C, raw birch pollen and dried lichen at –4 °C) or at room temperature in the case of MCC and they were made to suitable concentrations according to existing literature protocols. Snomax® and MCC were prepared as 0.05 % w/v and 0.1% w/v suspensions respectively in the same manner as the mineral samples. Lower concentrations of Snomax® were made by dilution of the 0.05% w/v suspension with deionised water. The birch pollen and lichen samples could not be immediately dispersed in water as they required additional filtration steps to produce visibly clear homogeneous extracts rather than particulate suspensions. A suspension of birch pollen washing water (BPWW) was prepared to a previously described protocol (O'Sullivan et al., 2015), wherein a 2 % w/v (20 mg mL<sup>-1</sup>) suspension of raw pollen powder was prepared by weighing 0.2 g of raw pollen and adding to 10 mL deionised water, before mixing via vortexing and shaking, and being allowed to soak overnight at 4 °C. The suspension was then filtered through a 0.2 µm cellulose acetate filter to remove the pollen grains, leaving only the washing water containing macromolecular INPs, thought to be anionic polysaccharides (Dreischmeier et al., 2017), for analysis. The lichen sample (*Evernia prunastri*) was collected from a tree during a field campaign at the Hyytiälä Forestry Station, Finland, in April 2018, was air dried and then stored in a sealed sterile plastic bag at 4 °C. The dried lichen was cut into millimetre-sized pieces, then 5 mL of purified water added to yield a lichen

concentration of 2 % w/v and placed on a rotary inverter for 2 h on a slow setting. The suspension was then filtered as per the BPWW procedure above to produce an aliquot of extract ready for analysis with or without subsequent dilution.

### **4.2.3 Heat treatments**

Each INP sample was subjected to heat treatment using two distinct methods: a ‘wet heating’ treatment wherein the INP was heated while in suspension and a ‘dry heating’ treatment wherein the INP sample was heated in dry powder form in air and subsequently mixed with water for analysis. The ‘standard’ temperature and duration for the wet heat test was 95 °C for 30 min (immersed in boiling water – see Fig. 4.9) and for the dry heat test was 250 °C for 4 h. These conditions have been used in previous work and our primary objective was to empirically test commonly used heat tests. For selected samples we varied heating temperature (for the dry test only) and durations for further analysis of the samples’ responses.

#### **4.2.3.1 Wet heating**

The ‘wet heating’ treatment comprised of a sealed vessel containing the INP suspensions, described in Section 4.2.2, being immersed in an open boiling water bath (hence at the boiling point of water at 1 atm: 100 °C). The vessels were sealed tightly to prevent the evaporation of water from the vessel causing an increase in concentration of the suspensions. After 30 min of immersion, the vessel was removed from the water bath and then allowed to cool to room temperature prior to the droplet freezing assay. In the case of the washing water samples (i.e., BPWW and lichen), the wet heat treatments took place following the filtration steps.

The temperature profile of the liquid inside 20 mL borosilicate glass vials and 50 mL polypropylene centrifuge tubes (Corning Falcon 352090) throughout the wet heat treatment procedure was measured (Fig. 4.9 in Appendix A) by inserting a thermocouple (Type K) through a small hole punched in the caps of the vessels, and was recorded using a data logger (TC-08,  $\pm 0.025$  °C, Pico Technology, UK). This showed that a 10 mL liquid aliquot inside the glass vial reached a maximum temperature of 96 °C after approximately 10 min of immersion in the boiling water bath, while the larger polypropylene vessel only reached 86 °C after 20 min. Samples of proteinaceous IN derived from lichen (Kieft 1988, Kieft and Ruscetti 1990, Moffat et al, 2015), fusarium fungi (Pouleur et al. 1992) and pseudomonas syringae bacteria

(Maki et al. 1974) all saw large deactivations after being heated in boiling water baths for less than 15 minutes, presumably due to denaturation. Therefore, it is presumed that 30 min of immersion under these conditions is sufficient to denature INP of proteinaceous origin. Both vessels returned to ambient temperature approximately 45 min after being removed from the bath.

In addition to our standard 30 min heat treatment, we performed extended wet heat treatments of up to 24 h for selected samples by immersing the vessels in a silicone oil bath heated to 100 °C rather than a water bath. The oil bath temperature was controlled using a thermostat alongside a magnetic stirrer bar and stirrer plate to ensure a homogeneous oil temperature.

#### **4.2.3.2 Dry heating**

‘Dry heating’ of samples was achieved by placing a 20 mL borosilicate glass vial containing a maximum of 0.2 g of dry sample in a standard laboratory oven at 250 °C for 4 h, before being allowed to cool to room temperature and then prepared as an aqueous suspension as described in Section 4.2.2 above. The dry heat treatment for the biogenic samples were performed on the raw, dry materials, then suspended in deionised water and, in the case of the BPWW and lichen, subject to the filtration process described above. A temperature of 250 °C for 4 h was selected for the ‘standard’ dry heat treatment as it far exceeded the highest documented temperature at which the most heat resistant biogenic INPs (birch pollen at around 180 °C (Pummer et al., 2012) and lignin at around 220 °C (Bogler et al, 2020)) are deactivated. Further, this temperature is lower than the maximum heat rating of polytetrafluoroethylene (PTFE) membrane and quartz filters that are often used to collect aerosol samples for INP analysis. We also Samples were weighed before and after standard dry heat treatment.

#### **4.2.4 Ice nucleation measurements by droplet freezing assay and determination of samples’ heat deactivations**

The INA of the mineral-based and biogenic sample suspensions both before and after heat treatments was determined by performing immersion mode droplet freezing assays (Vali, 1971) using the Microlitre Nucleation by Immersed Particle Instrument ( $\mu$ L-NIPI) (Whale et al., 2015), which has been used extensively for INP analysis in the literature and in several intercomparison studies (Hiranuma et al., 2015a; DeMott

et al., 2018). Here, 1  $\mu\text{L}$  droplets (up to a maximum of 50) of INP suspension were pipetted onto a hydrophobic glass coverslip (22 mm diameter, cat. no. HR3-231, Hampton Research, USA) that was located atop the aluminium cooling plate of a Grant-Asymptote EF600 cryocooler whilst at room temperature. The cooling plate was then enclosed in a Perspex chamber into which a flow of dry nitrogen gas was introduced at  $0.3 \text{ L min}^{-1}$  to flush the chamber of ambient air and to prevent the presence of moisture and airborne contaminants for the duration of each experimental run. The droplets were cooled at a rate of  $1 \text{ }^\circ\text{C min}^{-1}$  until all of the droplets were frozen. Droplet freezing events were detected visually using an optical camera (Microsoft LifeCam HD) mounted atop the clear Perspex flow chamber.

Analysis of the droplet freezing events allowed the determination of the fraction of droplets frozen as a function of temperature,  $f_{ice}(T)$ , as shown in Eq. (1), where  $n(T)$  is the number of droplets frozen at temperature  $T$ , and  $N$  is the total number of droplets in the assay.

$$f_{ice}(T) = \frac{n(T)}{N} \quad (4.1)$$

Blank tests were performed with droplets of filtered deionised water at the beginning of each day of experiments to confirm no contamination was introduced by the processes. In addition we performed handling blanks for the various heating methods and for the filtration of the BPWW and lichen samples (Fig. 4.14).

Quantification of a nucleator's INA was achieved by determining the surface density of ice-active sites,  $n_s(T)$  for particulate samples (minerals and MCC), or mass density of active sites,  $n_m(T)$ , for non-particulate biogenic samples. These allowed for comparison of our data with existing parameterisations for ice-nucleating materials (e.g., Fig 4.10b for BCS-376 Microcline or Fig 4.10e for Snomax<sup>®</sup>): If the surface area of nucleant present in each droplet,  $A$ , is known, then this can be used to calculate  $n_s(T)$  of an INP sample from  $f_{ice}(T)$ , as defined in Eq. (1).

$$n_s(T) = \frac{-\ln(1-f_{ice}(T))}{A} \quad (4.2)$$

Similarly if the mass of nucleant present in each droplet,  $M$ , is known,  $n_m(T)$  can be calculated:

$$n_m(T) = \frac{-\ln(1-f_{ice}(T))}{M} \quad (4.3)$$

Mass per droplet  $M$  is calculated from droplet size and the concentration of the INP suspension while the surface area,  $A$ , in our samples was derived mass of ice nucleant per droplet multiplied by the specific surface area (SSA,  $\text{m}^2 \text{g}^{-1}$ ) of the INP powders. We used literature values of SSA obtained by the Brauner-Emmet-Teller (BET)  $\text{N}_2$  gas adsorption technique (e.g. Harrison et al., 2019; Zolles et al., 2015; Paramonov et al., 2018) for all mineral samples apart from SSA of the BCS-376 microcline K-feldspar which we measured ourselves (Micrometrics TriStar 3000). For MCC we used a scanning electron microscope (SEM) based measurement from Hiranuma et al. (2019). This INA quantification approach assumes that each ice nucleation site has a characteristic temperature at which it always becomes active and time dependence is insignificant (Herbert et al., 2014), otherwise known as the singular description of heterogeneous ice nucleation (Koop and Zobrist, 2009; Murray et al., 2012; Vali, 1994; Pruppacher, 1978). Characterising ice-nucleating materials in terms of  $n_s(T)$  also forms the basis of models used for predicting the temperatures (and thus cloud regime) at which different classes of atmospheric INPs may become active (Vergara-Temprado et al., 2017; Hawker et al., 2021; Zhao et al., 2021; Murray et al., 2012).

### 4.3 Results and discussion

In Fig. 4.1 we have shown several examples of fraction frozen curves for heated (wet and dry) and unheated samples to illustrate the heat sensitivity of a range of ice nucleating materials. Similar plots for all materials we have tested here are shown in Figs. 4.12 and 4.13. In order to present this information in a more concise manner, we have plotted the same data in the form of boxplots of droplet freezing temperatures of mineral samples throughout the results section. In addition, changes in INA resulting from the heat treatments were evaluated by calculating the freezing temperature shifts between them and determining whether the shifts were significantly larger than the instrumental error. This was simply taken as the difference between the median droplet freezing temperature ( $T_{50}$ ) of the samples before and after the heat treatments to give a  $\Delta T_{50}$  value:  $\Delta T_{50}^{wet}$  for the wet heat treatment and  $\Delta T_{50}^{dry}$  for the dry heat treatment. Droplet freezing temperatures detected by the  $\mu\text{L-NIPI}$  instrument have a nominal error of  $\pm 0.4$  °C (Whale et al., 2015) so, as a simple test for significance, a change in  $\Delta T_{50}$  by more than 3 times this  $\pm 0.4$  °C error (i.e.,  $\pm 1.2$  °C) between  $f_{ice}(T)$  curves qualified as a significant shift. A significant shift in  $T_{50}$  to colder temperatures (i.e., a

negative  $\Delta T_{50}$  value) indicated a deactivation in INA of a sample in response to heating.

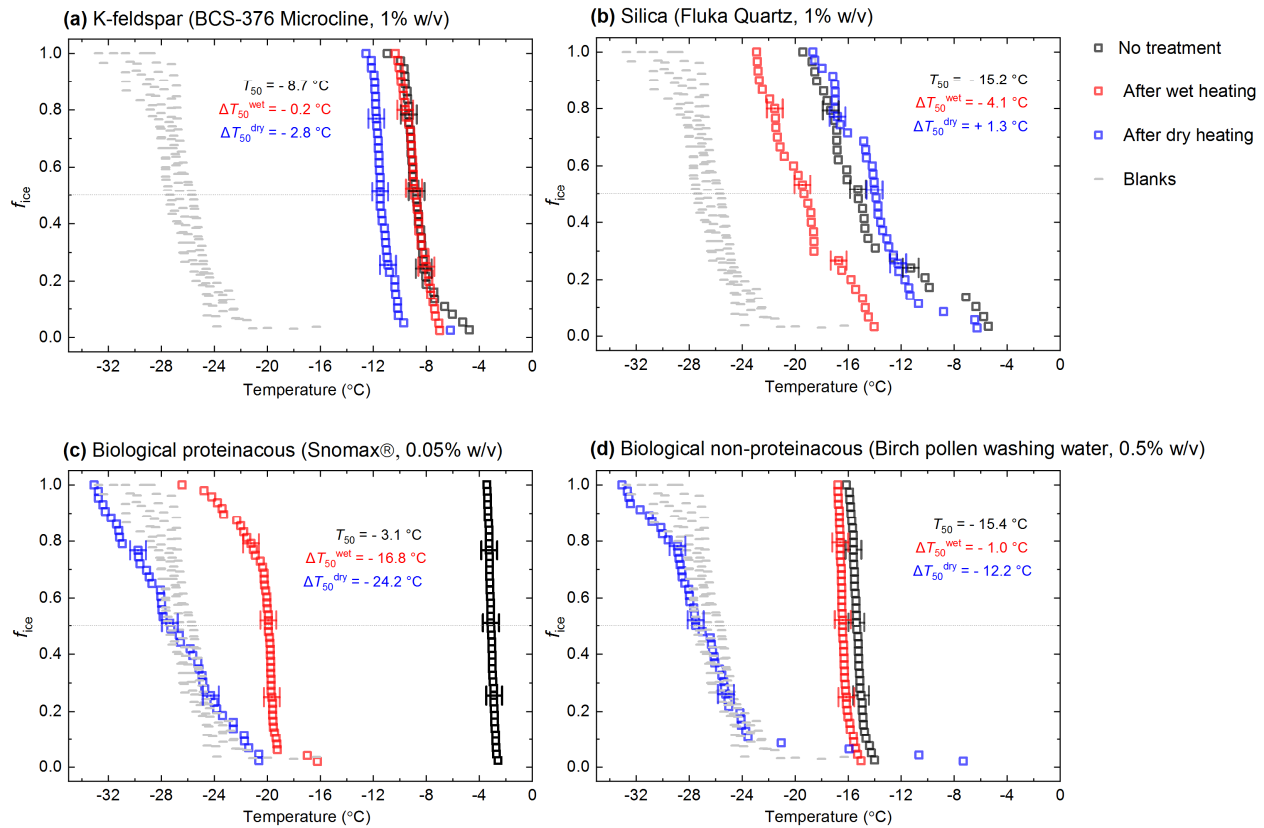


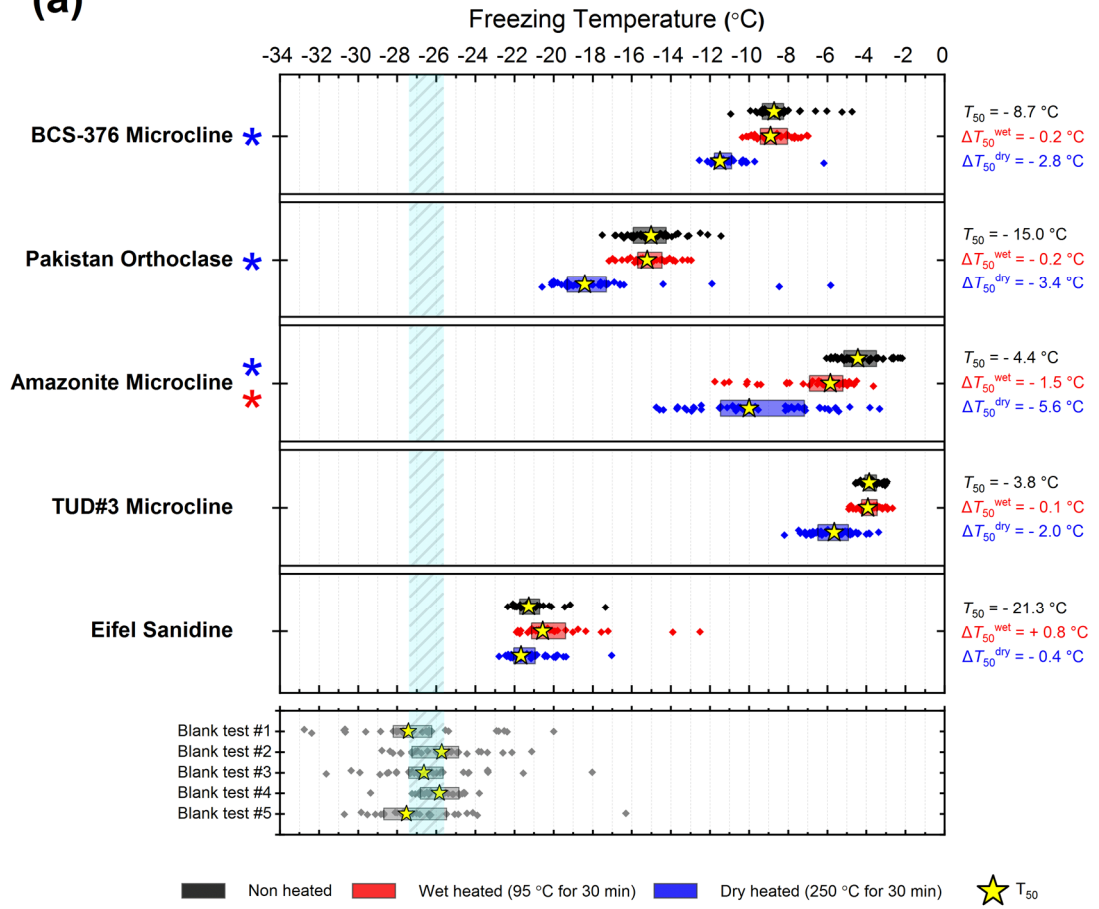
**Figure 4.1** Fraction of droplets frozen ( $f_{ice}(T)$ ) spectra illustrating characteristic heat treatment responses for: (a) A dry heat-sensitive mineral INP (BCS-376 Microcline). (b) A wet heat-sensitive mineral INP (Fluka Quartz). (c) A wet heat-sensitive proteinaceous biological INP (Snomax®). (d) A wet heat-insensitive non-proteinaceous biological INP (birch pollen washing water). On each plot, a dotted line is shown at  $f_{ice}(T) = 0.5$ , at which  $T_{50}$  temperatures can be read. Error bars on selected data points illustrate the 1.2 °C temperature range used to guide whether a shift in freezing temperatures after heating was considered to be significant.

### 4.3.1 Heat sensitivity of mineral-based INP samples

#### 4.3.1.1 *K-feldspars*

In general, the INA of K-feldspar samples did not respond substantially to wet heating for 30 mins with no significant reductions of  $T_{50}$  in four out of five of the samples of K-feldspar (see Figs. 4.1a and 4.2). An exception was Amazonite Microcline which showed a  $\Delta T_{50}^{wet}$  of  $-1.5$  °C, which was greater than the experimental uncertainty, as defined above (we discuss the possible reasons for this later in this section). The finding that K-feldspars are relatively insensitive to the wet heat test is consistent with the findings of O'Sullivan et al. (2014) and Peckhaus et al. (2016), who previously performed this test on BCS-376 Microcline and TUD#3 Microcline, respectively. Additional wet heat tests on less concentrated (0.1% and 0.02%) suspensions of BCS-376 Microcline also showed no response (Appendix B) indicating stability over a wide range of particle concentrations. We also conducted extended wet heat treatments of up to 22 h with BCS-376 Microcline that, although longer in duration than typical biological INP heat tests, were designed to ascertain whether wet deactivation was possible. The results, shown in Fig. 4.2b, are plotted in the form of  $n_s(T)$  to enable comparison with literature data. The results show that 24 h of wet heating resulted in a reduction in  $n_s(T)$  of approximately one order of magnitude, or 2 °C at  $n_s(T) = 1$  cm<sup>-2</sup>. However, some deactivation of the most active sites appeared to occur after only 60 min of heating. After 4 h, the reduction in  $n_s(T)$  was roughly the same as that seen after 16 months of immersion in water at room temperature, as determined by Harrison et al., (2016). Overall, we find that the INA of K-feldspar is retained after short term (30 min) wet heating but can be reduced if heated for longer periods.

(a)



(b)

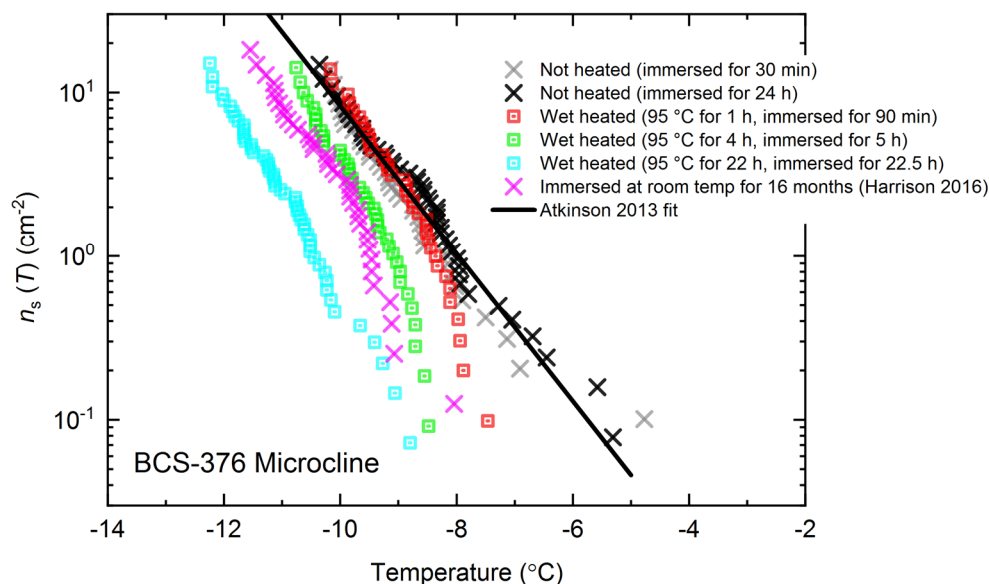


**Figure 4.2 (a) Boxplot showing freezing temperatures before (black) and after heat treatments (red for wet heat, blue for dry heat) for all K-feldspar samples. Asterisks (\*) next to sample name indicate significant deactivation by wet (red) or dry (blue) heating, this defined as a reduction in  $T_{50}$  of more than 1.2  $^{\circ}\text{C}$ . Boxes represent the 25-75 % percentile, points represent individual droplet freezing temperatures, and stars represent the temperature at which half of the droplet population had frozen (i.e.  $T_{50}$ ). Background freezing temperatures are illustrated by the blue band, which denotes the range of  $T_{50}$  temperatures obtained from four blank droplet freezing runs. Blank runs are shown below the main boxplot (b) Active site density per surface area ( $n_s(T)$ ) spectrum for BCS-376 Microcline after extended wet heat treatment compared to room temperature ageing experiments from Harrison et al. (2016). The parameterisation for the ice-nucleating activity of K-feldspar from Atkinson et al. (2013) is also shown.**

To discuss the reasons behind the deactivation of K-feldspar when wet heated for longer than 30 min, the nature of the ice-nucleating sites on minerals must first be considered. Ice nucleation on mineral surfaces such as feldspars has been shown to occur at specific sites that become active at a specific temperature (Holden et al., 2019;

Holden et al., 2021). Topographical features associated with exsolution microtexture (Whale et al., 2017; Kiselev et al., 2021) have been proposed as the locations of the highly active sites on K-feldspar. Moreover, Kiselev et al. (2017) observed that ice crystals growing from the vapour phase on the surface of microcline originated on steps and cracks and were preferentially orientated between the basal face of ice and the (100) cleavage plane. More recent work suggests that cracks caused by exsolution microtexture may expose the (100) face of feldspars (Kiselev et al., 2021). The chemical and physical nature of these sites is still unclear, however molecular dynamics studies such as those by Pedevilla et al. (2017) show that having a high density of functional groups like silanol groups (Si-OH), where water can hydrogen bond with the mineral surface and potentially order (such as those exposed at the (100) cleavage plane), may be important for nucleating ice (Harrison et al., 2019).

The most obvious physical cause of the INA deactivation of K-feldspar by wet heating would be the alteration of the mineral surface by dissolution via hydrolysis. This leaves an amorphous ‘leached’ layer at the surface (Lee et al., 2008; Chardon et al., 2006), destroying or at least disrupting the ice-active sites. Several studies have shown experimentally that acid treatment deactivates K-feldspar INPs (Augustin-Bauditz et al., 2014; Kulkarni et al., 2015; Kumar et al., 2018a). In pure water and at near-neutral pH, however, the supply of H<sup>+</sup> for hydrolysis is lower and therefore the dissolution rate is much slower, but may still occur at the less stable, higher energy sites and topographic features (Parsons et al., 2015), which are themselves proposed as the highly active sites in K-feldspars. As discussed above, Harrison et al. (2016) observed a gradual INA deactivation of BCS-376 Microcline while at room temperature in deionised water, but this occurred over several months rather than hours. It is reasonable to propose that the same INA deactivation process observed by Harrison et al. (2016) also occurred on the K-feldspar samples in this study but was accelerated in this case by heating.

Amazonite Microcline, one of our two highly ice-active microcline samples, was an exception to other K-feldspar samples in that short-term wet heating resulted in a significant but small deactivation ( $\Delta T_{50}^{wet} = -1.5$  °C). This could be because either the highly active sites of this sample were especially susceptible to dissolution and distinct from the more standard sites in the other K-feldspar samples, or is an indication of contamination with biological INPs. We return to this issue below.

Dry heating had a stronger deactivating effect on the K-feldspar samples than wet heating (Fig. 4.2a). Amazonite Microcline showed the largest  $\Delta T_{50}^{dry}$  of  $-5.6$  °C and we observed that this sample lost its pale green colour and turned white following the treatment, becoming more similar in appearance to the other K-feldspar samples. Dry heating resulted in deactivation of the Pakistan Orthoclase ( $\Delta T_{50}^{dry}$  of  $-3.4$  °C) and produced smaller deactivations in TUD#3 Microcline and BCS-376 Microcline ( $\Delta T_{50}^{dry}$  of  $-1.8$  °C and  $-2.8$  °C, respectively).

A potential alternative explanation for the apparent dry-heat sensitivity of K-feldspar is that there is a biological component mixed with the K-feldspar samples which nucleates ice and is deactivated on heating and, due to the high temperatures required for deactivation, is non-proteinaceous. Peckhaus et al. (2016) discussed the potential for biological ice nucleating material in TUD#3. They achieved a deactivation in TUD#3 Microcline by treatment with hot aqueous  $H_2O_2$  after a wet heat test (90 °C for 1 hr) showed no effect. They deliberated the presence of a polysaccharide based ice-nucleating component, but concluded this was unlikely given the unrealistic mass proportion of contaminant in the sample that would be required to produce such high ice-nucleating temperatures to start with. In the case of our affected K-feldspar samples, presence of non-proteinaceous biogenic material cannot be completely ruled out without further analysis, however there are no likely candidates of organic non-proteinaceous heat-labile material that nucleate ice at such high ( $> -5$  °C) temperatures. Hence, we suggest that the deactivation observed on dry heating K-feldspars is not related to the destruction of biological material.

Recalcitrant organic coatings have previously been proposed as the source of INA in mineral dusts that is lost upon dry heating (Paramonov et al., 2018; Peckhaus et al., 2016; Perkins et al., 2020). However others have reported that organic coatings suppress the INA of mineral dusts rather than enhance it (Boose et al., 2019; China et al., 2017; Pach et al., 2021) by blocking access to underlying active sites. For example, Pach et al (2021) treated slices of a K-feldspar crystal from the same locality as TUD#3 Microcline with oxygen plasma and observed an enhancement in INA which they attributed to the oxidation and removal of organic material from the surface that originated from ambient air. They suggested that the plasma treatment 'unblocked' the surface pores which contained the most active IN sites allowing water to enter during their freezing experiments. .

Alternatively the loss of a (non-organic) volatile component during dry heating may alter K-feldspar in a way that reduces its INA. As described above, Amazonite Microcline is a green or turquoise coloured variant of microcline and was observed here to lose its green colouration upon dry heating. This phenomenon has previously been observed (Hofmeister and Rossman, 1985) and was correlated to the loss of water molecules that were structurally bound within the feldspar crystal lattice. Although Amazonite is a relatively rare variety of microcline, all feldspars contain a minor water component either as lattice-bound H<sub>2</sub>O molecules or OH groups or fluid pockets (Johnson and Rossman, 2003) that can be driven off by high temperature (Liu et al., 2018), as could be the case in our dry heat treatment. Although it is not known whether this process would destroy the active ice nucleation sites, it is intriguing that microcline samples, the most ice-active variety, when surveyed were found to contain the most structurally bound water of all feldspars (Johnson and Rossman, 2004).

#### **4.3.1.2 Plagioclase feldspars**

BCS-375 Albite and TUD#2 Albite showed no significant changes to their  $T_{50}$  values after wet heating, but both samples lost much of the tail of INA that extended to above  $-15\text{ }^{\circ}\text{C}$  (Fig. 4.3 and Figs. 4.12f and 4.12g). Labradorite was sensitive to wet heating, with a  $\Delta T_{50}^{wet}$  of  $-2.4\text{ }^{\circ}\text{C}$ . All three samples in this mineral class were found to be insensitive to dry heat treatment, which means that biological contaminants was unlikely to be the source of the wet heat-labile INA (since all biological samples we looked at were sensitive to dry heat, see Section 4.3.2). The wet heat sensitivity was consistent with accelerated dissolution of the mineral surface, as discussed above for K-feldspars (and below for quartz). The Si dissolution rate for plagioclase feldspar is similar to that of quartz, but two orders of magnitude higher than that of K-feldspar microcline (Kumar et al., 2019a). This was consistent with the observation that, for example, both Labradorite and Fluka Quartz (see Sections 4.3.1.2 and 4.3.1.3) deactivated after 30 min of wet heating while BCS-376 Microcline took several hours to show deactivation. The wet heat reactions of the two albite samples were more difficult to interpret due to their varying impurities of other feldspars and quartz, and as such the deactivations could be a result of deactivation of those impurities rather than the plagioclase feldspar itself.

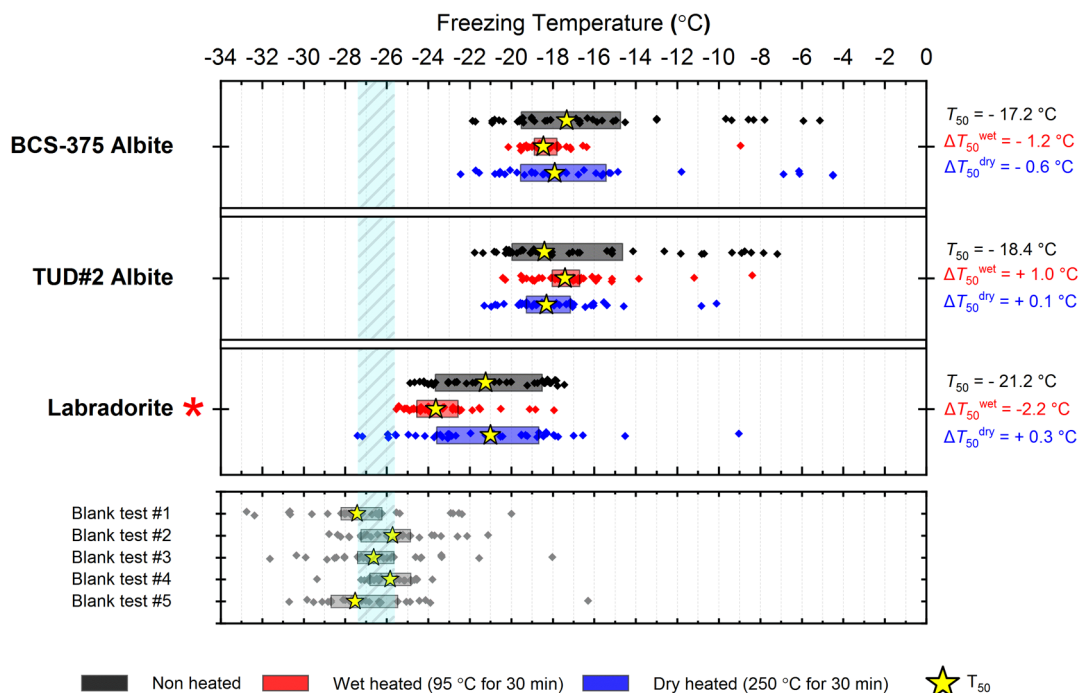
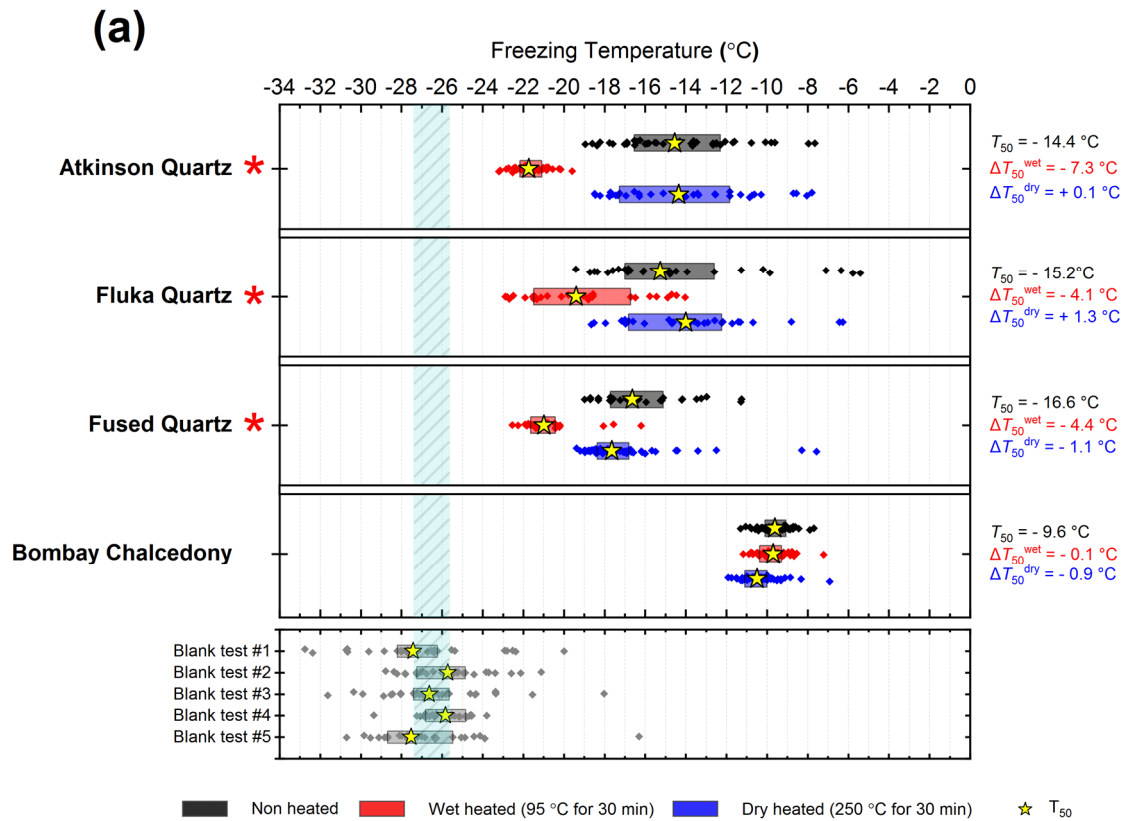


**Figure 4.3** Boxplot showing freezing temperatures before (black) and after heat treatments (red for wet heat, blue for dry heat) for all plagioclase feldspar samples along with blank runs.

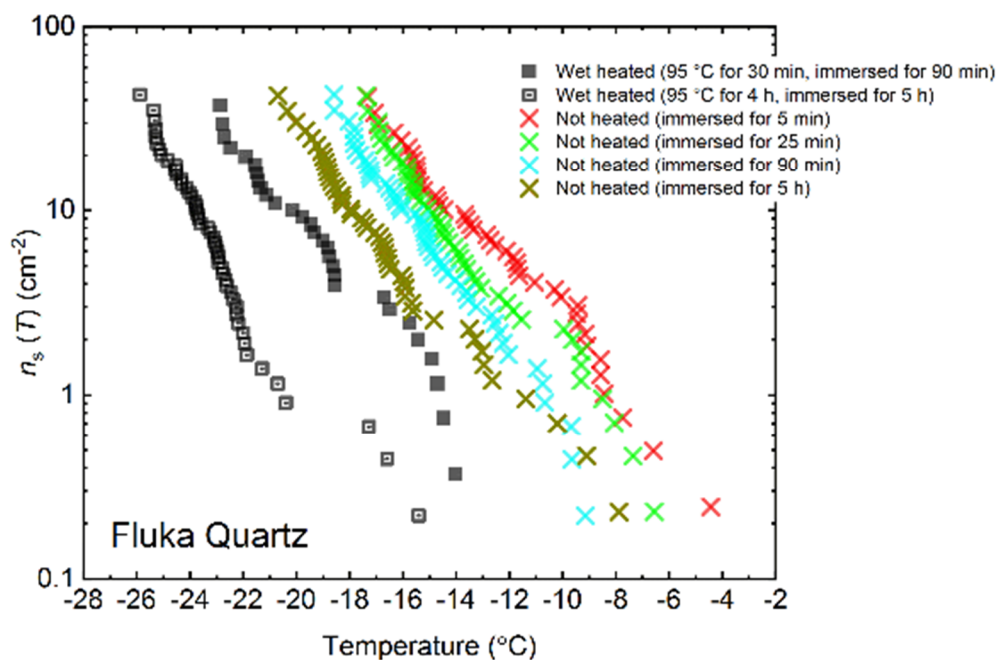
#### 4.3.1.3 .Silicas

Atkinson Quartz, Fluka Quartz and Fused Quartz all exhibited similar reactions to both wet and dry heat treatments (see Fig. 4.4a). In each case, the INA experienced significant deactivation upon wet heating ( $\Delta T_{50}^{\text{wet}}$  of  $-7.3$ ,  $-4.1$  and  $-4.4$  °C for Atkinson Quartz, Fluka Quartz and Fused Quartz, respectively), but no significant changes when dry heated. We repeated the standard wet and dry heat tests on Fluka Quartz at higher (2.5%) and lower (0.1%) suspension concentrations (Appendix B) and saw that the wet heat deactivation was consistent at approximately one order of magnitude of  $n_s(T)$  and dry heat consistently non-deactivating, apart from a small number of droplets active above  $-6$  °C. In contrast, Bombay Chalcedony showed no significant change in INA following either type of heat treatment. Kumar et al. (2019a) proposed that in their study that the quartz INP suspensions deactivated only as an artefact of being contained in glass vessels, however when we repeated our wet heat treatment in plastic containers deactivation was still observed (see Figs. 4.8 and 4.9 and Appendix A for discussion). While the INA deactivation of quartz by dry heating has previously been described by Zolles et al. (2015), this is the first time that the wet

heat treatment and resultant INA lability of quartz has been reported.



**Figure 4.4 (a) Boxplot showing freezing temperatures before (black) and after heat treatments (red for wet heat, blue for dry heat) for all silica samples along with blank runs**

**(b)**

**Figure 4: (b)  $n_s(T)$  spectrum for Fluka Quartz after wet heat treatment and room temperature ageing, illustrating their relative rates of INA deactivation.**

Being sensitive to wet heat, yet virtually resistant to dry heat treatment, is an indirect but strong indication that the heat labile ice-nucleating sites on Atkinson Quartz, Fluka Quartz and Fused Quartz are not biological in nature. This is because our dry heat treatment would be expected to reduce the activity of both proteinaceous and non-proteinaceous biological INPs (as our results with biogenic materials show in Section 4.3.2). In addition, it is interesting that the glassy Fused Quartz sample had very similar responses to both dry and wet heat. This indicates that the active sites on these three silica samples are not dependent on crystallinity. Given that Bombay Chalcedony was the exception in this mineral class in that it was insensitive to heat, it seems that the active sites on this material were distinct to the other silica samples we studied. The high INA and stability to heat of Bombay Chalcedony is comparable to several of the K-feldspar samples. Bombay Chalcedony is also a microcrystalline material possessing micropores, much like K-feldspar, and this may give rise to stable active sites (Harrison et al., 2019).

Given the INA deactivation in silica samples upon heating appears to be abiotic and only occurs in water, but not dry heat, then the most obvious explanation is that it is

due to the accelerated dissolution of surface features associated with the active sites. Active sites are thought to be most abundant where defects and fractures occur, as milling has consistently been found to increase the INA of quartz (Zolles et al., 2015; Kumar et al., 2018b; Harrison et al., 2019). They may also be the most unstable sites as Harrison et al. (2019) observed measurable ‘ageing’ in quartz samples (including Atkinson Quartz and Fluka Quartz) that were immersed in room temperature water for only 1 h. Our wet heat treatment of Atkinson Quartz resulted in an INA deactivation of similar magnitude ( $\Delta T_{50}^{wet}$  around 7 °C) to that achieved after 16 months of aqueous room temperature ageing by Harrison et al. (2019). To demonstrate the ‘accelerated’ deactivation speeds of quartz in water at different temperatures, we performed parallel room-temperature ‘ageing’ and also wet heating (30 min and 4 h) experiments with Fluka Quartz, with the results shown in Fig. 4.4b. When the heated sample and room-temperature sample had both been immersed in water for the same time, the heated sample always had a lower activity. In addition, the longer the sample was immersed in water (heated or room temperature), the greater the deactivation (where the deactivation was accelerated at higher temperatures).

A similar apparent phenomenon of room-temperature ageing being accelerated by heating has also been observed for BCS-376 Microcline K-feldspar (Harrison et al., 2016), except that the process appears to be much slower. At room temperature, INA deactivations of similar magnitude (up to 2 °C) were observed after only 1 h for Atkinson Quartz (Harrison et al., 2019), compared to 16 months required for deactivation of BCS-376 Microcline (Harrison et al., 2016). Similarly, we needed to wet heat K-feldspar for at least 1 h to detect a small deactivation compared to 30 min for Fluka Quartz. However, crucially the deactivation of quartz is, unlike K-feldspar, fast enough to occur on a timescale relevant to biogenic INP heat tests (about 30 min). It is possible that the same deactivation mechanism for both K-feldspar and Atkinson Quartz occurs during the wet heat treatments and is consistent with active site degradation by surface dissolution for two possible reasons. Firstly, surface dissolution rates for quartz are faster than for microcline ( $10^{-13}$  to  $10^{-12}$  Si-m<sup>-2</sup> s<sup>-1</sup> compared with  $4 \times 10^{-14}$  to  $8 \times 10^{-14}$  Si-m<sup>-2</sup> s<sup>-1</sup> at neutral pH and 25 °C (Kumar et al., 2019b)). Secondly, quartz and feldspar break apart differently when ground. Quartz, lacking cleavage planes, fractures conchoidally, while feldspar can more easily cleave along its two perfect cleavages situated on the (001) and (010) faces. Fracturing rather

than cleaving may result in a surface topography dense in high energy but unstable ice nucleation sites that are more susceptible to dissolution (Harrison et al., 2019) than the bulk of the surrounding surface.

#### ***4.3.1.4 Clay-based mineral samples***

While neither kaolinite sample were significantly sensitive to dry heat (the Fluka sample was only marginally sensitive), the Fluka Kaolinite showed clear sensitivity to wet heating while KGa-1b Kaolinite did not (see Fig. 4.5). We can perhaps attribute this to the comparatively purer state of the latter (96 % kaolinite) compared to the former (83 %) that includes a 6 % component of quartz, which was shown to be sensitive to wet heating in Section 4.3.1.3.

The results for the montmorillonite samples were harder to interpret because both possessed quite low purities and showed responses to heat treatments that are not easily explained by their feldspar and quartz components. A notable result was that the INA of the Sigma montmorillonite sample increased after dry heat treatment. An increase in INA in the deposition mode after dry heating has previously been observed in a smectite-rich Saharan dust sample that had been dry heated at 300 °C for 10 h during a study by Boose et al. (2019). The authors discussed potential reasons for this, including the volatilisation and removal of an organic INA inhibiting coating, as well as purely inorganic processes such as the growth of new anhydrite crystals from gypsum in the sample or alterations to the lattice spacing of smectite clay. Our sample, which became more active upon heating, did not contain any gypsum impurities, hence conversion to the highly active anhydrite (Maters et al., 2020; Grawe et al., 2018) was not a possibility. Smectites are characterised by their ability to swell or shrink by taking up or losing loosely bound water molecules in the crystal lattice. However, the same effect of dry heating was not observed for SW-y2 Montmorillonite, which demonstrated no deactivation of INA with dry heating and only a minor deactivation upon wet heating. Hence, the changes in the INA of Sigma Montmorillonite during dry heating could not be related to its swelling properties.

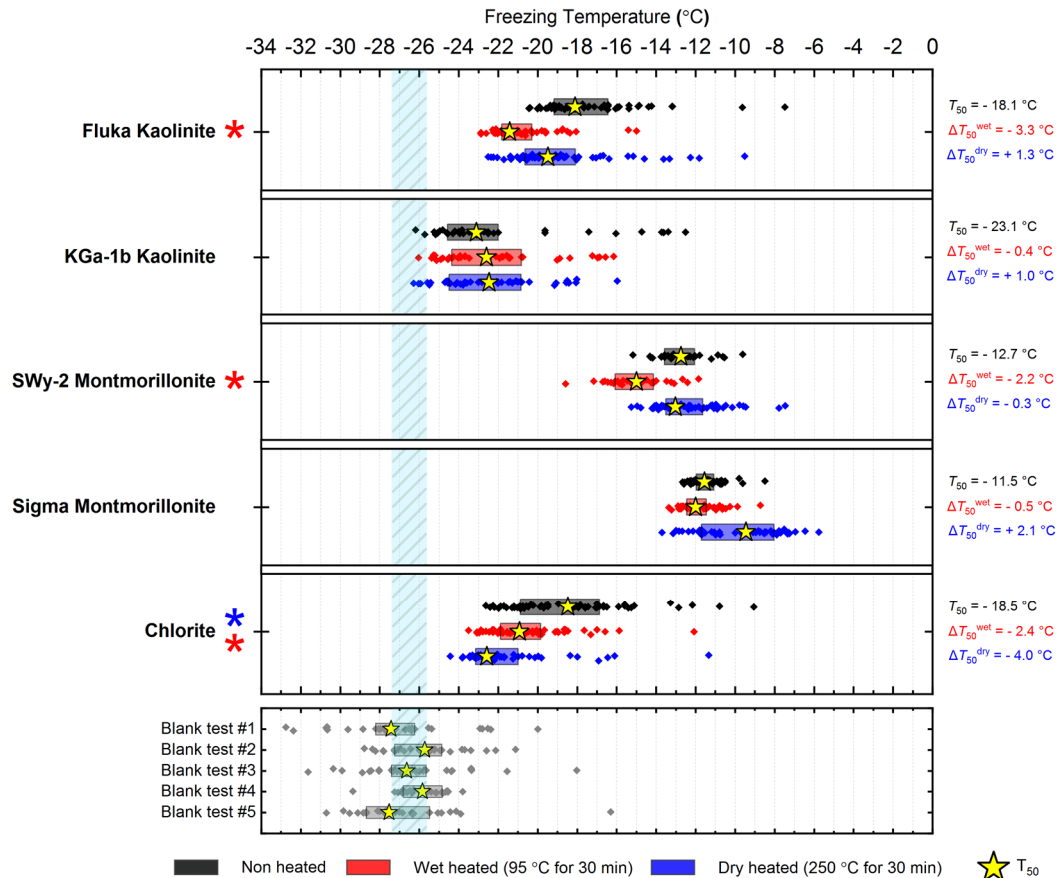


**Figure 4.5** Boxplot showing freezing temperatures before (black) and after heat treatments (red for wet heat, blue for dry heat) for clays based mineral samples

The results for chlorite, with its high purity (99.6 %), indicated heat-lability in both the wet and dry heat modes. However, chlorite likely has only limited atmospheric importance as an INP due to both its relatively low INA and typically low (around 5 %) proportional make-up of airborne mineral dusts (Murray et al., 2012; Kandler et al., 2009; Glaccum and Prospero, 1980).

#### 4.3.1.5 Mineral dust analogues and calcite

The boxplots with droplet freezing temperatures for NX Illite and ATD are shown in Fig. 4.6a. NX Illite was unresponsive to wet heating, as was previously demonstrated by O'Sullivan et al. (2015), but deactivated after dry heating with a  $\Delta T_{50}^{dry}$  of  $-2.0$  °C. ATD was clearly deactivated by wet heating ( $\Delta T_{50}^{wet}$  of  $-4.5$  °C, with activity almost eliminated above  $-10$  °C) and slightly affected by dry heating ( $\Delta T_{50}^{dry}$  of  $-1.4$  °C). In the case of both these samples the responses were independent of suspension

concentration (Appendix B). We further investigated the wet heat sensitivity of ATD by performing extended heat treatments of up to 22 h and also room-temperature ageing for 24 h, and these are plotted as  $n_s(T)$  plots in Fig. 4.6b. This shows a similar behaviour to that observed for Fluka Quartz (Fig. 4.4b), where room temperature deactivation was observed but deactivation was greatly increased by heating. However, in the case of ATD, the sites active at above  $-10\text{ }^\circ\text{C}$  retained activity when immersed in room temperature water, while the activity of sites active at lower temperatures was reduced (Fig. 4.6b). A previous instance of the wet heating of ATD in the literature also showed a wet heat lability (Yadav et al., 2019), while dry heating using a range of different methodologies also showed slight reductions in ATD's INA (Sullivan et al., 2010; Perkins et al., 2020; Zolles et al., 2015), thus corroborating the results shown here. Perkins et al. (2020) found that ATD lost some INA after dry heating to  $500\text{ }^\circ\text{C}$ , yet was deactivated to roughly the same degree by 'ageing' in water at room temperature for 2 days. Both dry heating to  $600\text{ }^\circ\text{C}$  and aqueous oxidation treatment by boiling in 30 %  $\text{H}_2\text{O}_2$  led to more significant deactivations. They attributed the dry heat deactivation to oxidation of an organic coating stable in air up to  $500\text{ }^\circ\text{C}$  but removed readily in the aqueous mode. They did not, however, boil the ATD in water alone which would have determined if the  $\text{H}_2\text{O}_2$  deactivation was merely a result of being heated in water.

(a)

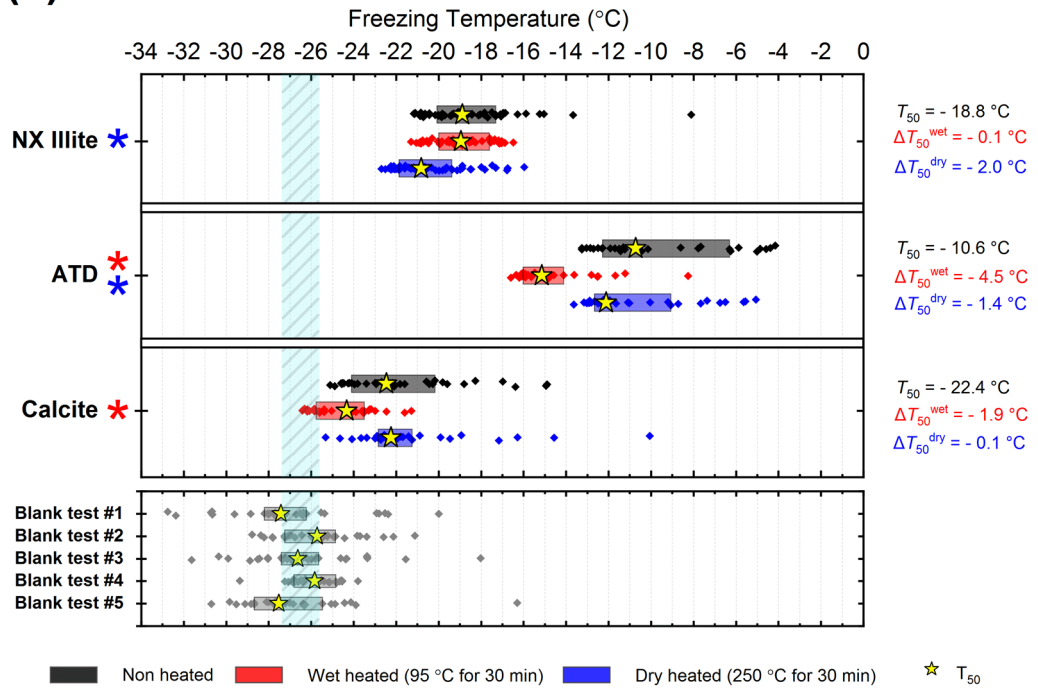


**Figure 4.6. a). Boxplot showing freezing temperatures before (black) and after heat treatments (red for wet heat, blue for dry heat) for mineral dust analogues and calcite.**

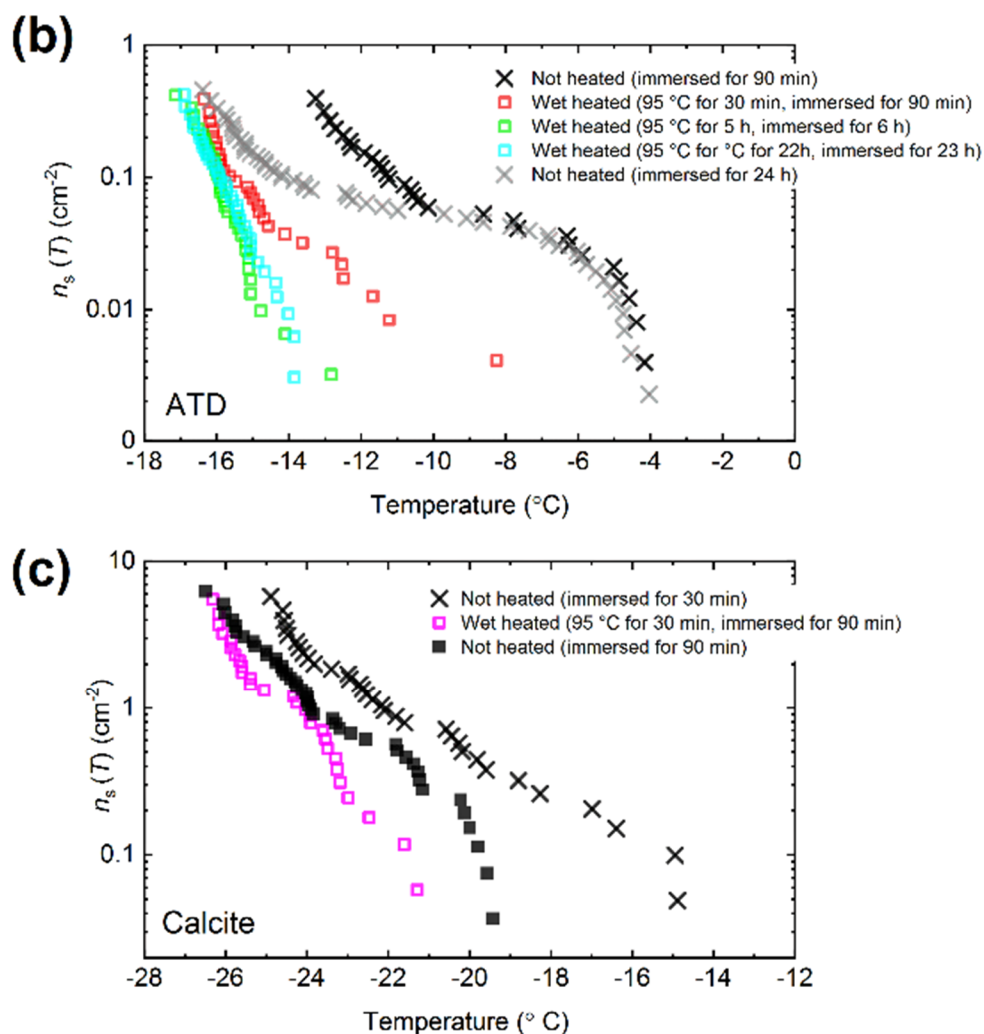


**Figure 4.6:** (b)  $n_s(T)$  spectrum for ATD after extended wet heat treatments and room temperature ageing, illustrating their relative rates of INA deactivation. (c)  $n_s(T)$  spectrum for Calcite after 30 min of wet heating and being immersed in water for equal amount of time.

As described above, K-feldspar is mostly only sensitive to dry heating while quartz is only sensitive to wet heating, which implies that the observed changes in INA for NX Illite may be controlled by the K-feldspar component while the INA of ATD may be controlled by milled quartz particles. Alternative explanations to the deactivations include biological contamination. However, similar to the results obtained for the silica samples, the greater deactivation seen in ATD from wet heating compared with that from dry heating suggests that the heat-labile component is not biological.

The calcite sample displayed a reduction in INA after wet-heating ( $\Delta T_{50}^{wet}$  of  $-1.9$  °C) but not after dry heating. This case was distinct from that of other minerals that were sensitive to wet heating (e.g., Fluka Quartz) where a similar degree of deactivation occurred in a control experiment when suspended in water at room temperature for the same duration as the heated sample (Fig. 6c). If the dissolution of active sites on calcite resulted in INA deactivation in water, then the fact that heating did not significantly speed up INA deactivation can be explained by calcite exhibiting retrograde solubility in water. Dissolution of calcium carbonate in water occurs when water equilibrates with atmospheric CO<sub>2</sub> and forms weak carbonic acid. Hence, the solubility, and reduction in activity, is limited by the amount of CO<sub>2</sub> dissolved in water, hence the lack of additional effects upon heating.

#### **4.3.2 Biological INP surrogates**

Four biological INP analogue samples were subjected to the same wet and dry heat treatments (95 °C for 30 min and 250 °C for 4 h respectively). The results are summarised in Fig. 4.7 as boxplots of freezing temperatures, Fig 4.11 as  $n_s(T)$  and  $n_m(T)$  plots for samples over extended concentration ranges and in Fig. 4 as  $f_{ice}(T)$  curves. We also performed wet and dry tests with varying durations and temperatures on Snomax<sup>®</sup> and birch pollen to compare the effects of heating in different media at equivalent conditions, these results are presented in Fig 4.11.

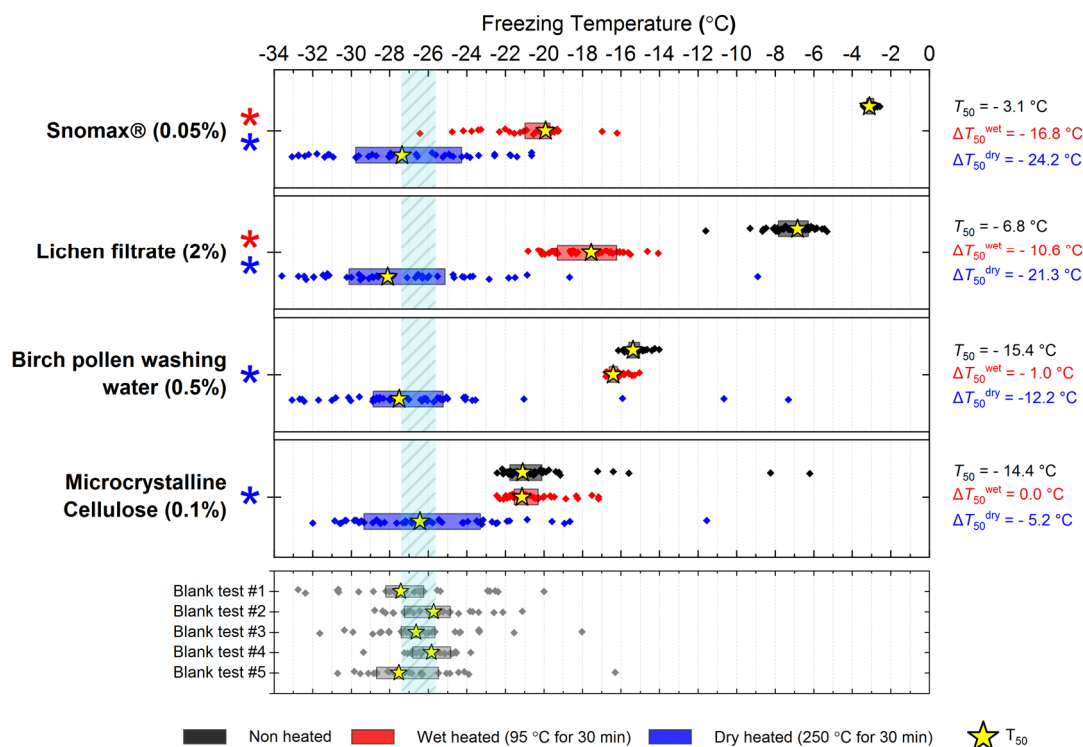


**Figure 4.7: Boxplot showing freezing temperatures before (black) and after heat treatments (red for wet heat, blue for dry heat) for biological INP samples.**

After the standard heat tests Snomax® (0.05 % w/v) was significantly deactivated by wet heating ( $\Delta T_{50}^{wet}$  of  $-16.8^{\circ}\text{C}$ ) and was also deactivated to background levels by the dry heat test with the material appearing carbonised (turning into a black substance) after the treatment. Clearly, both the wet and dry heats test denatured or destroyed ice-nucleating proteins in Snomax® although some residues with INA activity around  $-20^{\circ}\text{C}$  were left behind by wet heat test. The activity was reduced to near background levels when the wet heating time was increased to 4 h (Fig 4.11). Dry heating Snomax® at  $250^{\circ}\text{C}$  for only 30 min instead of 4 h had the same results, with carbonisation and complete deactivation. Reducing the dry heat temperature to  $95^{\circ}\text{C}$  only resulted in a very small deactivation ( $\sim 1.2^{\circ}\text{C}$ , i.e. of borderline significance) after either 30 min or 4 h, with the Snomax® pellets appearing unchanged by the treatment. Lichen (2% w/v filtrate) showed similar behaviour to that of Snomax®, that of being carbonised and deactivated to background levels by the dry heat test while the wet heat test achieved

a significant deactivation but left residual activity between -15 °C and -20 °C, at slightly warmer temperatures than with Snomax<sup>®</sup>.

Birch pollen washing water (0.5 % w/v) was not significantly deactivated by wet heating ( $\Delta T_{50}^{wet}$  of -1.0 C after 30 min and -1.6 °C after 4 h) but dry heating at 250 °C, resulted in deactivation of INA to background when heated for 4 h and slightly above after 30 min. These wet heat deactivations were consistent when repeated with over 20- and 200-fold dilutions (Fig B2h). Dry heating at 95 °C for up to 4h, however did not result in any change to INA or any change in appearance of the raw pollen powder. Finally, microcrystalline cellulose (0.1% w/v) was unchanged by wet heating (95 °C for 4h) but was completely deactivated by dry heating at 250 °C for 4 h and, like the other biogenic samples, was carbonised after this treatment.

Overall, the results showed that the proteinaceous samples (Snomax<sup>®</sup> and lichen) clearly suffered substantial deactivation by the standard wet and complete deactivation to standard dry heat treatments, while non-proteinaceous samples showed no or very little sensitivity wet heating but dry heating. For all four biogenic samples the magnitude of active site loss in terms of  $n_m(T)$  and  $n_s(T)$  was largely consistent when more dilute samples were tested (Fig. 4.10) suggesting these tests are representative to a wide range of concentrations. The stability of the INA in pollen and cellulose heated in water is consistent with reports of the relative resistance of polysaccharide-based ice-nucleating materials similar treatment (Conen et al., 2011; Conen et al., 2015; Bogler and Borduas-Dedekind, 2020). We also corroborate results from Pummer et al., (2012) where Snomax<sup>®</sup> was able to be heated dry to 112 °C with only slight loss of activity. This clearly demonstrates the difference responses of this particular substance to being heated in air or water under similar conditions and suggests that being in a desiccated form protects proteinaceous INP from being denatured at temperatures (~ 100 °C) that would otherwise denature them when suspended in water.

#### **4.4 Summary and implications for using INP heat treatments**

We performed both wet and dry heat tests on a range of mineral and biological ice-nucleating materials and directly compared their characteristic INA responses to both modes of heat treatment. Our findings, summarised in Table 4, show that the general assumption that the INA of minerals is insensitive to heat is too simplistic and we

identified sensitivities characteristic to important mineral classes. For example, quartz and plagioclase feldspar INPs were found to be sensitive to wet heating in a comparable way to proteinaceous INPs (bacteria and lichen), but were insensitive to dry heating at considerably higher temperature (250 °C). In contrast, K-feldspars are generally insensitive to the 30 min wet heat test (with the exception of Amazonite, which happens to be a relatively rare type of microcline), but slightly sensitive to the dry heating at 250 °C. Fluka Quartz and ATD, that were wet heat sensitive but not deactivated by dry heat, showed small INA deactivations after being dispersed in water but kept at room temperature for less than 1 hr.. This suggests that the deactivation process for these samples is an aqueous process accelerated by increased temperature. Calcite showed similar behaviour in water except the room temperature and wet heat deactivations were similar. Of the other mineral samples we tested their interpretations were more difficult due to their INA possibly being controlled by impurities (Fluka Kaolinite with its quartz content, for example) but, overall, we found that mineral samples were more likely to be deactivated by wet heating than by dry heating (with the important exception of K-feldspars).

The biogenic INP samples showed the clear heat sensitivity of proteinaceous- and heat resistance of polysaccharide-based INPs in wet mode while dry heating at 250 °C served to eliminate all INA for both classes. Dry heating at 95 °C for 4 h did not deactivate BPWW and only slightly deactivated Snomax<sup>®</sup> in contrast to wet heating at the same temperature and duration, which severely deactivated the latter and unaffected the former. The magnitude of deactivations in terms of  $n_s(T)$  did not depend on the concentration of INP during heating (Appendix B) nor the material of the vessel used (Appendix A). In the case of both mineral and biogenic samples longer heating duration lead to greater degree of INA deactivation when wet heating but not when dry heating.

**Table 4.4: Summary of the characteristic responses of classes of INPs to wet and dry heat treatments.**

INP type	Characteristic sensitivity of INA to wet heating (100 °C for 30 min)	Characteristic sensitivity of INA to dry heating (100 °C for 4 h)	Characteristic sensitivity of INA to dry heating (250 °C for 4 h)
<b>K-feldspar</b>	Stable <sup>1</sup>	Stable	Slightly heat sensitive <sup>2</sup>
<b>Plagioclase feldspar</b>	Slightly heat sensitive	(Stable)	Stable
<b>Quartz</b>	Heat sensitive <sup>3</sup>	(Stable)	Stable
<b>Clays</b>	Stable <sup>4</sup>	(Stable)	Stable <sup>5</sup>
<b>Carbonates</b>	Sensitive to water at room temperature <sup>6</sup>	(Stable)	Stable
<b>Biological, proteinaceous</b>	Heat sensitive	Slightly heat sensitive	Heat sensitive
<b>Biological, non-proteinaceous</b>	Stable	Stable	Heat sensitive

Notes: (Stable) denotes assumed stability as heating to higher temperatures resulted in no deactivation; 1. Hyperactive varieties may have slight sensitivity; 2. Hyperactive varieties are very sensitive; 3. Slight sensitivity in room temperature water; 4. Apart from chlorite; 5. Montmorillonite may increase in INA when dry heated; 6. INA deactivation does not increase when heated.

An implication of this work is that reduced INA of INP samples subject to a heat test may be incorrectly attributed to biological INPs when heated, particularly in wet mode. But crucially, since the INA of K-feldspar is not reduced by short-term wet heating, the standard wet heat test (30 min immersed in boiling water) remains a valid method for distinguishing *proteinaceous* INPs from mineral dusts, so long as the INA of the mineral dust component is controlled by K-feldspar. Nevertheless, the INA heat lability of some commonly occurring minerals raises the possibility that a false positive detection of biological INPs could be made following a wet heat test, i.e., a loss of INA of quartz or plagioclase feldspar may be misconstrued as a loss of biological INA. This could occur during a scenario in which a wet heat test is performed on a sample whose mineral component INA is dominated by its silica or plagioclase feldspar content rather than K-feldspar and in which proteinaceous biological INPs are absent. The importance of quartz and plagioclase feldspars as ice-nucleating components of mineral aerosols are second only to K-feldspar, hence the possibility of this scenario occurring should not be dismissed. However, feldspars and

quartzes tend to be found together in desert dust assemblages, thus K-feldspar will likely control the INA of desert dust on most occasions.

Performing heat tests on minerals in parallel with biological samples allowed the magnitude of mineral wet-heat sensitivity to be put into context. For example, Yadav et al. (2019), performed wet heat tests on rainwater and dust samples collected from Northern India, with a heat test of ATD performed as a control. The results showed a resultant deactivation of INA that was consistent with our results. The authors attributed this to the presence of organic matter in their ATD sample. However, the magnitude of deactivation ( $\sim 1$  °C) observed in the ATD control was far smaller than in their rainwater samples (up to 10 °C), which was interpreted as evidence of 'biological influence'. In other words, the 'signal' produced by the mineral INP heat deactivation should be weak compared to that of proteinaceous INP deactivation, hence the loss of INA in ATD may not have been influenced by the presence of biological components after all. Generally, marginal heat deactivations of a few degrees should be interpreted with caution and generally should not be attributed to the presence of proteinaceous ice-nucleating materials. This especially applies if heat deactivations have been used to calculate the ambient concentration of biological INPs in addition to identifying their presence.

We also consider the issue of whether the heat-sensitive active sites we found in our mineral samples are an artefact of the milling process and therefore not representative of particles present in the environment. The INA of quartz (Kumar et al., 2019a; Zolles et al., 2015; Harrison et al., 2019), hematite (Hiranuma et al., 2014) and also natural desert dusts (Boose et al., 2016) are increased by milling. This might imply that heat-labile mineral INPs do not occur naturally. Conversely, it has been argued that quartz particles in desert dusts are naturally 'milled' by collisions during the process of saltation prior to being lofted into the air (Harrison et al., 2019). If this is correct, then it would mean that only quartz INPs originating from desert dust, with their active surfaces exposed following saltation, would be wet heat-labile, whereas quartz particles that have been in contact with water, for example in soil or sediments, would have already been 'aged' and so may be less susceptible to further wet heat treatment.

Here, we provide some further caveats and considerations for the use of heat tests to identify biological, specifically proteinaceous, INPs in environmental and atmospheric samples:

*a) Dry heating INP samples as an alternative to wet heating*

Wet heating is the dominant mode of heat test used by others in past studies to detect biological (or more correctly, proteinaceous) INP (Table 1), yet wet heating deactivated some mineral INPs (e.g., quartz and plagioclase feldspars) much more strongly than dry heating did. Therefore, dry heating of aerosol filters or any INP sample available in an initially dry form could be considered as an alternative or parallel heating method that is more selective than wet heat treatment. Dry heating at 250 °C is expected to carbonise and deactivate all biological INP, including proteinaceous and polysaccharide, however the dry heat sensitivity of K-feldspar that we observed at this temperature could negate this approach. Our data shows that dry heating at a lower temperature of 95 °C preserved the activity of K-feldspar, however, it did not deactivate heat-resistant polysaccharide INP and denatured proteinaceous INP (Snomax<sup>®</sup>) far less than when heated at the same temperature in water. This means that for detection of proteinaceous INP dry heating at 95 °C holds no advantage over wet heating at 95 °C. Bounded by the conditions tested here, further experimentation would help to determine if there is an optimal dry heating protocol that both preserves the INA of K-feldspar and deactivates all biological INP (or even selectively deactivates different types of biological INP). Ideally, this should be conducted using a combination of model materials like we used in this study, but also natural materials such as fertile soils, desert dusts, surface waters and precipitation samples. Some consideration also needs to be given to how a dry heat test would be conducted on aerosol sampled from the atmosphere. It may be possible to conduct a heat test on filters loaded with aerosol particles where filters could perhaps be split in two, one half to be heated and one half for the standard INP analysis. For this to be feasible, the effects and suitability of alternative dry heat protocols on aerosol filters should be investigated. Another potential approach might be to use an inlet system with a heated component that would heat aerosol to some specified temperature. However, the timescales that aerosol would be exposed to elevated temperature would be relatively short (seconds) and tests would be needed to find the appropriate conditions.

### *b) Optimise wet heat tests to avoid mineral deactivations*

As K-feldspar was seen to deactivate after prolonged (>30 min) wet heating, ensuring wet-heat tests are as short in duration as possible (i.e. no longer than the time it takes for the sample to reach, for example, 95 °C) and are then cooled and tested for INA as soon as possible would theoretically minimise wet-heat mineral deactivations. Also an overlooked consequence of the wet heat treatment is that the INP sample may be immersed in water for longer than non-heated counterparts. This could result in an apparent deactivation of non-biological INPs due to the room temperature ‘ageing’ effects of mineral INPs in water (as demonstrated in this study and in the literature (Harrison et al., 2019; Kumar et al., 2019a)), which we hypothesise are sometimes sped up by heating. Two adaptations to the method that could mitigate this include: (i) conducting tests on samples for room temperature ‘ageing’, similar to those for Fluka Quartz and ATD performed here; (ii) ensuring that all heated and non-heated samples are immersed in water for an equal duration before running tests for INA.

### *c) Control heat tests on mineral and biological INP references*

Relatively few of the previous studies listed in Table 1, where heat treatments were performed to identify the presence of biological INPs in the environment, also included a control to test whether their protocol deactivated the INA of a reference material of known INA. Considering this study, future implementations of the heat test could benefit from testing a set of reference materials (e.g., microcline K-feldspar, albite plagioclase feldspar, quartz, Snomax<sup>®</sup> and pollen), to ‘calibrate’ a specific heat test protocol. Alternatively, the specific protocol described in this study could be used in future work.

## **4.5 Conclusions**

In this study, we have tested and characterised the changes in ice-nucleating ability of the principal mineral components of desert dust in response to heat treatments in both wet and dry modes and in parallel with biological INP analogues (bacterial, fungal, pollen and cellulose). The main purpose of this was to assess the efficacy of heat treatments for the ‘detection’ of biological INPs in environmental sample media such as ambient aerosol, surface waters, soils and desert dusts. Understanding how the sources and distribution of biological INPs and mineral dust INPs differ in the environment may be crucial for understanding their current and future impact on the

climatic impacts of clouds. It has been previously assumed that mineral INPs are inert to moderate heat treatments that are sufficient to denature proteins. However, we found that while the INA of (most) K-feldspars was unchanged on wet heating for 30 min, as expected, quartz and plagioclase-rich feldspars were heat-labile. The INA of quartz and plagioclase-rich feldspar samples was unchanged when exposed to dry heat (250 °C for 4 h). Given that all biogenic INP samples were strongly deactivated by the dry heat test, it is clear that the loss of activity in quartz and plagioclase feldspars was related to the minerals themselves, rather than some biological contamination.

We suggest that the loss of INA on wet heating of quartz and plagioclase feldspars is related to aqueous dissolution of features acting as active sites on the mineral surface. This is supported by the observation that the relative dissolution rates of the different mineral types correlate with their relative heat sensitivities. Moreover, several studies have previously reported aqueous room temperature ‘ageing’ of mineral INP samples and our results are consistent with the same process being accelerated by heating. As quartz and plagioclase feldspars are ubiquitous components of mineral dusts, this raises the possibility of false positives being produced by minerals in wet heat tests, which are more commonly used compared to dry heat tests. However, if the mineral-based INA of an environmental sample being tested for INP is controlled by K-feldspar then wet heat tests are valid.

Dry heating produced stronger deactivations compared to wet heating in the biological INP analogues, while overall being less likely to deactivate minerals. This could mean that dry heating has less potential to produce false-positive detection of biological INPs, so could be a more appropriate method for INP heat tests since wet heating is the method usually employed in these investigations. However, this may be precluded by the finding that most of our K-feldspar samples exhibited dry heat deactivations. Due to its practical simplicity and potential for high throughput of samples, heat treatments will likely continue to be the primary method used in future studies where biological INPs need to be differentiated from other types present in a collected sample. Interpretation of results may be aided by identification of the mineral phases present in a sample using techniques such as XRD or SEM. Overall, we have highlighted potential limitations where INP heat tests are applied and the need for deeper interpretation of results and have outlined possible improvements to INP heat

treatment methods. Further studies should focus on finding the optimum physical conditions that would result in the most selective deactivations of biological INPs.

#### **4.6 Appendix A: The effect of vessel type used for wet heating of silica INP suspensions.**

In our wet heating experiments, the mineral INP suspensions were heated while inside 20 mL borosilicate glass vials containing 10 mL of suspension. Kumar et al. (2019a) observed that ageing of quartz INP suspensions over several days occurred at room temperature in glass vials but not in polypropylene centrifuge tubes. For this they proposed an alternative explanation to the active sites on the quartz INP being irreversibly degraded by ageing in water, in which silicic acid leaches out from the glass vial walls and re-precipitates onto the active sites of the mineral, effectively blocking them. When polypropylene is the suspension container, however, the Si concentration remains too low for this to occur, so the INA does not reduce. Therefore, to rule out that quartz wet heat deactivations are only an artefact of heating in glass containers, we repeated our wet heat test for Fluka Quartz in an alternative glass vessel type (20 mL non-borosilicate vial with 10 mL of INP suspension) and plastic vessels (50 mL polypropylene centrifuge tube and 1.5 mL polypropylene microcentrifuge tube (Sarstedt Micro Tube 72.690) containing 10 mL and 1 mL of INP suspension, respectively) and compared the deactivations with those seen for our standard wet heat treatment in borosilicate glass. The results in  $f_{ice}(T)$  from are shown in Fig. 4.8.

Similar or larger wet heat deactivations occurred for the 1.5 mL microcentrifuge tube ( $\Delta T_{50}^{wet}$  of  $-6.0$  °C) and non-borosilicate glass vial ( $\Delta T_{50}^{wet}$  of  $-4.8$  °C) samples compared to that of borosilicate glass vial ( $\Delta T_{50}^{wet}$  of  $-4.1$  °C). With the 50 mL polypropylene tube sample, however, a smaller deactivation occurred:  $\Delta T_{50}^{wet}$  of  $-1.8$  °C. This may simply be because the suspension in the polypropylene tube did not reach as high a temperature as that inside the glass vials while immersed in the water bath, as demonstrated in Fig. 4.9 based on temperature measurements in both vessel types during the heat test procedure. This may have been due to the thicker wall and lower thermal conductivity of the polypropylene tube compared to the glass vials and microcentrifuge tube. Nevertheless, deactivation of quartz INP was still achieved when suspension were heated within plastic tubes, suggesting that aqueous silica leached from a glass container does not play a role in the deactivation of INA.

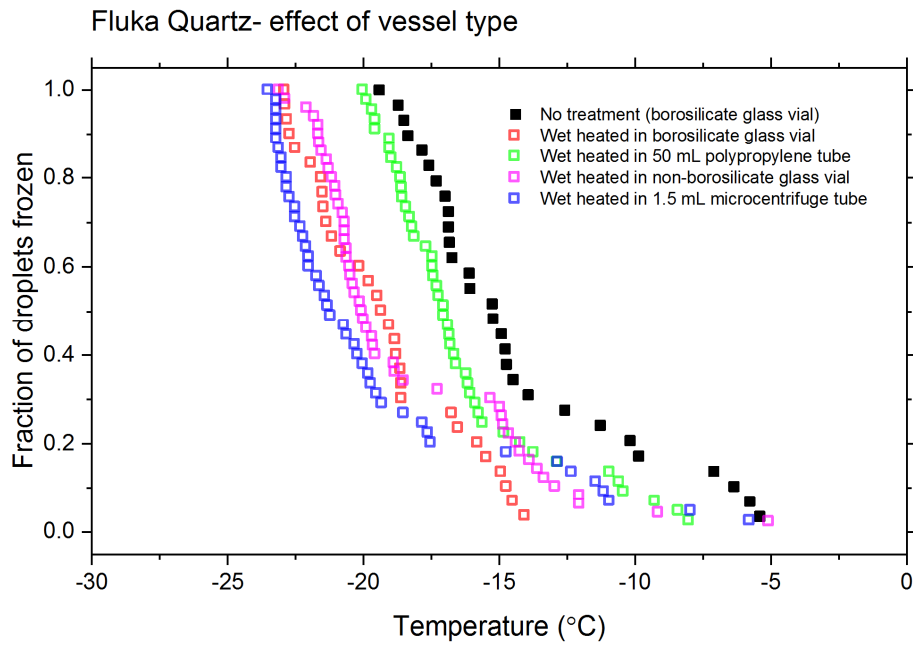


**Figure 4.8** Plot showing the fraction of droplets frozen ( $f_{ice}(T)$ ) for wet heated Fluka Quartz suspensions (all 1 % w/v) repeated using a range of different container types.

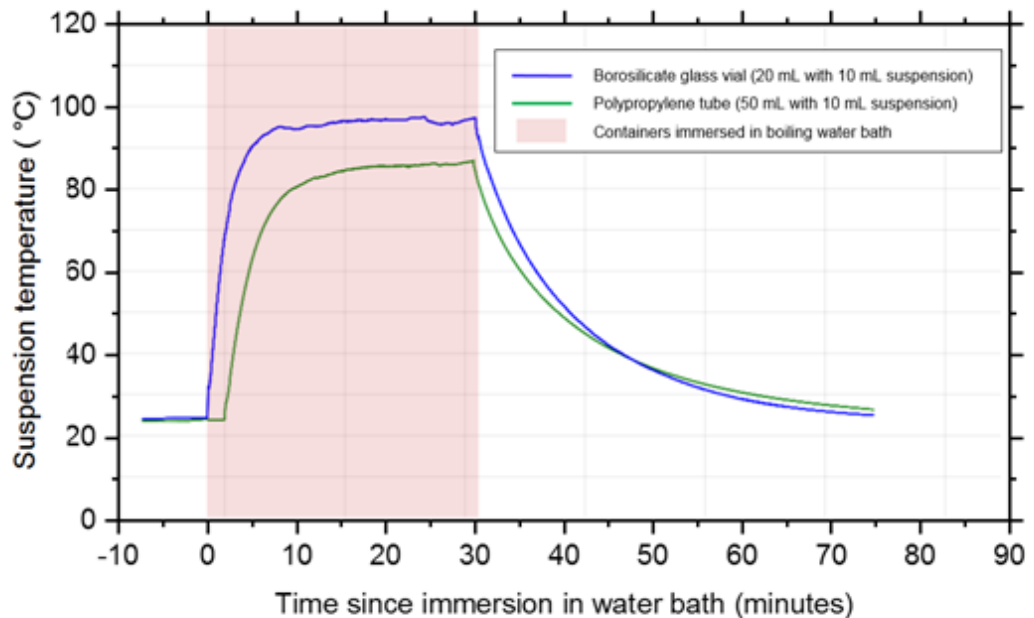


**Figure 4.9:** Thermocouple measurements of suspension temperature inside both glass and plastic vessels during the wet heat treatment procedure.

#### **4.7 Appendix B: Dependence of INA heat deactivations on temperature, duration and suspension concentration**

Several mineral samples' INA were significantly deactivated by heating in this study and we hypothesise that their ice-active sites are degraded by elevated temperature but also dependent on whether the mineral samples were heated while immersed in water or dry in air. Here we explore the dependence of additional variables on heat treatments using some of the mineral INP samples and the biogenic INP samples included in this study.

We used relatively concentrated suspensions of minerals and biogenic INP for the experiments shown in section 4.3 in order to ensure their droplet freezing temperatures were well above the instrumental background. However, there are potential mechanisms for the concentration of the suspension itself to affect the INA independently from the heat treatments. For example, species dissolved from the mineral powders may potentially interact with the nucleation to reduce the INA (Koop and Zobrist, 2009; Kumar et al., 2018a; Whale et al., 2018). Agglomeration of particles causing loss of INP surface area has been proposed to cause lower than expected INA with increasing INP concentrations (Emersic et al., 2015; Hiranuma et al., 2019). Also, more concentrated suspensions are more likely to contain rarer, warmer temperature IN sites which may be of different nature, and thus, different heat sensitivity to lower temperature IN sites. We therefore repeated both wet and dry heat tests for BCS-376 Microcline, Fluka Quartz, NX-Illite and ATD at both higher and lower concentrations than the standard 1% w/v reported in Section 4.3. This allowed us to ascertain if the observed heat deactivations are an artefact of the relatively concentrated suspensions that we used and are still pertinent to the lower particle concentrations involved with, for example, aerosol filter wash-offs. We also performed this with the biogenic samples for wet-heat tests only, since dry heat tests deactivated all these samples to background levels.

The resultant droplet freezing data is plotted in  $n_s(T)$  and  $n_m(T)$  form and shown in Figs. 4.10a-i. Plotting  $n_s(T)$  or  $n_m(T)$  data for the same INP sample repeated at multiple concentrations should result in a coherent 'curve' with data for lower concentrations reaching into higher values of  $n_s(T)$  (or  $n_m(T)$ ) and vice-versa. This is indeed the case

for all samples we tested whether they were sensitive to wet heat (e.g. Fluka Quartz, Lichen) or dry heat (e.g. BCS-376 microcline, NX Illite) (Fig 4.10). If, however, there was a concentration dependence on INP deactivations then the  $n_s(T)$  data for wet heated suspensions would be ‘staggered’ rather than coherent and would not be parallel with the unheated sample’s  $n_s(T)$  curve. In Fig. 4.10 we see that for all samples, for both wet and dry heating, the  $n_s(T)$  or  $n_m(T)$  curves are largely coherent and parallel with those for the unheated data showing that the rare, high temperature active sites are equally as heat sensitive as the more abundant low temperature sites.

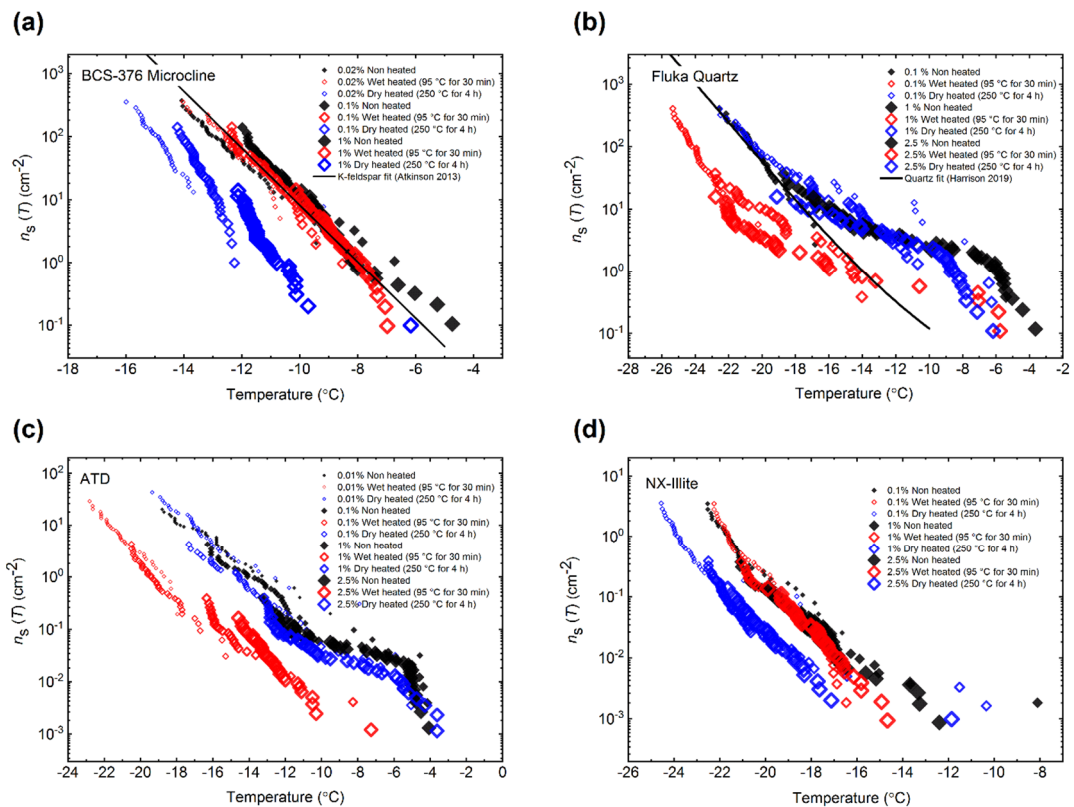


**Figure 4.10a-d: Plots of  $n_s(T)$  or  $n_m(T)$  illustrating heat test responses over an extended range of suspension concentrations for a) BCS-376 Microcline, b) Fluka Quartz, c) ATD, d) NX-Illite**

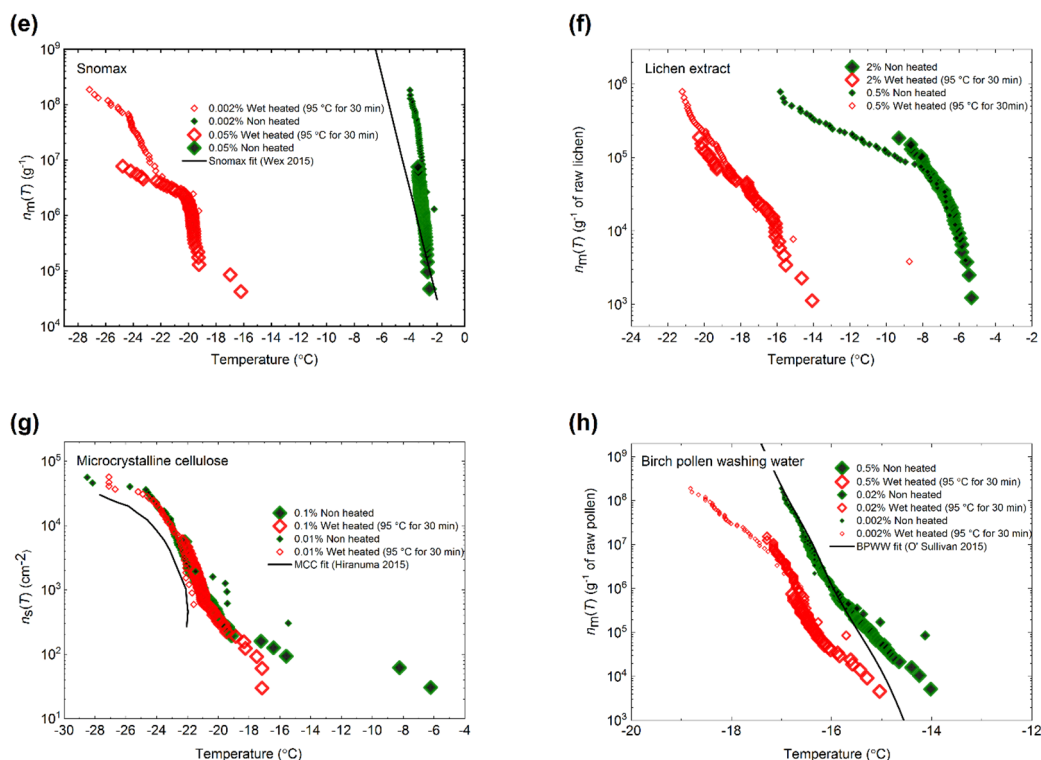


**Figure 4.10e-h: Plots of  $n_s(T)$  or  $n_m(T)$  illustrating heat test responses over an extended range of suspension concentrations for e) Snomax<sup>®</sup> f) Lichen extract g) MCC and h) Birch pollen washing water.**

In section 4.3 all samples were subject to ‘standard’ heat treatment conditions of 95  $^{\circ}C$  for 30 min for wet heating and 250  $^{\circ}C$  for 4 h for dry heating. We did this to empirically test these two distinct heat test procedures, but from a mechanistic perspective these experiments are not ideal since we are varying heating mode, temperature and duration. Hence, we performed a set of experiments with a subset of samples (BCS-376 Microcline, Snomax and Birch pollen washing water) as follows: Dry heat at 95  $^{\circ}C$  for 30 min, 95  $^{\circ}C$  for 4 h, 250  $^{\circ}C$  for 30 min and wet heat at 95  $^{\circ}C$  for 4 h. These results are shown in Fig. 4.11. Fluka Quartz is also included but without extra dry heat tests as it did not deactivate after dry heating at 250  $^{\circ}C$  for 4 hr so we assumed it would not deactivate if dry-heated at a lower temperature and/or for a shorter duration. Overall this allowed us to conclude that heating duration is a more important variable when wet heating than in dry heating where it appears secondary in importance to temperature. Also, Snomax, and to a lesser extent BCS-376 microcline, showed differences in their response to being heated wet and heated dry at the same duration and temperature.

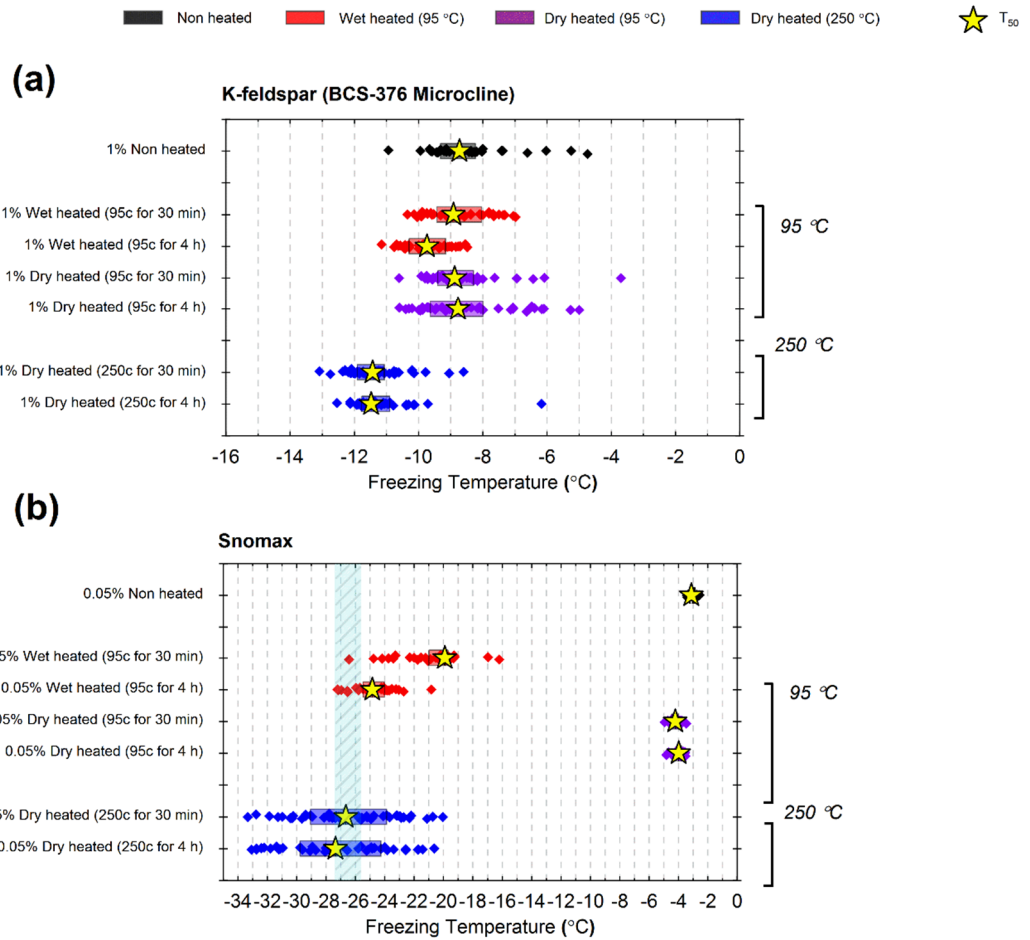


**Figure 4.11 a-b** Boxplots of freezing temperatures for droplet freezing assays of suspensions of a) BCS-376 Microcline (1 % w/v) and b) Snomax<sup>®</sup> (0.05 % w/v) before and after wet heating and dry heating at varying temperatures and durations.

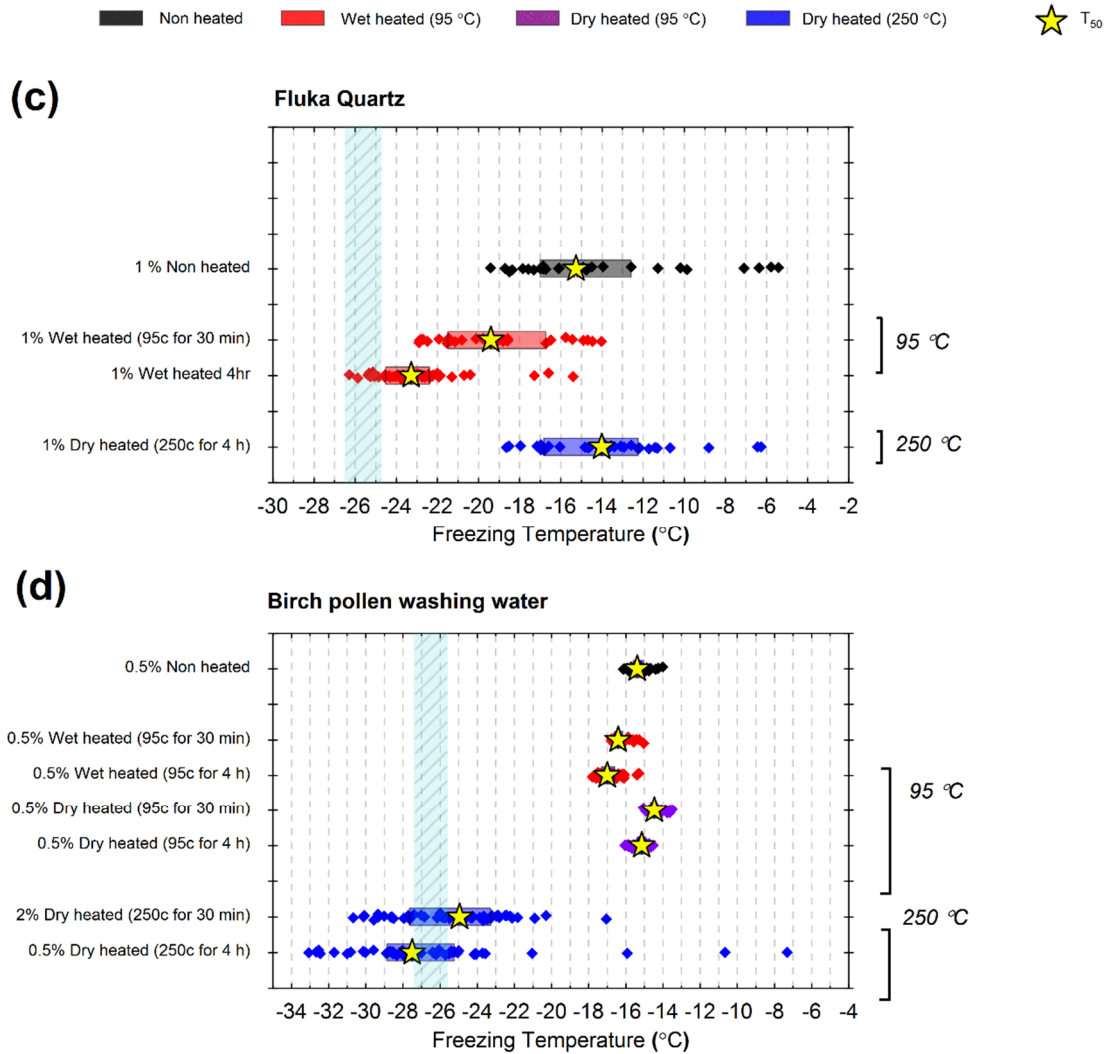


**Figure 4.11 c-d: Boxplots of freezing temperatures for droplet freezing assays of suspensions of c) Fluka Quartz (1 % w/v), and d) Birch pollen washing water (0.5 % w/v) before and after wet heating and dry heating at varying temperatures and durations.**

## 4.8 Supplementary Information

### 4.8.1 Background information on classes of mineral INPs

#### *K-feldspar*

Alkali feldspars rich in potassium (K-feldspars) are considered to be the most important single ice-nucleating mineral component in atmospheric mineral dust due to their exceptional ability to nucleate ice in both immersion (Atkinson et al., 2013; Zolles et al., 2015; Harrison et al., 2019) and deposition mode (Yakobi-Hancock et al., 2013) in combination with its ubiquitous atmospheric abundance (Arnold et al., 1998; Murray et al., 2012; Glaccum and Prospero, 1980; Kandler et al., 2009). As such, even in the presence of other minerals in higher proportions, the INA of a mineral dust will likely be controlled by the K-feldspar content (Harrison et al., 2016). Ice nucleation on mineral surfaces such as feldspars has been shown to occur at specific sites that become active at a specific temperature (Holden et al., 2019; Holden et al., 2021) and topographical features associated with exsolution microtexture (Whale et al., 2017; Kiselev et al., 2021) have been proposed as the locations of the highly active sites on K-feldspar. Moreover, Kiselev et al. (2017) observed that ice crystals growing from the vapour phase on the surface of microcline originated on steps and cracks and were preferentially orientated between the basal face of ice and the (100) cleavage plane. More recent work suggests that cracks caused by exsolution microtexture may expose the (100) face of feldspars (Kiselev et al., 2021). The chemical and physical nature of these sites is, however, still unclear.

#### *Plagioclase feldspar*

Plagioclase feldspars are the most abundant mineral in the Earth's crust and are defined as having feldspar compositions between that of the Na endmember albite ( $\text{NaAlSi}_3\text{O}_8$ ) and the Ca endmember anorthite ( $\text{CaAl}_2\text{Si}_2\text{O}_8$ ). Solid solutions between these two endmembers are more stable than in alkali feldspars, therefore plagioclase feldspars do not exhibit the 'perthitic' texture (exsolution microtexture) characteristic of K-feldspars. It has been suggested that the lack of these textures is the reason (Whale et al., 2017) that plagioclase feldspars are typically much less efficient INPs than K-feldspars (Harrison et al., 2016).

#### *Silica*

Quartz is the most common crustal mineral after the feldspars and is also highly chemically and physically resistant to weathering. It is often a major component of soils and sediments and is the most abundant non-phyllosilicate mineral component of atmospheric mineral dust (Arnold et al., 1998; Murray et al., 2012; Glaccum and Prospero, 1980; Kandler et al., 2009). Quartz is the crystalline form of silica ( $\text{SiO}_2$ ) and occurs in nature as several different polymorphs. However,  $\alpha$ -quartz is by far the most abundant polymorph and as such is usually referred to as 'quartz'. Previous laboratory studies have indicated that quartz particles have an atmospheric importance as INPs superior to that of clays but lower than alkali and plagioclase feldspars (Atkinson et al., 2013; Harrison et al., 2019), although there is variability in INA seen between different studies (Kumar et al., 2019a). Re-milling quartz powders has been seen to enhance their INA more than what may be expected based on the increase in surface area (Zolles et al., 2015), suggesting that the process creates active sites rather than simply exposing them. This has led to uncertainty as to whether the documented INA of quartz is representative of that found in the environment or whether it is simply an artefact of the laboratory milling process. The active sites of quartz are proposed to arise from fracturing that produce patches of 'dangling' Si- and Si-O sites on the mineral surface that can readily hydroxylate and order water molecules. Another characteristic of quartz is that it can lose its INA while immersed in room temperature water over a few days (Kumar et al., 2019a; Harrison et al., 2019).

#### *Clay-based minerals*

Clay minerals are present in abundance in soils, sedimentary and some metamorphic rocks, as well as in airborne samples of mineral dust. Clays fall into the phyllosilicate group of minerals, with its principal subgroups comprising kaolin (which includes kaolinite), smectite (which includes montmorillonite), illite and chlorite. They are secondary minerals, meaning that they are weathering products of igneous and metamorphic minerals and, as such, samples often contain relic traces of their parent minerals (for example K-feldspar in the case of kaolinite or illite) and also of quartz as a weathering reaction product. Clays were previously considered (Hoose and Möhler, 2012) to be the most important mineral ice-nucleating component of atmospheric mineral owing to early experimental work (Mason and Maybank, 1958) until the greater importance of feldspars was established (Atkinson et al., 2013). They are, however, still overall the most abundant type of mineral found in atmospheric

mineral dust, their concentration tending to increase proportionally in transported dusts owing to their smaller particle size (Murray et al., 2012). Therefore, clay minerals may be more likely to control the INA of desert dusts sampled far from their source and of the finer particle fraction.

#### *Mineral dust analogues*

Mineral dust analogue samples NX Illite and Arizona Test Dust (ATD) are two commercially available mineral dust mixtures that have been used as atmospheric mineral dust analogues in laboratory investigations into the properties of INPs (Marcolli et al., 2007; Broadley et al., 2012; Niemand et al., 2012; Hiranuma et al., 2015a). ATD contains a much higher proportion (~50 %) of quartz and feldspars than NX Illite (~20 %), with the remainder of both comprising clay minerals and a small amount of carbonate. It has been suggested that the INA of ATD may be artificially enhanced by the milling process used in its production (Perkins et al., 2020). Both mineral dust samples contain a higher proportion of K-feldspar than quartz (Broadley et al., 2012; Hiranuma et al., 2015a) meaning that K-feldspar should be the main contributor to the INA of both samples. This is consistent with the relatively high INA of ATD, in which the dominant polymorph of K-feldspar is microcline (Kaufmann et al., 2016). However, NX Illite is less active than would be expected given its K-feldspar content, which may be due to weathering or that the K-feldspar may have an INA at the lower end of the K-feldspar INA range (Harrison et al., 2016).

#### *Calcite*

Calcite ( $\text{CaCO}_3$ ), along with other carbonates such as gypsum and dolomite, has been found to be an ineffective mineral INP (Atkinson et al., 2013; Zolles et al., 2015; Kaufmann et al., 2016), however it can often be the dominant component of some surface dust sources, especially the deserts of north-western Africa (Knippertz and Stuut, 2014).

#### 4.8.2 Mass changes of samples after dry heating

**Table 4.5: Mass changes of samples after dry heat treatment (250 °C for 4 h)**

Sample name	Classification	% Change in mass after dry heating (250°C for 4 h)
Empty 15ml borosilicate glass vial (mean of 5)	-	-0.02 (mean) 0.10 (standard deviation)
BCS-376 Microcline (mean of 5)	K-feldspar	-0.25 (mean) 0.44 (standard deviation)
TUD#3 Microcline	K-feldspar	-2.53
Amazonite Microcline	K-feldspar	-0.68
Pakistan Orthoclase	K-feldspar	-0.96
TUD#2 Albite	Plagioclase feldspar	-1.39
BCS-375 Albite	Plagioclase feldspar	-2.32
Atkinson Quartz	Quartz	
Fluka Quartz (average of 5)	Quartz	-0.27 (mean) 0.52
Fused Quartz	Quartz	-1.72
Bombay Chalcedony	Quartz	-0.59
KGa-1b Kaolinite	Clay based	-1.01
Fluka Kaolinite	Clay based	-0.78
Sigma Montmorillonite	Clay based	-10.01
SWy-2 Montmorillonite	Clay based	-8.44
Chlorite	Clay based	
Arizona Test Dust (ATD)	Dust surrogate	-1.57
NX Illite	Dust surrogate	-3.47
Calcite	Carbonate	-3.40
Snomax (pellets)	Biological proteinaceous	-37.4
Lichen (raw)	Biological proteinaceous	-58.8
Birch Pollen (raw)	Biological non-proteinaceous	-56.3
Microcrystalline cellulose	Biological non-proteinaceous	-52.6

## 4.8.3 Supplementary figures

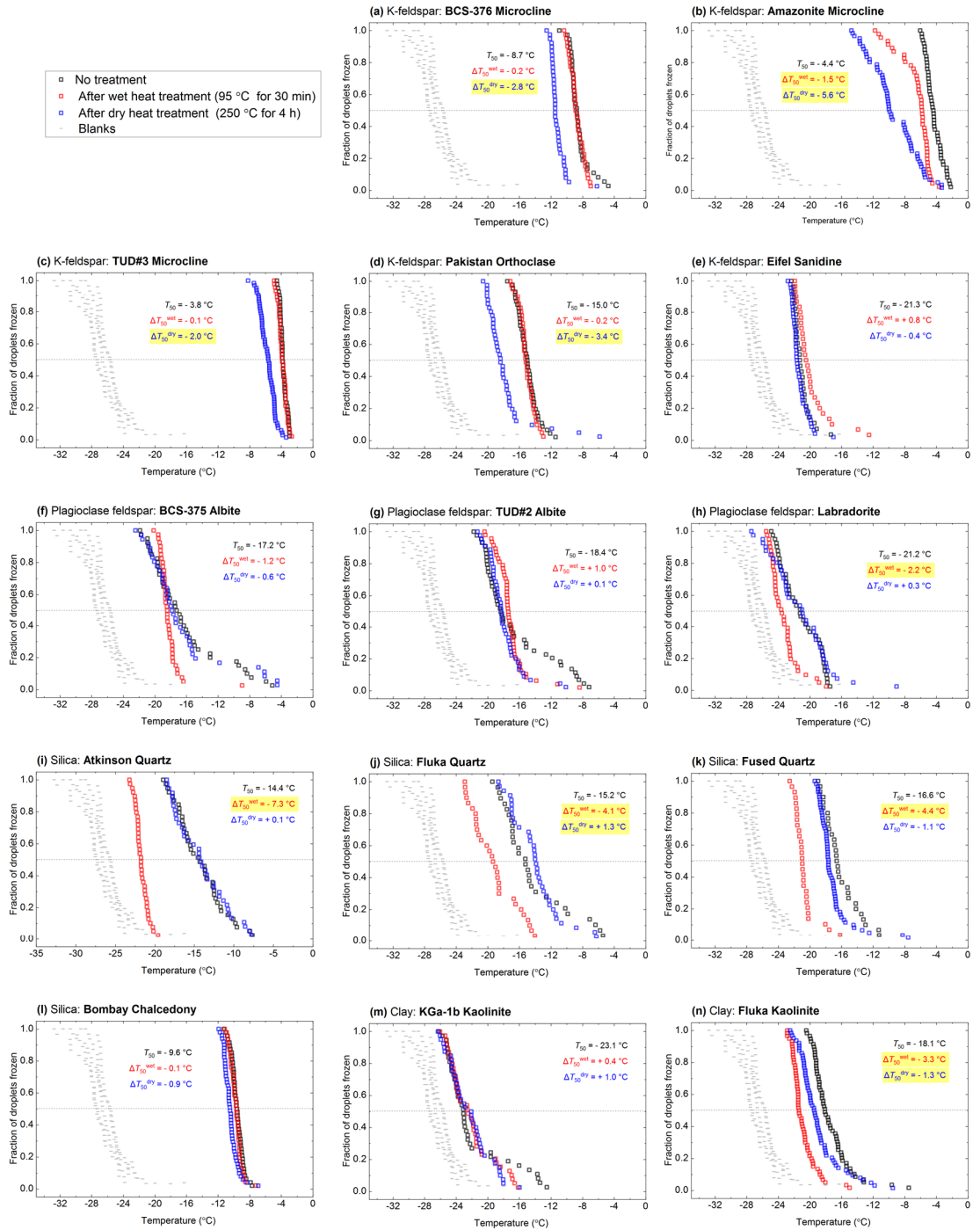
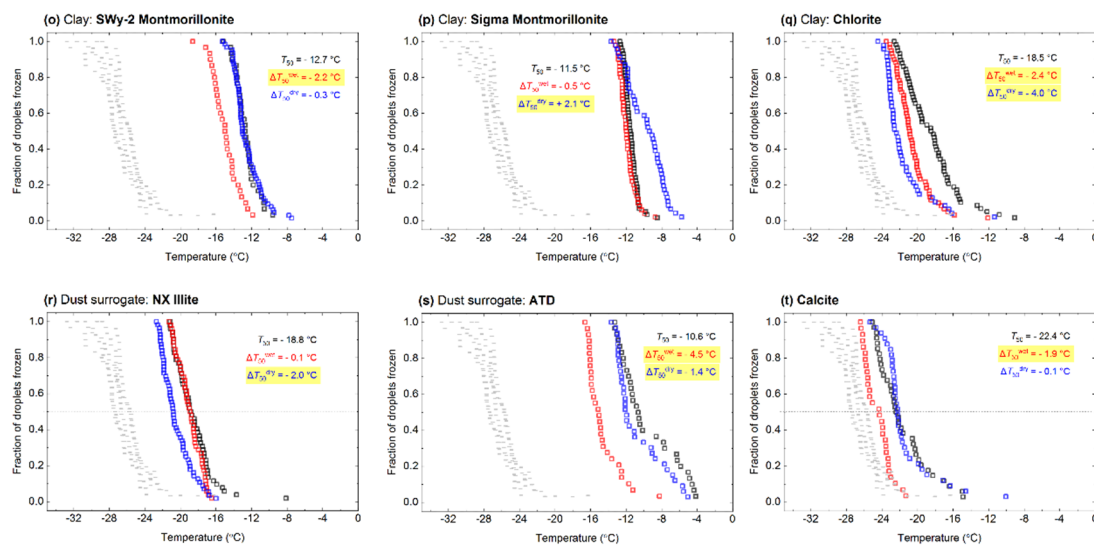
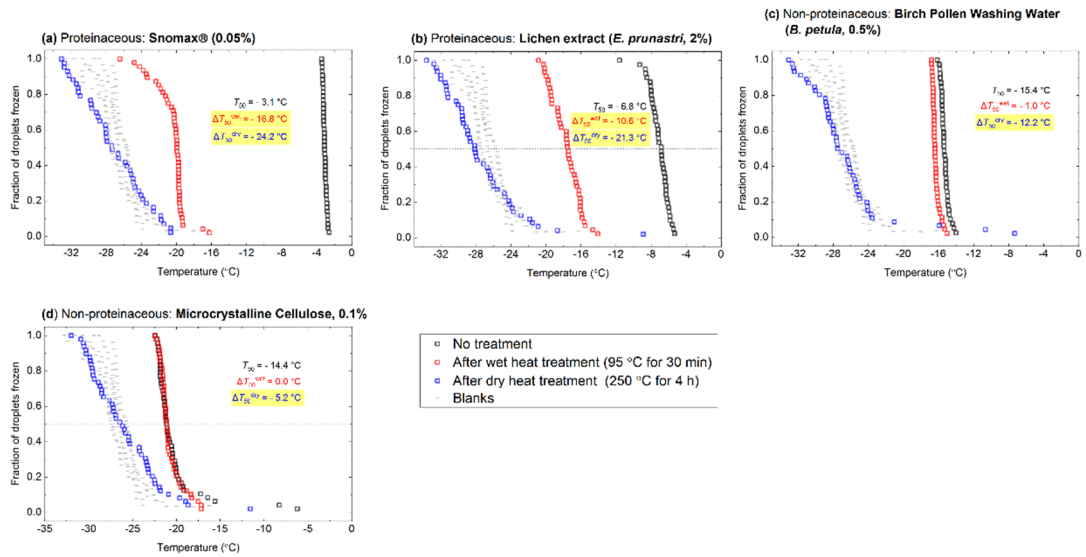


Figure continued overleaf...



**Figure 4.12: Fraction of droplets frozen ( $f_{ice}(T)$ ) curves for all mineral-based INP samples. Data for four background runs are shown in each plot. A dotted horizontal line denotes  $f_{ice}(T) = 0.5$ , from which  $T_{50}$  values were determined. All suspensions were prepared to a concentration of 1 % w/v. Denoted in each panel are  $T_{50}$ ,  $\Delta T$  wet and  $\Delta T_{50}$  dry values for the sample, with significant ( $\Delta T_{50}$  greater than  $\pm 1.2^\circ\text{C}$ ) values highlighted in yellow.**



**Figure 4.13** Fraction of droplets frozen ( $f_{\text{ice}}(T)$ ) curves for all biological analogue INP samples. Data for four background runs are shown in each plot. A dotted horizontal line denotes  $f_{\text{ice}}(T) = 0.5$ , from which  $T_{50}$  values were determined. All suspensions were prepared to a concentration of 1 % w/v. Denoted in each panel are  $T_{50}$ ,  $\Delta T$  wet and  $\Delta T_{50}$  dry values for the sample, with significant ( $\Delta T_{50}$  greater than  $\pm 1.2\text{ }^{\circ}\text{C}$ ) values highlighted in yellow.

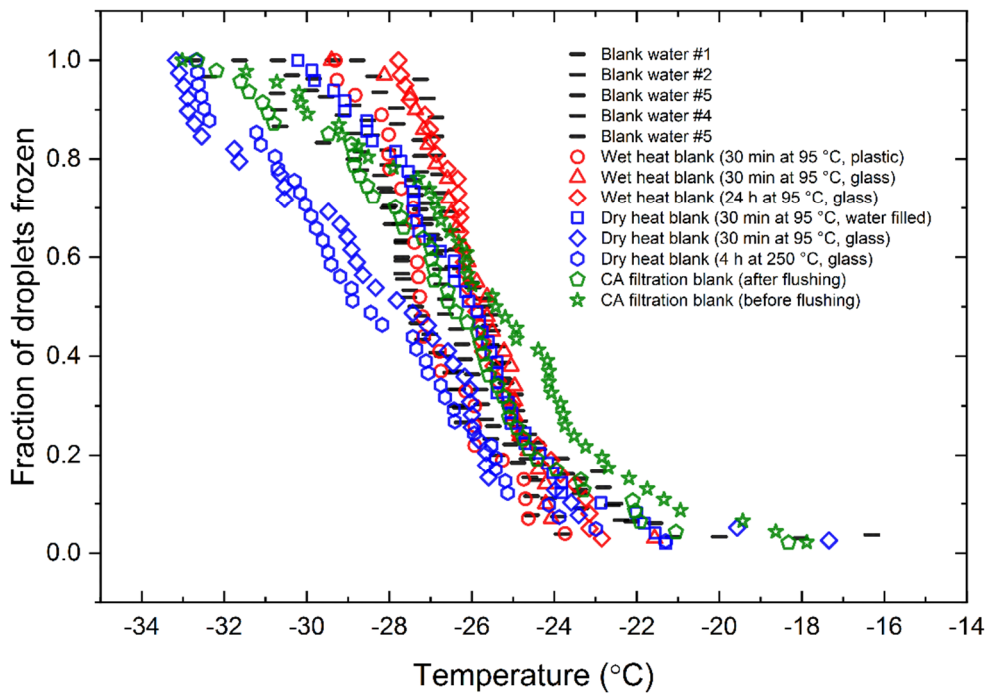


**Figure 4.14** Plot showing  $f_{ice}(T)$  data for background water in borosilicate glass vials (Blanks #1 to #5) and handling blanks for various modes of wet and dry heat tests in borosilicate and polypropylene containers. ‘CA’ denotes the use of a 0.2  $\mu\text{m}$  cellulose acetate filter used for filtration of raw lichen and birch pollen.

## References

- Ansmann, A., Tesche, M., Althausen, D., Müller, D., Seifert, P., Freudenthaler, V., Heese, B., Wiegner, M., Pisani, G., Knippertz, P., and Dubovik, O.: Influence of Saharan dust on cloud glaciation in southern Morocco during the Saharan Mineral Dust Experiment, *J. Geophys. Res.-Atmos.*, 113, <https://doi.org/10.1029/2007JD008785>, 2008.
- Arnold, E., Merrill, J., Leinen, M., and King, J.: The effect of source area and atmospheric transport on mineral aerosol collected over the North Pacific Ocean, *Global. Planet. Change.*, 18, 137-159, [https://doi.org/10.1016/S0921-8181\(98\)00013-7](https://doi.org/10.1016/S0921-8181(98)00013-7), 1998.
- Atkinson, J. D., Murray, B. J., Woodhouse, M. T., Whale, T. F., Baustian, K. J., Carslaw, K. S., Dobbie, S., O'Sullivan, D., and Malkin, T. L.: The importance of feldspar for ice nucleation by mineral dust in mixed-phase clouds, *Nature*, 498, 355-358, [10.1038/nature12278](https://doi.org/10.1038/nature12278), 2013.

- Augustin-Bauditz, S., Wex, H., Kanter, S., Ebert, M., Niedermeier, D., Stolz, F., Prager, A., and Stratmann, F.: The immersion mode ice nucleation behavior of mineral dusts: A comparison of different pure and surface modified dusts, *Geophys. Res. Lett.*, 41, 7375-7382, <https://doi.org/10.1002/2014GL061317>, 2014.
- Augustin, S., Wex, H., Niedermeier, D., Pummer, B., Grothe, H., Hartmann, S., Tomsche, L., Clauss, T., Voigtländer, J., Ignatius, K., and Stratmann, F.: Immersion freezing of birch pollen washing water, *Atmos. Chem. Phys.*, 13, 10989-11003, 10.5194/acp-13-10989-2013, 2013.
- Baloh, P., Els, N., David, R. O., Larose, C., Whitmore, K., Sattler, B., and Grothe, H.: Assessment of Artificial and Natural Transport Mechanisms of Ice Nucleating Particles in an Alpine Ski Resort in Obergurgl, Austria, *Frontiers in Microbiology*, 10, 2278, 2019.
- Bedjanian, Y., Romanias, M. N., and El Zein, A.: Uptake of HO<sub>2</sub> radicals on Arizona Test Dust, *Atmos. Chem. Phys.*, 13, 6461-6471, 10.5194/acp-13-6461-2013, 2013.
- Bogler, S., and Borduas-Dedekind, N.: Lignin's ability to nucleate ice via immersion freezing and its stability towards physicochemical treatments and atmospheric processing, *Atmos. Chem. Phys.*, 20, 14509-14522, 10.5194/acp-20-14509-2020, 2020.
- Boose, Y., Baloh, P., Plötze, M., Ofner, J., Grothe, H., Sierau, B., Lohmann, U., and Kanji, Z. A.: Heterogeneous ice nucleation on dust particles sourced from nine deserts worldwide – Part 2: Deposition nucleation and condensation freezing, *Atmos. Chem. Phys.*, 19, 1059-1076, 10.5194/acp-19-1059-2019, 2019.
- Broadley, S. L., Murray, B. J., Herbert, R. J., Atkinson, J. D., Dobbie, S., Malkin, T. L., Condliffe, E., and Neve, L.: Immersion mode heterogeneous ice nucleation by an illite rich powder representative of atmospheric mineral dust, *Atmos. Chem. Phys.*, 12, 287-307, 10.5194/acp-12-287-2012, 2012.
- Chardon, E. S., Livens, F. R., and Vaughan, D. J.: Reactions of feldspar surfaces with aqueous solutions, *Earth-Sci. Rev.*, 78, 1-26, <https://doi.org/10.1016/j.earscirev.2006.03.002>, 2006.
- China, S., Alpert, P. A., Zhang, B., Schum, S., Dzepina, K., Wright, K., Owen, R. C., Fialho, P., Mazzoleni, L. R., Mazzoleni, C., and Knopf, D. A.: Ice cloud formation potential by free tropospheric particles from long-range transport over the Northern Atlantic Ocean, *Journal of Geophysical Research: Atmospheres*, 122, 3065-3079, 2017.
- Christner, B. C., Cai, R., Morris, C. E., McCarter, K. S., Foreman, C. M., Skidmore, M. L., Montross, S. N., and Sands, D. C.: Geographic, seasonal, and precipitation chemistry influence on the abundance and activity of biological ice nucleators in rain and snow, *Proc Natl Acad Sci U S A*, 105, 18854-18859, 2008a.
- Christner, B. C., Morris, C. E., Foreman, C. M., Cai, R., and Sands, D. C.: Ubiquity of Biological Ice Nucleators in Snowfall, *Science*, 319, 1214, 10.1126/science.1149757, 2008b.
- Christner, B. C., Cai, R., Morris, C. E., McCarter, K. S., Foreman, C. M., Skidmore, M. L., Montross, S. N., and Sands, D. C.: Geographic, seasonal, and precipitation

chemistry influence on the abundance and activity of biological ice nucleators in rain and snow, *Proc Natl Acad Sci U S A*, 105, 18854-18859, 2008a.

Conen, F., Morris, C. E., Leifeld, J., Yakutin, M. V., and Alewell, C.: Biological residues define the ice nucleation properties of soil dust, *Atmos. Chem. Phys.*, 11, 9643-9648, 10.5194/acp-11-9643-2011, 2011.

Conen, F., Rodríguez, S., Hülin, C., Henne, S., Herrmann, E., Bukowiecki, N., and Alewell, C.: Atmospheric ice nuclei at the high-altitude observatory Jungfraujoch, Switzerland, *Tellus. B.*, 67, 25014, 10.3402/tellusb.v67.25014, 2015.

Conen, F., Eckhardt, S., Gundersen, H., Stohl, A., and Yttri, K. E.: Rainfall drives atmospheric ice-nucleating particles in the coastal climate of southern Norway, *Atmos. Chem. Phys.*, 17, 11065-11073, 10.5194/acp-17-11065-2017, 2017.

Conen, F., and Yakutin, M. V.: Soils rich in biological ice-nucleating particles abound in ice-nucleating macromolecules likely produced by fungi, *Biogeosciences*, 15, 4381-4385, 10.5194/bg-15-4381-2018, 2018.

Creamean, J. M., Suski, K. J., Rosenfeld, D., Cazorla, A., DeMott, P. J., Sullivan, R. C., White, A. B., Ralph, F. M., Minnis, P., Comstock, J. M., Tomlinson, J. M., and Prather, K. A.: Dust and Biological Aerosols from the Sahara and Asia Influence Precipitation in the Western U.S, *Science*, 339, 1572, 10.1126/science.1227279, 2013.

Creamean, J. M., Cross, J. N., Pickart, R., McRaven, L., Lin, P., Pacini, A., Hanlon, R., Schmale, D. G., Cenicerros, J., Aydell, T., Colombi, N., Bolger, E., and DeMott, P. J.: Ice Nucleating Particles Carried From Below a Phytoplankton Bloom to the Arctic Atmosphere, *Geophys. Res. Lett.*, 46, 8572-8581, <https://doi.org/10.1029/2019GL083039>, 2019.

Creamean, J. M., Hill, T. C. J., DeMott, P. J., Uetake, J., Kreidenweis, S., and Douglas, T. A.: Thawing permafrost: an overlooked source of seeds for Arctic cloud formation, *Env. Res. Lett.*, 15, 084022, 10.1088/1748-9326/ab87d3, 2020.

Daily, M. I., Whale, T. F., Partanen, R., Harrison, A. D., Kilbride, P., Lamb, S., Morris, G. J., Picton, H. M., and Murray, B. J.: Cryopreservation of primary cultures of mammalian somatic cells in 96-well plates benefits from control of ice nucleation, *Cryobiology*, 93, 62-69, <https://doi.org/10.1016/j.cryobiol.2020.02.008>, 2020.

D'Souza, N. A., Kawarasaki, Y., Gantz, J. D., Lee, R. E., Beall, B. F. N., Shtarkman, Y. M., Koçer, Z. A., Rogers, S. O., Wildschutte, H., Bullerjahn, G. S., and McKay, R. M. L.: Diatom assemblages promote ice formation in large lakes, *ISME. J.*, 7, 1632-1640, 2013.

DeMott, P. J., Sassen, K., Poellot, M. R., Baumgardner, D., Rogers, D. C., Brooks, S. D., Prenni, A. J., and Kreidenweis, S. M.: African dust aerosols as atmospheric ice nuclei, *Geophys. Res. Lett.*, 30, <https://doi.org/10.1029/2003GL017410>, 2003.

DeMott, P. J., Möhler, O., Cziczo, D. J., Hiranuma, N., Petters, M. D., Petters, S. S., Belosi, F., Bingemer, H. G., Brooks, S. D., Budke, C., Burkert-Kohn, M., Collier, K. N., Danielczok, A., Eppers, O., Felgitsch, L., Garimella, S., Grothe, H., Herenz, P., Hill, T. C. J., Höhler, K., Kanji, Z. A., Kiselev, A., Koop, T., Kristensen, T. B., Krüger, K., Kulkarni, G., Levin, E. J. T., Murray, B. J., Nicosia, A., O'Sullivan, D., Peckhaus, A., Polen, M. J., Price, H. C., Reicher, N., Rothenberg, D. A., Rudich, Y.,

Santachiara, G., Schiebel, T., Schrod, J., Seifried, T. M., Stratmann, F., Sullivan, R. C., Suski, K. J., Szakáll, M., Taylor, H. P., Ullrich, R., Vergara-Temprado, J., Wagner, R., Whale, T. F., Weber, D., Welti, A., Wilson, T. W., Wolf, M. J., and Zenker, J.: The Fifth International Workshop on Ice Nucleation phase 2 (FIN-02): laboratory intercomparison of ice nucleation measurements, *Atmos. Meas. Tech.*, 11, 6231-6257, 10.5194/amt-11-6231-2018, 2018.

Dreischmeier, K., Budke, C., Wiehemeier, L., Kottke, T., and Koop, T.: Boreal pollen contain ice-nucleating as well as ice-binding 'antifreeze' polysaccharides, *Sci Rep*, 7, 41890, 10.1038/srep41890, 2017.

Field, P. R., Lawson, R. P., Brown, P. R. A., Lloyd, G., Westbrook, C., Moisseev, D., Miltenberger, A., Nenes, A., Blyth, A., Choulaton, T., Connolly, P., Buehl, J., Crosier, J., Cui, Z., Dearden, C., DeMott, P., Flossmann, A., Heymsfield, A., Huang, Y., Kalesse, H., Kanji, Z. A., Korolev, A., Kirchgaessner, A., Lasher-Trapp, S., Leisner, T., McFarquhar, G., Phillips, V., Stith, J., and Sullivan, S.: Secondary Ice Production: Current State of the Science

Du, R., Du, P., Lu, Z., Ren, W., Liang, Z., Qin, S., Li, Z., Wang, Y., and Fu, P.: Evidence for a missing source of efficient ice nuclei, *Sci Rep*, 7, 39673, 2017.

Fröhlich-Nowoisky, J., Hill, T. C. J., Pummer, B. G., Yordanova, P., Franc, G. D., and Pöschl, U.: Ice nucleation activity in the widespread soil fungus *Mortierella alpina*, *Biogeosciences*, 12, 1057-1071, 10.5194/bg-12-1057-2015, 2015.

Garcia, E., Hill, T. C. J., Prenni, A. J., DeMott, P. J., Franc, G. D., and Kreidenweis, S. M.: Biogenic ice nuclei in boundary layer air over two U.S. High Plains agricultural regions, *J. Geophys. Res.-Atmos.*, 117, n/a-n/a, 10.1029/2012jd018343, 2012.

Glaccum, R. A., and Prospero, J. M.: Saharan aerosols over the tropical North Atlantic — Mineralogy, *Mar. Geol.*, 37, 295-321, [https://doi.org/10.1016/0025-3227\(80\)90107-3](https://doi.org/10.1016/0025-3227(80)90107-3), 1980.

Gong, X., Wex, H., van Pinxteren, M., Triesch, N., Fomba, K. W., Lubitz, J., Stolle, C., Robinson, T. B., Müller, T., Herrmann, H., and Stratmann, F.: Characterization of aerosol particles at Cabo Verde close to sea level and at the cloud level – Part 2: Ice-nucleating particles in air, cloud and seawater, *Atmos. Chem. Phys.*, 20, 1451-1468, 2020.

Grawe, S., Augustin-Bauditz, S., Clemen, H. C., Ebert, M., Eriksen Hammer, S., Lubitz, J., Reicher, N., Rudich, Y., Schneider, J., Staacke, R., Stratmann, F., Welti, A., and Wex, H.: Coal fly ash: linking immersion freezing behavior and physicochemical particle properties, *Atmos. Chem. Phys.*, 18, 13903-13923, 10.5194/acp-18-13903-2018, 2018.

Hara, K., Maki, T., Kakikawa, M., Kobayashi, F., and Matsuki, A.: Effects of different temperature treatments on biological ice nuclei in snow samples, *Atmos. Env.*, 140, 415-419, 2016a.

Hara, K., Maki, T., Kobayashi, F., Kakikawa, M., Wada, M., and Matsuki, A.: Variations of ice nuclei concentration induced by rain and snowfall within a local forested site in Japan, *Atmos. Env.*, 127, 1-5, 2016b.

Harrison, A. D., Whale, T. F., Carpenter, M. A., Holden, M. A., Neve, L., and Murray, B. J.: Not all feldspars are equal: a survey of ice nucleating properties across the feldspar group of minerals, *Atmos. Chem. Phys.*, 16, 10927-10940, 10.5194/acp-16-10927-2016, 2016.

Harrison, A. D., Lever, K., Sanchez-Marroquin, A., Holden, M. A., Whale, T. F., Tarn, M. D., McQuaid, J. B., and Murray, B. J.: The ice-nucleating ability of quartz immersed in water and its atmospheric importance compared to K-feldspar, *Atmos. Chem. Phys.*, 19, 11343-11361, 10.5194/acp-19-11343-2019, 2019.

Hartmann, M., Adachi, K., Eppers, O., Haas, C., Herber, A., Holzinger, R., Hünnerbein, A., Jäkel, E., Jentsch, C., van Pinxteren, M., Wex, H., Willmes, S., and Stratmann, F.: Wintertime Airborne Measurements of Ice Nucleating Particles in the High Arctic: A Hint to a Marine, Biogenic Source for Ice Nucleating Particles, *Geophys. Res. Lett.*, 47, e2020GL087770, <https://doi.org/10.1029/2020GL087770>, 2020.

Hawker, R. E., Miltenberger, A. K., Wilkinson, J. M., Hill, A. A., Shipway, B. J., Cui, Z., Cotton, R. J., Carslaw, K. S., Field, P. R., and Murray, B. J.: The temperature dependence of ice-nucleating particle concentrations affects the radiative properties of tropical convective cloud systems, *Atmos. Chem. Phys.*, 21, 5439-5461, 10.5194/acp-21-5439-2021, 2021.

Henderson-Begg, S. K., Hill, T., Thyrhaug, R., Khan, M., and Moffett, B. F.: Terrestrial and airborne non-bacterial ice nuclei, *Atmos. Sci. Lett.*, 10, 215-219, <https://doi.org/10.1002/asl.241>, 2009.

Herbert, R. J., Murray, B. J., Whale, T. F., Dobbie, S. J., and Atkinson, J. D.: Representing time-dependent freezing behaviour in immersion mode ice nucleation, *Atmos. Chem. Phys.*, 14, 8501-8520, 10.5194/acp-14-8501-2014, 2014.

Herbert, R. J., Murray, B. J., Dobbie, S. J., and Koop, T.: Sensitivity of liquid clouds to homogenous freezing parameterizations, *Geophys. Res. Lett.*, 42, 1599-1605, <https://doi.org/10.1002/2014GL062729>, 2015.

Hill, T. C. J., Moffett, B. F., Demott, P. J., Georgakopoulos, D. G., Stump, W. L., and Franc, G. D.: Measurement of ice nucleation-active bacteria on plants and in precipitation by quantitative PCR, *Appl Environ Microbiol*, 80, 1256-1267, 10.1128/AEM.02967-13, 2014.

Hill, T. C. J., DeMott, P. J., Tobo, Y., Fröhlich-Nowoisky, J., Moffett, B. F., Franc, G. D., and Kreidenweis, S. M.: Sources of organic ice nucleating particles in soils, *Atmos. Chem. Phys.*, 16, 7195-7211, 10.5194/acp-16-7195-2016, 2016.

Hiranuma, N., Hoffmann, N., Kiselev, A., Dreyer, A., Zhang, K., Kulkarni, G., Koop, T., and Möhler, O.: Influence of surface morphology on the immersion mode ice nucleation efficiency of hematite particles, *Atmos. Chem. Phys.*, 14, 2315-2324, 10.5194/acp-14-2315-2014, 2014.

Hiranuma, N., Augustin-Bauditz, S., Bingemer, H., Budke, C., Curtius, J., Danielczok, A., Diehl, K., Dreischmeier, K., Ebert, M., Frank, F., Hoffmann, N., Kandler, K., Kiselev, A., Koop, T., Leisner, T., Möhler, O., Nillius, B., Peckhaus, A., Rose, D., Weinbruch, S., Wex, H., Boose, Y., DeMott, P. J., Hader, J. D., Hill, T. C. J., Kanji, Z. A., Kulkarni, G., Levin, E. J. T., McCluskey, C. S., Murakami, M.,

- Murray, B. J., Niedermeier, D., Petters, M. D., O'Sullivan, D., Saito, A., Schill, G. P., Tajiri, T., Tolbert, M. A., Welti, A., Whale, T. F., Wright, T. P., and Yamashita, K.: A comprehensive laboratory study on the immersion freezing behavior of illite NX particles: a comparison of 17 ice nucleation measurement techniques, *Atmos. Chem. Phys.*, 15, 2489-2518, 10.5194/acp-15-2489-2015, 2015a.
- Hiranuma, N., Möhler, O., Yamashita, K., Tajiri, T., Saito, A., Kiselev, A., Hoffmann, N., Hoose, C., Jantsch, E., Koop, T., and Murakami, M.: Ice nucleation by cellulose and its potential contribution to ice formation in clouds, *Nat. Geosci.*, 8, 273-277, 10.1038/ngeo2374, 2015b.
- Hiranuma, N., Adachi, K., Bell, D. M., Belosi, F., Beydoun, H., Bhaduri, B., Bingemer, H., Budke, C., Clemen, H. C., Conen, F., Cory, K. M., Curtius, J., DeMott, P. J., Eppers, O., Grawe, S., Hartmann, S., Hoffmann, N., Höhler, K., Jantsch, E., Kiselev, A., Koop, T., Kulkarni, G., Mayer, A., Murakami, M., Murray, B. J., Nicosia, A., Petters, M. D., Piazza, M., Polen, M., Reicher, N., Rudich, Y., Saito, A., Santachiara, G., Schiebel, T., Schill, G. P., Schneider, J., Segev, L., Stopelli, E., Sullivan, R. C., Suski, K., Szakáll, M., Tajiri, T., Taylor, H., Tobo, Y., Ullrich, R., Weber, D., Wex, H., Whale, T. F., Whiteside, C. L., Yamashita, K., Zelenyuk, A., and Möhler, O.: A comprehensive characterization of ice nucleation by three different types of cellulose particles immersed in water, *Atmos. Chem. Phys.*, 19, 4823-4849, 10.5194/acp-19-4823-2019, 2019.
- Hiranuma, N., Auvermann, B. W., Belosi, F., Bush, J., Cory, K. M., Georgakopoulos, D. G., Höhler, K., Hou, Y., Lacher, L., Saathoff, H., Santachiara, G., Shen, X., Steinke, I., Ullrich, R., Umo, N. S., Vepuri, H. S. K., Vogel, F., and Möhler, O.: Laboratory and field studies of ice-nucleating particles from open-lot livestock facilities in Texas, *Atmos. Chem. Phys.*, 21, 14215-14234, 2021.
- Hofmeister, A. M., and Rossman, G. R.: A model for the irradiative coloration of smoky feldspar and the inhibiting influence of water, *Phys. Chem. Miner.*, 12, 324-332, 10.1007/BF00654342, 1985.
- Holden, M. A., Whale, T. F., Tarn, M. D., O'Sullivan, D., Walshaw, R. D., Murray, B. J., Meldrum, F. C., and Christenson, H. K.: High-speed imaging of ice nucleation in water proves the existence of active sites, *Sci Adv*, 5, eaav4316, 10.1126/sciadv.aav4316, 2019.
- Holden, M. A., Campbell, J. M., Meldrum, F. C., Murray, B. J., and Christenson, H. K.: Active sites for ice nucleation differ depending on nucleation mode, *P. Nat. Acad. Sci. USA.*, 118, e2022859118, 10.1073/pnas.2022859118, 2021.
- Hoose, C., Kristjánsson, J. E., and Burrows, S. M.: How important is biological ice nucleation in clouds on a global scale?, *Environ. Res. Lett.*, 5, 024009, 10.1088/1748-9326/5/2/024009, 2010.
- Hoose, C., and Möhler, O.: Heterogeneous ice nucleation on atmospheric aerosols: a review of results from laboratory experiments, *Atmos. Chem. Phys.*, 12, 9817-9854, 10.5194/acp-12-9817-2012, 2012.
- Huang, S., Hu, W., Chen, J., Wu, Z., Zhang, D., and Fu, P.: Overview of biological ice nucleating particles in the atmosphere, *Environ. Int.*, 146, 106197, <https://doi.org/10.1016/j.envint.2020.106197>, 2021.

Huffman, J. A., Prenni, A. J., DeMott, P. J., Pöhlker, C., Mason, R. H., Robinson, N. H., Fröhlich-Nowoisky, J., Tobo, Y., Després, V. R., Garcia, E., Gochis, D. J., Harris, E., Müller-Germann, I., Ruzene, C., Schmer, B., Sinha, B., Day, D. A., Andreae, M. O., Jimenez, J. L., Gallagher, M., Kreidenweis, S. M., Bertram, A. K., and Pöschl, U.: High concentrations of biological aerosol particles and ice nuclei during and after rain, *Atmos. Chem. Phys.*, 13, 6151-6164, 10.5194/acp-13-6151-2013, 2013.

Ickes, L., Welti, A., Hoose, C., and Lohmann, U.: Classical nucleation theory of homogeneous freezing of water: thermodynamic and kinetic parameters, *Phys Chem Chem Phys*, 17, 5514-5537, 10.1039/c4cp04184d, 2015.

Johnson, E. A., and Rossman, G. R.: The concentration and speciation of hydrogen in feldspars using FTIR and <sup>1</sup>H MAS NMR spectroscopy, *Am. Mineral.*, 88, 901-911, 10.2138/am-2003-5-620, 2003.

Johnson, E. A., and Rossman, G. R.: A survey of hydrous species and concentrations in igneous feldspars, *American Mineralogist*, 89, 586-600, doi:10.2138/am-2004-0413, 2004.

Irish, V. E., Elizondo, P., Chen, J., Chou, C., Charette, J., Lizotte, M., Ladino, L. A., Wilson, T. W., Gosselin, M., Murray, B. J., Polishchuk, E., Abbatt, J. P. D., Miller, L. A., and Bertram, A. K.: Ice-nucleating particles in Canadian Arctic sea-surface microlayer and bulk seawater, *Atmos. Chem. Phys.*, 17, 10583-10595, 2017.

Iwata, A., Imura, M., Hama, M., Maki, T., Tsuchiya, N., Kuniyama, R., and Matsuki, A.: Release of Highly Active Ice Nucleating Biological Particles Associated with Rain, *Atmosphere*, 10, 2019.

Joly, M., Amato, P., Deguillaume, L., Monier, M., Hoose, C., and Delort, A. M.: Quantification of ice nuclei active at near 0 °C temperatures in low-altitude clouds at the Puy de Dôme atmospheric station, *Atmos. Chem. Phys.*, 14, 8185-8195, 10.5194/acp-14-8185-2014, 2014.

Joly, M., Amato, P., Deguillaume, L., Monier, M., Hoose, C., and Delort, A. M.: Quantification of ice nuclei active at near 0 °C temperatures in low-altitude clouds at the Puy de Dôme atmospheric station, *Atmos. Chem. Phys.*, 14, 8185-8195, 2014.

Joyce, R. E., Lavender, H., Farrar, J., Werth, J. T., Weber, C. F., D'Andrilli, J., Vaitilingom, M., and Christner, B. C.: Biological Ice-Nucleating Particles Deposited Year-Round in Subtropical Precipitation, *Appl Environ Microbiol*, 85, e01567-01519, 10.1128/AEM.01567-19, 2019.

Kandler, K., SchütZ, L., Deutscher, C., Ebert, M., Hofmann, H., Jäckel, S., Jaenicke, R., Knippertz, P., Lieke, K., Massling, A., Petzold, A., Schladitz, A., Weinzierl, B., Wiedensohler, A., Zorn, S., and Weinbruch, S.: Size distribution, mass concentration, chemical and mineralogical composition and derived optical parameters of the boundary layer aerosol at Tinfou, Morocco, during SAMUM 2006, *Tellus B: Chemical and Physical Meteorology*, 61, 32-50, 10.1111/j.1600-0889.2008.00385.x, 2009.

Kanji, Z. A., Ladino, L. A., Wex, H., Boose, Y., Burkert-Kohn, M., Cziczo, D. J., and Krämer, M.: Overview of Ice Nucleating Particles, *Meteorol. Monogr.*, 58, 1.1-1.33, 10.1175/amsmonographs-d-16-0006.1, 2017.

- Kaufmann, L., Marcolli, C., Hofer, J., Pinti, V., Hoyle, C. R., and Peter, T.: Ice nucleation efficiency of natural dust samples in the immersion mode, *Atmos. Chem. Phys.*, 16, 11177-11206, 10.5194/acp-16-11177-2016, 2016.
- Kieft, T. L., and Ruscetti, T.: Characterization of biological ice nuclei from a lichen, *J Bacteriol*, 172, 3519-3523, 10.1128/jb.172.6.3519-3523.1990, 1990.
- Kiselev, A., Bachmann, F., Pedevilla, P., Cox, S. J., Michaelides, A., Gerthsen, D., and Leisner, T.: Active sites in heterogeneous ice nucleation-the example of K-rich feldspars, *Science*, 355, 367-371, 10.1126/science.aai8034, 2017.
- Kiselev, A., Keinert, A., Gaedecke, T., Leisner, T., Sutter, C., Petrishcheva, E., and Abart, R.: Effect of chemically induced fracturing on the ice nucleation activity of alkali feldspar, *Atmos. Chem. Phys. Discuss.*, 2021, 1-17, 10.5194/acp-2021-18, 2021.
- Knackstedt, K. A., Moffett, B. F., Hartmann, S., Wex, H., Hill, T. C. J., Glasgo, E. D., Reitz, L. A., Augustin-Bauditz, S., Beall, B. F. N., Bullerjahn, G. S., Fröhlich-Nowoisky, J., Grawe, S., Lubitz, J., Stratmann, F., and McKay, R. M. L.: Terrestrial Origin for Abundant Riverine Nanoscale Ice-Nucleating Particles, *Environ. Sci. Technol.*, 52, 12358-12367, 10.1021/acs.est.8b03881, 2018.
- Knippertz, P., and Stuut, J.: *Mineral Dust: A Key Player in the Earth System*, Mineral Dust, 2014.
- Koop, T., and Zobrist, B.: Parameterizations for ice nucleation in biological and atmospheric systems, *Phys Chem Chem Phys*, 11, 10839-10850, 10.1039/b914289d, 2009.
- Kulkarni, G., Zhang, K., Zhao, C., Nandasiri, M., Shutthanandan, V., Liu, X., Fast, J., and Berg, L.: Ice formation on nitric acid-coated dust particles: Laboratory and modeling studies, *J. Geophys. Res.-Atmos.*, 120, 7682-7698, <https://doi.org/10.1002/2014JD022637>, 2015.
- Kumar, A., Marcolli, C., Luo, B., and Peter, T.: Ice nucleation activity of silicates and aluminosilicates in pure water and aqueous solutions – Part 1: The K-feldspar microcline, *Atmos. Chem. Phys.*, 18, 7057-7079, 10.5194/acp-18-7057-2018, 2018a.
- Kumar, A., Marcolli, C., and Peter, T.: Ice nucleation activity of silicates and aluminosilicates in pure water and aqueous solutions. Part 2; Quartz and amorphous silica, *Atmos. Chem. Phys. Discussions*, 1-35, 10.5194/acp-2018-1020, 2018b.
- Kumar, A., Marcolli, C., and Peter, T.: Ice nucleation activity of silicates and aluminosilicates in pure water and aqueous solutions – Part 2: Quartz and amorphous silica, *Atmos. Chem. Phys.*, 19, 6035-6058, 10.5194/acp-19-6035-2019, 2019a.
- Kumar, A., Marcolli, C., and Peter, T.: Ice nucleation activity of silicates and aluminosilicates in pure water and aqueous solutions – Part 3: Aluminosilicates, *Atmos. Chem. Phys.*, 19, 6059-6084, 10.5194/acp-19-6059-2019, 2019b.
- Kunert, A. T., Lamneck, M., Helleis, F., Pöschl, U., Pöhlker, M. L., and Fröhlich-Nowoisky, J.: Twin-plate Ice Nucleation Assay (TINA) with infrared detection for high-throughput droplet freezing experiments with biological ice nuclei in laboratory and field samples, *Atmos. Meas. Tech.*, 11, 6327-6337, 10.5194/amt-11-6327-2018, 2018.

- Lee, M. R., Hodson, M. E., Brown, D. J., MacKenzie, M., and Smith, C. L.: The composition and crystallinity of the near-surface regions of weathered alkali feldspars, *Geochimica et Cosmochimica Acta*, 72, 4962-4975, <https://doi.org/10.1016/j.gca.2008.08.001>, 2008.
- Liu, W. D., Yang, Y., Zhu, K. Y., and Xia, Q. K.: Temperature dependences of hydrous species in feldspars, *Physics and Chemistry of Minerals*, 45, 609-620, 10.1007/s00269-018-0946-1, 2018.
- Lu, Z., Du, P., Du, R., Liang, Z., Qin, S., Li, Z., and Wang, Y.: The Diversity and Role of Bacterial Ice Nuclei in Rainwater from Mountain Sites in China, *Aerosol. Air. Qual. Res.*, 16, 640-652, 2016.
- Lundheim, R.: Physiological and ecological significance of biological ice nucleators, *Philos Trans R Soc Lond B Biol Sci*, 357, 937-943, 10.1098/rstb.2002.1082, 2002.
- Maki, L. R., Galyan, E. L., Chang-Chien, M. M., and Caldwell, D. R.: Ice nucleation induced by *Pseudomonas syringae*, *Appl Microbiol*, 28, 456-459, 10.1128/am.28.3.456-459, 1974.
- Marculli, C., Gedamke, S., Peter, T., and Zobrist, B.: Efficiency of immersion mode ice nucleation on surrogates of mineral dust, *Atmos. Chem. Phys.*, 7, 5081-5091, 10.5194/acp-7-5081-2007, 2007.
- Martin, A. C., Cornwell, G., Beall, C. M., Cannon, F., Reilly, S., Schaap, B., Lucero, D., Creamean, J., Ralph, F. M., Mix, H. T., and Prather, K.: Contrasting local and long-range-transported warm ice-nucleating particles during an atmospheric river in coastal California, USA, *Atmos. Chem. Phys.*, 19, 4193-4210, 2019.
- Mason, B. J., and Maybank, J.: Ice-nucleating properties of some natural mineral dusts, *Q. J. R. Meteorol. Soc.*, 84, 235-241, <https://doi.org/10.1002/qj.49708436104>, 1958.
- McCluskey, C. S., Hill, T. C. J., Sultana, C. M., Laskina, O., Trueblood, J., Santander, M. V., Beall, C. M., Michaud, J. M., Kreidenweis, S. M., Prather, K. A., Grassian, V., and DeMott, P. J.: A Mesocosm Double Feature: Insights into the Chemical Makeup of Marine Ice Nucleating Particles, *J. Atmos. Sci.*, 75, 2405-2423, 10.1175/JAS-D-17-0155.1, 2018a.
- McCluskey, C. S., Ovadnevaite, J., Rinaldi, M., Atkinson, J., Belosi, F., Ceburnis, D., Marullo, S., Hill, T. C. J., Lohmann, U., Kanji, Z. A., O'Dowd, C., Kreidenweis, S. M., and DeMott, P. J.: Marine and Terrestrial Organic Ice-Nucleating Particles in Pristine Marine to Continentally Influenced Northeast Atlantic Air Masses, *J. Geophys. Res.-Atmos.*, 123, 6196-6212, 2018b.
- Michaud, A. B., Dore, J. E., Leslie, D., Lyons, W. B., Sands, D. C., and Priscu, J. C.: Biological ice nucleation initiates hailstone formation, *J. Geophys. Res.-Atmos.*, 119, 12,186-112,197, <https://doi.org/10.1002/2014JD022004>, 2014.
- Moffett, B. F., Getti, G., Henderson-Begg, S. K., and Hill, T. C. J.: Ubiquity of ice nucleation in lichen — possible atmospheric implications, *Lindbergia*, 38, 39-43, 10.25227/linbg.01070, 2015.

- Moffett, B. F., Hill, T. C. J., and DeMott, P. J.: Abundance of Biological Ice Nucleating Particles in the Mississippi and Its Major Tributaries, *Atmosphere*, 9, 10.3390/atmos9080307, 2018.
- Morris, C. E., Conen, F., Alex Huffman, J., Phillips, V., Pöschl, U., and Sands, D. C.: Bioprecipitation: a feedback cycle linking Earth history, ecosystem dynamics and land use through biological ice nucleators in the atmosphere, *Global Change Biology*, 20, 341-351, <https://doi.org/10.1111/gcb.12447>, 2014.
- Morris, G. J., and Lamb, S.: Improved Methods for Cryopreservation of Biological Material, U.S. Patent Application # 15/557320, 2018.
- Murray, B. J., O'Sullivan, D., Atkinson, J. D., and Webb, M. E.: Ice nucleation by particles immersed in supercooled cloud droplets, *Chem Soc Rev*, 41, 6519-6554, 10.1039/c2cs35200a, 2012.
- Murray, B. J., Carslaw, K. S., and Field, P. R.: Opinion: Cloud-phase climate feedback and the importance of ice-nucleating particles, *Atmos. Chem. Phys.*, 21, 665-679, 10.5194/acp-21-665-2021, 2021.
- Niemand, M., Möhler, O., Vogel, B., Vogel, H., Hoose, C., Connolly, P., Klein, H., Bingemer, H., DeMott, P., Skrotzki, J., and Leisner, T.: A Particle-Surface-Area-Based Parameterization of Immersion Freezing on Desert Dust Particles, *J. Atmos. Sci.*, 69, 3077-3092, 10.1175/jas-d-11-0249.1, 2012.
- O'Sullivan, D., Murray, B. J., Malkin, T. L., Whale, T. F., Umo, N. S., Atkinson, J. D., Price, H. C., Baustian, K. J., Browse, J., and Webb, M. E.: Ice nucleation by fertile soil dusts: relative importance of mineral and biogenic components, *Atmos. Chem. Phys.*, 14, 1853-1867, 10.5194/acp-14-1853-2014, 2014.
- O'Sullivan, D., Murray, B. J., Ross, J. F., Whale, T. F., Price, H. C., Atkinson, J. D., Umo, N. S., and Webb, M. E.: The relevance of nanoscale biological fragments for ice nucleation in clouds, *Scientific Reports*, 5, 8082, 10.1038/srep08082, 2015
- O'Sullivan, D., Murray, B. J., Ross, J. F., and Webb, M. E.: The adsorption of fungal ice-nucleating proteins on mineral dusts: a terrestrial reservoir of atmospheric ice-nucleating particles, *Atmos. Chem. Phys.*, 16, 7879-7887, 10.5194/acp-16-7879-2016, 2016.
- O'Sullivan, D., Adams, M. P., Tarn, M. D., Harrison, A. D., Vergara-Temprado, J., Porter, G. C. E., Holden, M. A., Sanchez-Marroquin, A., Carotenuto, F., Whale, T. F., McQuaid, J. B., Walshaw, R., Hedges, D. H. P., Burke, I. T., Cui, Z., and Murray, B. J.: Contributions of biogenic material to the atmospheric ice-nucleating particle population in North Western Europe, *Sci. Rep.*, 8, 13821, 2018.
- Obata, H., Nakai, T., Tanishita, J., and Tokuyama, T.: Identification of an ice-nucleating bacterium and its ice nucleation properties, *J. Ferment. Bioeng.*, 67, 143-147, [https://doi.org/10.1016/0922-338X\(89\)90111-6](https://doi.org/10.1016/0922-338X(89)90111-6), 1989.
- Pach, E. and Verdager, A.: Freezing efficiency of feldspars is affected by their history of previous freeze-thaw events, *Physical Chemistry Chemical Physics*, 23, 24905-24914, 2021.

- Paramonov, M., David, R. O., Kretzschmar, R., and Kanji, Z. A.: A laboratory investigation of the ice nucleation efficiency of three types of mineral and soil dust, *Atmos. Chem. Phys.*, 18, 16515-16536, 10.5194/acp-18-16515-2018, 2018.
- Parsons, I., Fitz Gerald, J. D., and Lee, M. R.: Routine characterization and interpretation of complex alkali feldspar intergrowths, *Am. Mineral.*, 100, 1277-1303, 10.2138/am-2015-5094, 2015.
- Peckhaus, A., Kiselev, A., Hiron, T., Ebert, M., and Leisner, T.: A comparative study of K-rich and Na/Ca-rich feldspar ice-nucleating particles in a nanoliter droplet freezing assay, *Atmos. Chem. Phys.*, 16, 11477-11496, 10.5194/acp-16-11477-2016, 2016.
- Pedevilla, P., Fitzner, M., and Michaelides, A.: What makes a good descriptor for heterogeneous ice nucleation on OH-patterned surfaces, *Phys. Rev. B*, 96, 10.1103/PhysRevB.96.115441, 2017.
- Perkins, R. J., Gillette, S. M., Hill, T. C. J., and DeMott, P. J.: The Labile Nature of Ice Nucleation by Arizona Test Dust, *ACS. Earth. Space. Chem.*, 4, 133-141, 10.1021/acsearthspacechem.9b00304, 2020.
- Pietsch, R. B., Vinatzer, B. A., and Schmale, D. G.: Diversity and Abundance of Ice Nucleating Strains of *Pseudomonas syringae* in a Freshwater Lake in Virginia, USA, *Front. Microbiol.*, 8, 318, 2017.
- Polen, M., Lawlis, E., and Sullivan, R. C.: The unstable ice nucleation properties of Snomax<sup>®</sup> bacterial particles, *J. Geophys. Res.-Atmos.*, 121, 11,666-611,678, <https://doi.org/10.1002/2016JD025251>, 2016.
- Pouleur, S., Richard, C., Martin, J. G., and Antoun, H.: Ice Nucleation Activity in *Fusarium acuminatum* and *Fusarium avenaceum*, *Appl Environ Microbiol*, 58, 2960-2964, 10.1128/AEM.58.9.2960-2964.1992, 1992.
- Pruppacher, H. R.: *Microphysics of clouds and precipitation* / by Hans R. Pruppacher and James D. Klett, Accessed from <https://nla.gov.au/nla.cat-vn946461>, edited by: Klett, J. D., D. Reidel Pub. Co, Dordrecht, Holland ; Boston, 1978.
- Pummer, B. G., Bauer, H., Bernardi, J., Bleicher, S., and Grothe, H.: Suspendable macromolecules are responsible for ice nucleation activity of birch and conifer pollen, *Atmos. Chem. Phys.*, 12, 2541-2550, 10.5194/acp-12-2541-2012, 2012.
- Pummer, B. G., Budke, C., Augustin-Bauditz, S., Niedermeier, D., Felgitsch, L., Kampf, C. J., Huber, R. G., Liedl, K. R., Loerting, T., Moschen, T., Schauperl, M., Tollinger, M., Morris, C. E., Wex, H., Grothe, H., Pöschl, U., Koop, T., and Fröhlich-Nowoisky, J.: Ice nucleation by water-soluble macromolecules, *Atmos. Chem. Phys.*, 15, 4077-4091, 10.5194/acp-15-4077-2015, 2015.
- Rosenfeld, D., Yu, X., Liu, G., Xu, X., Zhu, Y., Yue, Z., Dai, J., Dong, Z., Dong, Y., and Peng, Y.: Glaciation temperatures of convective clouds ingesting desert dust, air pollution and smoke from forest fires, *Geophys. Res. Lett.*, 38, <https://doi.org/10.1029/2011GL049423>, 2011.
- Roy, P., House, M. L., and Dutcher, C. S.: A Microfluidic Device for Automated High Throughput Detection of Ice Nucleation of Snomax<sup>®</sup>, *Micromachines*, 12, 10.3390/mi12030296, 2021.

Sanchez-Marroquin, A., West, J. S., Burke, I. T., McQuaid, J. B., and Murray, B. J.: Mineral and biological ice-nucleating particles above the South East of the British Isles, *Environ. Sci.: Atmos.*, 1, 176-191, 10.1039/D1EA00003A, 2021.

Šantl-Temkiv, T., Sahyoun, M., Finster, K., Hartmann, S., Augustin-Bauditz, S., Stratmann, F., Wex, H., Clauss, T., Nielsen, N. W., Sørensen, J. H., Korsholm, U. S., Wick, L. Y., and Karlson, U. G.: Characterization of airborne ice-nucleation-active bacteria and bacterial fragments, *Atmos. Env.*, 109, 105-117, 2015.

Šantl-Temkiv, T., Lange, R., Beddows, D., Rauter, U., Pilgaard, S., Dall'Osto, M., Gunde-Cimerman, N., Massling, A., and Wex, H.: Biogenic Sources of Ice Nucleating Particles at the High Arctic Site Villum Research Station, *Environ. Sci. Technol.*, 53, 10580-10590, 10.1021/acs.est.9b00991, 2019.

Schneider, J., Höhler, K., Heikkilä, P., Keskinen, J., Bertozzi, B., Bogert, P., Schorr, T., Umo, N. S., Vogel, F., Brasseur, Z., Wu, Y., Hakala, S., Duplissy, J., Moisseev, D., Kulmala, M., Adams, M. P., Murray, B. J., Korhonen, K., Hao, L., Thomson, E. S., Castarède, D., Leisner, T., Petäjä, T., and Möhler, O.: The seasonal cycle of ice-nucleating particles linked to the abundance of biogenic aerosol in boreal forests, *Atmos. Chem. Phys. Discuss.*, 2020, 1-18, 10.5194/acp-2020-683, 2020.

Schnell, R. C., and Vali, G.: Biogenic Ice Nuclei: Part I. Terrestrial and Marine Sources, *J. Atmos. Sci.*, 33, 1554-1564, 10.1175/1520-0469, 1976.

Steinke, I., Funk, R., Busse, J., Iturri, A., Kirchen, S., Leue, M., Möhler, O., Schwartz, T., Schnaiter, M., Sierau, B., Toprak, E., Ullrich, R., Ulrich, A., Hoose, C., and Leisner, T.: Ice nucleation activity of agricultural soil dust aerosols from Mongolia, Argentina, and Germany, *J. Geophys. Res.-Atmos.*, 121, 13,559-513,576, 2016.

Storelvmo, T., and Tan, I.: The Wegener-Bergeron-Findeisen process - Its discovery and vital importance for weather and climate, *Meteorol. Z.*, 24, 455-461, 2015.

Sullivan, R. C., Petters, M. D., DeMott, P. J., Kreidenweis, S. M., Wex, H., Niedermeier, D., Hartmann, S., Clauss, T., Stratmann, F., Reitz, P., Schneider, J., and Sierau, B.: Irreversible loss of ice nucleation active sites in mineral dust particles caused by sulphuric acid condensation, *Atmos. Chem. Phys.*, 10, 11471-11487, 10.5194/acp-10-11471-2010, 2010.

Suski, K. J., Hill, T. C. J., Levin, E. J. T., Miller, A., DeMott, P. J., and Kreidenweis, S. M.: Agricultural harvesting emissions of ice nucleating particles, *Atmos. Chem. Phys. Discussions*, 1-30, 10.5194/acp-2018-348, 2018.

Tarn, M. D., Sikora, S. N. F., Porter, G. C. E., O'Sullivan, D., Adams, M., Whale, T. F., Harrison, A. D., Vergara-Temprado, J., Wilson, T. W., Shim, J.-u., and Murray, B. J.: The study of atmospheric ice-nucleating particles via microfluidically generated droplets, *Microfluid. Nanofluid.*, 22, 52, 10.1007/s10404-018-2069-x, 2018.

Tarn, M. D., Sikora, S. N. F., Porter, G. C. E., Wyld, B. V., Alayof, M., Reicher, N., Harrison, A. D., Rudich, Y., Shim, J.-u., and Murray, B. J.: On-chip analysis of atmospheric ice-nucleating particles in continuous flow, *Lab. Chip.*, 20, 2889-2910, 10.1039/D0LC00251H, 2020.

- Tesson, S. V. M. and Šantl-Temkiv, T.: Ice Nucleation Activity and Aeolian Dispersal Success in Airborne and Aquatic Microalgae, *Front. Microbiol.*, 9, 2681, 2018.
- Tobo, Y., DeMott, P. J., Hill, T. C. J., Prenni, A. J., Swoboda-Colberg, N. G., Franc, G. D., and Kreidenweis, S. M.: Organic matter matters for ice nuclei of agricultural soil origin, *Atmos. Chem. Phys.*, 14, 8521-8531, 10.5194/acp-14-8521-2014, 2014.
- Tobo, Y., Adachi, K., DeMott, P. J., Hill, T. C. J., Hamilton, D. S., Mahowald, N. M., Nagatsuka, N., Ohata, S., Uetake, J., Kondo, Y., and Koike, M.: Glacially sourced dust as a potentially significant source of ice nucleating particles, *Nat. Geosci.*, 12, 253-258, 10.1038/s41561-019-0314-x, 2019.
- Tobo, Y., Uetake, J., Matsui, H., Moteki, N., Uji, Y., Iwamoto, Y., Miura, K., and Misumi, R.: Seasonal Trends of Atmospheric Ice Nucleating Particles Over Tokyo, *J. Geophys. Res.-Atmos.*, 125, e2020JD033658, 2020.
- Ullrich, R., Hoose, C., Möhler, O., Niemand, M., Wagner, R., Höhler, K., Hiranuma, N., Saathoff, H., and Leisner, T.: A New Ice Nucleation Active Site Parameterization for Desert Dust and Soot, *J. Atmos. Sci.*, 74, 699-717, 10.1175/jas-d-16-0074.1, 2017.
- Vali, G.: Quantitative Evaluation of Experimental Results on the Heterogeneous Freezing Nucleation of Supercooled Liquids, *J. Atmos. Sci.*, 28, 402-409, 10.1175/1520-0469(1971)028<0402:QEOERA>2.0.CO;2, 1971.
- Vali, G.: Freezing Rate Due to Heterogeneous Nucleation, *J. Atmos. Sci.*, 51, 1843-1856, 10.1175/1520-0469(1994)051<1843:FRDTHN>2.0.CO;2, 1994.
- Vergara-Temprado, J., Murray, B. J., Wilson, T. W., and Sullivan, D., Browse, J., Pringle, K. J., Ardon-Dryer, K., Bertram, A. K., Burrows, S. M., Ceburnis, D., DeMott, P. J., Mason, R. H., and Dowd, C. D., Rinaldi, M., and Carslaw, K. S.: Contribution of feldspar and marine organic aerosols to global ice nucleating particle concentrations, *Atmos. Chem. Phys.*, 17, 3637-3658, 10.5194/acp-17-3637-2017, 2017.
- Vergara-Temprado, J., Miltenberger, A. K., Furtado, K., Grosvenor, D. P., Shipway, B. J., Hill, A. A., Wilkinson, J. M., Field, P. R., Murray, B. J., and Carslaw, K. S.: Strong control of Southern Ocean cloud reflectivity by ice-nucleating particles, *Proc Natl Acad Sci U S A*, 115, 2687-2692, 10.1073/pnas.1721627115, 2018.
- Warren, G. J.: Bacterial Ice Nucleation: Molecular Biology and Applications, *Biotechnology and Genetic Engineering Reviews*, 5, 107-136, 10.1080/02648725.1987.10647836, 1987.
- Welti, A., Lohmann, U., and Kanji, Z. A.: Ice nucleation properties of K-feldspar polymorphs and plagioclase feldspars, *Atmos. Chem. Phys. Discussions*, 1-25, 10.5194/acp-2018-1271, 2019.
- Wex, H., Augustin-Bauditz, S., Boose, Y., Budke, C., Curtius, J., Diehl, K., Dreyer, A., Frank, F., Hartmann, S., Hiranuma, N., Jantsch, E., Kanji, Z. A., Kiselev, A., Koop, T., Möhler, O., Niedermeier, D., Nillius, B., Rösch, M., Rose, D., Schmidt, C., Steinke, I., and Stratmann, F.: Intercomparing different devices for the investigation of ice nucleating particles using Snomax<sup>®</sup> as test substance, *Atmos. Chem. Phys.*, 15, 1463-1485, 10.5194/acp-15-1463-2015, 2015.

Whale, T. F., Murray, B. J., O'Sullivan, D., Wilson, T. W., Umo, N. S., Baustian, K. J., Atkinson, J. D., Workneh, D. A., and Morris, G. J.: A technique for quantifying heterogeneous ice nucleation in microlitre supercooled water droplets, *Atmos. Meas. Tech.*, 8, 2437-2447, 10.5194/amt-8-2437-2015, 2015.

Whale, T. F., Holden, M. A., Kulak, A. N., Kim, Y. Y., Meldrum, F. C., Christenson, H. K., and Murray, B. J.: The role of phase separation and related topography in the exceptional ice-nucleating ability of alkali feldspars, *Phys Chem Chem Phys*, 19, 31186-31193, 10.1039/c7cp04898j, 2017.

Wilson, T. W., Ladino, L. A., Alpert, P. A., Breckels, M. N., Brooks, I. M., Browse, J., Burrows, S. M., Carslaw, K. S., Huffman, J. A., Judd, C., Kilhau, W. P., Mason, R. H., McFiggans, G., Miller, L. A., Najera, J. J., Polishchuk, E., Rae, S., Schiller, C. L., Si, M., Temprado, J. V., Whale, T. F., Wong, J. P., Wurl, O., Yakobi-Hancock, J. D., Abbatt, J. P., Aller, J. Y., Bertram, A. K., Knopf, D. A., and Murray, B. J.: A marine biogenic source of atmospheric ice-nucleating particles, *Nature*, 525, 234-238, 10.1038/nature14986, 2015.

Wragg, N. M., Tampakis, D., and Stolzing, A.: Cryopreservation of Mesenchymal Stem Cells Using Medical Grade Ice Nucleation Inducer, *Int. J. Mol. Sci.*, 21, 10.3390/ijms21228579, 2020.

Yadav, S., Venezia, R. E., Paerl, R. W., and Petters, M. D.: Characterization of Ice-Nucleating Particles Over Northern India, *J. Geophys. Res.-Atmos.*, 124, 10467-10482, 10.1029/2019JD030702, 2019.

Yakobi-Hancock, J. D., Ladino, L. A., and Abbatt, J. P. D.: Feldspar minerals as efficient deposition ice nuclei, *Atmos. Chem. Phys.*, 13, 11175-11185, 10.5194/acp-13-11175-2013, 2013.

Zhao, X., Liu, X., Burrows, S. M., and Shi, Y.: Effects of marine organic aerosols as sources of immersion-mode ice-nucleating particles on high-latitude mixed-phase clouds, *Atmos. Chem. Phys.*, 21, 2305-2327, 10.5194/acp-21-2305-2021, 2021.

Zinke, J., Salter, M. E., Leck, C., Lawler, M. J., Porter, G. C. E., Adams, M. P., Brooks, I. M., Murray, B. J., and Zieger, P.: The development of a miniaturised balloon-borne cloud water sampler and its first deployment in the high Arctic, *Tellus. B. Chem. Phys.*, 73, 1-12, 10.1080/16000889.2021.1915614, 2021.

Zolles, T., Burkart, J., Hausler, T., Pummer, B., Hitzenberger, R., and Grothe, H.: Identification of ice nucleation active sites on feldspar dust particles, *J Phys Chem A*, 119, 2692-2700, 10.1021/jp509839x, 2015.

## 5 Conclusions and future work

Three objectives for this project were defined in Chapter 1 and they were addressed by the research papers that constituted chapters two to four. In this concluding chapter these objectives are now each revisited in terms of how they were met and then the potential future avenues of research are discussed and final remarks on the project are offered.

### 5.1 Objective one: Demonstrate importance of controlling ice-nucleating in 96-well plates and the effectiveness of IceStart™ for cryopreserving cells

#### 5.1.1 Conclusions

This objective is a product of the industrial collaboration aspect of the project and sought to overcome the technical challenge of cryopreserving cells in 96-well plates which could facilitate a greater supply of more uniformly cryopreserved biological material for *in-vitro* toxicology screening. There were two approaches to meet the objective, firstly directly linking the controlling of ice-nucleation to better post-thaw cell survival and secondly performing plate cryopreservation trials with IceStart™ arrays.

The former approach was crucial as it showed a causal link between the IceStart array deployment and better cell freezing performance. First, it was necessary to quantify the typical supercooling that occurs in 96-well plates when ice-nucleation was left uncontrolled and this was investigated in Chapter 2. The IR-NIPI instrument allowed us to quantify that supercoolings of 10°C to 20°C in both water and cryoprotectant 100 µL aliquots are to be expected in 96-well plates (Fig. 2.2). To highlight that this was part of an empirical trend of smaller volumes resulting in more supercooling (Morris and Acton, 2013) this was plotted (Fig 2.5) to place it in context with what occurs in other cryobiological containers such as cryovials and straws. A trend predicting ice-nucleation temperature and volume emerges which agrees remarkably well with a similar plot based on literature values of droplet freezing temperatures (Fig. 1.4 in chapter one). In Chapter 2 and Chapter 3 higher survival of frozen plated

cultures of both primary cells (bovine granulosa) and immortalised cells (human hepatocytes) were linked to control of ice-nucleation. In Chapter 3 the ability to simultaneously cryopreserve 96-well plate cultures and measure well-to-well ice-nucleation temperatures meant allowed a direct relationship to be plotted (Fig. 3.6d). This is significant as, while there are previous reports of cryopreserving cell monolayers in 96-well plates (Campbell and Brockbank, 2014, 2012; Katkov et al., 2011; Wells and Price, 1983), the benefit of controlling ice-nucleation has not before been clearly shown due to the practical difficulty of measuring well-to-well ice-nucleation temperatures. There is also value in the preservation of primary cells compared to immortalised cell lines as they are also generally more difficult to cryopreserve. Finally, plate freezing trials with HepG2 cultures loaded with IceStart arrays (Chapter 3) clearly improved survival compared to plates without ice-nucleation control.

How exactly did controlled ice-nucleation lead to better post-thaw recovery of plated cells? An observation for both cell systems (see Figs 2.4c-e and 3.8) was that in wells where supercooling was severe the monolayer was more likely to suffer detachment - an obstacle previously reported when attempting to freeze cell monolayers (Campbell and Brockbank, 2014; Corsini et al., 2002; Ebertz and McGann, 2004). This leads to the hypothesis that the controlled ice-nucleation prevented thermal fluctuations caused by latent heat release, which is more severe when deeply supercooled, and in turn prevented mechanical stresses between the well substrate and cell monolayer (Eskandari et al., 2018; Rutt et al., 2019). Also, the deeper the level of supercooling of CPA in the well the greater the deviation from the intended rate of cooling after latent heat release back down to the bulk plate temperature after ice crystallisation is complete. According to the two-factor hypothesis of controlled-rate cell cryopreservation (Mazur et al., 1972) this leads to a greater risk of lethal intracellular ice formation.

### **5.1.2 Future work**

From a commercial point of view, the plate cultures that were produced here are probably of limited value, yet the experiments have provided valuable insight into the importance of ice-nucleation control. Demonstrating comparable results with IceStart on plate cultures of primary hepatocytes or cardiomyocytes, cells more commonly used in toxicology screening (though more expensive and not as conveniently sourced

as bovine granulosa or immortalised cell lines), is the next step towards commercial realisation.

The metric of success used for cryopreservation was cell viability as this is a first order indication of cryopreservation success. Any commercialised product would need validation that upon thawing cells are functioning as well as viable. In Chapter 3 the well-to-well correlation of ice-nucleation temperature and viability was achieved using the IR-NIPI to record ice-nucleation temperatures during the freezing process. An interesting potential further application of this method could be to rapidly characterise different types of cells' response to ice-nucleation temperature both in terms of viability and functionality markers.

## **5.2 Objective two: Optimise performance of mineral ice nucleator**

### **5.2.1 Conclusions**

In Chapter 3 the ice-nucleating material used in IceStart arrays, a K-feldspar variant called LDH1, was introduced. K-feldspar is an ideal choice of ice-nucleating agent for use in IceStart arrays due to its relative inertness compared to other potent ice-nucleators such as Snomax and silver iodide. Different specimens of K-feldspar, however, have wildly different ice-nucleating abilities (Harrison et al., 2016; Welti et al., 2019; Whale et al., 2017), likely due to natural mineralogical variations from samples collected from different geological localities. Certain variants of K-feldspar are known to have ice-nucleating active site densities which are orders of magnitude higher than BCS-376 microcline, a sample which K-feldspar parameterisation are based on (Atkinson et al., 2013; Harrison et al., 2019). The reasons for this are unclear and contamination by proteinaceous INP is unlikely due to its heat resistance (Peckhaus et al., 2016). One example of these 'hyperactive' feldspars is a microcline sample from Mt. Malosa in Malawi and has been known to nucleate ice in microlitre droplets as warm as  $-2\text{ }^{\circ}\text{C}$  (Harrison et al., 2016). In Harrison et al. (2016) a sample from this locality was called TUD#3 (also used in Chapter 4) and was chosen as the optimum candidate of ice-nucleant for IceStart arrays. A new specimen of Mt Malosa microcline, named LDH1 (Leeds Hyperactive feldspar 1), was sourced that would provide enough material to be able to perform many more experiments. It was necessary to confirm that the new sample contained the same hyperactive material as reported previously and it was not due to contaminants or minor constituents (see

Section 3.5.1 in Chapter 3). It was indeed found to be of similar activity as previously reported and quantities of this new material that were well below those used in IceStart arrays nucleated ice at least as warm as  $-1\text{ }^{\circ}\text{C}$  in  $100\text{ }\mu\text{L}$  water droplets, almost eliminating supercooling. Although this material has been previously investigated, this is nonetheless a remarkable finding as it is more active than established ice-nucleating agents such as Snomax, cholesterol and silver iodide (Fig. 3.4). It also renders potential treatments to increase the existing ice-nucleation ability of minerals such as milling (Hiranuma et al., 2014), chemically inducing cracks (Kiselev et al., 2021b) or addition of ammonium salts (Whale et al., 2018), redundant.

It may be up for debate whether total elimination of supercooling is necessary and mere prevention of severe supercooling is sufficient for small volume cryopreservation protocols (Morris and Acton, 2013). For example, in a study published during the preparation of this thesis, Wragg et al. (2020) demonstrated improved cryopreservation of mesenchymal stem cells in 96-well plates also using IceStart arrays. They used a formulation which allowed  $2^{\circ}\text{C}$  to  $5\text{ }^{\circ}\text{C}$  of supercooling to take place in wells in contrast to almost no supercooling as was the case in Chapter 3. There are, however two major advantages of hyperactive feldspars for ice-nucleation control in cryopreservation over ‘standard’ K-feldspars. Firstly, ice-nucleation temperatures can be so consistently high that supercooling is effectively eliminated and also no longer an unpredictable process. Secondly the amount of material needed to induce warm ice-nucleation is orders of magnitude less than ‘standard’ K-feldspars meaning delivery devices such as IceStart arrays can be re-imagined as physically smaller and much less intrusive.

### **5.2.2 Future work**

The ability of LDH1 to nucleate ice with very small quantities opens the possibility of freezing cells in the next smallest well volume format of 384-well plates. This would theoretically enable up to four times as many experiments to be carried out on a single plate of cells. It also poses more of a challenge for ice-nucleation control due to the even smaller well working volume of  $25\text{ }\mu\text{L}$  which would be expected to produce supercoolings of around  $15^{\circ}\text{C}$  to  $25^{\circ}\text{C}$ . Only hyperactive feldspars would be active enough to be effective in volumes small enough to not interfere with the well contents - the experiments used in Chapters 2 and 3 could confirm this. Also, alternative delivery systems such as encapsulation in alginate beads (Kojima et al., 1988; Massie

et al., 2011; Teixeira et al., 2017), incorporation into cryoprotectant solutions or even immobilisation onto containers could be explored as alternatives to array inserts. Finally, the toxicity tests shown in Fig 3.15 are a useful screening for potential toxicity from LDH1, however more specialised biocompatibility testing would be needed for LDH1 to be approved for routine commercial use.

Of more fundamental importance is to ascertain the nature of the active sites in hyperactive ice-nucleating feldspars and what distinguishes them from those in 'standard' feldspars. Hyperactive feldspars have been noted in atmospheric INP research on feldspars, but due to their atypical nature have received relatively little attention. At least three varieties have been reported in the literature which are potential candidates. These include Mt Malosa microcline (also known as TUD#3 (Harrison et al., 2016), FS04 (Kiselev et al., 2021a; Peckhaus et al., 2016) and LDH1 in Chapter 4), a microcline from the Former Yugoslavia, (Kaufmann et al., 2016) an amazonite (Chapter 4) and a microcline from Namibia in (Welti et al., 2019). Another example is Amelia albite, which shows hyperactive activity yet is a plagioclase feldspar. An interesting and overlooked common feature of these samples is their common geological origin as pegmatites. Pegmatites are bodies of igneous rock associated with the late stages of a cooling magma intrusion. They are distinctive for containing exceptionally large crystals with unusual chemical compositions which result from extreme fractionation of incompatible elements and volatile components of the magma (London, 2011) during their formation. A clear trend of ice-nucleating activity with an elemental signature (Sr/Rb) indicative of fractionated magma origin was observed by Welti et al. (2019) which may support this. Also, ion specific effects that enhance ice-nucleation were observed by He et al., (2016) to be caused by  $\text{Li}^+$  and  $\text{Cs}^+$ , ions of incompatible elements which may be enriched in pegmatite rocks. However, Pach et al. (2021) found using SEM imaging that the active sites on a sample of Mt Malosa microcline seemed to be associated with micropores indicating a topological origin, corroborating the findings of (Holden et al., 2019). Either way, identifying a specific geological origin for hyperactive feldspars would enable added resources for the material to be sourced from to be identified, their potential atmospheric relevance to be determined and even the potential for synthetic hyperactive ice-nucleating materials to be manufactured.

## **5.3 Objective three: Investigate stability of mineral ice-nucleators and compare with biological ice-nucleators**

### **5.3.1 Conclusions**

In Chapter 4 the stability of mineral ice-nucleators to heating, both in water and in air was investigated. This has some interesting implications for the potential use of minerals for ice-nucleation control for cryopreservation in terms of whether they retain their ice-nucleating ability while stored in aqueous cryoprotectant solutions or after being sterilised by heating. However, the main motivation is that heating is used to determine the relative contributions of biological INP and mineral INP in samples collected from the environment. As explained in Section 1.4.2, being able to understand the emissions, distribution, and sources of mineral dust and biological INP will be crucial for modelling the radiative response of mixed phase clouds to a warming climate. As such, more than 20 publications have documented using this methodology to date. In Chapter four I challenged the assumption that heating in water does not affect any type of mineral's ice-nucleating ability (Conen et al., 2011). Evidence to doubt this comes from several studies which show that mineral samples, such as quartz, see their ice-nucleating ability reduce while stored in water at room-temperature (Harrison et al., 2019; Perkins et al., 2020). Also, it was pointed out that heating samples in air and water could produce different reactions, yet this is not usually experimentally considered. The set of droplet freezing assay experiments in Chapter 4 fully characterised the heat responses of all the principle mineral classes in wet and dry modes and compared them with those of biological INP analogues. Overall, it was found that the INA of some atmospherically important mineral dust components, such as quartz and plagioclase feldspar, are heat sensitive in water but not in air. This is a surprising result due to the chemical inertness of quartz compared to other minerals and may be due to a combination of dissolution and fracturing, possible artificially exacerbated by the process of grinding to produce a powder. K-feldspar was slightly sensitive to dry heating for reasons that are unclear, and this may preclude dry heating as an alternative to wet heating to avoid false positives from wet heating heat sensitive minerals. Overall Chapter 4 highlights the need for making complementary measurements and analyses to using heat tests when determining what component of a sample collected from the environment contributes to ice-nucleating activity.

Finally, other findings throughout this thesis also contributed to Objective three but with pertinence to cryopreservation. For example, one of the key advantages of using minerals as chemical ice-nucleation control agents (Table 1.1) is that they are assumed to be stable and unreactive. In Chapter 3 it was shown that feldspars, both ‘standard and hyperactive, are largely resistant in terms of their ice-nucleating ability to chemical sterilisation by ethanol and storage in 10% DMSO solution. Also, the sensitivity of some minerals in water is pertinent as, for example quartz has been proposed as a potential mineral ice-nucleation control agent for cryopreservation (Jiang et al., 2021).

### **5.3.2 Future work**

A by-product of the assessment of the INP heat test that forms Chapter 4 is some interesting insights into the nature of the ice-nucleating sites on minerals. For example, why are the active sites on quartz so unstable in water compared to other minerals such as the feldspars? As the main hypothesis is dissolution of particle surfaces that house active sites, scanning electron microscopy could be used to look for changes in mineral particle morphology after heating test to this hypothesis. A practical difficulty of this could be imaging the same active site before and after a heat treatment. One issue raised by the sensitivity of some minerals to aqueous heating is the use of hot (~60 °C) aqueous hydrogen peroxide (H<sub>2</sub>O<sub>2</sub>) treatment, which is similar to the heat test but intended to eliminate all organic matter from a sample (Suski et al., 2018; Tobo et al., 2019; Tobo et al., 2014), and can be used in addition to the heat test. This obviously could inadvertently affect heat sensitive mineral INP. There is also some evidence that H<sub>2</sub>O<sub>2</sub> treatment can attack mineral surfaces (Mikutta et al., 2005). An alternative to this method for eliminating organic INP could be to add an oxidant that does not require raised temperatures, such as sodium hypochlorite. Alternatively dilute boric acid has been shown to denature polysaccharide INPs and this could be used in parallel with existing heat tests to detect polysaccharide and proteinaceous INP respectively.

## 5.4 Final remarks

Since the turn of the century the threat of climate change has driven intense research into ice-nucleation and substances that facilitate it. As a result, our fundamental knowledge of minerals and biological matter that efficiently nucleate ice has expanded greatly. A new generation of instrumentation has also been developed. Despite this, this project has shown that there is still much to learn about ice-nucleating minerals in the context of how they affect cloud properties. Re-assessing the heat test will aid future field campaigns that seek to survey the nature of INP in the environment. This will aid the urgent issue of understanding the role mixed-phase clouds play in climate sensitivity in a warming world. An offshoot of this is the potential applied science driven by industry that has taken advantage of thriving ice-nucleation research. As this project has revealed, the unpredictable nature of ice-nucleation may finally be controlled during cryopreservation with a potentially biocompatible substance. This was demonstrated in a system where hazardous supercooling is extreme. The end application of frozen format cells may accelerate development of new drugs and therapies. There is still, however, much to learn about how minerals as it is still unclear why some are so active. Hyperactive feldspars, such as LDH1, as almost perfect ice-nucleators, may be an ideal model system to unravel mysterious nature of active sites. This may involve focusing on and understanding geological processes that formed them. Ultimately this could open the door to the manufacture of ice-nucleating materials and could have applications in other fields such as food preservation (Kobayashi et al., 2018) and water desalination (Kalista et al., 2018).

## References

- Atkinson, J. D., Murray, B. J., Woodhouse, M. T., Whale, T. F., Baustian, K. J., Carslaw, K. S., Dobbie, S., O'Sullivan, D., and Malkin, T. L.: The importance of feldspar for ice nucleation by mineral dust in mixed-phase clouds, *Nature*, 498, 355-358, 2013.
- Campbell, L. H. and Brockbank, K. G. M.: Cryopreservation of Adherent Cells on a Fixed Substrate, *IntechOpen*, doi: 10.5772/58618, 2014. 2014.
- Campbell, L. H. and Brockbank, K. G. M.: Culturing with trehalose produces viable endothelial cells after cryopreservation, *Cryobiology*, 64, 240-244, 2012.
- Conen, F., Morris, C. E., Leifeld, J., Yakutin, M. V., and Alewell, C.: Biological residues define the ice nucleation properties of soil dust, *Atmospheric Chemistry and Physics*, 11, 9643-9648, 2011.

- Corsini, J., Maxwell, F., and Maxwell, I. H.: Storage of various cell lines at -70 degrees C or -80 degrees C in multi-well plates while attached to the substratum, *Biotechniques*, 33, 42, 44, 46, 2002.
- Ebertz, S. L. and McGann, L. E.: Cryoinjury in endothelial cell monolayers, *Cryobiology*, 49, 37-44, 2004.
- Eskandari, N., Marquez-Curtis, L. A., McGann, L. E., and Elliott, J. A. W.: Cryopreservation of human umbilical vein and porcine corneal endothelial cell monolayers, *Cryobiology*, 85, 63-72, 2018.
- Harrison, A. D., Lever, K., Sanchez-Marroquin, A., Holden, M. A., Whale, T. F., Tarn, M. D., McQuaid, J. B., and Murray, B. J.: The ice-nucleating ability of quartz immersed in water and its atmospheric importance compared to K-feldspar, *Atmos. Chem. Phys.*, 19, 11343-11361, 2019.
- Harrison, A. D., Whale, T. F., Carpenter, M. A., Holden, M. A., Neve, L., and Sullivan, D., Vergara Temprado, J., and Murray, B. J.: Not all feldspars are equal: a survey of ice nucleating properties across the feldspar group of minerals, *Atmospheric Chemistry and Physics*, 16, 10927-10940, 2016.
- He, Z., Xie Wen, J., Liu, Z., Liu, G., Wang, Z., Gao Yi, Q., and Wang, J.: Tuning ice nucleation with counterions on polyelectrolyte brush surfaces, *Science Advances*, 2, e1600345, 2016.
- Hiranuma, N., Hoffmann, N., Kiselev, A., Dreyer, A., Zhang, K., Kulkarni, G., Koop, T., and Möhler, O.: Influence of surface morphology on the immersion mode ice nucleation efficiency of hematite particles, *Atmospheric Chemistry and Physics*, 14, 2315-2324, 2014.
- Holden, M. A., Whale, T. F., Tarn, M. D., O'Sullivan, D., Walshaw, R. D., Murray, B. J., Meldrum, F. C., and Christenson, H. K.: High-speed imaging of ice nucleation in water proves the existence of active sites, *Sci Adv*, 5, eaav4316, 2019.
- Jiang, B., Li, W., Stewart, S., Ou, W., Liu, B., Comizzoli, P., and He, X.: Sand-mediated ice seeding enables serum-free low-cryoprotectant cryopreservation of human induced pluripotent stem cells, *Bioactive Materials*, 6, 4377-4388, 2021.
- Kalista, B., Shin, H., Cho, J., and Jang, A.: Current development and future prospect review of freeze desalination, *Desalination*, 447, 167-181, 2018.
- Katkov, I. I., Kan, N. G., Cimadamore, F., Nelson, B., Snyder, E. Y., and Terskikh, A. V.: DMSO-Free Programmed Cryopreservation of Fully Dissociated and Adherent Human Induced Pluripotent Stem Cells, *Stem Cells Int*, 2011, 981606-981606, 2011.
- Kaufmann, L., Marcolli, C., Hofer, J., Pinti, V., Hoyle, C. R., and Peter, T.: Ice nucleation efficiency of natural dust samples in the immersion mode, *Atmospheric Chemistry and Physics*, 16, 11177-11206, 2016.
- Kiselev, A., Keinert, A., Gaedecke, T., Leisner, T., Sutter, C., Petrishcheva, E., and Abart, R.: Effect of chemically induced fracturing on the ice nucleation activity of alkali feldspar, *Atmos. Chem. Phys. Discuss.*, 2021, 1-17, 2021a.

Kiselev, A. A., Keinert, A., Gaedeke, T., Leisner, T., Sutter, C., Petrishcheva, E., and Abart, R.: Effect of chemically induced fracturing on the ice nucleation activity of alkali feldspar, *Atmos. Chem. Phys.*, 21, 11801-11814, 2021b.

Kobayashi, A., Horikawa, M., Kirschvink, J. L., and Golash, H. N.: Magnetic control of heterogeneous ice nucleation with nanophase magnetite: Biophysical and agricultural implications, *Proceedings of the National Academy of Sciences*, 115, 5383, 2018.

Kojima, T., Soma, T., and Oguri, N.: Effect of ice nucleation by droplet of immobilized silver iodide on freezing of rabbit and bovine embryos, *Theriogenology*, 30, 1199-1207, 1988.

London, D.: Granitic pegmatites, *Earth and Environmental Science Transactions of the Royal Society of Edinburgh*, 87, 305-319, 2011.

Massie, I., Selden, C., Hodgson, H., and Fuller, B.: Cryopreservation of Encapsulated Liver Spheroids for a Bioartificial Liver: Reducing Latent Cryoinjury Using an Ice Nucleating Agent, *Tissue Engineering Part C: Methods*, 17, 765-774, 2011.

Mazur, P., Leibo, S. P., and Chu, E. H.: A two-factor hypothesis of freezing injury. Evidence from Chinese hamster tissue-culture cells, *Exp Cell Res*, 71, 345-355, 1972.

Mikutta, R., Kleber, M., Kaiser, K., and Jahn, R.: Organic Matter Removal from Soils using Hydrogen Peroxide, Sodium Hypochlorite, and Disodium Peroxodisulfate, *Soil Science Society of America Journal*, 69, 120-135, 2005.

Morris, G. J. and Acton, E.: Controlled ice nucleation in cryopreservation--a review, *Cryobiology*, 66, 85-92, 2013.

Peckhaus, A., Kiselev, A., Hiron, T., Ebert, M., and Leisner, T.: A comparative study of K-rich and Na/Ca-rich feldspar ice-nucleating particles in a nanoliter droplet freezing assay, *Atmospheric Chemistry and Physics*, 16, 11477-11496, 2016.

Perkins, R. J., Gillette, S. M., Hill, T. C. J., and DeMott, P. J.: The Labile Nature of Ice Nucleation by Arizona Test Dust, *ACS Earth and Space Chemistry*, 4, 133-141, 2020.

Rutt, T., Eskandari, N., Zhurova, M., Elliott, J. A. W., McGann, L. E., Acker, J. P., and Nychka, J. A.: Thermal expansion of substrate may affect adhesion of Chinese hamster fibroblasts to surfaces during freezing, *Cryobiology*, 86, 134-139, 2019.

Suski, K. J., Hill, T. C. J., Levin, E. J. T., Miller, A., DeMott, P. J., and Kreidenweis, S. M.: Agricultural harvesting emissions of ice nucleating particles, *Atmospheric Chemistry and Physics Discussions*, doi: 10.5194/acp-2018-348, 2018. 1-30, 2018.

Teixeira, M., Buff, S., Desnos, H., Loiseau, C., Bruyère, P., Joly, T., and Commin, L.: Ice nucleating agents allow embryo freezing without manual seeding, *Theriogenology*, 104, 173-178, 2017.

Tobo, Y., Adachi, K., DeMott, P. J., Hill, T. C. J., Hamilton, D. S., Mahowald, N. M., Nagatsuka, N., Ohata, S., Uetake, J., Kondo, Y., and Koike, M.: Glacially sourced dust as a potentially significant source of ice nucleating particles, *Nature Geoscience*, 12, 253-258, 2019.

Tobo, Y., DeMott, P. J., Hill, T. C. J., Prenni, A. J., Swoboda-Colberg, N. G., Franc, G. D., and Kreidenweis, S. M.: Organic matter matters for ice nuclei of agricultural soil origin, *Atmospheric Chemistry and Physics*, 14, 8521-8531, 2014.

Wells, D. E. and Price, P. J.: Simple rapid methods for freezing hybridomas in 96-well microculture plates, *J Immunol Methods*, 59, 49-52, 1983.

Welti, A., Lohmann, U., and Kanji, Z. A.: Ice nucleation properties of K-feldspar polymorphs and plagioclase feldspars, *Atmospheric Chemistry and Physics Discussions*, doi: 10.5194/acp-2018-1271, 2019. 1-25, 2019.

Whale, T. F., Holden, M. A., Kulak, A. N., Kim, Y. Y., Meldrum, F. C., Christenson, H. K., and Murray, B. J.: The role of phase separation and related topography in the exceptional ice-nucleating ability of alkali feldspars, *Phys Chem Chem Phys*, 19, 31186-31193, 2017.

Whale, T. F., Holden, M. A., Wilson, Theodore W., O'Sullivan, D., and Murray, B. J.: The enhancement and suppression of immersion mode heterogeneous ice-nucleation by solutes, *Chemical Science*, 9, 4142-4151, 2018.

Wragg, N. M., Tampakis, D., and Stolzing, A.: Cryopreservation of Mesenchymal Stem Cells Using Medical Grade Ice Nucleation Inducer, *International Journal of Molecular Sciences*, 21, 2020.